**Title**
Peptide Repertoire Changes Caused by Defects in Antigen Processing



**Author**
Lind, Kristin

**Publication Date**
2013

Peer reviewed|Thesis/dissertation

# Peptide Repertoire Changes Caused by Defects in Antigen Processing

By

Kristin Camfield Lind

A dissertation submitted in partial satisfaction of the

requirements for the degree of

Doctor of Philosophy

in

Molecular and Cell Biology

in the

Graduate Division

of the

University of California, Berkeley

Committee in Charge:

Professor Nilabh Shastri, Chair
Professor Ellen Robey
Professor Greg Barton
Professor Fenyong Liu

Spring 2013

# Abstract

## Peptide Repertoire Changes Caused by Defects in Antigen Processing

By

Kristin Camfield Lind

Doctor of Philosophy in Molecular and Cell Biology

University of California, Berkeley

Professor Nilabh Shastri, Chair

MHC I molecules display peptides derived from intracellular proteins on the cell surface for recognition by CD8+ T cells. Presentation of these peptide:MHC I complexes (pMHC I) is important for elimination of viruses and transformed cells. In order to generate an effective CD8 T cell response, a high-quality set of pMHC I must be presented. However, the editing mechanisms that select these optimal pMHC I are not clear. In these studies, we used biochemical and immunological methods to examine the role of two ER-resident pMHC I editors, tapasin and ERAAP in shaping the pMHC I repertoire.

Analysis of tapasin-deficient mice revealed a qualitative loss as well as gain of some pMHC I. However, these changes did not overlap with the ERAAP-unedited pMHC I repertoire, indicating that tapasin edits peptides in a distinct way. Sequencing of peptides unique to tapasin-deficient cells revealed altered C-termini, suggesting that tapasin determines the peptide C-terminus while ERAAP shapes the peptide N-terminus.

We separately examined the allele-specific effects of ERAAP-deficiency on the H-$2^d$ pMHC I repertoire. In addition to $K^d$ and $D^d$, these mice express $L^d$, an MHC I molecule which is particularly affected by loss of ERAAP. We found that ERAAP-deficiency has distinct effects on the peptide repertoire presented by each MHC I molecule. Analysis of the peptide sequences revealed unique peptides bound to all three MHC I, although long, structurally unique peptides were only found on $D^d$ and $K^d$. Furthermore, using a T cell hybridoma specific for loss of ERAAP function, we identified and characterized an ERAAP-unedited peptide presented by $D^d$. Together, these findings highlight the importance of both tapasin and ERAAP in determining an optimal pMHC I repertoire.

# Table of Contents:

## List of Tables and Figures:

### Chapter 1:



### Chapter 2:



### Chapter 3:



### Chapter 4:



### Chapter 5:

## Chapter 6:



## Appendix:

## Acknowledgements

This work was not done in a bubble. I would like to recognize the colleagues, friends and family that made completing this journey possible.

First and foremost, I would like to thank Nilabh for giving me the opportunity to work in his lab and steering me through this process. You gave me the space to make my mistakes and the guidance to grow intellectually so that I could overcome them. Thank you for always having an open door - even when I know you were busy – for questions big or small.

I would also like to thank the past and present members of the Shastri Lab who made coming in to work something to look forward to even when the science wasn't going my way. Thanks to the Postdocs (Shelley, Nico, Takayuki and Soo Jung) whose helpful comments helped keep me on the right track and remember my controls. Fellow Shastri lab graduate students Harshi, Sharanya and Keling for commiserating when the going got tough and celebrating when things were good. My bay-mate Arne for your friendship and opinions on things both science and non-science. Fred for keeping the lab running and for making sure nobody's head got unduly big. And, of course Niranjana – My mini-PI – for taking me under your wing to guide me in all things ERAAP. Thanks for always being there to offer advice and friendship. Here's to many more coffee and lunch dates in the future!

I would also like to thank my family for inspiring a love for science and, in particular, biology. To Mom and Dad, thanks you for your unwavering support for me and my passions and for always encouraging me to do my best. Who else would let their kid grow frogs in her bedroom? I hope one day to be as good a parent to my kids as you were to me. To my sister, and fellow science nerd, Katie for always finding the positive in any situation. And for being the only other person I know who remembers way too many lines from Spaceballs and Wayne's World.

To my husband and best friend Nick, for encouraging me to fulfill my ambitions and for being my rock. There is no way I could have finished grad school without you. You are the best best! And of course to little Philip – for just being amazing and for all his writing 'help' in completing this thesis.

# Chapter 1: Introduction

## Overview

### The immune system distinguishes between self and non-self to protect from infection and tumors

The immune system is responsible for protecting the host from infection by a wide variety of non-self pathogens, such as protozoans, bacteria and viruses. To this end, it has a number of ways to distinguish self from the non-self invaders. Our immune system has both an innate and adaptive branch. By working together, both arms of the immune system protect the host from microbial invaders.

The innate immune defenses depend on pattern recognition receptors encoded by germline DNA to detect conserved microbial associated molecular patterns (MAMPs). Generally, these are features of microbes distinct from our own cells. Diverse receptor families have evolved to recognize these conserved patterns, and can be found in the cytosol, on the cell surface or are secreted (1). Using these receptors, the immune system can either eliminate invading pathogens or contain them until the infection can be fully cleared by the adaptive immune system.

Stimulation of some innate immune receptors, such as toll-like receptors, is important for activating B and T cell-mediated adaptive immunity. The hallmark of the adaptive immune system is its ability to generate non-germline encoded receptors to recognize microbial pathogens. Furthermore, the adaptive immune system has the ability to form memory responses such that it can recognize and respond to re-infection with the same microbe more robustly.

In addition to protection from infection, the immune system also eliminates malignant cells. Recognition of altered-self, such as the intracellular changes that often accompany the transformation of a healthy cell to a potentially tumorogenic one, can serve to protect the host.

### CD8 T cells protect against viral infection and cancer

CD8+ T cells are important components of the adaptive immune system. They are key in protection from a wide range of assaults, notably viruses, intracellular parasites, bacteria and tumors. However, due to their potent cytotoxic abilities, misregulation of CD8+ T cells can cause autoimmune disease, and as such, it is important to tightly manage their responses.

CD8+ T cells express T cell receptors (TCR) that recognize small peptide antigens presented on the cell surface by MHC I molecules. In the thymus, T cells undergo an education process that selects cells with TCRs capable of recognizing peptide-MHC I complexes (pMHC I), termed positive selection. However, in a process termed negative selection, T cells that express TCRs with a high affinity for self-pMHC I are deleted, thus eliminating potentially autoreactive cells. Although this process removes a majority of potential T cells, a large T cell pool with TCRs capable of recognizing diverse pMHC I remain. These exit the thymus and enter into the periphery(2).

To become activated, peripheral CD8+ T cells require encounter with antigen presenting cells (APCs), resulting in stimulation through their specific TCR, co-stimulation via CD28 as well as other cytokine signals. This activation step generally occurs in the secondary lymphoid organs, and is followed by a rapid clonal expansion of the responding T cells. Upon encounter with an infected cell in the periphery, CD8+ T cells utilize an arsenal of effector mechanisms to eliminate compromised cells, including production of effector cytokines such IFN-γ and release

of granules containing cytotoxic material like perforin and granzyme B. After clearance of the pathogen, a majority of the CD8+ T cells die, although a subset of memory cells remain to protect from future rechallenge with the same pathogen(3).

**MHC I molecules present a diverse set of antigenic peptides:**

The MHC I antigen presentation pathway generates peptides that are presented on MHC I molecules as peptide:MHC I complexes (pMHC I). These pMHC I are expressed on the surface of almost all cells in the body. They serve as ligands for CD8+ T cell recognition, and are important for immune surveillance.

Humans co-dominantly express allelic variants of three MHC I molecules: HLA-A, HLA-B and HLA-C, which are encoded on chromosome 6. Murine homologs of these MHC I molecules, H-2D, H-2K and H-2L are found on the mouse chromosome 17. The peptides generated by the MHC I antigen presentation pathway can be of endogenous origin (self) or foreign (non-self) origin. Recognition of a non-self pMHC I by a CD8+ T cell results in subsequent release of cytotoxic granules that kill the presenting cell.

In 1987, the first crystal structures of MHC I molecules were published by Wiley and colleagues(4). The MHC I molecule resolved consisted of two alpha helices upon eight anti-parallel beta strands, representing the peptide binding groove. Between the two alpha helices was electron dense material, presumed to be the source of antigenic activity. We now understand that this material represents peptides, and it could not be resolved because of the large diversity of peptides each MHC I can present. Work from Rammensee and colleagues determined that peptide binding motifs for MHC I molecules have a fixed length (5). In addition, for any given MHC I molecule, there are 2-3 residues that are called 'anchor residues' that serve to bind the peptide to the MHC I. There are some preferences for certain residues outside of the anchor positions, however, by and large almost any amino acid can fill these positions. This means that MHC I molecules are capable of presenting a broad repertoire of peptides to CD8+ T cells.

A second class of MHC I molecules, the non-classical or MHC Ib molecules, have a role in both innate and adaptive immunity (6). This is a diverse group of molecules, which is varied in function. They share structural similarities with MHC I, often require TAP and beta2M and several are found linked to the MHC loci. Unlike classical MHC I, which is highly polymorphic, these molecules are relatively conserved between individuals. While some of these non-classical MHC I molecules present peptides, many present different classes of antigen to both T cells and innate immune cells, like NK cells. Alternative classes of antigen include lipids presented by CD1 or microbial vitamin metabolites presented by MR-1 (7, 8).

**Beta2-microglobin deficiency**

Beta2 microglobin (beta2M) is a small molecule that binds the MHC I heavy chain in the ER prior to entry into the PLC and is required for expression of most MHC I on the cell surface (9). To determine the importance of beta2M in antigen presentation, cells and mice deficient in this protein were analyzed.

Beta2M-deficiency causes a pronounced immune phenotype. Examination of beta2M-deficient cell lines R1E (mouse) and Daudi (human) demonstrated that they are highly deficient in MHC I surface expression. $D^b$ and $L^d$ were exceptions to this beta2M dependence, as they were found at very low levels on the cell surface after transfection(10-12).

Although beta2M-deficient mice were viable and otherwise healthy in other aspects (13, 14), beta2M is required for optimal cell surface expression of MHC I molecules, including both classical and non-classical MHC I. The diminished levels of MHC I also affected selection of CD8+ alpha/beta T cells. In beta2M-deficient mice, the percentage of peripheral CD8+ T cells was only 0.2% relative to a typical 11% found in TAP +/- cells (15), reflecting a defect in positive selection(13). Interestingly, the small percentage of CD8 T cells in these mice is sufficient to reject tumors and allogeneic splenocytes in an MHC I-specific manner (16), indicating that a subset of T cells can be selected on the highly restricted pMHC I repertoire available. Beta2M-deficient mice may also have a defect in negative selection, as beta2M-deficient T cells had enhanced responses to self-MHC I complexes.

Overall, these mice are highly deficient in antigen presentation and CD8 T cell responses. They have been an invaluable tool for the study of MHC I antigen presentation and the contribution of CD8+ T cells relative to other immune cells in protection from a variety of different pathogens and tumors.

**The effects of MHC I deficiency**

Due to their important role in both thymic selection of T cells and mediating peripheral immune responses, it is not surprising that loss of MHC I has severe effects on the CD8+ T cell compartment. Single $K^b$ or $D^b$-deficient mice were generated and characterized with varying degrees of difference(17). Loss of $D^b$ did not lead to significant reduction in peripheral CD8+ T cells, while Kb-deficient mice had about half as many mature T cells. However, mice lacking both $K^b$ and $D^b$ only had about 10% of both their peripheral and thymic CD8+ T cells (17, 18). Non-classical MHC I molecules, including Qa-1, were not deficient in their expression (17). Qa-1 is notable as it primarily presents the peptide ligand Qdm derived from the signal sequence of some MHC I molecules which is absent in $K^bD^b$-deficient mice. These double-deficient mice have subsequently been used to study the role of non-classical MHC I molecules in response to various pathogens, including viruses (19, 20).

## The generation of antigenic peptides for MHC I

Formation of pMHC I complexes has two major steps: generation of the antigenic peptide and selection and loading of that peptide onto MHC I molecules. In this section, I will discuss the factors involved in the origination of antigenic peptides and the effects of deficiency in these factors on the quality of the pMHC I repertoire and CD8 T cell immunity.

**Antigenic Peptide Sources**

Peptides presented by MHC I molecules provide the immune system with a cellular status report, allowing for detection of any problems caused by infection or mutation. Antigenic peptides presented on MHC I molecules typically originate from endogenously synthesized cellular proteins. To ensure any detrimental change is detected, it is important that the immune system can sample a diverse set of the components and cellular processes.

Initially it was thought that antigenic peptides resulted as byproducts of normal cellular turnover. In support of that hypothesis, introduction of full-length protein into cells was sufficient for presentation of its known antigenic peptide(21). However, it was observed that peptides from viral proteins were presented faster than would be expected based on the stability of the source protein, which suggested that normal turnover was not the only source of antigenic peptides(22). Furthermore, a considerable fraction of newly synthesized proteins are rapidly

degraded (23, 24). A recent study in which the stability of a protein can be controlled by drug treatment indicated that a higher fraction of short-lived peptides are presented relative to the more stable version. Together, the evidence now suggests that the majority of antigenic peptides come from rapidly degraded sources. This faster rate of sampling allows the immune system to detect infected or transformed cells before they become a problem.

Exactly what conditions determine which proteins are destined to become antigenic peptides is not well understood. However, it is of great interest as these define the set of peptides available for presentation to T cells. Diverse cellular sources of antigenic peptides have been reported. For example, mistakes in mRNA translation, protein folding or truncated proteins can result in presented peptides (25-27). These are broadly referred to as Defective Ribosomal Products, or DRiPs(28). Cryptic sources of antigenic peptides also exist, including the use of alternative reading frames or non-AUG start codons (29, 30). While the exact contribution of each of these remains unclear, it should be appreciated that such diverse sources for antigenic peptides allows the immune system to broadly sample the intracellular state.

**The Proteasome/Immunoproteasome is responsible for the breakdown of proteins into antigenic peptide precursors**

The multicatalytic proteasome is a large enzymatic complex responsible for degrading cellular proteins. It contains a core catalytic domain consisting of four stacked rings made up of fourteen subunits (alpha1-alpha7 and beta1-beta7). The alpha subunits make up the outer rings and are responsible for regulation of the proteins that enter the inner catalytic core, which is made up of the beta subunits. Three of the subunits (beta1, beta2 and beta5) have defined catalytic activity (31, 32).

The proteasome is responsible for breaking down a majority of cellular proteins targeted for degradation into smaller peptide fragments. Most of these proteins are targeted to the proteasome by ubiquitin side chains (33). The resulting peptides are generally between 3 and 25 amino acids in length (34). While a majority of the peptide fragments generated from these cytoplasmic proteolytic events are destroyed (35) a small percentage are shuttled into the MHC I antigen presentation pathway as antigenic peptide precursors.

Identification of the proteasome as the major enzyme responsible for generating peptides presented by MHC I was demonstrated using chemical inhibitors. Treatment of cells with proteasome inhibitors lead to overall decreases in antigen presentation due to an inability to process the full-length protein, as reflected by the failure of MHC I heavy chain molecules to dimerize with beta2M and to generate the antigenic SIINFEKL epitope from full-length OVA protein (36).

In response to the cytokine IFN-γ, new proteasomal components and regulators are expressed and are preferentially integrated into assembling proteasome complexes, forming the immunoproteasome. These include beta-1i (LMP2), beta-2i (MECL-1) and beta 5i (LMP7). These new subunits increase the rate of processing and change the cleavage preferences of the proteasome (37-40). In this state, the peptide fragments released tend to favor either a hydrophobic or basic residue at the C-terminus (41), which is in line with MHC I binding preferences. Further evidence of the relation of the proteasome to antigen presentation is demonstrated by the fact that two of these subunits, LMP2 (beta-1i) and LMP7 (beta-5i) are found in the MHC II locus (42, 43). Several studies have examined how loss of the

immunoproteasome affects MHC I antigen presentation by examining how loss of each of the immunoproteasome subunits affects MHC I presentation and T cell responses.

Loss of MECL-1 (beta-2i) did not significantly affect MHC I surface expression, however, there were about 20% fewer T cells in the periphery (44). There were no changes in thymic populations. When MECL-1-deficient T cells were tested for their ability to respond to LCMV epitopes, a slight decrease in response to GP276 and NP205 were detected, however, the amount of these peptides generated was not noticeably different from MECL-1 sufficient cells. This indicates that any difference in the response is likely a result of altered T cell development.

LMP2 (beta-1i)-deficient mice were generated almost 20 years ago (45). Using fluorogenic substrates, changes in peptidase activity from lymphoblasts lacking LMP2 were observed. While $K^b$ and $D^b$ surface expression of these mice was not different from WT, 20-50% fewer CD8+ T cells were detected. In addition, decreased CTL responses against an influenza epitope were observed, and there were fewer responding T cells upon influenza virus infection. These altered T cell responses may have reflected changes in thymic selection of CD8+ T cells. However, no differences were seen in responses or antigen immunodominance hierarchies between LMP2-deficient and WT mice upon LCMV infection (46). This suggests that any effects of the single LMP2 KO may be compensated for by other components *in vivo* or may be specific to generation of particular yet untested epitopes.

A similar analysis was performed on LMP7 (beta-5i)-deficient mice which resulted in a stronger phenotype. As seen with LMP2-deficiency, LMP7-deficient proteasomes have altered proteolytic activity and cleavage site preferences (41, 47). Furthermore, LMP7-deficient mice had a 50% decrease in $K^b$ and $D^b$ MHC I surface expression, although normal numbers of B and T cells were reported, and presentation of an endogenous H-Y antigen was affected in these mice (48). Subsequent studies identified broader qualitative changes to endogenous pMHC I in LMP7-deficient cells. T cell lines from LMP7-deficient mice were raised which lysed WT cells, indicating that some WT pMHC I need LMP7 for their presentation (49). Furthermore, Osterloh et al demonstrated that optimal positive selection of OT-I T cells required LMP7(50).

The above single-knockouts of the immunoproteasome subunits MECL-1, LMP2 and LMP7 showed variable effects on antigen presentation. To examine whether some of these results were complicated by compensation from remaining subunits, Kincaid et. al. made triple-mutant mice which lack all three subunits. They observed surface MHC I decreases of about 50%, similar to those seen in LMP7-deficient mice. However, there were decreased responses to both self and viral epitopes by the triple-KO T cells relative to WT or single KO and the changes in endogenous peptides were significant enough to result in rejection of triple-KO cells by WT hosts (51).

Together, the evidence suggests that the proteasome is key in generating antigenic peptide precursors for MHC I antigen presentation. Although several other cytoplasmic proteases have been tested for their ability to generate antigenic peptides, no other enzyme has thus far been discovered that can fully compensate for proteasome function (52), as is discussed below.

**The limited role of cytoplasmic proteases in antigen presentation**

The proteasome is responsible for general recycling of cellular proteins, and its products vary in length from approximately 7-20 amino acids. Additional cytoplasmic proteases are necessary for further breakdown of proteasome-generated fragments into amino acids. Some studies have suggested that these cytoplasmic proteases can also participate in generating and destroying antigenic peptides, although their overall effect seems to be limited. Individual cytoplasmic proteases and the evidence supporting their involvement in antigen presentation is discussed below.

*Tripeptidyl peptidase II (TPPII):* TPPII is a large cytoplasmic protease which removes amino acids in groups of three from oligopeptides and may also have some endopeptidase activity (53). It was identified from cells adapted to proteasome inhibitors and it was hypothesized that it might be capable of replacing some functions of the proteasome, including the generation of peptides for MHC I(53). While some studies show TPPII may participate in processing for a subset of peptides, the relative contribution of TPPII to overall antigen presentation remains unclear.

Studies using inhibitors and *in vitro* trimming assays with purified components have found that TPPII can generate individual epitopes (54, 55). At least *in vitro*, TPPII cooperated with LAP to generate one antigenic peptide (56)and generated the C-terminus of another(55), presumably through its endopeptidase activity. In these studies, TPPII favored peptides longer than 16 amino acids. However, results from knockdown of TPPII by siRNA indicated that while it had a role in generating epitopes from long peptides, TPPII is not essential for most antigen presentation (57).

A limited role for TPPII was further supported by *in vivo* studies which examined the effects of TPPII-deficiency on antigen presentation. Cells from TPPII-gene trapped mice, in which TPPII expression was decreased by 90%, were able to elicit similar T cell responses against LCMV epitopes (58). Furthermore, TPPII-knockout mice had slightly increased surface expression of MHC I molecules, suggesting that TPPII may negatively regulate overall antigen presentation. Although the T cell compartment in TPPII-deficient mice has increased cell death(59), CD8+ T cells from these mice responded similarly to LCMV infected cells(60). Together, it seems that, while TPPII can participate in antigen presentation for a subset of antigens, it is not important for most pMHC I and T cell responses.

*Thimet Oligopetpidase* (TOP): TOP is a cytoplasmic protease that cleaves 3-5 amino acids off the C-terminus of peptides in the cytoplasm (61). This carboxypeptidase activity contributed to the hypothesis that TOP might be responsible for generating some C-termini of antigenic peptides. Indeed, one study suggested that TOP could work in concert with the cytoplasmic metalloprotease nardylisin to release one epitope which does not contain a typical proteasome-generated C-terminus(62). However, this enzyme is thought to have an overall negative effect on antigen presentation by destroying epitopes (63, 64). Overexpression of TOP led to decreased MHC I surface expression and destruction of the model SIINFEKL epitope(64). These results suggest a limited role for TOP in general antigen presentation and CD8+ T cell immunity.

*Bleomycin Hydrolase (BH):* BH is a cytoplasmic aminopeptidase with broad substrate specificity. Purified BH and BH-containing fractions from soluble cell extracts are capable of trimming N-terminally extended precursors of the VSV-NP epitope (65), suggesting BH may participate in generating antigenic peptides. Furthermore, treatment of cells with aminopeptidase inhibitors blocked presentation of this same VSV-NP epitope to T cells. However, as with other cytoplasmic proteases, the overall contribution of BH to antigen presentation appears limited. A subsequent study examining the ability of BH, among other proteases, to generate a final epitope from extended precursors found that the residual proteasome activity was still required for this process.

In human cells expressing a variety of MHC I, siRNA knockdown of BH identified allele-specific differences in which surface expression of some alleles was affected while others were not(66). However, no change in surface expression of $K^b$ and $D^b$ MHC I was seen in BH-deficient mice(67). In addition, there was no difference in the ability of WT or BH-deficient cells to generate the final SIINFEKL peptide from extended epitopes. Although BH alone may not be sufficient to generate epitopes, it may work with other cytoplasmic proteases to do so on some set of antigenic peptides. Future studies should seek to further understand the allele-specific effects of BH on generation of antigenic peptides.

*Leucine Aminopeptidase (LAP):* Another cytoplasmic aminopeptidase is LAP. An initial report identified LAP from HeLa cell cytoplasmic extracts as an IFN-γ inducible aminopeptidase capable of trimming N-terminally extended model peptides (68). Furthermore, injection of LAP into cells increased the overall trimming of peptides(69). However, when the effects of LAP-deficiency on antigen presentation were examined through *in vitro* siRNA knockdown or in cells from LAP-knockout mice no defects were found(70). To test whether the lack of effect is due to compensation by other cytoplasmic aminopeptidases, BH and LAP mice were crossed together and CTL responses against several known epitopes were examined(67). The only epitope tested that showed a difference was increased relative to WT, suggesting that it is normally destroyed by BH and LAP. It appears that, while LAP has the ability to trim antigenic peptides in vitro, it does not play a significant role in editing the N-termini of antigenic peptides

*Puromycin-Sensitive Aminopeptidase (PSA):* A third cytoplasmic aminopeptidase with a putative role in antigen trimming is PSA. As with BH, PSA was biochemically isolated from cytoplasmic extracts as a peak of aminopeptidase activity capable of cleaving fluorogenic substrates (65). Purified PSA was also able to trim extended precursors to final products. However, analysis of PSA-deficient mice suggested that, *in vivo*, PSA may actually degrade antigenic peptide precursors rather than generate them, as increased MHC I surface expression was found on dendritic cells(71). In addition, no differences in the overall T cell compartment or responses to viral epitopes were observed. As with BH, there may be some allele-specific effects, as siRNA knockdown caused decreased expression of HLA-A68 but increased expression of HLA-B8 and HLA-B15(66). Again, while it is possible that PSA is required for a small subset of antigens, overall it does not appear to be a major player in the generation of antigenic peptides.

**Chaperones: getting the peptides from the cytoplasm to the ER**

Proteasomal degradation of proteins results in a large number of peptide fragments, only a small number of which are of suitable length for presentation on MHC I (72, 73). Shortly after the peptides have left the proteasome, most are rapidly degraded into single amino acids for new protein synthesis by cytoplasmic proteases such as TOP (63). For efficient presentation, antigenic peptide precursors must be protected from cytoplasmic degradation and shuttled to the TAP transporter and the MHC I antigen presentation pathway. This section details the roles of cytoplasmic chaperones in protecting peptides and facilitating MHC I antigen presentation.

*Heat Shock Protein 90, Heat-shock protein 70 and gp96:* HSPs, including HSP90, HSP70 and gp96, which are discussed individually in more detail below, have long been known to associate with a variety of antigenic peptides. HSP90, HSP70 and gp96 may all play a role in antigen presentation by directly binding either the final peptide or peptide precursors(74). A growing body of literature suggests that this association appears to be important for cross-presentation of antigens in addition to endogenous antigen presentation (75-77).

Heat-shock protein-90 (HSP90) is a cytoplasmic chaperone that is abundantly expressed in cells. Antigenic peptides introduced into the cytoplasm in complex with HSP-90 or HSP-70 were more highly presented to specific CTLS (78) than free peptides, linking HSP90 to antigen presentation by suggesting it protects peptides from degradation by binding them. Furthermore, knockdown of the alpha isoform of HSP90 by siRNA resulted in the intracellular loss of a series of C-terminal proteolytic intermediates and decreased presentation of the final pMHC I on the cell surface (79). Treatment of cells with HSP inhibitors, such as geldanamycin and radcicol, reduced overall surface pMHC I levels of H-$2^b$ and H-$2^d$ MHC I by approximately 50% (80) as well as association of HSP90 with N-terminally extended peptide precursors. HSP90a may also indirectly affect peptide generation, as it is may participate in chaperoning the folding of subunits of the 26S proteasome.

As with HSP90, immunization of peptide complexed with HSP70 increased the efficiency of the CTL response than when mice were immunized with peptide alone (81). Immunization of mice with these complexes is also sufficient to break tolerance and induce autoimmunity (82).

In contrast to HSPs 70 and 90, gp96 is an ER-resident chaperone which has been suggested to play an analogous role in shielding antigenic peptides from destruction in the ER. In support of this, gp96 has been shown to be capable of binding to peptides transported by TAP (83). Furthermore, gp96 purified from TAP-deficient cells was unable to prime CTLs, whereas when it was purified gp96 from TAP-sufficient cells was able to do so (84). As with the other HSPs, immunization of mice with gp96 complexed with peptide generated an adjuvant effect, suggesting it is able to protect the antigenic peptides from destruction (Li H, 2005 JI). However, examination of gp96-deficient cell lines found no impact on surface expression of $K^b$ (85).

These chaperones may have redundant functions in protecting antigenic peptides from destruction (75), making the task of identifying the individual contributions of each chaperone difficult. Additional studies examining the effects of loss of some or all of these chaperones in MHC I antigen presentation are needed to clarify their role in endogenous antigen presentation, including whether some sequences are favored over others, as this could be an important

selection step that determines which peptides are available to the MHC I antigen presentation pathway.

*Tailless Complex Polypeptide-1 Ring Complex (TRiC)*: TRiC is a large cytoplasmic chaperone which facilitates peptide folding (86). It also has a secondary but important function to protect antigenic peptide precursors from destruction by cytoplasmic proteases. This protection was established by Kunisawa et. al. who used biochemical methods to identify model proteolytic intermediates bound to TRiC(87). Further supporting a role in antigen presentation, they found that TRiC was essential for optimal HLA surface expression and presentation of endogenous peptides by $K^b$. Administration of TRiC-peptide complexes was found to stimulate efficient cross-presentation(88), demonstrating the protection of peptides by TRiC in a different way. Future studies should examine whether any sequence specificity exists for TRiC binding of antigenic peptides and clarify the role of TRiC in endogenous antigen presentation.

## Loading Antigenic Peptides onto MHC I: The PLC

Cytoplasmic peptide fragments are transported into the endoplasmic reticulum (ER) by the transporter associated with antigen processing (TAP)(89). Upon entering the ER, the peptides encounter the peptide loading complex (PLC) which facilitates optimal peptide loading onto MHC I(90, 91). The PLC consists of TAP, tapasin, calreticulin, the thiol oxidoreductase ERp57, beta2M and the MHC I heavy chain. As the mediator of the final loading step, the PLC determines which peptides make the cut for surface presentation to CD8+ T cells. In this section, I will detail the role that individual PLC components play in MHC I antigen presentation, particularly with respect to determining which peptides are presented.

### Chaperones calnexin and calreticulin facilitate MHC I folding

As new MHC I heavy chain molecules are synthesized into the ER, chaperones calnexin and calreticulin bind to them, protect them from misfolding and deliver them to the PLC (89). Both chaperones bind to monoglucosylated N-linked glycans, although not necessarily the same ones (92, 93). Calnexin is reported to bind to the heavy chain right after translocation into the ER, prior to binding of peptide . Calreticulin, on the other hand, was found in complexes with other PLC components (94-96), presumably indicating it chaperones the MHC I during peptide binding. Thus, it seems that these two chaperones have successive, yet distinct, roles in antigen presentation (93, 97). Mice and cell lines deficient in either calnexin or calreticulin have provided insight into the role of these chaperones.

Prior to examination of calnexin-deficient mice, it was found that overexpression of calnexin leads to decreased expression of MHC I, indicating that it retains MHC I molecules in the ER (98). This effect on antigen presentation, coupled with biochemical evidence that calnexin binds the MHC I heavy chain (99)implied an important role in antigen presentation. Surprisingly, examination of calnexin knockout cell lines (100)and calnexin gene-trapped mice (101)indicated that the loss of calnexin does not result in an immune phenotype. There was normal assembly and retention of MHC I molecules in the cell lines (98)and there were no major changes in the CD4/CD8 profiles of these mice in either the spleen or the thymus (101). One

explanation for this discrepancy may be that other chaperones, such as BiP, are able to compensate for calnexin's absence.

Calreticulin, on the other hand, has a stronger link to antigen presentation and peptide selection. Unfortunately, calreticulin-deficient mice are not viable, which has limited the study of the effects of loss of calreticulin on immunity. Broadly, calreticulin has two primary roles: to regulate calcium homeostasis in the ER in and to facilitate folding of glycoproteins. The inability to regulate calcium affects heart development (102), and is embryonic lethal unless the chaperone calcineurin is overexpressed to compensate for its loss (103). As mentioned above, calreticulin is found in the PLC and directly binds to ERp57 and glycans on the MHC I heavy chain (104). Loss of calreticulin leads to decreased surface presentation of MHC I (93). This appeared to be due to a general instability of the calreticulin-deficient MHC I molecules, as they were more rapidly transported from the ER yet were found at decreased levels on the cell surface. When examination of the effects of calreticulin-deficiency on presentation of particular epitopes was examined, epitope-specific effects were identified. B3Z hybridoma cells recognized calreticulin-deficient and sufficient cells equally, although lower SL8/Kb complexes were detected by antibody staining. Furthermore, when two separate CTL clones specific for different MCMV epitopes were tested for the ability to kill calreticulin-sufficient or deficient cells, one killed the calreticulin-sufficient cells better while the other killed both equally, suggesting that some antigens are capable of being presented in the absence of calreticulin. The likely model for calreticulin's contribution is that it maintains a lower threshold for peptide binding, thus facilitating antigen presentation (105).

**TAP transports peptides into the ER**

Peptides are transported from the cytoplasm into the endoplasmic reticulum by a protein heterodimer called the Transporter Associated with Antigen Processing or TAP. Using different methods, four groups independently identified the TAP genes at about the same time (106-109). Genes for TAP1 and TAP2 are both located in the MHC locus and their expression is rapidly increased in response to IFN-γ treatment(110). When expressed, TAP1 and TAP2 heterodimerize to form an ABC-like transporter. They each have multiple transmembrane domains and a C-terminal ATP-binding domain, characteristic features of an ABC transporter. TAP resides primarily in the ER-membrane and requires ATP hydrolysis to pump peptides from the cytoplasm to the ER lumen (111). The ER-lumen side of the TAP heterodimer is linked to the peptide loading complex (PLC) by tapasin. This association brings the transport of peptides in close proximity to the empty MHC I molecules and stabilizes TAP expression.

Prior to transport, peptides bind to membrane-spanning domains on the cytoplasmic side of both TAP1 and TAP2 (112). Because a large majority of the peptides presented by MHC I require TAP for their transport, the selectivity is an important determinant of what will actually be presented, thus a broad specificity is important. Interestingly, human and mouse TAP transporters have slightly different peptide preferences which correspond with the binding preferences of their respective MHC I molecules. Human TAP translocates peptides with either basic or hydrophobic C-termini more efficiently, and peptide binding is primarily dictated by the three N-terminal and the C-terminal position of the peptide (113, 114). The presence of a proline at the first or second N-terminal position was found to be strongly deleterious for peptide transport by human TAP (113). As with its human analog, mouse TAP favors transport of peptides with hydrophobic C-termini and it does not favor peptides with a proline at positions 1-

3 (114, 115). Furthermore, inefficient peptide translocation could be overcome by the substitution of the proline at position 3 or addition of flanking amino acids (116).

The inability to transport peptides with a proline at the beginning of the sequence, particularly at position 2 (P2), has consequences for several MHC I molecules, such as the murine $L^d$ and human HLA-B07 among others (117). The consensus motif for these MHC I is an X-P-$X_n$ motif, which is not favored by TAP. This means that in order for these epitopes to be presented efficiently, TAP would need to transport an N-terminally extended version that is subsequently trimmed in the ER, likely by ERAAP. This is further discussed below.

Loss of TAP is devastating for surface expression of MHC I molecules. Human cell line 721.134, which lacks the TAP1 gene, had almost undetectable levels of MHC I which could be rescued by transfection of TAP1 cDNA (106, 118). Similarly, TAP2 deficiency in RMA-s cells was rescued by addition of the TAP2 cDNA, supporting the hypothesis that the two molecules form a heterodimer, as they cannot compensate for one another. The decreased surface expression was also found *in vivo*, as TAP1 deficient mice showed striking surface expression loss (119).

While most antigens are absent in TAP-deficient cells, TAP-independent pMHC I do exist. Some antigens derive from signal sequences, which are removed when peptides enter the ER (120). Interestingly, T cell lines specific for endogenous TAP-independent peptides identified CTL lines restricted to $K^b$, $D^b$ and Qa-1b, suggesting that all MHC I are capable of presenting TAP-independent peptides (121). Furthermore, several endogenous peptides from TAP1-deficient LCL721.174 cells were sequenced by quantitative mass spectrometry and about half came from other sources other than signal sequences, indicating that some antigens use alternative pathways to be presented (122). Notably, these peptides had lower predicted binding affinity than their TAP-sufficient counterparts, again suggesting that these may only be presented when more optimal peptides are missing.

As might be expected, the severe effects seen on the pMHC I also affect CD8+ T cell selection and responses. Although the percentages of DP thymocytes are similar between TAP-deficient and sufficient mice, the percentages of CD8+ T cells in TAP1-deficient mice are decreased 30-40%, suggesting altered positive selection (119). In further support of defects in pMHC I presentation, TAP-deficient APCs require 25-times as many CTLs for lysis.

**ERp57 facilitates MHC I folding and tapasin action**

Also part of the PLC is ERp57, a member of the protein disulphide isomerase family. It is known to participate in disulfide bond oxidation and isomerization during the folding of newly synthesized glycoproteins through its interactions with calnexin and calreticulin (123, 124). It binds to the MHC I heavy chain and mediates formation of disulfide bonds prior to binding of beta2M and entry into the PLC (125). Upon entry into the PLC, ERp57 interacts with tapasin via a disulfide linkage, forming a stable dimer, for which the crystal structure was recently solved (126, 127). Indeed, a growing body of evidence suggests that many functions of tapasin, including editing and PLC formation, require the presence of ERp57 (128). The crystal structure indicates that tapasin binds both active sites on ERp57, preventing it from mediating disulfide bond formation within the PLC. Therefore, once in the PLC, ERp57 likely acts to recruit and stabilize the empty MHC I and calreticulin rather than as a thioloxidoreductase.

Constitutive ERp57 knock-out mice are not viable, however, Garbi et al generated B-cell specific conditional knock-out cell lines that enabled study of the effects of ERp57-deficiency on antigen presentation (129). Surface expression of $K^b$ was decreased about 50%, and expression

of $D^b$ was down about 20%. These moderate decreases did not fully phenocopy the effects of tapasin-deficiency, in which surface expression is diminished by about 90% relative to WT (130), but they are substantial. Furthermore, both presentation of endogenous antigens to the Des TCR transgenic T cell line and transfected OVA to the B3Z hybridoma were diminished in ERp57-deficient cells (129). Together, this data suggests that, ERp57 may, at least indirectly, be required for the presentation of certain antigens.

**Tapasin stabilizes the PLC and edits pMHC I**

Tapasin is known to play several key roles in presentation of peptides on MHC I. Through its interactions with TAP, MHC I heavy chain and ERp57 it anchors together the components of the PLC to keep the empty MHC I close to the source of incoming peptides (90, 91, 131, 132). Thus, in many ways, loss of tapasin reflects a loss of the PLC. (91, 126, 127, 132-135). Additionally, tapasin upregulates the peptide transport function of TAP, presumably by stabilizing it (136).

Consistent with these functions, $K^b$ and $D^b$ surface expression in mice is decreased by 90% in the absence of tapasin ($Tpn^0$). Similar dependence on tapasin for optimal MHC I expression is seen with some HLA alleles, such as HLA-B4402 and HLA-B3501 when expressed in the tapasin-deficient cell line 720.221. However, expression of other HLA molecules, such as HLA-B2705 and HLA-A0201, is unaffected in the absence of tapasin. This allele variability has been linked to residues in the peptide binding groove of MHC I (137).

To examine the role of tapasin in the PLC, the structure of the ERp57/tapasin heterodimer was solved (126). Tapasin contains two domains: An N-terminal domain with an Ig-like fold fused with a beta-barrel and a C-terminal domain which is also an Ig-like fold. From this structure, a functionally significant interface was identified which is required for surface expression of tapasin-dependent allele HLA-B*4402. This binds the MHC I molecule at the N-terminal segment of helix alpha-2. It has been hypothesized that tapasin functions to stabilize an open conformation of the MHC I molecule, which is supported by molecular modeling studies and the fact that tapasin is found associated most predominantly with an intermediately-folded MHC I molecule (138, 139).

In addition to its role in the PLC, tapasin also edits the pMHC I repertoire through mechanisms that are not yet fully understood. Evidence from the study of several human MHC I molecules (HLA) has indicated that pMHC I in $Tpn^0$ cells dissociate more quickly than WT (140, 141). This suggests the presence of an altered, suboptimal set of peptides that are presented when tapasin function is lost. Furthermore, based on molecular modeling, it was reported that tapasin destabilizes peptide binding at the C-terminus to promote dissociation of low-affinity peptides (142). Similar support for changes to the pMHC I repertoire was also found with mouse $K^b$ and $D^b$. Furthermore, when a series of SIINFEKL mutants with varied C-termini were tested for presentation in the absence of tapasin, it was found that WT cells presented the variant with the highest affinity, whereas $Tpn^0$ cells favored a variant with a moderate affinity (143). The precise nature of these pMHC I changes has not yet been described, as peptides from $K^b$ and $D^b$ in their endogenous context have not been sequenced. Further characterization of the effects of tapasin-deficiency on the pMHC I repertoire will better define tapasin's role in peptide presentation.

## ER-resident Proteases:

Many antigenic precursors are longer in length than the preferred 8-10 amino acids needed to form stable complexes with MHC I molecules. Furthermore, peptides that have the X-P-$X_n$ motif are not readily transported by TAP, despite it being a common consensus motif used by many MHC I, including $L^d$. Together, these suggest a need for further trimming of antigenic peptide precursors after entry into the ER. Below, enzymes known to participate in this role are discussed.

**ERAAP defines the final pMHC I repertoire**

ERAAP is a member of the M1 family of zinc metalloproteases (144). This family is characterized by the exopeptidase-specific GAMEN and the H-E-X-X-H-$(X)_{18}$-E zinc binding motifs which are part of the catalytic domain. There have been reports that ERAAP has functions outside of antigen processing pathway, such as in shedding of TNF receptors(145) as well as in regulating blood pressure (146, 147). However, ERAAP has been best characterized for its role in trimming N-terminal extensions from antigenic peptides. ERAAP is expressed most highly in cells with active antigen presentation, such as the lungs, liver, spleen and thymus, and its expression is upregulated by IFN-gamma(144).

Two recently published structures of human ERAP1 have provided insight into the mechanism by which peptide substrates are trimmed(148)(Kochan, Krojer et al. 2011). Both structures identify four domains in ERAP1, similar to those found in the structures of related aminopeptidases. The catalytic domain II is responsible for cleaving the N-terminal amino acid of the substrate. Domain I and Domain IV interact to form the substrate binding pocket. Domain III is the smallest of the four and acts as a hinge or lever to open domain IV, allowing it to capture substrates. The substrate binding pocket of ERAP1 is deeper as compared to other aminopeptidases which may account for the long substrates, 9-16 amino acids in length that ERAP1 favors. From the structure, Nguyen et. al. proposed a model for the mechanism by which ERAP1 trims its substrates which are consistent with the independent findings of Kochan, Krojer et al. In the open structure of ERAP1, the residues are disordered and not in close contact. Peptide substrates are 'captured' by ERAP1 in the open conformation, which causes domains I and IV to close around the substrate. The resulting conformational change brings the catalytic residues into an active position and cleaves the N-terminal amino acid from the peptide. The peptide must be released and re-bound in order to remove the next amino acid. Mouse and human ERAAPs are similar (86% amino acid similarity), and it is likely that the mouse version acts in an analogous fashion.

The structure of ERAAP informs its substrate specificity. It is important that ERAAP be able to trim a large range of substrates in order for it to generate the variety of antigenic peptides presented on all types of MHC I molecules. Although the mechanism of ERAAP trimming is not entirely known, reports have indicated that ERAP1 more efficiently trims substrates 9-16 amino acids in length and with a hydrophobic C-terminus(149). Hearn et. al. looked at the N-terminal substrate specificity of ERAAP and found that some residues are favored while others can negatively affect the generation of antigenic epitopes. Using *in vitro* trimming of ER-targeted constructs that have the OVA derived SL8 peptide with a variety of N-terminal amino acids, Hearn et. al. showed that, while many different amino acids were capable of being removed, a Leucine, Methionine or Tyrosine in front of the antigenic peptide released it more quickly than other amino acids. Having a Proline was the least favorable in terms of greater epitope production. Trimming assays with model peptides demonstrated that mutating the

internal residues affected their trimming, indicating that ERAAP has some preferences with regard to the internal sequence of its substrate(150).

Simply trimming peptides is not the whole story of how ERAAP shapes the peptide repertoire. The importance of MHC I molecules in the composition of peptides has been established for several years(5). Browenstein et. al. identified N-terminally extended precursors of the Ova-derived peptide SIINFEKL bound to $K^b$(151). In living cells, Kanaseki et. al. (152) showed that the type of MHC I available determined which peptide was generated. They used a system in which a single peptide could lead to the generation of either a $K^b$ or a $D^b$ epitope. In the presence of $K^b$, that epitope was generated, but not the $D^b$ epitope and vice versa. These findings indicate that ERAAP and MHC I molecules synergize to establish the pMHC I repertoire. While these findings point to a model in which ERAAP and the MHC I interact closely, it remains to be determined whether there is a direct interaction between the two.

To test the importance of ERAAP for presentation *in vivo*, ERAAP-deficient (ERAAP KO) mice were generated. The Shastri lab made a targeted deletion in the ERAAP locus in mice in which exons 4-8, those that maintain the enzymatic activity, were deleted(153). When compared to WT mice, ERAAP KO mice have decreased expression of MHC I molecules, but not MHC II molecules. In addition, the pMHC I complexes are less stable in ERAAP KO cells. As had been previously observed using RNAi knock-down of ERAAP expression(144), the levels of some epitopes increase, while others decrease or stay the same. When the pMHC I repertoire of endogenous peptides was examined in these mice, Hammer et. al. identified extensive differences in the peptide repertoire (154). C57BL/6 (B6) T cells respond to altered peptides presented by ERAAP KO APCs on $K^b$ and $D^b$ and vice versa. In addition, the ERAAP KO pMHC I are more unstable, as the optimal peptide repertoire is unable to be generated in the absence of ERAAP.

While classical MHC I presents many novel and unstable peptides, when the WT anti-ERAAP KO T cell response was examined, the dominant response was against a novel peptide, FL9, presented by a non-classical MHC I, Qa-1. This pMHC I complex was not presented in WT cells and was highly immunogenic, dominating the anti-ERAAP KO CD8+ T cell response in B6 mice (155). Immunogenic peptides presented by classical MHC I were not readily detected due to the dominant nature of the non-classical anti-ERAAP KO response. Future studies using alternative mouse strains, such as $H\text{-}2^d$, may provide insight into *the in vivo* effects of ERAAP-deficiency.

Three other groups have independently generated ERAAP-deficient mice, and also examined the ERAAP KO pMHC I repertoire(156-158). Overall, these groups found similar effects on pMHC I expression as was seen by Hammer and colleagues. These groups studied antiviral responses and found that responses varied. York et. al. looked at expression of vaccinia and LCMV epitopes and found that ERAAP-deficiency prevented the generation of some epitopes while others were unaffected. Yan et. al. examined generation of the gp33 epitope in ERAAP KO and WT mice and found that it was increased upon ERAAP-deficiency, indicating that it is an ERAAP-sensitive peptide. Finally, Firat et. al. found no significant change in anti-LCMV CTL hierarchies or compromised *in vivo* anti-viral immunity.

The molecular basis for the pMHC I differences in $K^b$ and $D^b$ due to loss of ERAAP function was determined when peptides from ERAAP KO and WT were sequenced by mass spectrometry. Analysis of unedited peptides from ERAAP-deficient cells revealed peptides with increased length at the N-terminus or middle of the peptide but with a strongly conserved C-terminus(159).

**ERAP2 complements ERAP1 in human cells**

Humans have an additional ER aminopeptidase, ERAP2 (formerly known as L-RAP), which does not have a murine homolog. However, similar to ERAP1, it is a member of the M1 family of metalloproteases and its expression is induced by IFN-gamma (160). Examination of the substrate specificity of ERAP2 indicated that, distinct from ERAP1, it preferentially cleaves basic residues (160). *In vivo,* ERAP1 and ERAP2 are thought to form heterodimeric complexes with complementary activity, which would allow for efficient trimming of a wider set of substrates (161, 162). These substrate preferences were supported by the ERAP2 crystal structure (163). Future studies should better characterize the effects of ERAP2 deficiency on immunity.

**Angiotension Converting Enzyme (ACE) edits the C-terminus**

The proteasome is responsible for generating a majority of the antigenic peptide C-termini, however, there has also been reports that ER-resident carboxypeptidase ACE may participate in trimming the C-termini of antigenic peptides. ACE has a broad expression pattern (164), consistent with its role in many different physiological functions, ranging from vascular biology to kidney function. ACE is also expressed in antigen presenting cells such as dendritic cells and inflammatory macrophages (165-167) suggesting it has an immunological function.

Surface expression of MHC I molecules on DCs, macrophages and whole spleen appears to be affected by changes in ACE expression. If ACE is overexpressed, then there is a slight decrease in MHC I expression, however, in ACE-deficient cells there is a slight increase in $K^b$ and $D^b$ pMHC I surface expression. Using a viral overexpression system, Eisenlohr et. al. had demonstrated that increased ACE can enhance presentation of TAP-dependent endogenous antigens (168). ACE was also shown to have the ability to destroy model epitopes, which is also seen in other antigen presentation editors. There is some evidence that ACE can act as an editor, much like ERAAP does (167). Cross-immunization experiments using ACE-deficient cells elicited T cell responses from ACE-WT mice, suggesting that ACE-deficient cells present a new set of pMHC I.

Current evidence suggests that, while ACE clearly affects presentation of some antigens, it primarily works on products already cleaved by the proteasome rather than whole proteins. Questions remain about the overall contribution of ACE to the peptide repertoire and whether it is part of the PLC, since the current dogma is that the antigenic C-termini are generated by the proteasome.

## Altered ER-editing in disease

The importance of expressing a quality pMHC I repertoire is highlighted by the fact that so many pathogens and transformed cells target the antigen presentation machinery to evade the immune system. In doing so, they prevent presentation of non-self peptides and subsequent elimination by CD8+ T cells. Herpes viruses are notorious for targeting antigen processing in order to establish latent infections within cells, and they encode several genes that specifically downregulate antigen presentation machinery. Misregulation of antigen processing can also affect pMHC I presentation causing development of autoimmune disease. Below, I discuss more specifically the targeting of ER-resident peptide editors ERAAP and tapasin in relation to development of disease.

**Altered ERAAP processing and disease**

As ERAAP is an important editor of pMHC I quality, its down-regulation can prevent expression of some pMHC I, potentially allowing evasion of CD8 responses. To this end, ERAP1 is inhibited by HCMV as part of its immune evasion strategy (169). A microRNA, miR-US4-1, encoded by the virus specifically targets ERAP1, leading to decreased expression and affecting susceptibility to virus-specific CD8+ T cells. In contrast, examination of ERAP1 expression in various non-lymphoid transformed cell lines revealed a heterogeneous expression pattern (170). Although it is not a clear link, it seems that some tumors may find downregulation of ERAP1 advantageous for avoiding detection while others use a different route.

ERAAP has also been associated with autoimmunity, as several recent studies have found associations between variants of the human homolog of mouse ERAAP (ERAP1), particular MHC I molecules and autoimmune disease. A link between polymorphisms in ERAP1 and Ankylosing Spondylitis (AS) is the best established of these (171) (172), although GWAS studies have also suggested a link between psoriasis and ERAP1 SNPs. The genetic link found between ERAP1 and these autoimmune diseases begs the question of whether the disease might result from alterations in the processing of peptides for in affected individuals. It is imperative that we better understand the MHC I allele specific effects of ERAP trimming on the pMHC I repertoire.

**Altered tapasin editing and disease.**

Tapasin is a target for inhibition by viruses as they seek to avoid CD8+ T cell detection. Human cytomegalovirus blocks both tapasin transcription, through mechanisms that are not yet clear, and tapasin stability via the inhibitor US3 (173, 174). Furthermore, the murine γ2-Herpesvirus 68 expresses mk3 which leads to ubiquitination and subsequent degradation of tapasin (175), resulting in subsequent downregulation of susceptible MHC I alleles. Finally, loss of tapasin in human cancer, such as squamous cell carcinoma, is associated with a poorer prognosis (176). Because tapasin generally leads to decreases in MHC I presentation, this downregulation presumably prevents immune detection.

## Thesis Research:

The MHC I antigen presentation pathway selects for optimal pMHC I in order to enable a robust T cell response. Many cellular factors are involved in the generation of antigenic peptides and the loading of these peptides onto MHC I. Indeed, many potential peptides are generated which never make it to the surface. Many questions still exist regarding how ER-resident editors ERAAP and tapasin shape the peptide repertoire. How do they work together? Do they have over-lapping or distinct functions? As allele-specific differences in surface expression of MHC I have been demonstrated upon deficiency of either editor, do further differences exist when surface expression is the same? The following studies seek to examine these questions.

**Table 1: Summary of deficiencies in antigen presentation factors**

| Antigen Presentation Factor Lost | | MHC I Surface expression | MHC I Peptide Presentation | CTL Responses | CTL Selection |
|---|---|---|---|---|---|
| MHC I | $K^b$ | No $K^b$ expression. $D^b$ and nonclassical MHC I show no deficiency | Presentation normal for all but $K^b$? | | 30-50% reduction of T cell compartment |
| | $D^b$ | No $D^b$ expression. $K^b$ and nonclassical MHC I show no deficiency | Presentation normal for all but $D^b$? | Development of a $K^b$-restricted anti-LCMV CTL response upon infection | 10-20% reduction of T cell compartment |
| | $K^bD^b$ | No $K^b$ or $D^b$ expression. Nonclassical MHC I show no deficiency | Primarily presentation by non-classical MHC I | CTLs do not respond to allogeneic MHC Ia expressing APCs unless primed first | 90% reduction of T cell compartment |
| beta2M | | no detectable MHC I expression (except very low $D^b$ and $L^d$) | Peptide-free MHC I heavy chains? | CTLs from beta2M-deficient hosts can reject tumors and allogeneic cells after priming | 98% reduction of CD8 Tcell compartment. Selection mediated by low levels of free heavy chains? |
| Proteasome/ Immunoproteasome | MECL-1 (beta-2i) | no defect | normal amouts of model peptides generated from MECL-1 deficient cells | Slight decrease in response to some LCMV epitopes | 20% fewer T cells in periphery (normal thymus compartment) |
| | LMP2 (beta-1i) | no defect | altered peptidase activity affects generation of model epitopes | decreased responses against one model influenza epitope but not against LCMV epitopes | 20-50% reduction in CD8 T cells |
| | LMP7 (beta-5i) | 50% reduction in $K^b$ and $D^b$ surface expression | decreased presentation of endogenous H-Y epitope and altered presentation of endogenous antigens | CTL lines from LMP7-deficient cells capable of lysing WT APCs | normal numbers of CD8 T cells |
| | MECL-1/LMP-2/LMP-7 Triple knockout | 50% reduction in $K^b$ and $D^b$ surface expression | altered presentation of endogenous antigens | decreased responses against self and viral epitopes | 50% reduction in CD8+ T cells |

**Table 1: Summary of deficiencies in antigen presentation factors**

| Antigen Presentation Factor Lost | | MHC I Surface expression | MHC I Peptide Presentation | CTL Responses | CTL Selection |
|---|---|---|---|---|---|
| Cytoplasmic proteases | TPPII | TPPII downregulation causes increased MHC Ia and TPPII overexpression decreases Kb and Db surface levels. | Reported to participate in generation of some model epitopes. No changes in viral epitope generation in gene-trapped mice | similar responses to LCMV infected cells. | ? |
| | TOP | TOP overexpression decreases MHC I surface levels | Reported to distroy model SIINFEKL epitopes but also participate with nardilysin to generate other epitopes | ? | ? |
| | BH | No change with siRNA knockdown | Can trim model VSV epitope *in vitro*. Cells with siRNA knockdown fully able to generate SIINFEKL epitopes | Towne et al tested 8 epitopes and saw a slight increase in response against one of them. | No defect? |
| | LAP | Normal | Can trim model epitopes *in vitro*. Presentation appears normal | ? | ? |
| | PSA | allele-specific effects of siRNA knockdown on various HLAs | Can trim model epitopes *in vitro*. Deficient mice show no change in response to viral epitopes | No difference in T cell responses to viral epitopes | No defect |

**Table 1: Summary of deficiencies in antigen presentation factors**

| Antigen Presentation Factor Lost | | MHC I Surface expression | MHC I Peptide Presentation | CTL Responses | CTL Selection |
|---|---|---|---|---|---|
| Cytoplasmic Chaperone | HSPs | Cells treated with HSP inhibitors have a 50% decrease in surface expression of H-2b and H-2d MHC I. Gp96-deficient cell lines have normal Kb expression. | siRNA knockdown of HSP90 decreases expression of model antigens | ? | ? |
| | TrIC | TRiC expression is requried for optimal HLA surface expression | Necessary for optimal presentation of endogenous peptides by $K^b$ | ? | ? |
| PLC | Calnexin | overexpression decreases MHC I surface expression | ? | ? | Knockout mice show no defect in selection |
| | Calreticulin | Calreticulin-deficiency decreases MHC I surface expression | Decreased $K^b$/SL8 complexes relative to WT cells via antibody staining but B3Z hybridomas see no difference. MCMV epitopes show epitope-dependent response | ? | ? |
| | TAP | no detectable MHC Ia | lower affinitly peptides - some derived from signal sequences | 25x more APCs required for Cr51 lysis (see Van Kaer 1992 cell) | >90% reduction of T cell compartment |
| | ERp57 | $K^b$ decreased 50% and $D^b$ 20% in ERp57-deficient B cells | diminished presentation of endogenous and transfected antigens | ? | ? |

**Table 1: Summary of deficiencies in antigen presentation factors**

| Antigen Presentation Factor Lost | | MHC I Surface expression | MHC I Peptide Presentation | CTL Responses | CTL Selection |
|---|---|---|---|---|---|
| | Tapasin | Both $K^b$ and $D^b$ expression decreased by 90%. Various HLA alleles show a range of tapasin dependence for optimal surface expression. | Peptides presented by tapasin-dependent alleles tend to have a lower affinity and be more unstable | Decreased CTL responses against cells expressing viral epitopes. | ~90% reduction in T cell compartment |
| | ERAAP/ERAP 1 | Kb and Db both decreased 20-30% | altered, unstable endogenous peptide repertoire including immunogenic FL9/Qa-1 complex | Endogenous anti-ERAAP CTL responses against FL9/Qa-1 complexes. ERAAP CTLs respond to some WT $K^b$ and $D^b$ pMHC I | No defect in CD8 compartment |
| | ACE | overexpression decreases Kb and Db surface expression | altered, unstable endogenous peptide repertoire. Distroyed model epitope *in vitro* | ACE CTLs respond to pMHC I | No defect in CD8 compartment? |

## Chapter 2: Tapasin is a C-terminal editor of antigenic peptides.

## Summary:

Tapasin is the central factor in the PLC and is believed to play a key role in maintaining PLC integrity and optimal antigen presentation. Loss of tapasin in B6 mice leads to severely decreased levels of surface expression of $K^b$ and $D^b$ MHC I, (130, 177). Non-classical MHC Ib molecules Qa-1 and Qa-2 are also affected (178). In addition to these quantitative changes, qualitative changes have also been observed for some MHC I molecules (179), including presentation of suboptimal pMHC I, suggesting that tapasin may also have a peptide editing function (91, 134, 137, 140, 143, 177, 180). The goal of these studies is to better characterize how pMHC I editing by tapasin affects presentation of endogenous pMHC I. Using immunological approaches, we found that tapasin-deficiency causes qualitative changes in the pMHC I repertoire, including loss of some pMHC I found on WT cells as well as presentation of new pMHC I. These studies were done in close collaboration with Takayuki Kanaseki when he was a postdoctoral fellow in the Shastri lab.

ERAAP-deficiency has also been shown to cause pMHC I losses and gains. How ERAAP edits peptides and whether editing requires interaction with the PLC is not known. Because tapasin is required to maintain the PLC, we reasoned that the peptide editing events in the PLC might be evident in cells lacking tapasin and ERAAP. Using immunological assays, we found that tapasin-unedited pMHC I were distinct from ERAAP-unedited pMHC I. Thus, we conclude that tapasin and ERAAP shape the pMHC I repertoire in different ways.

## Results:

### Loss of antigenic peptide editors decreases surface pMHC I presentation

Perturbation of MHC I antigen processing pathway components is often manifested as altered surface expression. For example, loss of peptide supply due to TAP1 or TAP2-deficiency results in severe surface expression decreases and limited T cell selection. In tapasin-deficient mice ($Tpn^0$), the expression of $K^b$ and $D^b$ pMHC I are decreased by about 90% of WT (130) while the effects of ERAAP-deficiency ($ERAAP^0$) is less severe, with $K^b$ and $D^b$ surface expression reproducibly diminished by 20-30% (154). Our own examination of surface expression of $K^b$ and $D^b$ from $Tpn^0$ and $ERAAP^0$ mice replicated these findings. To examine the effects of loss of both ERAAP and tapasin on pMHC I expression, splenocytes from double-deficient mice ($ERAAP^0Tpn^0$) were stained with MHC I anti-$K^b$ and anti-$D^b$ antibodies or control MHC II anti-$A^b$ antibody and analyzed by flow cytometry. These results were compared with wild-type (WT), which has normal surface expression, or ERAAP, tapasin and TAP single knockouts to better estimate the general effects of deficiency (**Fig 1a-c**). Interestingly, $ERAAP^0Tpn^0$ $K^b$ and $D^b$ expression was slightly below $Tpn^0$ but was above $TAP^0$. Therefore, it appears that loss of both tapasin and ERAAP lead to separate and independent decreases in pMHC I expression. Whether these decreases are a result of pMHC I instability due to the inability to select quality peptides or whether there is overall decreased trafficking to the cell surface remains to be determined.

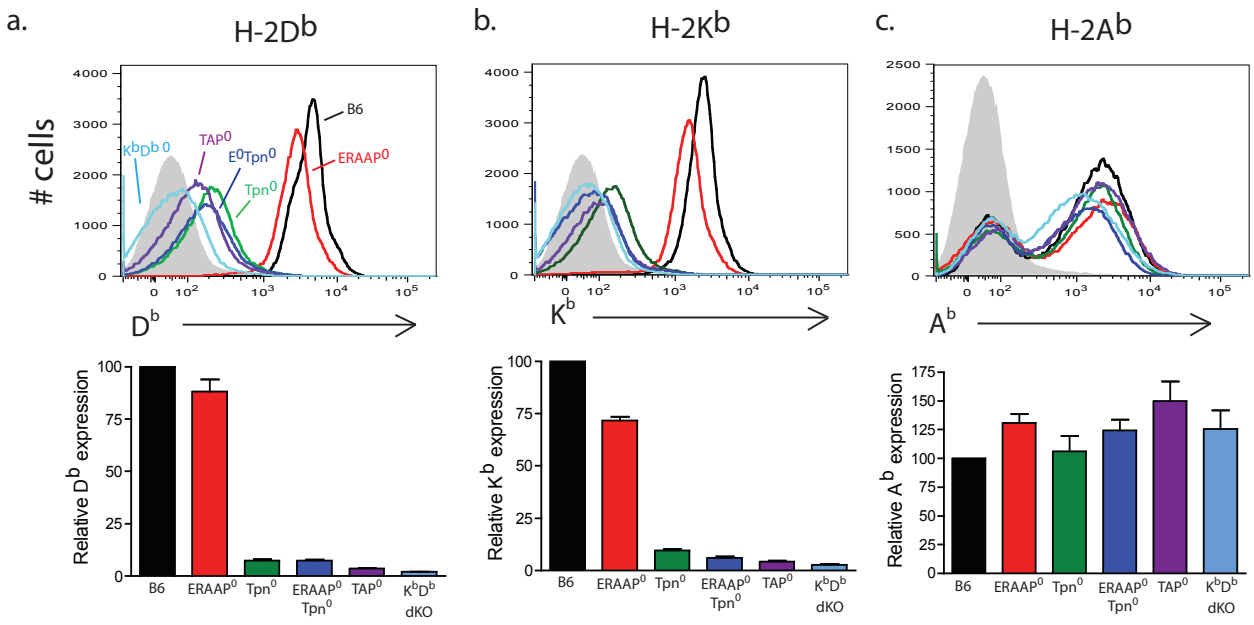


**Figure 1: Tapasin and ERAAP differentially affect surface pMHC I expression.** (a-c) Surface expression of (a) H-2D$^b$, (b) H-2K$^b$ and (c) H-2A$^b$ expression on spleen cells derived from WT, ERAAP$^0$, Tpn$^0$, ERAAP$^0$Tpn$^0$, TAP$^0$, K$^b$D$^b$ dKO mice. Bar graphs summarize the mean fluorescence intensity (MFI). Top panels show representative data and bottom panels show combined data from 3 independent experiments.

**Thymic development in ERAAP and tapasin double-deficient cells is phenotypically similar to tapasin-deficient cells**

As pMHC I complexes play an important role in T cell selection, altered expression also affects T cell development. For example, in beta2M deficient mice, in which no significant expression of MHC I can be detected, the CD8+ cells are absent from both the thymus and the periphery. To examine the effects of deficiency in both tapasin and ERAAP on CD8 T cell development, we examined the frequency of CD8 single-positive (SP) T cells from ERAAP$^0$Tpn$^0$ double-deficient mice relative to single tapasin or ERAAP-deficient or WT mice (**Fig 2a-b**). As was previously reported, loss of ERAAP alone did not affect the percentage of SP CD8+ T cells (153). However loss of tapasin (130) or both tapasin and ERAAP led to similar, striking decreases in percentages of SP CD8+ T cells. Similar trends were observed in the spleen. It is important to note the presence of a small population of T cells in ERAAP$^0$Tpn$^0$ mice. Even with severely diminished MHC I expression, there is still sufficient pMHC I to mediate positive selection. The exact nature of the selecting pMHC I, and whether it overlaps with the tapasin-deficient pMHC I, should be further explored.

**ERAAP and tapasin differentially influence generation of endogenous pMHC I**

Previous studies characterized the effect of ERAAP-deficiency on generation of specific pMHC I and found that in the absence of ERAAP, some pMHC I are enhanced while others are diminished. As we were interested in testing whether ERAAP and tapasin have a shared editing role, we wanted to examine whether tapasin-deficient cells expressed similar types of losses and gains of the same pMHC I.

To assess the influence of ERAAP and tapasin on the generation of specific peptides bound to MHC I, we measured the presentation of a panel of endogenously processed peptides on the surface of spleen cells from wild-type B6, Tpn$^0$, ERAAP$^0$ or ERAAP$^0$Tpn$^0$ mice (**Fig 3**). As expected, ERAAP-deficient APCs failed to stimulate the 11P9Z and LPAZ hybridomas, while presentation of pMHC I to the 30NXZ, 1AZ and BEko8Z hybridomas was enhanced. In contrast, hybridoma responses against Tpn$^0$ splenocytes were diminished for all pMHC I ligands tested, suggesting that tapasin is required for presentation of these pMHC I.

To examine the effects of ERAAP$^0$Tpn$^0$ double-deficiency on generation of these pMHC I, ERAAP$^0$Tpn$^0$ APCs were tested using the same set of hybridomas. Consistent with the strong surface down-regulation seen in the double-deficient splenocytes (**Fig 1**), ERAAP$^0$Tpn$^0$ APCs showed a striking overall decrease similar in magnitude to Tpn$^0$. Upon closer examination, however, ERAAP$^0$Tpn$^0$ APCs stimulated slightly higher responses in 30NXZ and slightly lower responses in LPAZ relative to Tpn$^0$, showing a similar pattern as is seen with ERAAP$^0$ relative to WT but on a different scale (**Fig 3**). These results highlight the importance of tapasin for presentation of many endogenous pMHC I and suggest that tapasin and ERAAP may differentially affect pMHC I.

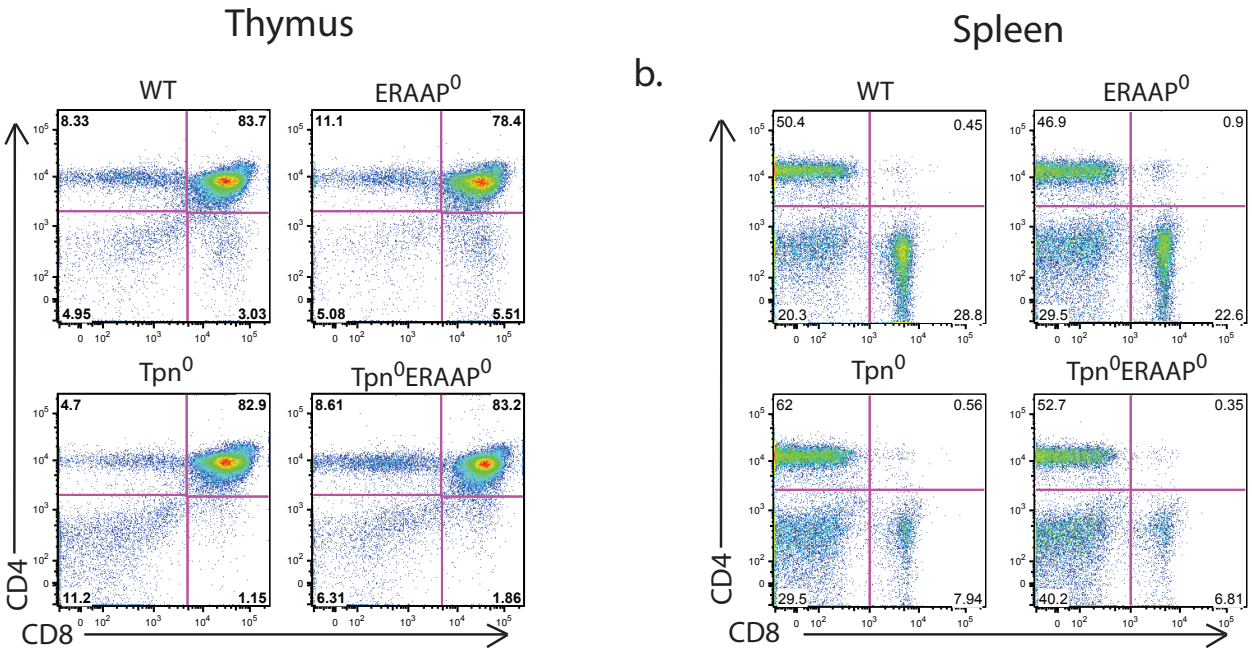


**Figure 2. Development of T cell subsets in tapasin-deficient and ERAAP-tapasin double-deficient mouse strains.** (a) Thymus and (b) Spleen from C57BL/6 (WT), ERAAP-deficient ($ERAAP^0$), tapasin-deficient ($Tpn^0$) or ERAAP and tapasin-double deficient ($ERAAP^0Tpn^0$) were harvested. A single cell suspension was stained with anti-mouse CD4 and CD8. Data are representative of two independent experiments.

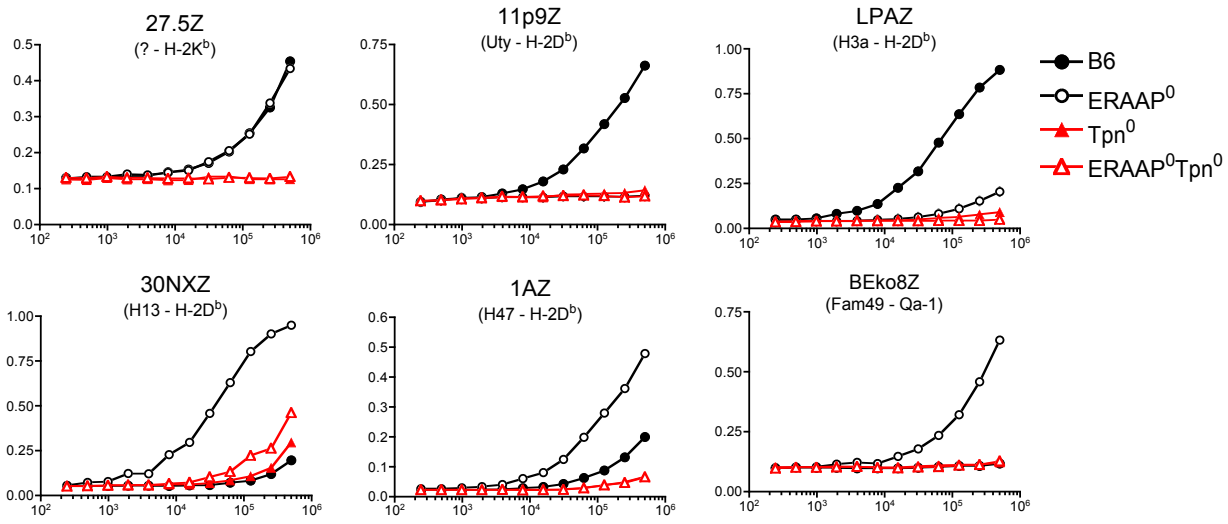


**Figure 3. Tapasin and ERAAP differentially affect presentation of endogenous pMHC I by spleen cells.**
Splenocytes from indicated male mice were stimulated with 200ng/ml LPS overnight prior to incubation with CD8$^+$ T cell hybridomas 27.5Z, LPAZ, 11P9Z, 1AZ, 30NXZ, or BEko8Z. Hybridomas specifically recognize peptides encoded by the indicated genes and presented on H-2D$^b$, H-2K$^b$, or Qa-1$^b$. Hybridoma response is determined by assessing conversion of the colorometric substrate CPRG to chlorophenol red measured at absorbance at 595 nm (A595). Data is representatives of three independent experiments.

**Tapasin-deficient T cells respond to WT pMHC I**

To further define the changes that occurred in pMHC I repertoire of tapasin-deficient mice, we took advantage of the immune systems' ability to detect differences between self- and non-self. If some WT pMHC I were not expressed in tapasin-deficient mice, then the $Tpn^0$ T cells would not encounter them during selection, and would therefore not be tolerant to the missing pMHC I. Immunization of tapasin KO mice with WT APCs would then result in the recognition of these missing pMHC I as foreign. In contrast, if there is simply a quantitative decrease in all pMHC I without the qualitative loss, then $Tpn^0$ T cells would be tolerant to all WT pMHC I as are normal self pMHC I.

To test for a qualitative loss of WT pMHC I in tapasin-deficient mice, $Tpn^0$ mice were immunized with wild-type spleen cells expressing the normally diverse pMHC I repertoire. For all immunizations, female mice were injected with male cells as they express H-Y antigens that can provide T cell 'help' to enhance CD8+ T cell responses. After ten days, splenocytes from recipient mice were restimulated for a week with WT spleen cells. The cultures were then analyzed for presence of $CD8^+$ T cells that produced IFN-γ in response to the indicated APCs. The $Tpn^0$ anti-WT $CD8^+$ T cells responded strongly to WT APCs but not to self APCs, suggesting that tapasin-deficiency did cause a selective loss of pMHC I(**Fig 4a-b**). As with a majority of peptides that bind MHC I, TAP is required for presentation, as $TAP^0$ APCs do not stimulate the $Tpn^0$ anti-WT T cells (**Fig 4b)**.

To evaluate which MHC presented the tapasin-dependent peptides, we used spleen cells from $K^b$ and $D^b$ ($K^bD^b$ dKO) double-deficient mice as APCs. The $Tpn^0$ anti-WT T cells did not respond to $K^bD^b$ dko spleen cells indicating that tapasin-dependent peptides were primarily presented by the $K^b$ and $D^b$ MHC I in WT cells, rather than non-classical MHC I molecules (**Fig 4b**). To further define the MHC I molecules presenting the immunogenic peptides, we used anti-$K^b$ or anti-$D^b$ blocking antibodies prior to incubation of APCs with $Tpn^0$ anti-WT T cells (**Fig 4c**). Of the three T cell lines tested, IFN-γ responses were decreased with $K^b$ blocking and in one line with $D^b$ blocking as well, indicating that immunogenic pMHC I were presented by either $K^b$ or $D^b$ MHC I.

**WT T cells respond to novel pMHC I presented by tapasin-deficient cells**

In addition to the qualitative loss of peptides from $Tpn^0$ cells, we hypothesized that if tapasin edits MHC I peptides then the loss of tapasin would result in presentation of new peptides. To test whether $Tpn^0$ cells present novel pMHC I, we immunized WT mice with $Tpn^0$ cells. The recipient T cells were restimulated *in vitro* as above and analyzed for responses to WT or $Tpn^0$ APCs. WT anti-$Tpn^0$ T cells produced IFN-γ in response to $Tpn^0$, but not to WT APCs, indicating presence of unedited pMHC I in $Tpn^0$ cells (**Fig 5a-b**). Tapasin expression appears to affect TAP stability and could thus influence peptide transport into the ER(136) Therefore, it was possible that the novel peptides presented in the absence of tapasin could be due to a TAP deficiency (121, 181).

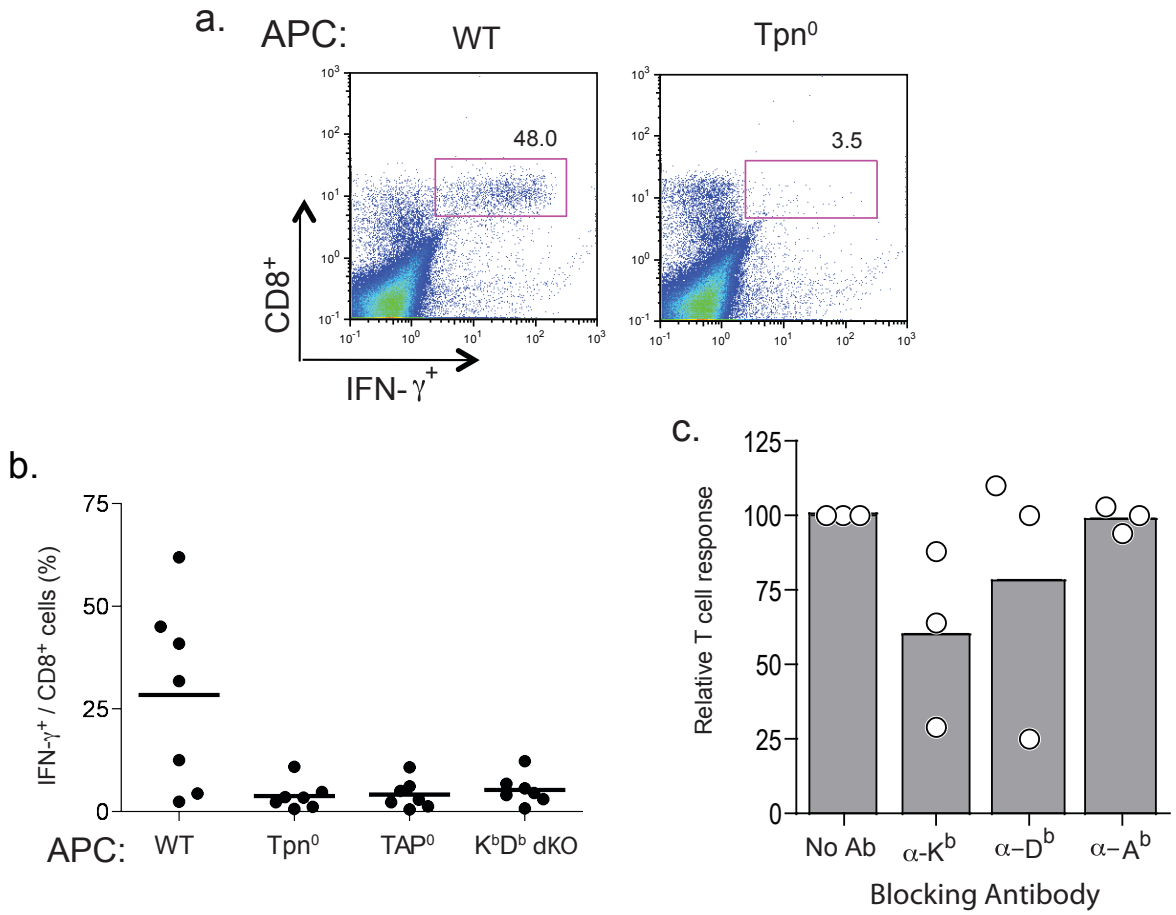


**Figure 4. Tapasin-deficient mice respond to pMHC I expressed by WT cells.**
**(a)** Intracellular IFN-γ produced by Tpn$^0$ anti-WT CD8$^+$ T cell lines in response to WT or Tpn$^0$ APCs. Numbers indicate percent IFN-γ positive cells of total CD8$^+$ T cells. **(b)** Tpn$^0$ anti-WT CD8$^+$ T cell IFN-γ+ response against WT, Tpn$^0$, TAP$^0$ or K$^b$ and D$^b$ double-deficient (K$^b$D$^b$ dKO) APCs. Each point represents an individual mouse. **(c)** Tpn$^0$ anti-WT CD8$^+$ T cell responses towards WT APCs previously treated with blocking antibodies to MHC I H-2K$^b$ (α-K$^b$) or H-2D$^b$ (α-D$^b$) or to MHC II H-2A$^b$ (α-A$^b$). Percentages of CD8$^+$ IFN-γ$^+$ cells were normalized to no antibody control. Data are from one of two independent experiments (a and c) or pooled from two independent experiments (b).

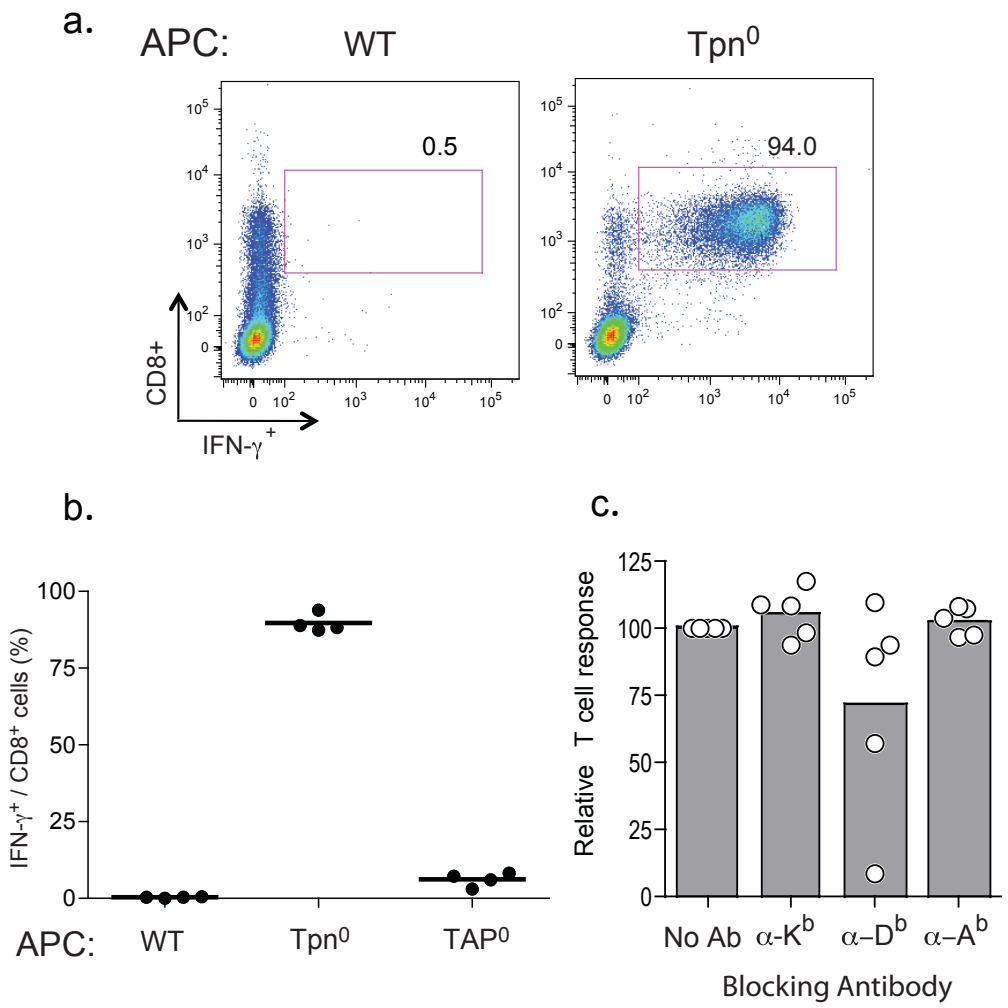


**Figure 5. Tapasin-deficient cells elicit CD8$^+$ T cell responses in wild-type mice**. **(a)** IFN-γ response of WT anti-Tpn$^0$ CD8$^+$ T cell lines against WT or Tpn$^0$ APCs. Numbers indicate percent IFN-γ positive cells of total CD8$^+$ T cells. **(b)** WT anti-Tpn$^0$ CD8$^+$ T cell responses against WT, Tpn$^0$ or TAP$^0$ APCs. Each point represents an individual mouse. **(c)** WT anti-Tpn$^0$ CD8$^+$ T cell responses against WT APCs previously treated with blocking antibodies to MHC I K$^b$ (α-K$^b$) or D$^b$ (α-D$^b$) or to MHC II A$^b$ (α-A$^b$). Percentages of CD8$^+$IFN-γ$^+$ cells were normalized to no antibody control (No Ab).

However, when we used $TAP^0$ cells as APCs, WT anti-$Tpn^0$ T cells did not produce IFN-γ (**Fig 5b**), indicating that peptide transport is required for presentation of these pMHC I and that this presentation is not a consequence of TAP-deficiency. Furthermore, while blocking the $A^b$ MHC class II molecule or the $K^b$ MHC I molecule did not inhibit IFN-γ production in any of the five lines tested, blocking with the anti-$D^b$ antibody inhibited T cell responses more effectively than blocking with anti-$K^b$ (**Fig 5c**). The possible contribution of $CD8^+$ T cells restricted by other non-classical MHC I to the overall $CD8^+$ T cell response is presently unclear. Alternatively, some ligands may represent novel pMHC I conformations that are not recognized by conventional anti-MHC I antibodies. Together, these results show that loss of tapasin not only caused a profound loss of pMHC I, it also allowed generation of new and immunologically distinct pMHC I.

**Distinct ligands are used *in vivo* for rejection of tapasin or ERAAP-deficient cells.**

Identification of pMHC I losses and gains in tapasin-deficient cells echoes the unedited pMHC I repertoire found in ERAAP-deficient cells and suggests that the function of these two editors could be linked. For example, ERAAP's role in trimming peptides for MHC I molecules could be more effective if it interacted with the PLC, thus providing access to incoming peptides and empty MHC I. If such an interaction exists, then we hypothesized that some ERAAP-unedited peptides might also be presented by $Tpn^0$ cells.

To rigorously determine whether there is an immunological distinction between tapasin or ERAAP-dependent ligands, we assessed the ability of WT mice to eliminate $ERAAP^0$ or $Tpn^0$ target cells *in vivo* (**Fig 6**). We primed WT mice with splenocytes from $ERAAP^0$, $Tpn^0$ or WT mice as a negative control. Seven days later, the mice were challenged with a cell mixture containing an equal number of WT, $ERAAP^0$ and $Tpn^0$ spleen cells as targets (**Fig 6b**). We depleted NK cells in host mice prior to immunization and challenge to obviate the possible effect of these cells in targeting $Tpn^0$ or $ERAAP^0$ cells with lower MHC I expression (177) (182). To distinguish the three populations of donor cells recovered from host animals *in vivo,* each target cell population was labeled with a different fluorescent dye as shown schematically (**Fig 6a**). After 20 hours, spleens from host WT mice were analyzed for the presence of each labeled cell population (**Fig 6b, OUTPUT**). A decrease in the percentage of cells recovered relative to the WT (self) targets indicates elimination of individual populations by the immune system of WT hosts.

Mice primed with $ERAAP^0$ cells efficiently eliminated $ERAAP^0$ targets, but did not influence the recovery of tapasin-deficient or self-WT cells (**Fig 6c**). In contrast, WT mice primed with $Tpn^0$ splenocytes eliminated $Tpn^0$ targets but not $ERAAP^0$ or WT targets. Finally, there was no specific loss of any of these target cells in mice primed with self-WT cells. Furthermore, the requirement for prior immunization for the *in vivo* elimination of $ERAAP^0$ or $Tpn^0$ targets suggests that these responses are mediated by the adaptive immune system. The *in vitro* and *in vivo* assessment of WT anti-$Tpn^0$ and WT-anti $ERAAP^0$ T cell lines demonstrates that the unedited peptide repertoires in cells deficient in ERAAP versus tapasin were distinct without any detectable overlap.

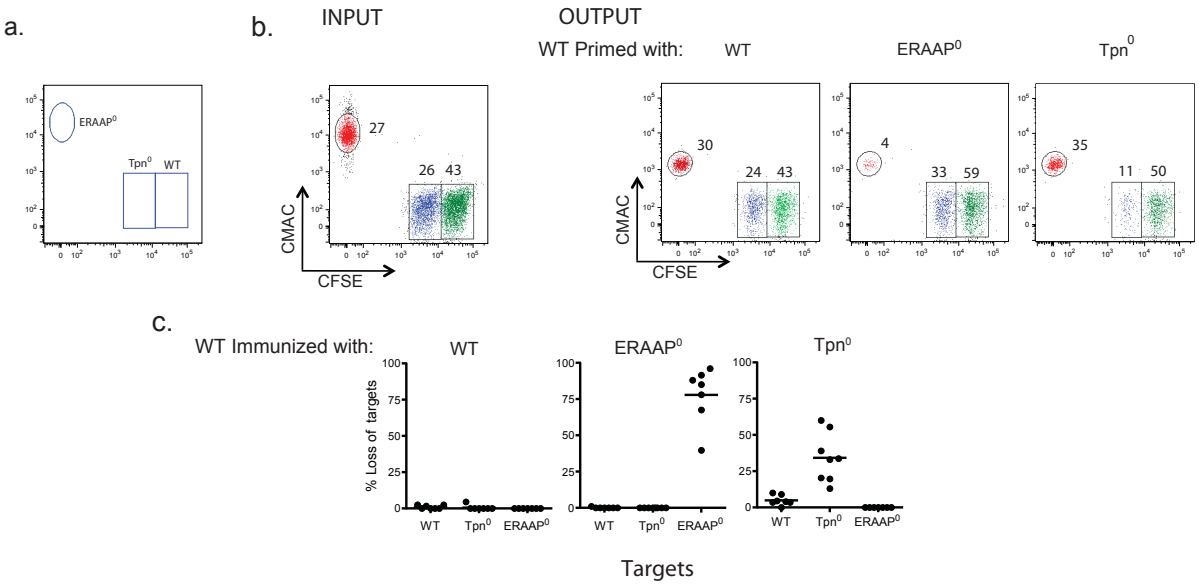


**Figure 6. Different ligands are used for rejection of tapasin- or ERAAP-deficient cells by WT mice *in vivo*.**

T cells from WT mice primed seven days earlier with male WT, Tpn$^0$ or ERAAP$^0$ splenocytes were assessed for their ability to specifically eliminate WT, Tpn$^0$ or ERAAP$^0$ female targets *in vivo*. Targets were given distinct labels so they could be compared in the same host mouse: WT = CFSE (high-dose; green ); Tpn$^0$ = CFSE (low-dose; blue); ERAAP$^0$ = CMAC (red). **(a)** Schematic indicating the populations which represent ERAAP$^0$, Tpn$^0$ and WT **(b)** Representative FACS plots of labeled targets before (input) and after (output) challenge. Input refers to proportion of each labeled cell type prior to challenge while output refers to the labeled populations identified 20 hours post-transfer **(c)** Summary of *in vivo* killing assay from b. Negative loss (gain) is plotted as zero. Data are representative of two independent experiments (b) or are pooled from two independent experiments (c).

**Discussion:**

The set of peptides presented by MHC I molecules in WT cells is incredibly diverse, such that a wide variety of self and foreign peptides are presented. However, there are certain key features, such as a length of 8-10 amino acids and the presence of conserved anchor residues, shared by almost all MHC I-bound peptides. Editing of the pMHC I by the PLC is crucial to ensure that only the most stable pMHC I reach the surface and are capable of triggering $CD8^+$ T cell responses. However, the mechanisms by which the PLC selects stable, high-affinity peptides for presentation on MHC I are not fully understood. Peptide editing by ERAAP is important for generating high-quality pMHC I (154). In its absence, many WT pMHC I are lost while new, unstable pMHC I are expressed. Using T cell lines specific for differences in pMHC I between $Tpn^0$ and WT, we determined that $Tpn^0$ cells have pMHC I losses and gains analogous to those seen in $ERAAP^0$ cells, suggesting that tapasin is also a key editor of pMHC I.

In this study, we also established that ERAAP and tapasin are distinct peptide editors required for generation of the optimal pMHC I repertoire. Given that the lack of pMHC I editing is reflected in the repertoire of self-peptides presented, we compared the pMHC I of $ERAAP^0$ with $Tpn^0$ to determine whether there were any similarities which would indicate overlapping editing functions. However, we found that the new pMHC I from $Tpn^0$ were immunologically distinct from $ERAAP^0$ peptides. WT T cells specific for either $ERAAP^0$ or $Tpn^0$ were highly specific and do not cross-react. Together, these results strongly indicate that loss of tapasin or ERAAP editing causes immunologically distinct changes to endogenous pMHC I that echo their role in peptide editing.

## Chapter 3: Mass Spectrometry of the Tapasin-deficient Peptide Repertoire

**Summary**:

MHC I molecules present a diverse set of peptides derived from endogenous proteins to CD8+ T cells to allow for surveillance of the intracellular state of the cell. The nature of antigenic peptides, including length and sequence requirements, was identified by sequencing peptides from several different mouse and human MHC I molecules using mass spectrometry (183). The peptide editing mechanisms that define these motifs are not yet entirely clear, however, peptide selection by tapasin and the PLC is likely be key in this process.

The use of mass spectrometry to identify peptides has been extended from characterization of the normal repertoire to the elucidation of the changes in pMHC I upon defects in the antigen processing pathway (51, 159). The cross-immunization experiments discussed in chapter 2 indicated that tapasin-deficient cells express new pMHC I not found on WT cells. In this chapter, I discuss the use of mass spectrometry to characterize the molecular nature of these differences and what they tell us about how tapasin shapes the pMHC I repertoire.

Mass spectrometry analysis of the tapasin-deficient peptide repertoire revealed several differences from WT peptides. First, there was an overall increase in peptide length and a decrease in binding affinity for $K^b$ and $D^b$ peptides eluted from tapasin-deficient cells. Strikingly, the changes were often found at the peptide C-terminus (PΩ). These findings highlight an important role for tapasin in ensuring that peptides containing compatible PΩ residue are presented.

**Results:**

### Tapasin-deficient cells present peptides lacking canonical consensus motif

To define the tapasin-dependent changes in the peptide repertoire, we isolated $K^b$ and $D^b$ pMHC I from WT as well as $Tpn^0$ splenocytes, eluted the bound peptides and determined their amino acid sequences by tandem mass spectrometry. From WT cells, we identified 210 and 163 peptides bound to $D^b$ and $K^b$ respectively. In contrast, the lower pMHC I expression in tapasin-deficient cells allowed recovery of fewer peptides; 63 and 22 peptides bound to $D^b$ and $K^b$ respectively. We did not find any obvious differences in the intracellular localization of the source proteins for these peptides (**Fig 9**). Many peptides in $Tpn^0$-deficient splenocytes were also found in WT mice (**Fig 7a; Fig 8a; Table 2-3**).

Remarkably, comparison of the unique peptides in $Tpn^0$ cells with their WT counterparts revealed significant differences. First, peptides in $Tpn^0$ cells were markedly longer than those in WT cells (**Fig 7b; Fig 8b**). Second, the canonical asparagine (N) residue at the p5 position of $D^b$ bound peptides was virtually absent

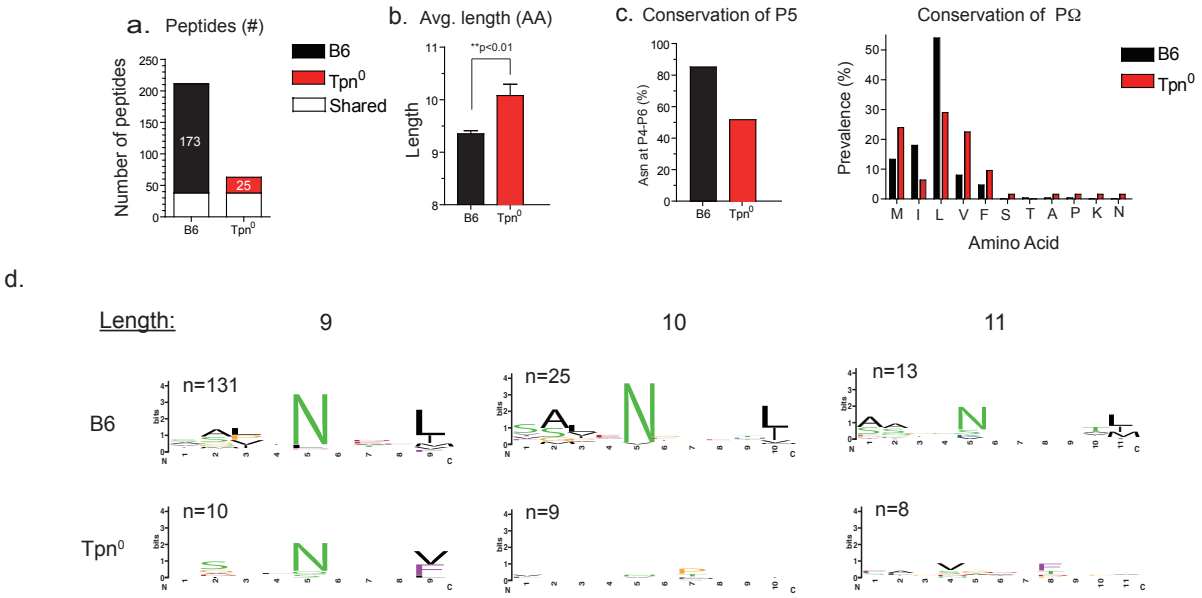


**Figure 7. $D^b$ MHC I in WT and tapasin-deficient cells present unique peptides.** The H-$2D^b$ MHC I were immunoprecipitated from WT and Tpn-deficient spleen cells. Eluted peptides were sequenced by mass spectrometry and manually validated. **(a)** Numbers of distinct or shared peptides found in pMHC I expressed by WT or Tpn-deficient cells. **(b-d)** Analysis of the unique peptides from WT and tapasin-deficient cells**.** (**b**) The average lengths of peptides recovered from WT or Tpn-deficient cells. The indicated p-value was calculated by two-tailed t-test. **(c)** Conservation of p5 and C-terminal anchor residues (PΩ). Plots represent frequency of Asn (N) at P4-6 or the frequency of indicated amino acids at PΩ of H-$2D^b$ peptides. **(d)** Logo representation of H-$2D^b$ peptides eluted from WT or Tpn-deficient cells. Peptides are grouped according to their lengths, and the numbers of peptides in each group is indicated. The height of each bar is proportional to the frequency of amino acid conservation and the height of each letter composing the column is proportional to its frequency at the given position. Amino acids are colored as follows: hydrophobic (black), aromatic (purple), acidic (red), basic (blue), neutral (green).

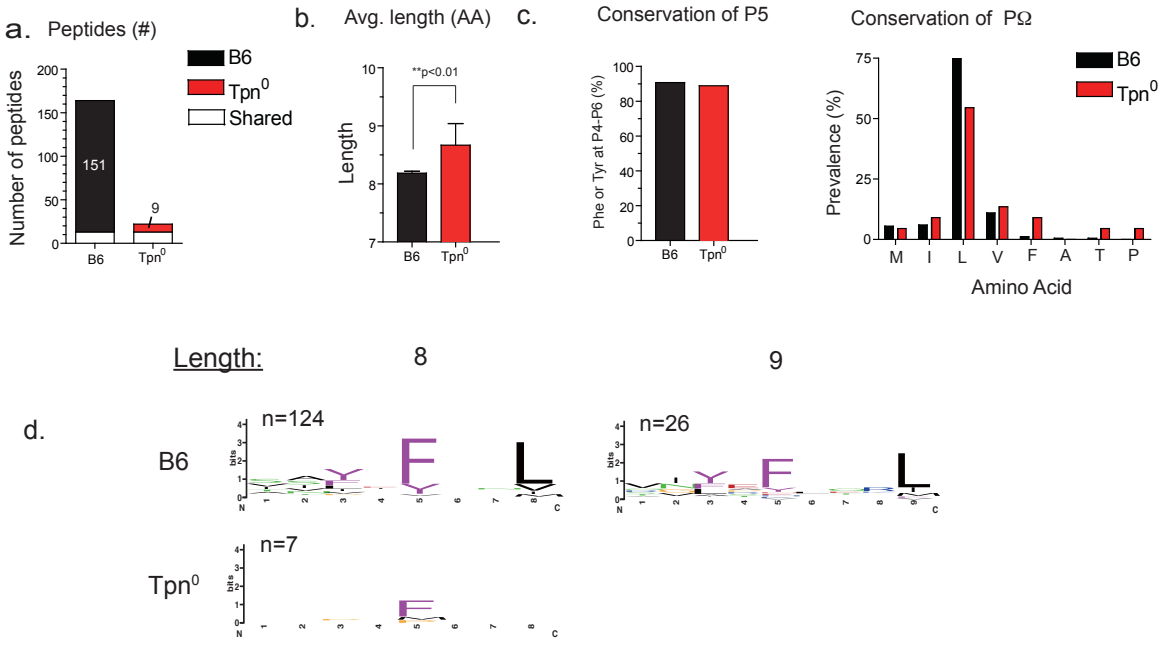


**Figure 8. $K^b$ MHC I in WT and tapasin-deficient cells present unique peptides.**
The H-2$K^b$ MHC I were immunoprecipitated from WT and Tpn-deficient spleen cells. Eluted peptides were sequenced by mass spectrometry and manually validated. (a) Numbers of distinct or shared peptides found in pMHC I expressed by WT or Tpn-deficient cells. (b-d) Analysis of the unique peptides from WT and tapasin-deficient cells. (b) The average lengths of peptides recovered from WT or Tpn-deficient cells. The indicated p-value was calculated by two-tailed t-test. (c) Conservation of p5 and C-terminal anchor residues (PΩ). Plots represent frequency of Phe or Tyr (F or Y) at P4-6 or the frequency of indicated amino acids at PΩ of H-2$K^b$ peptides. (d) Logo representation of H-2$K^b$ peptides eluted from WT or Tpn-deficient cells. Peptides are grouped according to their lengths, and the numbers of peptides in each group is indicated. The height of each bar is proportional to the frequency of amino acid conservation and the height of each letter composing the column is proportional to its frequency at the given position. Amino acids are colored as follows: hydrophobic (black), aromatic (purple), acidic (red), basic (blue), neutral (green)

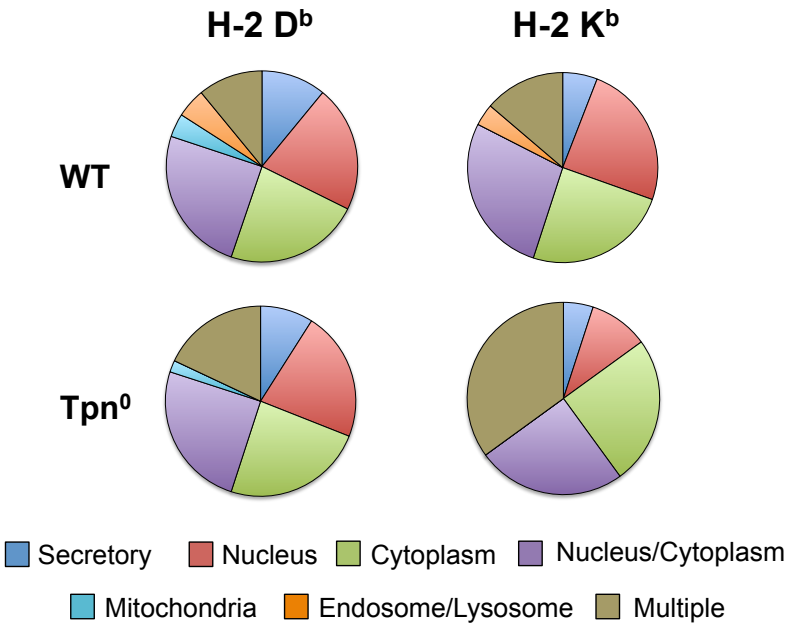


**Figure 9: Comparison of the source of Tpn$^0$ and WT peptides shows no significant differences.** Each slice of the pie chart represents the percentage of peptide source-proteins from a given cellular location as determined using GO terms. Both peptides shared between Tpn$^0$ and WT and unique peptides are included in each chart. Only peptides that were assigned a cellular location were included.

in peptides produced in absence of tapasin (**Fig 7c**). A loss of the conserved phenylalanine or tyrosine residues (F/Y) at the p5 anchor position was less obvious in peptides bound to $K^b$ (**Fig 8c**).

The most striking difference in the amino acid sequences was found in the C-terminal (PΩ) position of $K^b$ and $D^b$ peptides eluted from $Tpn^0$ samples. Typically, the C-terminal position is occupied by an aliphatic amino acid; Met (M), Ile (I), Leu (L) or Val (V), as seen in peptides found in WT cells (**Fig 7c; Fig 8c**). However, in the $Tpn^0$ samples, a higher frequency of abnormal amino acids was identified at PΩ. These included Lysine (K), Ser (S), Asn (N), Pro (P) and Ala (A) for $D^b$ (**Fig 7c**) and Thr (T) and Pro (P) for $K^b$ (**Fig 8c**). In contrast, the ability to choose the appropriate C-terminal amino acid - a key determinant of pMHC I stability - was lost in the absence of tapasin. These changes are easily visualized using Weblogo software **(Fig 7d; Fig 8d)**. The size of each letter is proportional to the frequency with which it is found at a particular position. While WT peptides contain the consensus P5 and PΩ residues, $Tpn^0$ peptides are missing these residues, particularly at the C-terminus. Thus, in contrast to the striking influence of ERAAP on the N-termini, tapasin primarily influenced the C-termini peptides presented by MHC I.

**Peptides unique to tapasin-deficient cells form less stable pMHC I**

The MHC I binding characteristics of a few representative peptides (**Table 4; Fig 10**) were verified by assessing their ability to stabilize $D^b$ or $K^b$ on the surface of TAP-deficient RMA/s cells. The set of peptides chosen included those with and without canonical lengths and anchor residues. Peptides at various concentrations were incubated with the TAP-deficient cell line RMA/s which had been left at room temperature overnight to enable surface expression of empty MHC I molecules. Peptides that can bind exogenously stabilize the MHC I molecules on the surface, allowing for detection by flow cytometry, while peptides that are unable to bind do not. Each peptide tested bound to its respective MHC I, although the binding was lower than the canonical $K^b$ (LYL8) and $D^b$ (WI9) binding peptides (**Fig 10**). Interestingly, even the peptides that contained both anchor residues, such as FSPLNPVRV ($D^b$) and SLNRFIPL ($K^b$), were suboptimal binders of MHC I. To examine this in a different way, the duration by which the peptides were able to stabilize MHC I on the surface was analyzed. Similar to the stability assay, the decay was faster for the $Tpn^0$ peptides than for the control LYL8 and WI9 peptides.

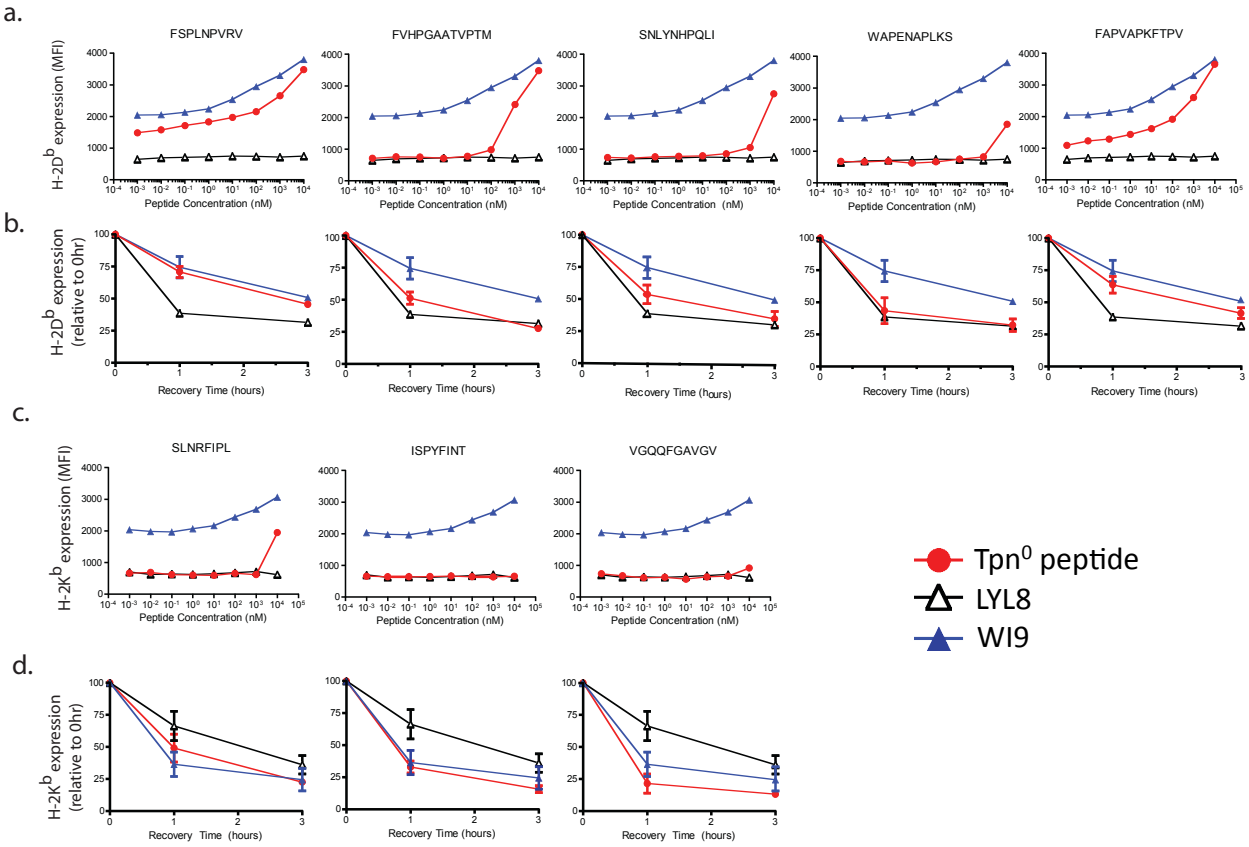


**Figure 10. Peptides from tapasin-deficient cells form less stable pMHC I on the surface and decay faster.**

(a). Stabilization of H-2D$^b$ MHC I with Tpn$^0$ peptides. RMA/s cells, incubated overnight to stabilize empty pMHC I on the surface, were incubated with indicated Tpn$^0$ peptides (top of each graph) or control LTFNYRNL (LYL8, K$^b$-binding) or WMHHNMDLI (WI9, D$^b$-binding) peptides for 1 hour at 22°C followed by incubation at 37°C for 3 hours prior to analysis by flow cytometry. (b) Decay of H-2D$^b$ surface expression. RMA/s cells were pulsed with 20μM peptide prior to treatment with brefeldin A (BfA). Recovery time represents time at 37°C after Bfa treatment and prior to staining for H-2D$^b$. MFI for each sample is normalized to 0hr recovery time. (c) Stability of K$^b$ peptides performed as in (a). (d) Decay of K$^b$ peptides as in (b). Data are representative of three independent experiments (a and c) or contain pooled data from at least three independent experiments (b and d).

## Discussion

Mass spectrometry analysis of ERAAP$^0$ and Tpn$^0$ peptides provided a molecular explanation for the immunogenic differences seen in their unedited pMHC I repertoires. In the absence of tapasin, the most distinct changes were found at the C-terminus where non-canonical amino acids at PΩ were much more frequent than in WT. In contrast, K$^b$ and D$^b$ peptides from ERAAP$^0$ mice contained additional amino acids either at the N-terminus or between the two anchor residues, but never at the C-terminus which always contained a canonical residue. Thus, even without ERAAP, tapasin edits all peptides and ultimately ensures they contain the correct C-terminal amino acid.

Previous studies have shown that enzymes such as the proteasome are important for generating peptides with a canonical C-terminal residue. However, this data suggests that tapasin is the editor that ultimately ensures that these peptides with the correct C-terminal residue are presented. Consistent with a role for tapasin-mediated editing at the C-terminus, the region of tapasin:MHC I interaction is believed to be the alpha-2 helix where the peptide C-terminus binds (141). While the direct mechanism by which tapasin edits peptides remains unclear, putative models for peptide optimization
via tapasin include accelerated dissociation of unfavorable peptides (184)or maintenance of the MHC I in an peptide-receptive conformation until binding of a high-affinity peptide (142). Further studies are required to better define the mechanism of tapasin action.

These results indicate that the effects of tapasin-deficiency are not equal across all MHC I alleles, even when they have similar surface expression. Although both K$^b$ and D$^b$ are only expressed at about 10% of WT levels, we identified further differences. Many more peptides were recovered from D$^b$ by mass spectrometry and several of them lacked the canonical P5 anchor. The same was not true for K$^b$. K$^b$ pMHC I appear to be highly unstable in the absence of tapasin, which may account for the decreased number of sequences recovered, as unstable pMHC I are likely to dissociate during the affinity purification step of the mass spectrometry. Previous studies involving several human HLA molecules concluded that there is a range of tapasin-dependence based on the amount of pMHC I downregulation in Tpn$^0$ cells. Our findings suggest that a more comprehensive analysis is required to detect the subtle pMHC I changes caused by the loss of PLC editing.

## Chapter 4: H-2$^d$ ERAAP KO cells present altered pMHC I on K$^d$, D$^d$ and L$^d$


### Summary

In addition to the presence of certain amino acids, MHC I molecules have a strong preference for peptides with a length of between 8 and 10 amino acids. This length allows the peptide to fit into the peptide binding groove. However, longer versions of many antigenic peptides are transported into the ER by TAP, necessitating further trimming of these precursors to generate final peptides of appropriate length. To date, the aminopeptidase ERAAP is the only ER-resident enzyme identified to carry out this function.

Recent genome-wide association studies have found significant association with polymorphisms in human ERAAP, ERAP1, with the presence of particular MHC I molecules and disease. Most notable is the link between ERAP1 polymorphisms, HLA-B27 and the autoimmune disease ankylosing spondylitis. These associations suggest that altered antigen processing by ERAAP may contribute to this disease and underscores the need for further study into the mechanisms by which ERAAP edits the pMHC I repertoire. In particular, it is key to understanding the allele-specific effects of ERAAP-deficiency.

Mice have three MHC I molecules: K, D and L. In the H-2$^d$ background they all bind peptides via an anchor residue at position 2 (P2) but they differ in terms of amino acid preference. The goal of these studies was to understand how loss of ERAAP editing affected peptide presentation by these three MHC I molecules.

Our examination of the effects of ERAAP-deficiency on surface expression confirmed previous findings: expression of all three MHC I is decreased and L$^d$ is the most affected (144, 153). Reciprocal-immunization experiments with H-2$^d$ ERAAP KO and WT cells indicated a qualitative loss of some WT pMHC I from ERAAP-deficient cells, primarily L$^d$, and a qualitative gain of a new, unedited set of pMHC I presented by all three MHC I. Together, these findings suggest that the effects of ERAAP-deficiency are not limited to loss of surface expression but also alter the peptide repertoire.


### ERAAP-deficiency affects pMHC I expression on professional APCs

Loss of ERAAP for antigen processing results in diminished surface presentation of murine pMHC I (153), suggesting that ERAAP is required for optimal expression. To examine in detail whether these decreases are consistent for H-2$^d$ pMHC I on all professional antigen presenting cell (APC) types, splenocytes isolated from B10.D2 ERAAP-deficient (ERAAP KO) or B10.D2 (WT) mice were co-stained with cell-type specific and MHC I antibodies and analyzed by flow cytometry. Consistent with previous results, L$^d$ expression is decreased by about 50% on spleen cells without cell-type specific staining (**Fig 11a**), while changes in K$^d$ and D$^d$ expression were less striking, with 20-30% decreases (**Fig 11a-b).** However, when distinct cell populations were differentiated based on surface markers, MHC I specific differences were observed. For all cell types examined, L$^d$ expression was similarly and profoundly decreased (**Fig 11a)**. In contrast, D$^d$ and K$^d$ expression were less affected in dendritic cells than in B cells and macrophages (**Fig 11b**). Together, these results suggest that in some cell types, such as dendritic cells, K$^d$ and D$^d$ are better able to compensate for loss of ERAAP whereas L$^d$ expression is dependent on ERAAP in all cell types. This finding identifies cell-type specific, in addition to MHC I specific, effects of ERAAP-deficiency.

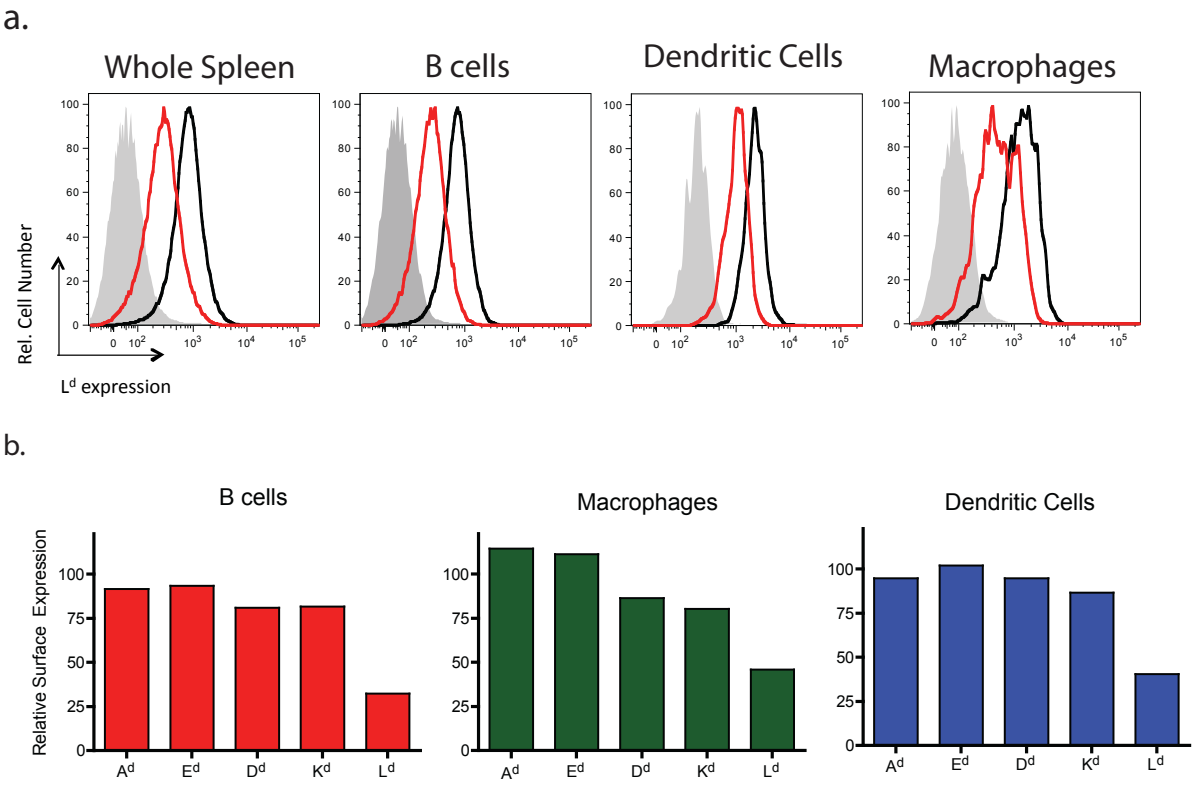


**Figure 11. H-2$^d$ pMHC I are differentially affected by ERAAP-deficiency.** Spleen cells isolated from either WT or **(a-c)** Surface expression on spleen cells derived from H-2$^d$ WT or ERAAP-deficient (ERAAP KO) mice. (a) Representative surface staining of L$^d$ on all splenocytes (whole spleen), dendritic cells (B220-CD11b+CD11c+), macrophages (B220-CD11b+F4/80+) or B cells (B220+). (b) Bar graphs summarize the mean fluorescence intensity (MFI) of ERAAP KO samples relative to WT samples for all H-2$^d$ MHC I. Data are representative of 3 or more experiments.

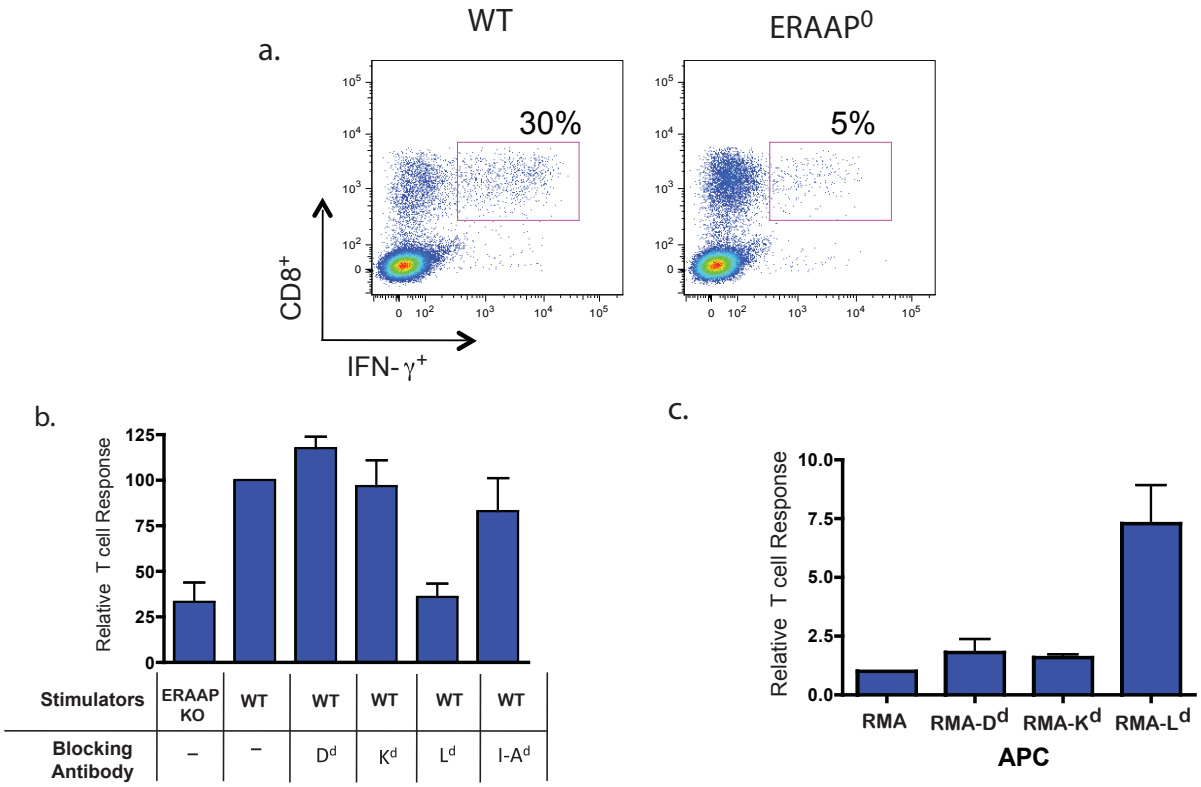


**Figure 12. ERAAP-KO T cells respond to pMHC I expressed by WT cells**. (a) IFN-γ$^+$ response of EkoF CD8$^+$ T cell lines against WT or ERAAP-deficient (ERAAP KO) APCs. Numbers indicate percent IFN-γ$^+$ positive cells of total CD8$^+$ T cells. **(b)** EkoF CD8$^+$ T cell responses against ERAAP KO or WT APCs in the presence of indicated MHC I blocking antibodies. Responses are normalized to WT. (c) EkoF responses against RMA APCs stably expressing indicated MHC I molecules. Responses are normalized to RMA.

**ERAAP KO cells are missing WT pMHC I:**

The surface pMHC I decreases for $K^d$, $D^d$ and $L^d$ may reflect a general quantitative loss of pMHC I complexes or may represent a qualitative loss of certain pMHC I. To distinguish between these two possibilities, we utilized the ability of CD8+ T cells to identify and respond to pMHC I repertoire differences (**Fig 12**). We reasoned that if some WT pMHC I were not expressed in ERAAP-deficient cells, then ERAAP KO T cells would not be tolerant to them and would recognize them as non-self. To test this, we generated ERAAP KO anti-WT, or 'EkoF', T cell lines, by immunizing female ERAAP-deficient mice with male WT splenocytes, as done with the $Tpn^0$ anti-WT T cell lines. These lines were assessed for their ability to respond to either ERAAP-KO (self) or WT (non-self) APCs through measurement of production of the effector cytokine IFN-γ. The EkoF T cells responded robustly to WT APCs, which caused 30% of the T cells to produce IFN-γ whereas only 5% of the EkoF T cells responded to self APCs (**Fig 12a)**. Therefore, we conclude that ERAAP-deficient cells are missing a set of pMHC I that are expressed in WT cells.

**ERAAP KO T cells are not tolerant to WT $L^d$ pMHC I.**

Based on the drastic changes in surface expression, $L^d$ is the most inhibited by ERAAP-deficiency. We hypothesized that this sharp decrease may reflect a qualitative loss of a number of pMHC I complexes, which would be manifested by the lack of tolerance of EkoF T cells for these $L^d$ pMHC I.

To determine the MHC I restriction of the EkoF T cells, two approaches were used. First, APCs were incubated with purified anti-MHC I antibodies shown to be capable of blocking TCR:MHC I interactions. T cell lines were tested for IFN-γ production in the presence of one of these blocking antibodies. Consistently, addition of the $L^d$ antibody diminished IFN-γ production, while the $K^d$ and $D^d$ blocking antibodies did not affect the response (**Fig 12b)**, suggesting that the EkoF T cells are indeed responding to ligands presented by $L^d$.

To test the restriction in a different and independent assay, EkoF T cells were examined for their ability to respond to RMA cells stably expressing only $K^d$, $D^d$ or $L^d$ (**Fig 12c**). Again, the EkoF T cells responded most dramatically to $L^d$ rather than $K^d$ or $D^d$. Therefore, ERAAP KO anti-WT responses are primarily directed against $L^d$ pMHC I.

**H-$2^d$ ERAAP KO cells present novel peptides.**

Finding a qualitative loss of pMHC I in H-$2^d$ ERAAP-deficient cells led us to ask whether there was also a qualitative gain of a novel, unedited set of pMHC I. In B6 mice, ERAAP limits presentation of certain pMHC I and enhances presentation of others, including some which are normally not presented (154). To determine whether ERAAP has a similar editing role for H-$2^d$ MHC I, we tested whether ERAAP-deficient cells presented an altered pMHC I repertoire that was immunogenic to

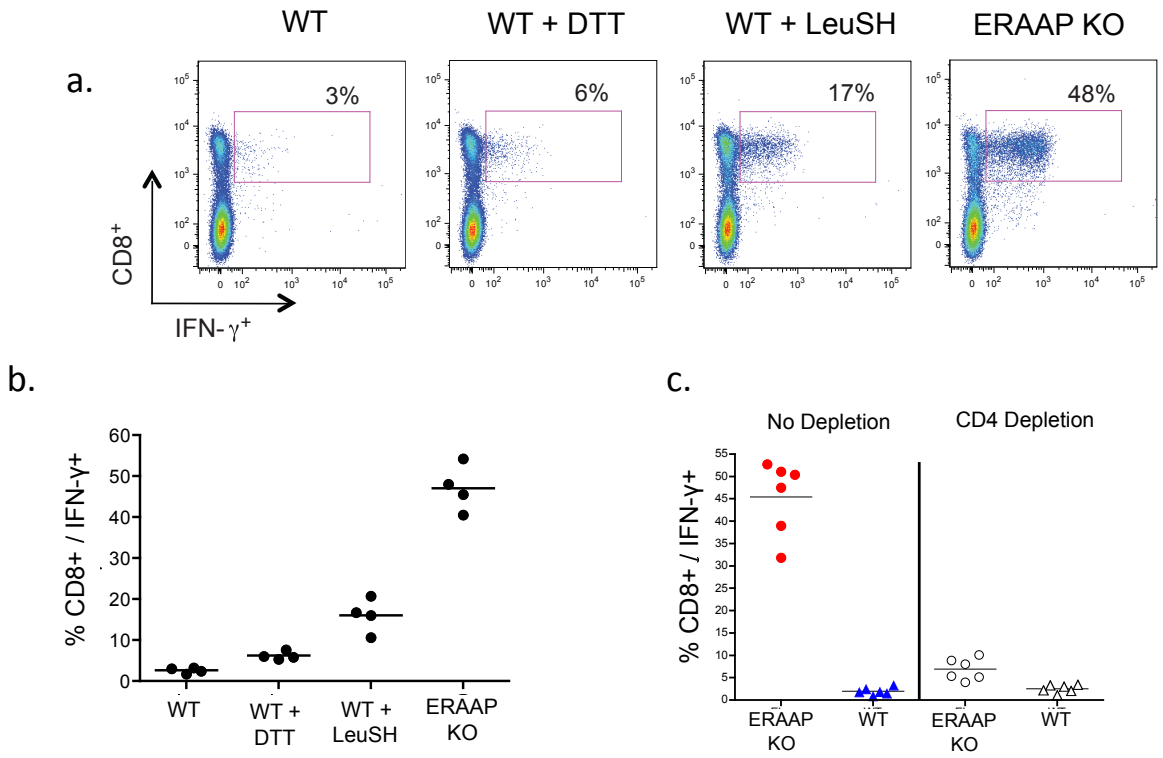


**Figure 13. WT cells respond to novel pMHC I expressed by ERAAP-deficient cells**. (a) Representative plot of FEko CD8$^+$ T cell line response against either untreated ERAAP-deficient (ERAAP KO) APCs, untreated WT APCs or WT APCs treated DTT and aminopeptidase inhibitor Leucinethiol (LeuSH). Numbers indicate percent IFN-γ$^+$ positive cells of total CD8$^+$ T cells. (b) Summary of FEko T cell responses from (a). Each dot represents an individual T cell line. (c) Generation of FEko T cells requires CD4 help. FEko T cell lines generated from mice with CD4 T cells (closed symbols) or depleted for CD4 T cells(open symbols) were assessed for responses against ERAAP KO or WT APCs.

WT T cells. As CD4 T cell help is important for optimal CD8 T cell responses, we chose to utilize $F_1$ cross of B6 and B10.D2 as our WT host mice. Alone, H-$2^d$ mice lack endogenous H-Y antigens which are important for generating CD4 help (185), however, these can be supplied by the H-$2^b$ MHC I in our F1 mice to enhance the quality of the CD8 response, as was done previously on the B6 background (154). All subsequent stimulations were done using H-$2^d$ ERAAP KO cells to direct the CTL response toward antigens presented by $D^d$, $K^d$ or $L^d$.

To determine whether ERAAP KO cells present unedited pMHC I, FEko T cells were analyzed for their ability to produce IFN-γ in response to B10.D2 WT or ERAAP KO APCs. Robust FEko T cell responses were directed against ERAAP-deficient (48%) but not WT (3%) APCs (**Fig 13a-b**).

The mice used in these experiments are a F1 cross and therefore have several minor histocompatability differences. To confirm that the FEko T cell responses are due to loss of ERAAP function rather than these genetic differences, WT spleen cells treated with the chemical aminopeptidase inhibitor Leucinethiol (LeuSH) were used as APCs in the IFN-γ assay. FEko T cells made robust responses against LeuSH-treated APCs (17%), although they were not as stimulatory as the ERAAP KO APCs (**Fig 13a-b**). Therefore, ERAAP-deficiency results in presentation of a novel, immunogenic pMHC I repertoire.

The importance of CD4 T cells for the FEko responses was confirmed by depleting CD4 T cells from F1 mice prior to immunization, which resulted in a diminished FEko T cell response (**Fig 13c**).

**All MHC I present unedited peptides in ERAAP-deficient mice**

To assess whether each MHC I molecule contributes equally to the FEko T cell response, or whether only certain MHC I molecules present the immunogenic peptides, a blocking antibody approach was utilized as above. ERAAP KO APCs were incubated with individual blocking antibodies that inhibited recognition of MHC I prior to addition of the FEko T cells. The T cells were then assessed for production of the effector cytokine IFN-γ. Adding the $K^d$ blocking antibody led to the greatest decrease in IFN-γ production, indicating that a majority of the T cells respond to unedited peptides presented by $K^d$ (**Fig 14a**). The $L^d$-blocking antibody led to partial inhibition of the response as well. In contrast, the $D^d$-blocking antibody did not prevent IFN-γ production, and actually enhanced it, suggesting that FEko T cells either do not respond to $D^d$ peptides or that the $D^d$ pMHC I are structurally distinct and thus are not blocked by the conformation-dependent blocking antibody.

As an alternative approach that is independent of the blocking antibodies, RMA cells expressing $K^d$, $D^d$ or $L^d$ were treated with Leucinethiol and used as APCs for FEko T cells. T cells responded to all three RMA cell types, although to different extents. RMA-$K^d$ cells elicited the highest response (**Fig 14b**), suggesting that a majority of FEko T cells are specific for altered peptides presented by $K^d$, which is consistent with the results of the blocking antibodies. RMA-$L^d$ and RMA-$D^d$ cells also stimulated T cell responses, but to a lower degree than RMA-$K^d$ cells. Together, these findings indicate that all MHC I molecules present unedited peptides upon ERAAP-deficiency, but that some pMHC I are more immunogenic than others.

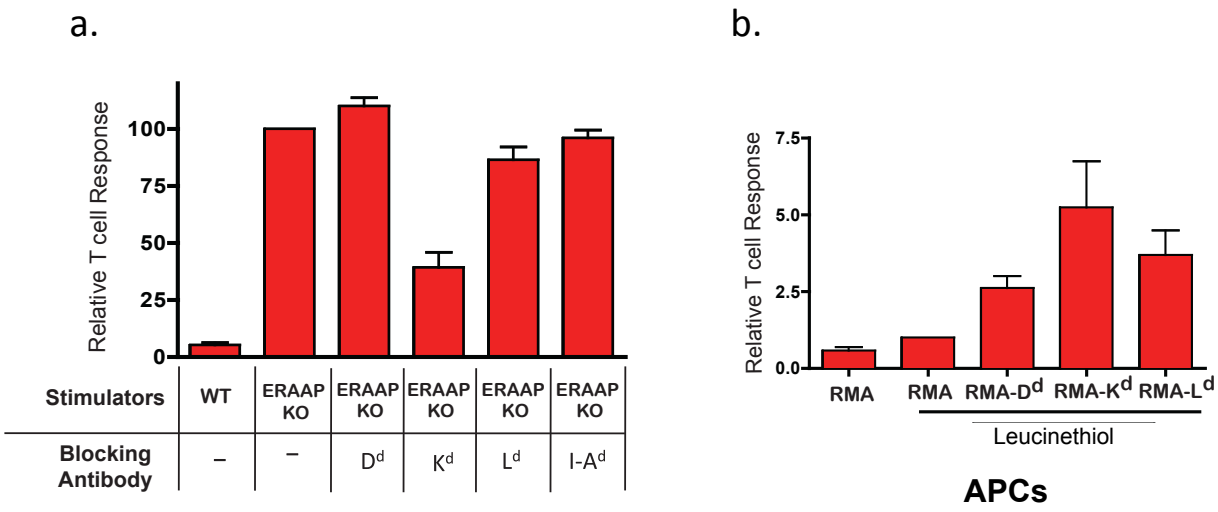


**Figure 14. WT T cells respond to novel pMHC I presented by Kd, Dd Ld**. (a) FEko CD8$^+$ T cell responses against ERAAP KO or WT APCs in the presence of indicated MHC I blocking antibodies. Responses are normalized to ERAAP KO (b) FEko CD8+ T cell responses against RMA APCs stably expressing indicated MHC I molecules. As indicated, cells were treated overnight with Leucinethiol to inhibit ERAAP prior to incubation with FEko T cells. Responses are normalized to RMA treated with Leucinethiol.

**Discussion:**

Overall, these findings indicate that loss of ERAAP has allele-specific effects. $L^d$ is highly downregulated on all ERAAP-deficient cells. Because many WT pMHC I are not expressed, and are therefore not available during selection, T cells from ERAAP-deficient mice are primarily restricted to these missing $L^d$ pMHC I. In contrast, WT T cell lines respond to novel, unedited pMHC I presented by all three MHC I in H-$2^d$ ERAAP-deficient cells. However, not all MHC I molecules are equally immunogenic, as a higher percentage of T cells recognize unedited peptides presented by $K^d$ than $D^d$ or $L^d$. Based on surface expression, $K^d$ and $D^d$ are downregulated to a similar extent, this suggests that further allele-specific differences in the types and immunogenicity of peptides presented exist.

Interestingly, although loss of ERAAP results in presentation of new pMHC I in the RMA-$D^d$ cells, unedited peptides presented by $D^d$ were not detectable with the antibody blocking experiments. The same $D^d$ blocking antibodies were capable of efficiently inhibiting T cell hybridoma AI9Z recognition of its $D^d$/AI9 epitope (**Fig. 25**), ruling out a problem with the reagents. Furthermore, the same result was seen with an additional anti-$D^d$ clone, 34-2-12 (data not shown). One intriguing explanation is that the immunogenic peptides presented by $D^d$ are structurally distinct, possibly due to N-terminal extensions, and therefore lack the epitope required for the antibody to bind.

$K^d$ and $L^d$-restricted T cells were blocked by their corresponding antibodies, which may indicate that similar altered pMHC I conformations are not found, or are not immunogenic, in these cells upon ERAAP-deficiency. This finding would further suggest that loss of ERAAP has distinct effects on different MHC I alleles.

In B6 mice, the anti-ERAAP KO response is almost exclusively restricted to a non-classical MHC Ib molecule, Qa-1, presenting the ligand FL9 (155). In contrast, FEko T cells respond to all three classical MHC I molecules, suggesting that ERAAP-deficiency on the H-$2^d$ background causes wide-ranging changes to the pMHC I repertoire. Subsequent chapters will discuss the molecular nature of these unedited pMHC I.

## Chapter 5: Characterization of the ERAAP KO pMHC I repertoire by mass spectrometry

**Summary**:

ERAAP-deficiency leads to immunogenic changes to the pMHC I repertoire that differ for each MHC I molecule. Using mass spectrometry to sequence and compare peptides from ERAAP-deficient and WT MHC I molecules, we sought to understand the molecular basis for these differences. These experiments were done in collaboration with the Delgado Lab at the University of Utah. $K^d$, $D^d$ and $L^d$ pMHC I complexes were isolated from primary spleen cell lysates using affinity purification. Peptides were eluted from the MHC I molecules and sequenced by tandem mass spectrometry. Recovered sequences were manually validated and pooled into three groups for each MHC I: those unique to WT, those unique to ERAAP-deficiency and those peptides shared by both WT and ERAAP-deficient samples. The findings revealed distinct sets of peptides, some with N-terminal extensions, bound to $K^d$ and $D^d$. These may reflect direct endogenous ERAAP substrates. Very few peptides eluted from $L^d$ and in both WT and ERAAP-deficient samples, and these maintained the consensus length and motif. Together, these results suggest that ERAAP-deficiency affects the peptides bound to each MHC I molecule differently.

### $L^d$-bound peptides have canonical length and consensus motifs in ERAAP-deficient cells:

The severe decrease in surface expression of $L^d$ indicates that it requires ERAAP for optimal presentation. The $L^d$ motif is distinguished by a proline at the P2 position and an aliphatic amino acid at the C-terminus, PΩ. Similar consensus motifs are found for several human MHC I molecules(186). To determine the nature of the ERAAP-deficient Ld pMHC I, the 28-14-8 antibody clone was used to affinity purify pMHC I complexes and peptides were sequenced by tandem mass spectrometry.

Consistent with the diminished $L^d$ surface expression (**Fig 11; Table 5**) very few peptides were recovered from ERAAP-deficient $L^d$ samples relative to WT. From WT samples, 81 peptides were found that were unique to WT and an additional 54 peptides were found in both the ERAAP KO and WT sets (**Fig. 15a**). However, only 18 peptides unique to ERAAP-deficient $L^d$ were found. This decreased recovery is likely due in part to the high degree of instability found in $L^d$ complexes (153).

Closer comparison of the composition of the peptides unique to WT and ERAAP KO yielded surprising results. First, peptides recovered from both sets did not contain N-terminal extensions and instead strongly conformed to the typical peptide length of 8-10 amino acids (**Fig. 15 b-c**). Furthermore, a majority (78%) of the peptides unique to ERAAP KO contained a proline at P2 (**Fig 15d)**, although it is slightly lower than the percentage found in WT (91% ) or shared (95% )sample sets. The strong conservation of the proline at this position can be seen when peptides are analyzed using the Weblogo Program **(Fig 16).** As TAP is thought to be limited in its ability to transport peptides with a proline at this position (187) and ERAAP is believed to be the only aminopeptidase in the ER(144), the mechanism by which these peptides encounter $L^d$ is unclear.

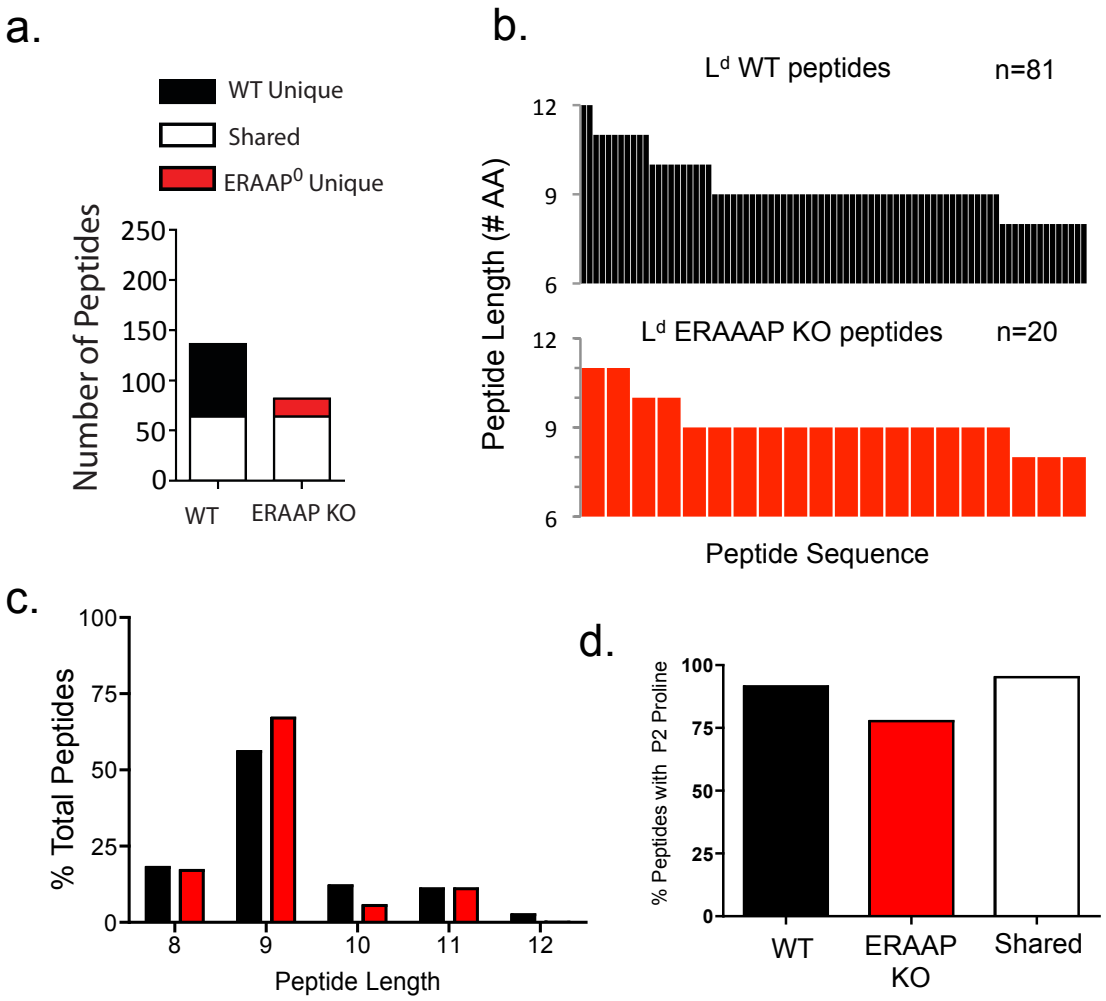


**Figure 15. $L^d$-bound peptides have canonical length in ERAAP-deficient cells.** (a-d). Analysis of H-2$L^d$ peptides from WT and ERAAP-deficient (ERAAP KO) spleen cells identified by tandem mass spectrometry. WT-unique peptides (black); ERAAP KO unique (red) and shared (white) (a) Numbers of distinct or shared peptides recovered from WT or ERAAP KO cells. (b) Analysis of the non-overlapping peptides from WT and ERAAP KO cells represented as single vertical bars and plotted according to amino acid length. (c) Lengths of recovered non-overlapping peptides represented as percentage of the total peptides. (d) Percentage of peptides of total from indicated set that have a proline at P2.

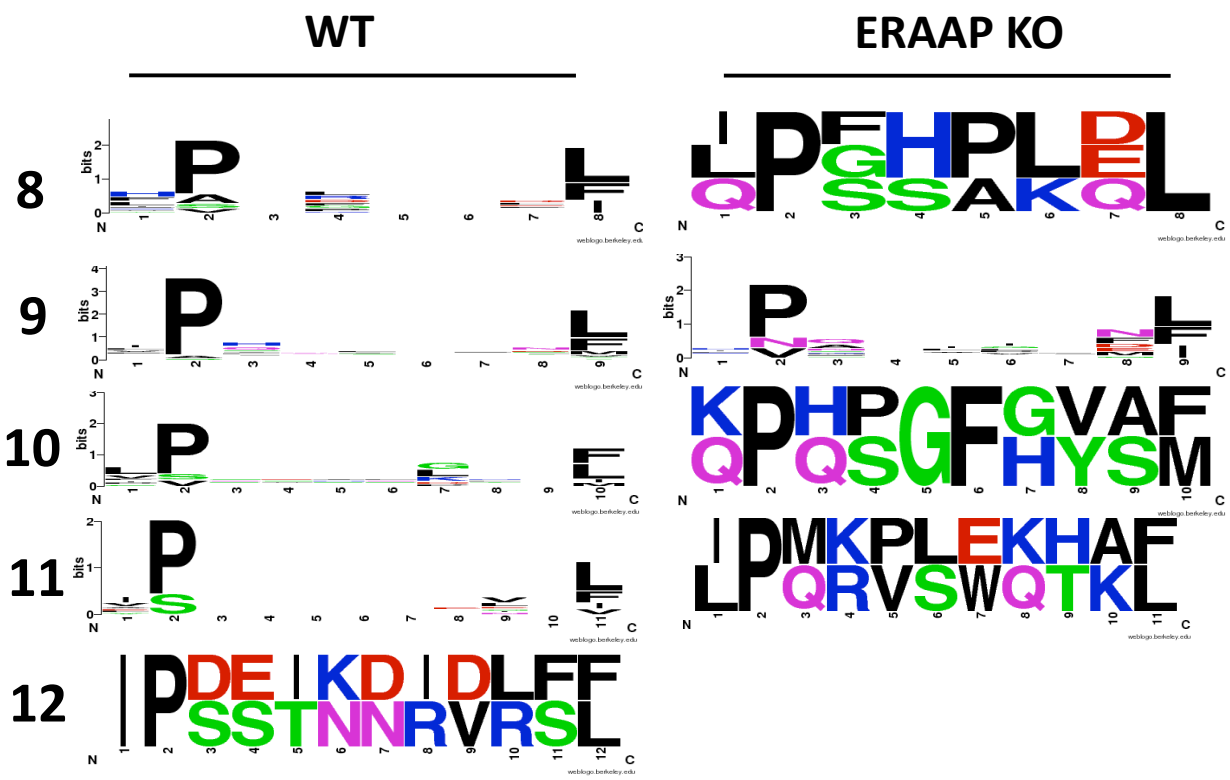


**Figure 16. $L^d$ peptides from ERAAP KO and WT maintain the canonical consensus motif**. Logo representation of H-2$L^d$ peptides eluted from WT or ERAAP-deficient cells. Peptides are grouped according to their lengths (left). The height of each bar is proportional to the frequency of amino acid conservation and the height of each letter composing the column is proportional to its frequency at the given position. Amino acids are colored as follows: hydrophobic (black), aromatic (purple), acidic (red), basic (blue), neutral (green).

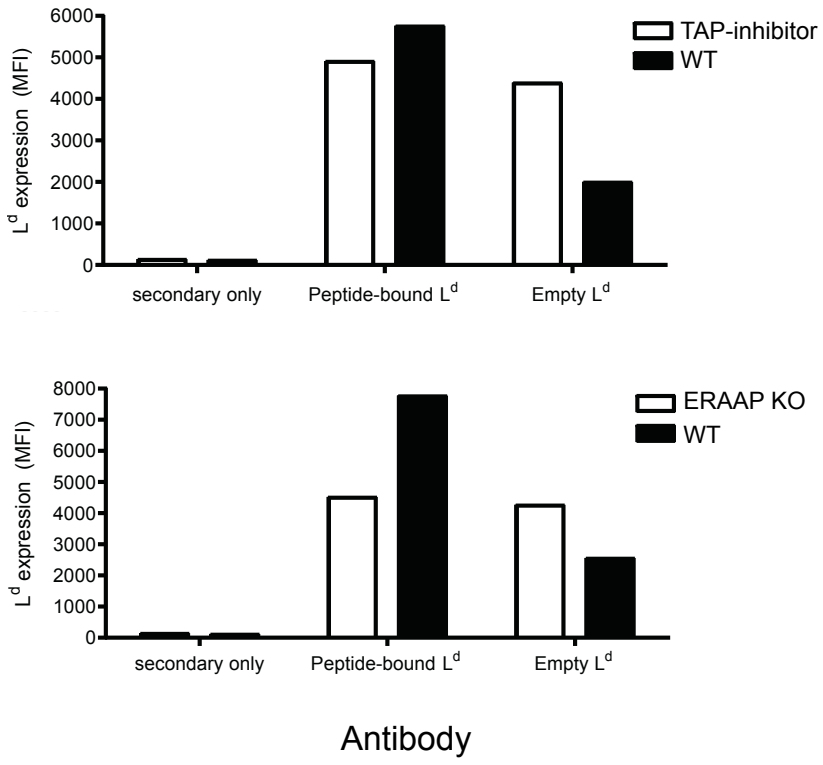


**Figure 17. Intracellular $L^d$ is empty in ERAAP-deficient cells.** Comparison of the relative amounts of peptide-bound $L^d$ versus empty $L^d$ in indicated cell lines. Cells were stained intracellularly with conformation-dependent antibodies prior to analysis by flow cytometry. 30-5-7 antibody detects folded $L^d$ with bound peptide and 64-3-7 antibody detects empty $L^d$. (a) WT J774 cells or J774 cells stably expressing the UL49.5 TAP inhibitor. GFP marker was used to identify positive cells. (b) BMDCs from B10.D2 ERAAP KO or WT mice.

**$L^d$ MHC I are empty in ERAAP-deficient cells**

To further explore the state of $L^d$ in ERAAP-deficient cells, Margret Veltman, a UC Berkeley undergraduate under my supervision, performed intracellular staining on cells using conformation-dependent $L^d$ antibodies. As a control, J774 cells were transfected with the TAP-inhibitor UL49.5 in a plasmid with a GFP marker. Thus, GFP-positive cells express UL49.5 while GFP-negative cells do not. These cells were stained intracellularly using 30-5-7 antibody, which is specific for peptide-bound $L^d$, or 64-3-7 antibody, which recognizes unfolded, 'empty' $L^d$. As expected, TAP-inhibited cells contained less peptide-associated $L^d$ and more empty $L^d$ relative to WT cells (**Fig 17a)**. When BMDCs from ERAAP-deficient or WT cells were stained with these antibodies, the same phenotype is observed, indicating that $L^d$ tends to remain unassociated with peptide in ERAAP KO cells (**Fig 17b**). It will be interesting to determine whether expression of the $L^d$ peptides identified by mass spectrometry into ERAAP-deficient cells would rescue this phenotype.

**ERAAP-deficient peptides from $K^d$ are longer and bind with distinct conformations.**

Unlike $L^d$, surface expression of $K^d$ is only moderately affected by ERAAP-deficiency. However, FEko T cells were primarily restricted to ERAAP KO peptides presented by $K^d$, suggesting that $K^d$ presents an alternative pMHC I repertoire. To determine the nature of these alterations, $K^d$ pMHC I were affinity purified using the SF1-1.1.1 antibody and sequenced by tandem mass spectrometry.

Similar numbers of $K^d$-bound peptides were recovered from ERAAP KO (101) and WT samples (98), as well as from the shared set (114) (**Fig 18a; Table 7**). The comparable recovery is consistent with the more moderate surface pMHC I decreases found for $K^d$ (**fig 11**). When the lengths of the peptides were more closely examined, a majority of the peptides from both sets unique to WT and to ERAAP KO were between 8-10 amino acids (**Fig 18b-c).** Strikingly, there were also several long peptides that were recovered only from ERAAP KO. These extended peptides ranged in length from 11-16 amino acids (**Fig 18b-c**).

In addition to length, we also examined changes in the composition of the peptides. As is readily seen from the weblogo analysis (**Fig 20a**), peptides of canonical length overwhelmingly contained the $K^d$ consensus motif. Long peptides from ERAAP KO also contained a tyrosine or phenylalanine, but not always at P2. They were grouped into two catagories: those expected to bind with a 'central bulge' phenotype, meaning that the anchor remained at P2 and the additional length comes from residues between the two anchor positions or those with N-terminal extensions, in which the residue expected to be used as the P2 anchor is in the middle of the peptide and the additional residues are at the N-terminus (**Fig 21a**). No significant changes were observed at the C-terminus.

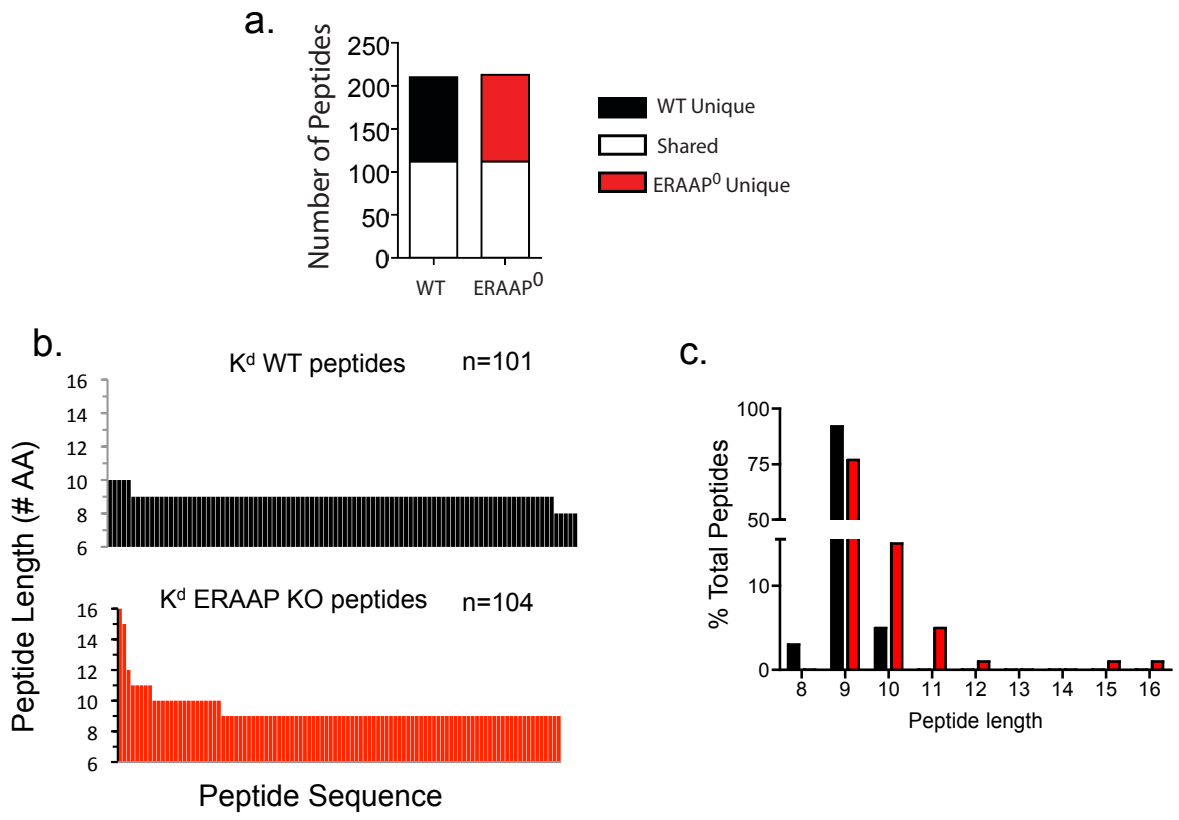


**Figure 18. Unique ERAAP KO peptides presented by $K^d$ longer than WT $K^d$ peptides.** (a-c). Analysis of H-2$K^d$ peptides from WT and ERAAP-deficient (ERAAP KO) spleen cells identified by tandem mass spectrometry. WT-unique peptides (black); ERAAP KO unique (red) and shared (white) (a) Numbers of distinct or shared peptides recovered from WT or ERAAP KO cells. (b) Analysis of the non-overlapping peptides from WT and ERAAP KO cells represented as single vertical bars and plotted according to amino acid length. (c) Lengths of recovered non-overlapping peptides represented as percentage of the total peptides.

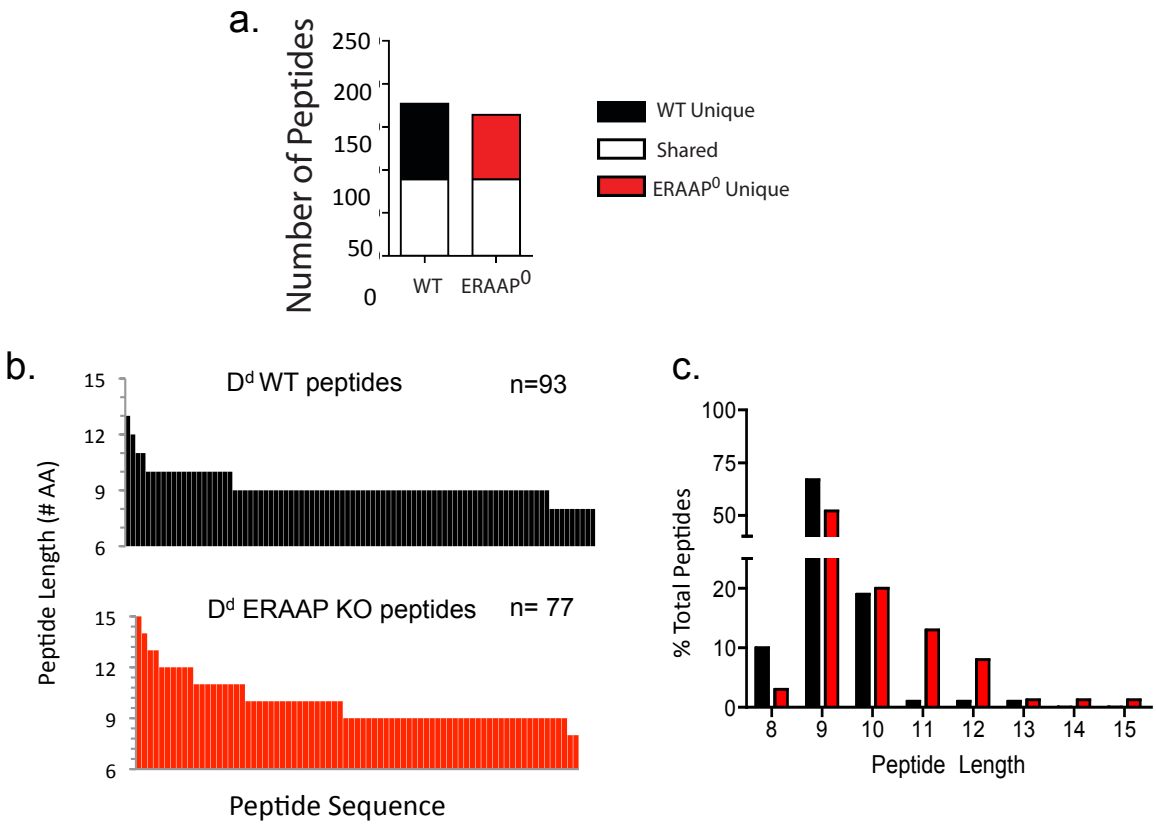


**Figure 19. Unique ERAAP KO peptides presented by $D^d$ are longer than WT $D^d$ peptides.** (a-c). Analysis of H-2$D^d$ peptides from WT and ERAAP-deficient (ERAAP KO) spleen cells identified by tandem mass spectrometry. WT-unique peptides (black); ERAAP KO unique (red) and shared (white) (a) Numbers of distinct or shared peptides recovered from WT or ERAAP KO cells. (b) Analysis of the non-overlapping peptides from WT and ERAAP KO cells represented as single vertical bars and plotted according to amino acid length. (c) Lengths of recovered non-overlapping peptides represented as percentage of the total peptides.

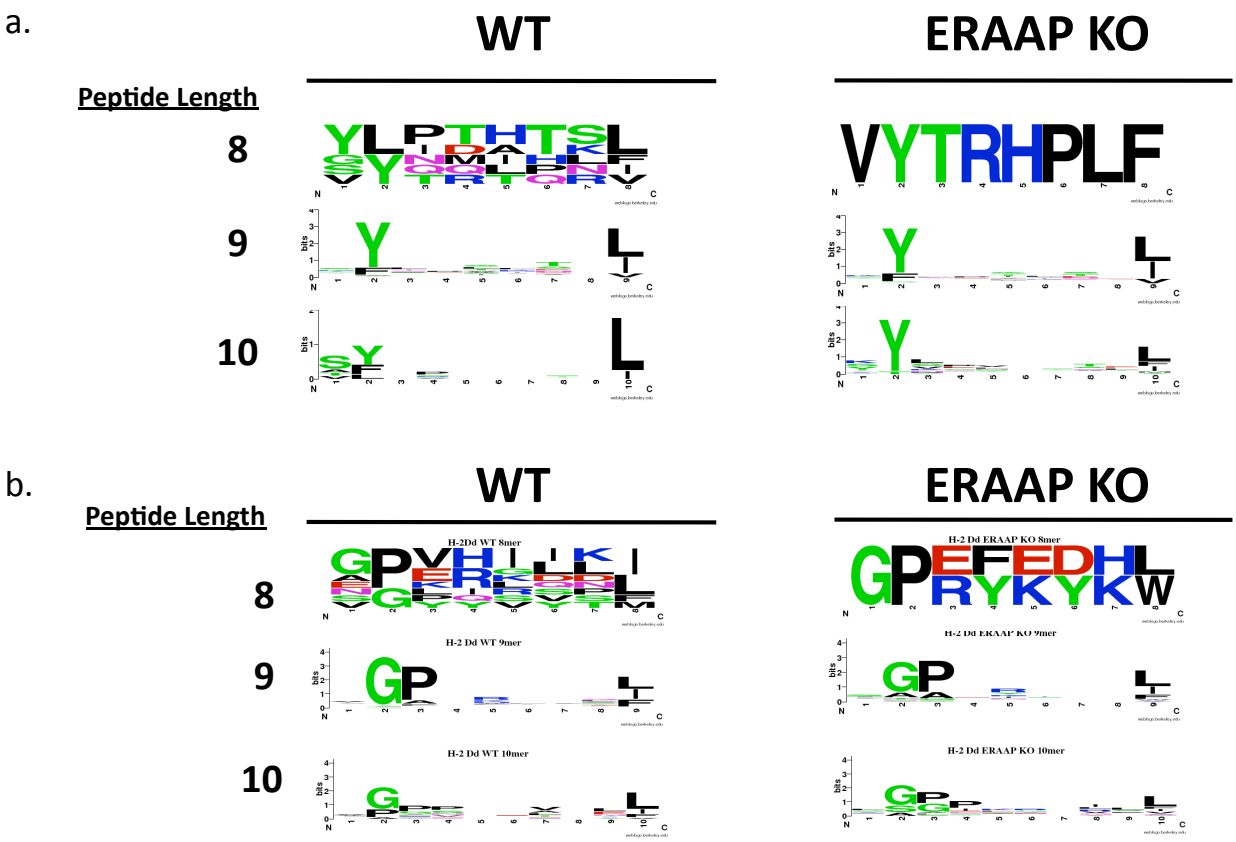


**Figure 20. $D^d$ and $K^d$ eluted peptides 8-10 amino acids in length maintain the consensus binding motif.** Composition of canonical length peptides eluted from (a) $K^d$ or (b) $D^d$ was analyzed with Weblogo program to determine frequency of amino acids at each position. Peptides are grouped according to their lengths, and the numbers of peptides in each group is indicated. The height of each bar is proportional to the frequency of amino acid conservation and the height of each letter composing the column is proportional to its frequency at the given position. Amino acids are colored as follows: hydrophobic (black), aromatic (purple), acidic (red), basic (blue), neutral (green).

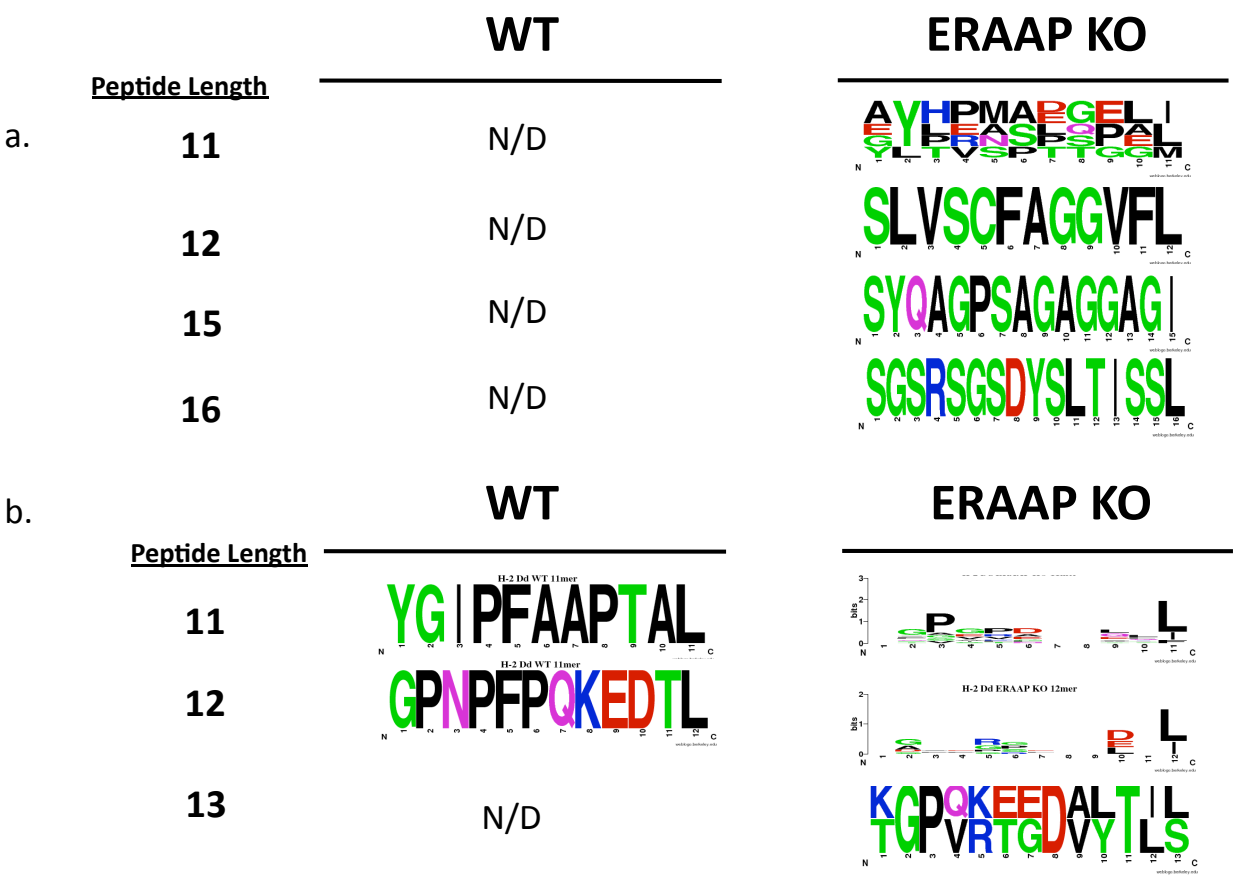


**Figure 21. Long $D^d$ and $K^d$ peptides bind with N-terminal or central bulges.** Composition of canonical length peptides eluted from (a) $K^d$ or (b) $D^d$ was analyzed with Weblogo program to determine frequency of amino acids at each position. N/D is not detected. Peptides are grouped according to their lengths, and the numbers of peptides in each group is indicated. The height of each bar is proportional to the frequency of amino acid conservation and the height of each letter composing the column is proportional to its frequency at the given position. Amino acids are colored as follows: hydrophobic (black), aromatic (purple), acidic (red), basic (blue), neutral (green).

| Sequence in ERAAP KO | Sequence in WT | Gene Name |
|---|---|---|
| AAFPGPLKEENL<br>AFPGPLKEENL | FPGPLKEENL | CREB-regulated transcription coactivaor 3 |
| KAAGPDRFVLL<br>AAGPDRFVLL<br>AGPDRFVLL | AGPDRFVLL | Zinc finger CCCH-type antiviral protein 1 |
| VSVPDSSGPERLISI<br>SVPDSSGPERLISI<br>PDSSGPERLISI<br>DSSGPERLISI<br>SSGPERLISI<br>SGPERLISI | VPDSSGPERLISI<br>PDSSGPERLISI<br>DSSGPERLISI<br>SSGPERLISI<br>SGPERLISI<br>GPERLISI | Heterogeneous Nuclear Ribonucleoprotein K |

Table 8. **Notable N-terminally extended nested peptide sets identified from $D^d$**

**ERAAP-deficient peptides from $D^d$ are longer and bind with distinct conformations:**

The final MHC I molecule analyzed was $D^d$. The consensus binding motif for $D^d$ is distinct from $K^d$ and $L^d$ in that it has three anchor residues: Both the P2 and P3 position as well as the PΩ position (XGPXXXXXXL). As with $K^d$, ERAAP-deficient cells show a moderate ~25% decrease in $D^d$ expression.

As seen with $K^d$, similar numbers of peptides were recovered from $D^d$ in WT and ERAAP KO samples, with 90 individual sequences unique to WT, 77 unique to ERAAP KO and 89 shared between the two (**Fig 19a; Table 6**). As observed in $K^d$, peptides that were 9 amino acids were the most frequent in the ERAAP KO-unique set and there was also an overall shift toward longer peptides relative to WT (**Fig 19 b-c**). Unlike the peptides recovered from $K^d$, however, there were also long peptides observed in the WT-unique group (**Fig 19 b-c**). Weblogos illustrated that canonical length peptides maintained the consensus motif while longer peptides did not (**Fig 20b**). As with $K^d$-binding peptides, the long peptides presumably bound with N-terminal extensions or a central bulge phenotype, but tended to have the correct C-terminal amino acid (**Fig 21b**).

More so than the $K^d$ and $L^d$ data sets, several N-terminally extended nested sets were recovered from $D^d$ (**Table 8**). As ERAAP trims the N-terminal end of peptides, these intermediates may represent endogenous ERAAP substrates. The most prominent of these nested peptide sets contained the entire range from 8 (GPERILSI) to 15 (VSVPDSSGPERILSI) amino acids. Interestingly, several of the intermediates were shared by WT and ERAAP KO sets, although the very longest peptides were only found in ERAAP KO samples. Other nested sets had fewer intermediates, but shared the same pattern with the N-terminally extended versions limited to ERAAP KO.

**$D^d$ and $K^d$ bind extended peptides:**

While examples of long peptides have been identified from MHC I molecules(188) the prevailing wisdom is that this increase in length comes at a cost to the overall stability of the pMHC I complex. Binding algorithms, such as that used by IEDB, are not able to assess the predicted binding of these long peptides. To test whether the long peptides from $K^d$ and $D^d$ were able to bind MHC I molecules, a RMA/s stability assay was performed. Briefly, a set of short and long peptides from the $K^d$ (TYAPPKPRSEL)/ (TYQDIQNTI) and $D^d$ (SGPERLISI)/PDSSGPERLISI) ERAAP KO data sets were chosen for analysis. These peptides were tested for their ability to stabilize MHC I by exogenously binding empty $K^d$ or $D^d$ stably expressed by RMA/s cells. The long peptides tested bound their appropriate MHC I molecule at similar concentrations as the canonical length peptides (**Fig 22**). Therefore, for those peptides tested, increased length is not inhibitory to peptide binding.

**Discussion:**

Sequencing peptides by mass spectrometry revealed the molecular nature of the altered peptide repertoire presented by $K^d$, $D^d$ and $L^d$ MHC I in the absence of ERAAP. Loss of ERAAP function has differential effects on each MHC I, as depicted by the schematic in **figure 23**. Consistent with the overall instability and decreased surface expression of $L^d$, very few peptides were recovered. Those peptides that were identified contained canonical lengths and consensus sequences. In contrast, while many of the

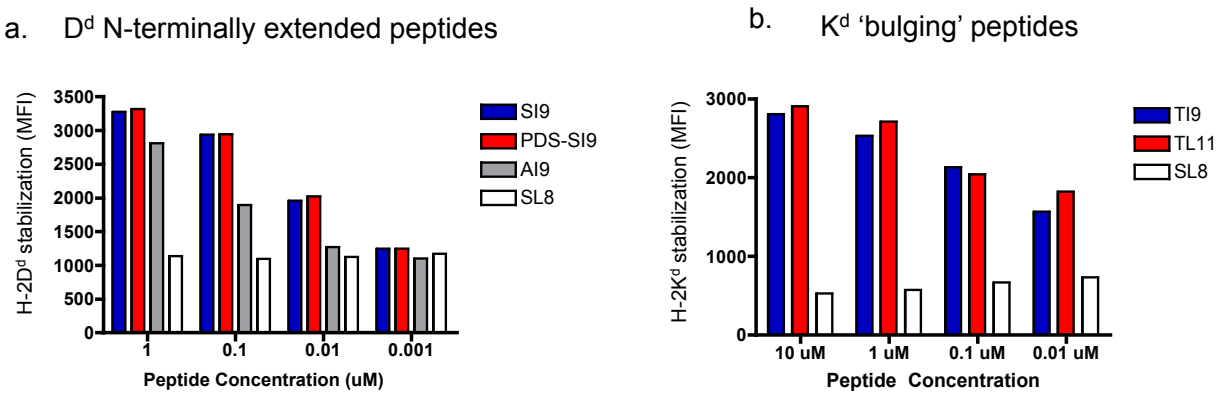


**Figure 22. Long peptides from ERAAP KO $D^d$ and Kd bind with similar affinity.** (a-b). Stabilization of H-2Dd MHC I with peptides. RMA/s cells, incubated overnight to stabilize empty pMHC I on the surface, were incubated with ERAAP-unique peptides or control AGPPRYSRI (AI9, $D^d$-binding) or SIINFEKL (SL8, $K^b$-binding) peptides for 1 hour at 22°C followed by incubation at 37°C for 3 hours. Cells were then fixed, stained with Kd or Dd fluorescently-conjugated antibodies and analyzed by flow cytometry. (a) $D^d$-binding peptides SGPERLISI (SI9) and PDSSGPERLISI (PI12). (b) $K^d$ peptides TYQDIQNTI (TI9) and TYAPPKPRSEL (TL11).

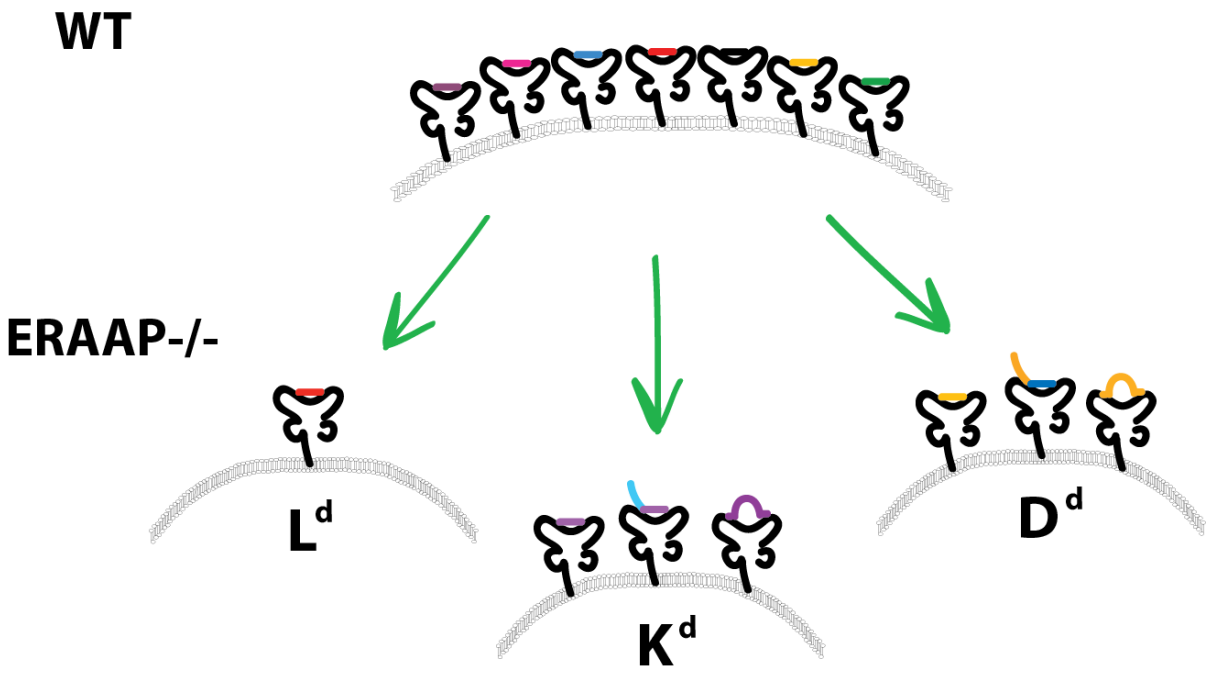


**Figure 23. Schematic depicting the allele-specific changes to the unedited pMHC I repertoire in H-2$^d$ ERAAP KO cells.** The top represents the endogenous WT pMHC I repertoire and the bottom represents the ways in which ERAAP-deficiency changes that repertoire. L$^d$ expression is decreased significantly, and the peptides presented are of canonical length. K$^d$ and D$^d$ surface expression is also decreased upon ERAAP deficiency. K$^d$ and D$^d$ present new peptides, many that have the canonical length and others which are extended. Extended peptides can bind with a bulge phenotype or may be N-terminally extended.

peptides recovered from $K^d$ and $D^d$ were of canonical length, there were also several examples of long peptides. These peptides either bound to the MHC I with a 'bulge' phenotype or with an N-terminally extended phenotype.

The use of mass spectrometry to sequence antigenic peptides has been invaluable for characterizing what peptides bind MHC I under normal and abnormal conditions. However, there are some caveats to this methodology that may affect interpretation of the results. First, the absence of a particular peptide sequence in a given data set may reflect the fact that it is below the limit of detection for the assay, but not necessarily that it is not present. As T cells are highly attuned to detect even small amounts of a given pMHC I complex, peptides that are not detected by mass spectrometry may still have immunological consequences. Along similar lines, immunodominance of certain antigens over others depends on several factors, and even peptides that are unique to ERAAP-deficient cells may not be immunologically significant. Nonetheless, the data obtained provides broad and important insights into the types of changes in the peptide repertoire caused by loss of ERAAP editing.

## Chapter 6: Characterization of immunogenic ERAAP-deficient pMHC I repertoire

**Summary**:

In chapters 4 and 5, I identified and characterized the presence of novel, unedited pMHC I presented on the surface of ERAAP-deficient cells by $K^d$, $D^d$ and $L^d$. Although mass spectrometry revealed the presence of longer, structurally unique peptides, this analysis does not reveal whether these longer peptides are presented on the cell surface or are capable of eliciting the WT anti-ERAAP KO T cell responses.

T cells are tolerant only to self-peptides and recognize changes in the pMHC I repertoire with specificity. Thus, one way to detect the presence of novel pMHC I is to generate T cell responses against the altered pMHC I which are missing from WT cells. Using this property, we sought to immortalize FEko T cells and characterize the molecular nature of their immunogenic ligands.

To immortalize the FEko T cells, I fused them with the BWZ.36 fusion partner in which TCR signaling results in expression of beta-galactosidase. These cells can be used in a colorometric assay in which CPRG cleavage is associated with the presence of the pMHC I ligand(189). Using an expression cloning strategy, we found that the resulting hybridoma, FEKo7Z, was specific for a peptide presented on $D^d$ from ribosomal protein L17 only in the absence of ERAAP function. The nonamer SSPCHIEMI is sufficient to elicit FEko7Z hybridoma responses and to cause lysis by FEko T cells. Consistent with the $D^d$ peptides identified via mass spectrometry, this antigen may be N-terminally extended and is missing the P2 anchor.

### Fusion of FEko T cell lines to generate WT anti-ERAAP KO hybridoma:

In order to identify the nature of the immunogenic pMHC I from ERAAP KO mice, FEko T cell lines (Chapter 4) were fused with the BWZ.36 fusion partner (Mendoza et. al.). Resulting hybridomas went through three rounds of subcloning by limiting dilution to select for a stable cell specific for ERAAP-deficient H-$2^d$ cells. Each round of subclones was screened against ERAAP KO spleen cells to confirm that the hybridoma maintained specificity for ERAAP KO H-$2^d$ APCs.

To assess whether FEko7Z maintained the same specificity as the FEko T cell lines, we tested its ability to respond to various spleen cell APCs (**Fig 24a**). As with the FEko T cells, responses were only observed against B6.bBy ERAAP-deficient or B10.D2 ERAAP-deficient APCs, which both contain $K^d$, $D^d$ and $L^d$. In contrast, WT H-$2^d$ APCs, B6 ERAAP KO APCs, which express allelic variants of K and D MHC I, and $K^bD^b$ ERAAP KO APCS, which lack classical MHC I molecules, are not capable of stimulating FEko7Z responses. Furthermore, chemical inhibition of ERAAP function in WT spleen cells using the aminopeptidase inhibitor LeuSH is sufficient to result in presentation of the unedited pMHC I (**Fig 24b**). Interestingly, although chemical inhibition led to presentation of FEko7Z's ligand on WT cells, these inhibited responses are never as high as when ERAAP-knockout cells were used as APCs. One explanation could be incomplete inhibition by LeuSH. Therefore, we conclude that FEko7Z is specific for an unedited pMHC I ligand presented only in the absence of ERAAP trimming by either $K^d$, $D^d$ or $L^d$.

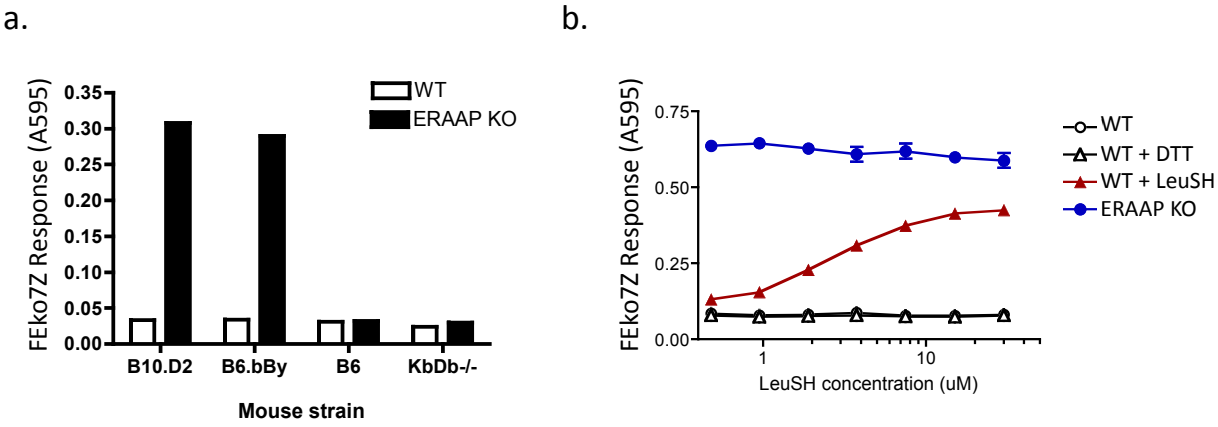


**Fig 24. T cell hybridoma FEko7Z is specific for ligands presented by H-2$^d$ cells in the absence of ERAAP function.** (a) FEko7Z responds to spleen cells from ERAAP-deficient H-2$^d$ mouse strains. FEko7Z hybridoma was incubated for 14-16 hours with LPS-treated spleen cells from the indicated ERAAP KO or WT mouse strains (b) FEko7Z is specific for loss of ERAAP function. WT cells treated with DTT alone or DTT and various doses of the ERAAP-inhibitor Leucinthiol (LeuSH) were incubated with FEko7Z for 14-16 hours before measurement of hybridoma response. WT and ERAAP KO spleen cells not treated with DTT or LeuSH were used as controls. Hybridoma response was determined by CPRG substrate cleavage measured at absorbance 595.

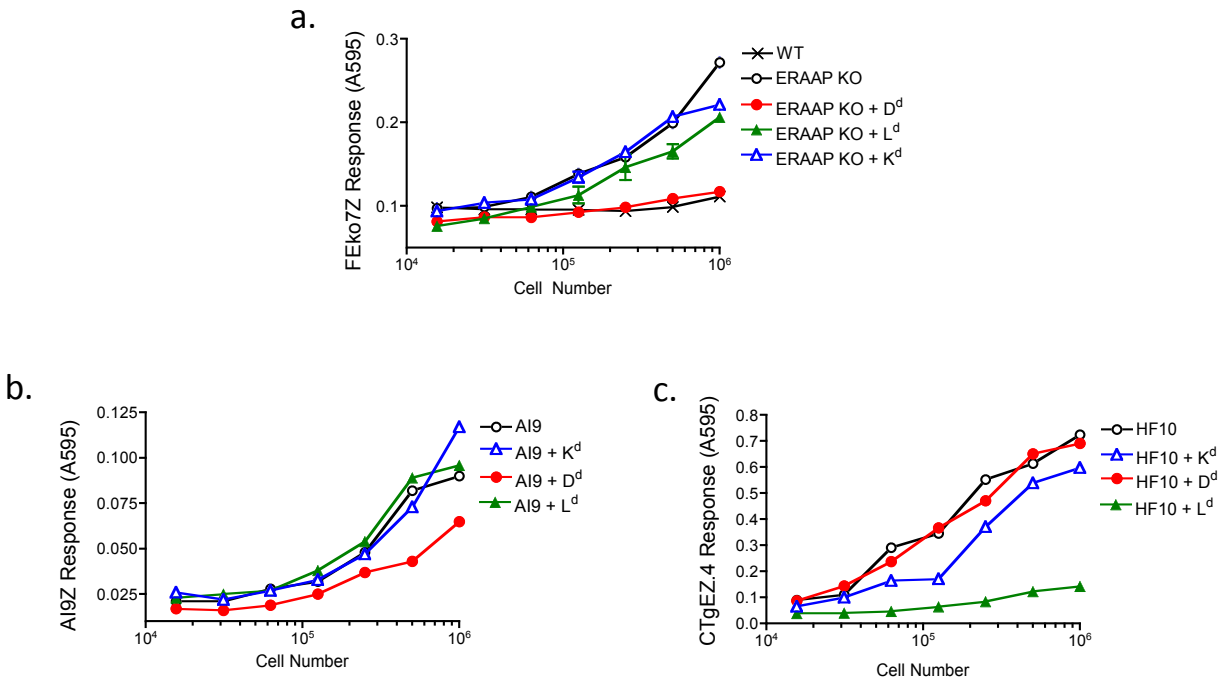


**Figure 25. FEko7Z is restricted to $D^d$** (a-c) Antibody blocking to determine hybridoma restriction. (a) Test of FEko7Z restriction.
WT or ERAAP KO splenocytes were incubated with the indicated blocking antibodies for 30 minutes on ice before addition of FEKo7Z hybridoma. (b-c) Controls for antibody specificity. (b) AI9 or (c) HF10 peptides were added to WT spleen cells before addition of blocking antibodies as in (a) and T cell hybridoma AI9Z (b) or CTgEZ.4 (c). T cell hybridoma responses were measured by CPRG substrate cleavage. Data is representative of 3 independent experiments.

As the $F_1$ mice likely have several minor histocompatability differences with B10.D2, it was possible that the FEko7Z hybridoma recognizes those differences. To confirm that FEko7Z recognition is specific for loss of ERAAP-function, APCs were
treated with varying dilutions of the aminopeptidase inhibitor L-leucinethiol (LeuSH) prior to incubation with FEko7Z hybridoma (**Fig 24b**). B10.D2 WT APCs treated with LeuSH are sufficient to stimulate FEko7Z responses, suggesting that this hybridoma is specific for ERAAP-deficient H-$2^d$ cells.

**FEko7Z is restricted to H-2D$^d$**

CD8+ T cells maintain a T cell receptor specific for a single restricting MHC I and peptide antigen. To determine which MHC I molecule presents the immunogenic peptide recognized by FEko7Z, we utilized blocking antibodies to inhibit recognition of each individual MHC I. Varying concentrations of spleen cells were treated with blocking antibodies specific for individual MHC I. After blocking, the FEko7Z hybridoma was added and a CPRG assay was performed. Incubation of APCs with anti-$K^d$, anti-$L^d$ and anti-$A^d$ did not inhibit the FEko7Z response, however, blocking $D^d$ with either the 34-2-12 (not shown) or 34-5-8 antibodies did diminish the response, suggesting that Feko7Z recognizes an antigen presented by $D^d$ (**Fig 25a**). To establish the specificity of the antibodies, the 34-5-8 antibodies were tested for the ability to block the HF10/CTgEZ.4 response ($L^d$-restricted) or the AI9/AI9Z response ($D^d$-restricted). As the antibody blocked AI9Z but not CTgEZ.4, the specificity was confirmed (**Fig 25b-c**).

**RPL17 cDNA contains the antigenic epitope for FEKo7Z**

To identify the antigen presented by $D^d$ and recognized by FEko7Z an expression cloning strategy was utilized. I generated a cDNA library in collaboration with F. Gonzalez using mRNA harvested from LPS-treated B10.D2 ERAAP-deficient spleen cells, which are potent stimulators of the FEko7Z hybridoma.

To screen for cDNAs containing antigenic activity, pools of these cDNAs were transfected into L cells stably expressing $D^d$ ($D^d$-L cells). The transfected cells were given 48 hours to allow expression of the genes, before ERAAP was inhibited by LeuSH treatment and a CPRG assay was performed with the FEKo7Z hybridoma.

Screening of several library pools resulted in the detection of antigenic activity in one 96 plate well at about two-fold above background (**Fig 26a**). To fractionate the various cDNAs in the positive well, the pool was re-transformed into competent bacteria and individual colonies were selected. When these individual cDNAs were expressed in $D^d$-L cells, several wells came up as positive**.** Of 5 individual cDNAs tested, 3 stimulated FEko7Z upon transfection in a dose-dependent manner (**Fig 5d**). Wells containing antigenic activity were sequenced, and all positive wells were found to contain the complete Ribosomal Protein L17 (RPL17) cDNA, including some 5' UTR. In contrast, the fractions that did not have antigenic activity were found to encode the TCR beta chain. Therefore, RPL17 cDNA contains the antigenic activity, and thus the peptide epitope, required for FEKo7Z activation.

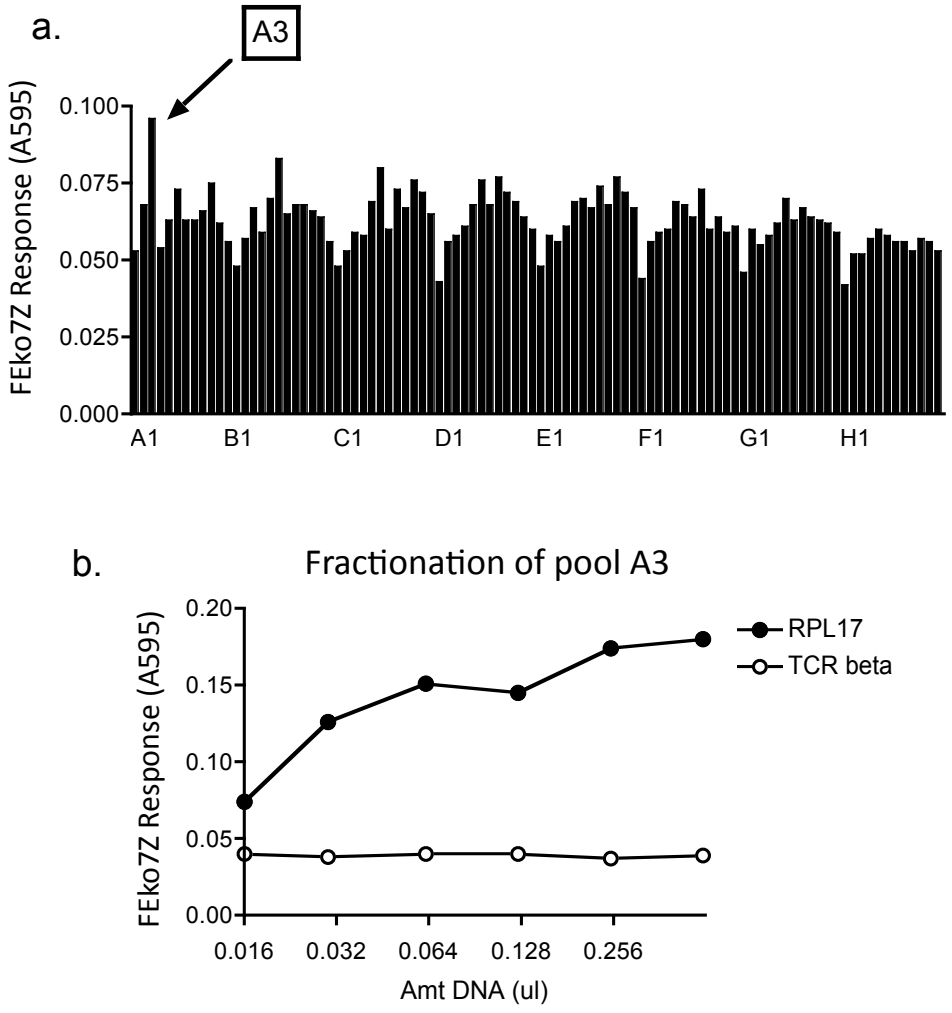


**Figure 26. The RPL17 gene is the source of a new antigen presented by Dd in the absence of ERAAP function.** (a and b) Pools of cDNA from ERAAP KO spleen cells were transfected into L cells stably expressing $D^d$. Cells were treated with the ERAAP inhibitor Leucinethiol and FEKo7Z hybridoma response was assessed by CPRG substrate cleavage. (a) A well containing antigenic activity was identified (b) Representative FEko7Z response to transfected cDNAs from well A3 fractionation.

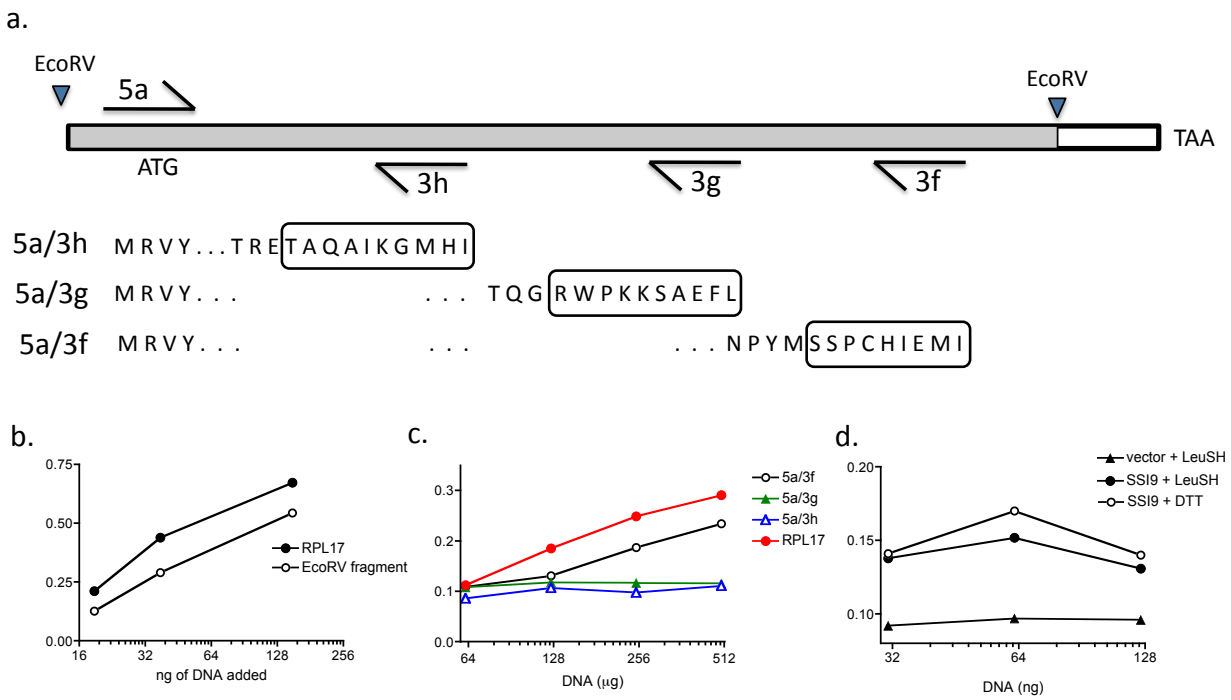


**Figure 27. SSI9 peptide presented by $D^d$ is the ligand for Feko7Z.** (a) Schematic of deletion mutants from RPL17 cDNA generated by restriction digest or PCR. Boxed regions indicate possible epitopes identified by prediction algorithm (IEDB) (b-d) Results of transfection of deletion mutant constructs into $D^d$-L cells. Leucinethiol and DTT were added to cells 48hr after transfection unless otherwise indicated followed by incubation with FEko7Z hybridoma (b) Cloned EcoRV fragment (grey bar from (a)) contains FEko7Z antigenic activity. (c) Longest PCR product 5a/3f contains antigenic activity in $D^d$-L cells treated with Leucinethiol (LeuSH), but shorter fragments 5a/3h and 5a/3g do not. (d) SSI9 minigene(SSPCHIEMI) in Ubiquitin-release vector stimulates ERAAP-independent FEko7Z response.

**Identification of SSI9 as the minimal antigenic peptide required for FEko7Z response**

To identify the peptide sequence responsible for FEKo7Z activity, deletion mutants of the RPL17 cDNA were generated. When the RPL17 cDNA sequence is analyzed with the $D^d$ epitope prediction algorithm from the Immune Epitope Database (IEDB), several putative antigens were found. As none of these epitopes contained the ideal XGPXXXXXXL $D^d$ motif, we utilized a deletion mutant approach to detect the sequence of the antigenic peptide presented by $D^d$ to FEko7Z.

First, I took advantage of existing EcoRV restiction sites near the 3' end of the RPL17 cDNA and upstream from the cDNA in the vector. Cutting with this enzyme and ligating the 5' portion resulted in a cDNA missing the final 55bp of RPL17 sequence. This portion was tested by transient transfection into $D^d$-L cells which were subsequently treated with LeuSH and used in a CPRG assay with FEko7Z. This region contained antigenic activity, indicating that FEko7Z's epitope does not include the final 18 amino acids (**Fig 27b**).

Next, several deletion constructs were generated using various sets of PCR primers. Various reverse primers were paired with a shared forward primer that placed the RPL17 initiating methionine in frame (see schematic **Fig 27a***)*. The reverse primers were designed such that the C-terminal end of the translated polypeptide will contain one of the most likely epitopes predicted based on IEDB analysis. The PCR products were digested and cloned into the pcDNA1 vector. The constructs were tested for antigenic activity by transfection in $D^d$-L cells as above. While the 5a/3g and 5a/3h constructs did not stimulate FEko7Z responses, the 5a/3f construct did (**Fig 27c)**, which suggested that the sequence encoding FEko7Z's epitope was between amino acids 91 and 147.

The 3' end of this construct encoded the peptide SSPCHIEMI, which was a strong candidate for $D^d$ binding based on IEDB prediction. To test whether this peptide was sufficient to stimulate FEko7Z hybridoma responses, DNA coding for the SSI9 peptide was expressed in the cytosol of $D^d$-L cells using a ubiquitin-release construct as previously described(56). This peptide robustly stimulated FEko7Z independently of LeuSH treatment, suggesting that this peptide alone is sufficient to stimulate FEko7Z response (**Fig 27c**).

**SSI9 and its N-terminally extended variants bind to $D^d$**

Based on the above results, we concluded that the SSI9 peptide is sufficient to generate the FEko7Z hybridoma response. However, as ERAAP trims peptides *in vivo* and several extended peptides unique to ERAAP KO were identified by mass spectrometry, the actual antigenic peptide may be an N-terminally extended variant of SSI9. To further characterize the MHC I binding and antigenic activity of N-terminally extended SSI9 variants, I utilized synthetic peptides made by David King (UC Berkeley). Each variant has the addition of a single amino acid at the N-terminus which corresponds to the natural amino acid sequence of the RPL17 protein, such that the sequence of the longest variant was NPYMSSPCHIEMI.

To test ability of N-terminally extended variants to bind $D^d$ MHC I, a RMA/s stability assay was performed. RMAs-Dd cells, which have diminished MHC I expression due to TAP-deficiency and stably express $D^d$, are left overnight at room temperature so that empty $D^d$ stabilizes on the cell surface. The following day, SSI9,

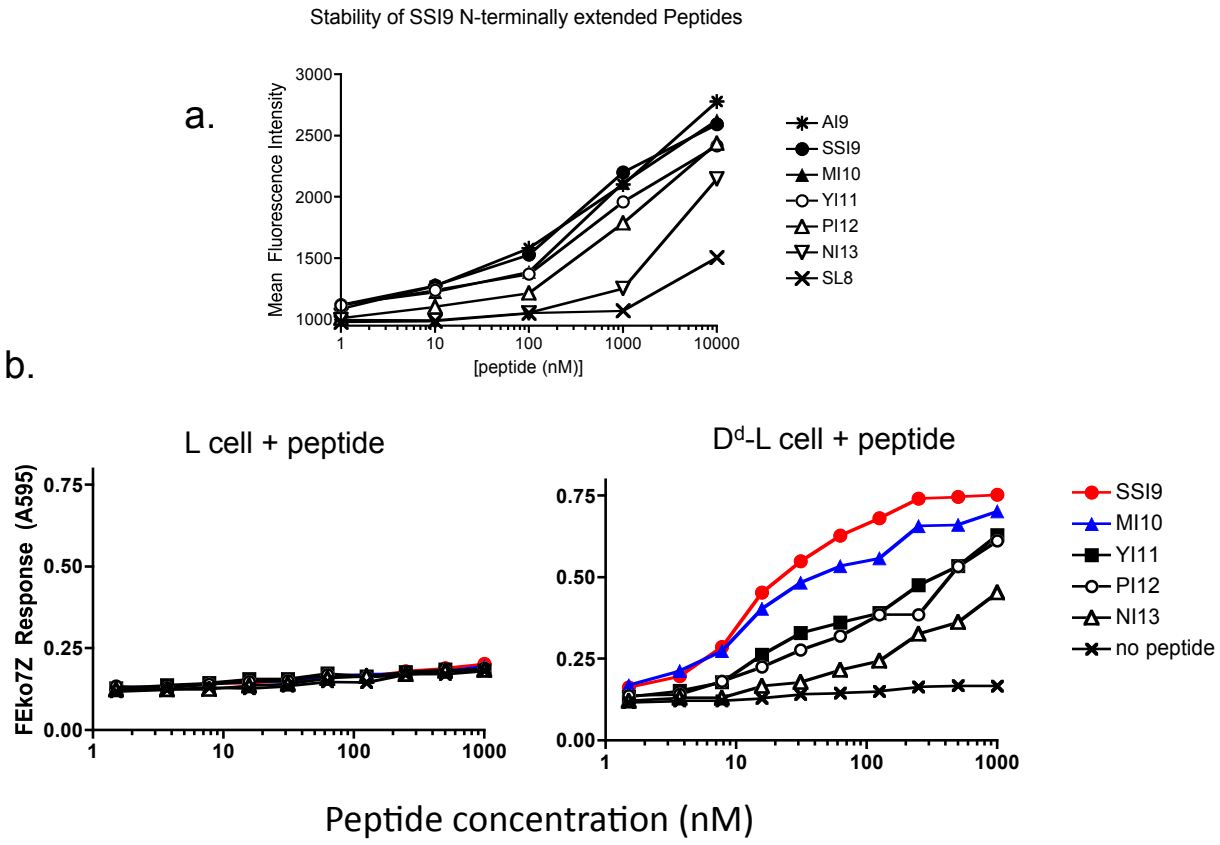


**Figure 28. N-terminally Extended variants of SSI9 bind $D^d$ and stimulate FEko7Z responses.** (a). Stabilization of H-$2D^d$ MHC I with synthetic peptides. RMAs-$D^d$ cells, incubated overnight to stabilize empty pMHC I on the surface, were incubated with indicated SSI9 N-terminally extended peptides or control AGPPRYSRI (AI9) peptides for 1 hour at 22°C followed by incubation at 37°C for 3 hours. Cells were fixed, stained for $D^d$ and analyzed by flow cytometry for $D^d$ expression. (b) FEko7Z recognizes all SSI9 variants, but to different extents. FEko7Z hybridoma and $D^d$-L APCs were added to titrated synthetic SSI9 variants. Hybridoma responses were assessed by measuring cleavage of CPRG substrate at absorbance 595 (A595).

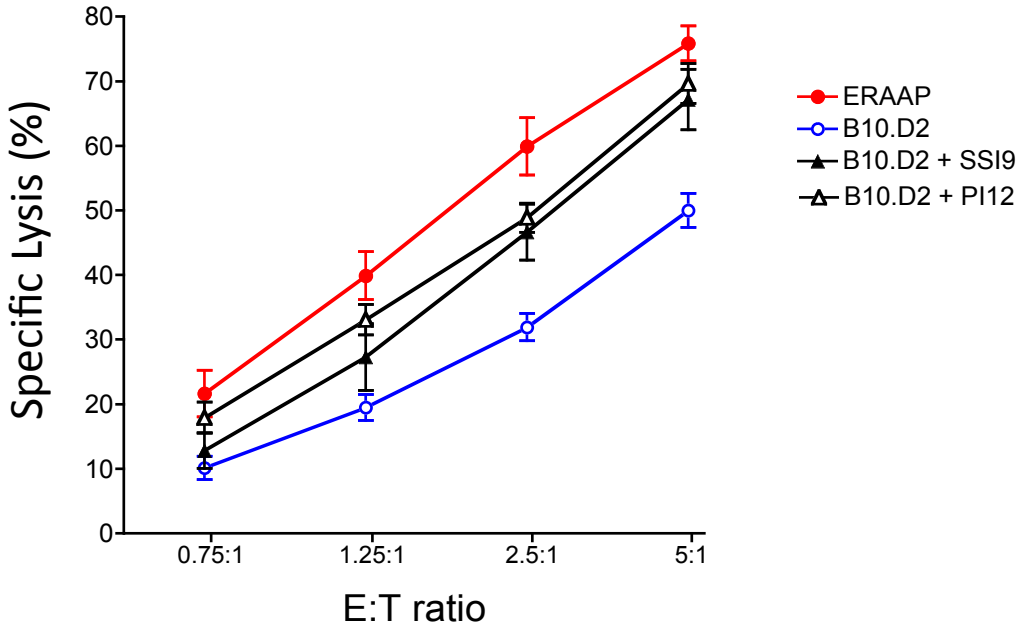


**Figure 29. FEko T cells kill SSI9 pulsed targets *in vitro*.** (a) WT anti-ERAAP KO T cell line was incubated with labeled ERAAP KO targets, unpulsed WT targets or WT targets pulsed with SSI9 or PI12 synthetic peptide for 2 hours at indicated effector to target ratios (E:T). Cells were then co-stained with Yo-Pro-1 viability dye and analyzed by flow cytometry. Percent specific lysis of target cells at each E:T ratio was determined. Data is pooled from one experiment with 5 replicates and is representative of 2 independent experiments.

MI10, YI11, PI12 or NI13 peptides are added to the RMAs-Dd cells and left at room temperature to allow the peptide to exogenously bind the empty $D^d$ molecules. After 1 hour, excess peptide was removed and the plates were put at 37°C. After 3 hours, cells were analyzed for remaining $D^d$ surface expression levels. The SSI9 and MI10 peptides were able to stabilize $D^d$ to a similar extent as the established high-affinity $D^d$-binding peptide AI9. Variants YI11 and PI12 had slightly lower than the shorter peptides and NI13 stabilization activity was substantially reduced (**Fig 28a**). Although a clear hierarchy of stability based on length was seen, all peptides were capable of binding $D^d$.

To determine the extent to which these variants are recognized by the FEko7Z hybridoma, peptides were exogenously loaded on $D^d$-L cells and a CPRG assay was performed. Similar to the RMA/s stabilization assay, a hierarchy of FEko7Z response was observed (**Fig 28b**). SSI9 and MI10 triggered the best FEko7Z response, followed by YI11 and PI12. Lmtk- (L) cells lacking the $D^d$ MHC I molecule did not stimulate the hybridoma, confirming that the FEko7Z response is $D^d$ specific.

**SSI9-$D^d$ complex is immunologically significant**

As the FEko7Z hybridoma was generated from a responding T cell line, its ligand likely has immunologically significance. To determine whether SSI9 is important in FEko T cell responses, FEko T cell lines were tested for their ability to kill target cells pulsed with the SSI9 peptide variants *in vitro*. Exogenously presented SSI9 and PI12 resulted in similar lysis of target cells (**Fig 29**), as did the other N-terminally extended variants (data not shown). While they were well above the background WT control, none of the variants was as efficient at stimulating lysis as ERAAP KO APCs. This suggests that SSI9 is an immunologically significant ligand, however, there are likely other unedited pMHC I important for this response *in vivo*.

**Discussion**

CD8+ T cell hybridomas have proven to be valuable tools for identifying and characterizing immunogenic changes to pMHC I that occur under a variety of circumstances. In this work, I have generated a T cell hybridoma, FEko7Z, which is specific for loss of ERAAP function in cells containing $D^d$. Through expression cloning, the SSI9 peptide was found to contain sufficient antigenic activity to stimulate FEko7Z responses, although the actual epitope *in vivo* may be an N-terminally extended variant of SSI9. Interestingly, although the SSI9 peptide was not found in the mass spectrometry data sets, it appears to be consistent with ERAAP KO $D^d$ peptides as it is suboptimal and is missing the P2 anchor residue.

Identification of the final epitope recognized by FEko7Z has been challenging. Detection of exogenous loading or with tetramers requires an unusually high concentration of peptide. RPL17 has been reported to be phosphorylated on both serines in the antigenic peptide sequence *in vivo*, so it is possible that our synthetic peptides don't properly mimic the phospho-peptide ligand. Another challenge has been that the SSI9 peptide is not presented in all cells, despite being a ubiquitous translation factor.

It remains unknown whether to classify SSI9 as an ERAAP-unedited peptide or an ERAAP-sensitive peptide. Is FEKO7Z's ligand only found in ERAAP KO cells? This would indicate that this SSI9 variant is typically destroyed by ERAAP *in vivo*. Alternatively, it may also be found in WT cells and, due to competition with other peptides in the ER, simply not be presented.

To determine the endogenous peptide found in ERAAP KO cells and presented to FEko7Z, one method would involve fractionating ERAAP KO splenic cell extracts by HPLC follwed by analysis of the peptides present using the FEko7Z hybridoma. Resulting positive fractions could be identified with synthetic peptides run under the same conditions. Although it would be challenging to isolate enough material, this would allow identification *in vivo* of an ERAAP-unedited peptide.

Overall, the generation of this hybridoma has allowed us to identify an example of pMHC I only presented in the absence of ERAAP. Future applications of FEko7Z include detection of loss of ERAAP function in transformed cells or due to viral inhibition.

## Future Directions

### What is the Mechanism of tapasin action?

Using immunological and biochemical methods, we have determined that tapasin is indeed an editor of the endogenous pMHC I repertoire. Our data suggests that it is responsible for ensuring that a high-affinity peptides are presented by editing out peptides with inappropriate C-termini or overall low binding affinities. However, the direct mechanism of tapasin action remains unclear.

The foremost challenge preventing the establishment of a model of action is that it is difficult to distinguish between any direct role of tapasin-editing versus overall PLC function. Tapasin is the key adaptor which holds the PLC together, so its absence may prevent other factors from carrying out their roles. In particular, tapasin-deficiency decreases TAP stability, and therefore overall peptide supply (136). Generation of soluble tapasin molecules, which do not interact with TAP, were assessed for ability to mediate pMHC I presentation to attempt to distinguish between the roles for TAP and tapasin. The results were mixed, however, with rescue of surface expression for human HLA-B8 but not murine $K^d$, $K^b$ or $L^d$ (93, 190).

Tapasin interacts with MHC I at the alpha-2 helix where the peptide C-terminus binds. This fits with a putative role in editing the PΩ amino acid to ensure an optimal residue is used, and is consistent with our finding that tapasin-deficient cells present an increased frequency of peptides with altered C-termini. Several possible models for how tapasin might edit at the C-terminus exist, and include maintaining the MHC I molecule in an open, peptide-receptive conformation (191), such that several peptides can be tried until a high-affinity match is found or accelerated dissociation of unfavorable peptides (142, 184, 192). However, questions about tapasin's mechanism of action still remain. What constitutes an acceptable peptide? How does tapasin identify the presence of a high-affinity peptide? One possible hypothesis is that conformational changes in the MHC I upon binding of an optimal C-terminal amino acid allow release of tapasin, although this has yet to be tested (193).

Also unknown is whether tapasin interacts with other PLC editors. We tested for a functional interaction between ERAAP and tapasin, but were unable to identify any overlap in the unedited pMHC I from ERAAP or tapasin-deficient cells, thus leading us to conclude that ERAAP-editing shapes the N-terminus while tapasin-editing shapes the peptide C-terminus. What about carboxypeptidases such as ACE? Perhaps ACE requires tapasin to finalize the C-termini of a subset of antigenic peptides. Similar types of cross-immunization experiments as were performed here with tapasin and ERAAP would allow this hypothesis to be tested.

These findings provide broad insight into the effects of tapasin-deficiency on the endogenous peptide repertoire. Further large-scale analyses coupled with biochemical and structural data will allow us to continue refining the models for tapasin's mechanism of action. It will be particularly important to continue getting data from several different MHC I molecules, as, based on surface expression, some alleles are more affected by tapasin-deficiency than others (179, 194).

**Allele-specific effects of ER-editors: consequences for immunity**

Our study highlights that the effects of both tapasin-deficiency and ERAAP-deficiency are not equal across all MHC I molecules and suggests that a comprehensive analysis is required to detect subtle pMHC I changes caused by the loss of PLC editing.

*Tapasin:* In tapasin-deficient mice, although surface expression of $K^b$ and $D^b$ is similarly reduced, we find that there are further differences. Assessment of the WT anti-$Tpn^0$ lines showed that $D^b$ was more immunogenic than $K^b$ (**Fig 5).** In addition, many more peptides were recovered from $D^b$ by mass spectrometry, suggesting that some $D^b$ peptides may be less tapasin-dependent (**Fig 7**). While we identified several $D^b$ peptides that lacked the canonical P5 anchor, the same was not true for $K^b$ (**Fig 8).** In the absence of tapasin, $K^b$ pMHC I appear to be highly unstable, such that they are unable to be recognized by WT anti-$Tpn^0$ T cells and difficult to recover through affinity purification.

Studies with several human HLA molecules have concluded that there is a range of tapasin-dependence based on the amount of surface pMHC I downregulation in $Tpn^0$ cells (195). For example, it was found that tapasin was required for optimal surface expression of HLA-A1, HLA-B8 and HLA-B*4402 while surface expression of HLA-A_0201 and HLA-B*2705 was unaffected in the absence of tapasin (179, 194). However, it is possible that, just as we found further differences exist with $K^b$ and $D^b$, they may also be immunologically significant differences might be present on HLA molecules which that have normal surface expression upon loss of tapasin editing. More thorough immunological and biochemical analyses, such as the mass spectrometry analysis of peptides from chapter 3, should be performed for a broader set of HLA molecules.

*ERAAP:* Strong evidence supports the participation of MHC I molecules in shaping the composition of peptides that are presented in the presence of ERAAP (5, 151, 152). However, *in vitro* studies indicated that ERAAP can also trim peptides without MHC I, meaning that ERAAP-deficiency also affects the pool of peptides available for presentation on MHC I.

Our studies indicate that loss of ERAAP affects each allele and the composition of peptides it presents in different ways. Although all three MHC I molecules presented novel pMHC I, long peptides, some with N-terminal extensions, were found bound to $K^d$ and $D^d$ but not $L^d$. Furthermore, we showed that these allele-specific differences have immunological consequences. FEko T cell responses were not equally distributed in their restriction, but rather a larger fraction of the response was directed at $K^d$ than at $D^d$ or $L^d$. Furthermore, an immunologically-significant ligand from RPL17 was found to be presented by $D^d$. Future studies should aim to better understand the consequences of the allele-specific effects of ERAAP-deficiency. The link between ankylosing spondylitis, an autoimmune disease tightly linked to a particular MHC I molecule, and ERAP1 highlights the need to better understand the allele-specific effects of ERAAP-editing of pMHC I.

$L^d$ should be a particular focus of future studies. It was previously hypothesized that the reason for decreased $L^d$ expression was that it had a limited peptide pool, as TAP must transport peptides with extended versions of its consensus motif. However, although few ERAAP-deficient peptides were identified, most of the ones that were found contained the consensus

motif. How and where does $L^d$ encounter these peptides? Furthermore, why were $D^d$ and $K^d$ capable of accommodating N-terminally extended peptide but Ld was not? These questions can be addressed with straight-forward biochemical experiments. Additionally, it will be interesting to determine whether $L^d$ is more dependent on ERAAP for more than generation of peptides. This may demonstrate a direct interaction of ERAAP and MHC I, and would be important for future disease studies.

**Targeting ER-editing to evade immune detection**

In order to prevent detection by the host immune system, viruses employ various immune evasion strategies. Because they seek to establish long-term infections within host cells, herpes viruses in particular, are notorious for targeting the MHC I antigen presentation pathway and encode several genes to this effect (196). ER-editors tapasin and ERAAP have both been shown to be targets of viral inhibition, although the consequences of this inhibition are not fully understood. A better characterization of how and why tapasin and ERAAP are targeted can teach us both about their function, the biology of the virus, and interactions between host and pathogen.

*Tapasin:* A better understanding of the nature of the unique peptides presented in the absence of tapasin may provide insight into how this escape can be diminished. Human cytomegalovirus (HCMV) expresses inhibitor US3 (174) which directly binds tapasin and prevents it from participating in peptide loading onto MHC I. Murine herpes virus-68 (MHV-68) also contains a gene, mk3, (175) which inhibits tapasin, in this case causing its ubiquitination and subsequent degradation. Our findings demonstrated that in the absence of tapasin-editing, $D^b$ MHC I present new pMHC I complexes capable of stimulating T cell responses. One open question whether viral inhibition of tapasin is sufficient to generate these complexes. If so, this begs the question of whether WT anti-tapasin T cells recognize mk3-expressing cells and, if so, whether the presence of these pMHC I are sufficient for protection from MHV-68 infection.

*ERAAP:* The human homolog of mouse ERAAP, ERAP1, is also targeted by HCMV. Early in infection, HCMV expresses a microRNA found to target ERAP1 and cause its degradation (169). Analogous downregulation by a murine herpes virus has not yet been identified, and it would be of interest because mouse models are more tractable to characterize the *in vivo* effects of ERAAP deficiency. The FEko T cell lines and hybridoma will be invaluable to detect immunologically significant loss of ERAAP function. While murine herpes viruses are a natural place to start, it is possible that other viruses or pathogens have independently developed methods to inhibit ERAAP expression, and these should be tested as well. Furthermore, if loss of ERAAP is found, it will be important to then look at *in vivo* infection models to determine whether it is sufficient to generate T cell responses and whether there are any allele-specific effects.

## Chapter 8: Materials and Methods:

**Mice:** B6 ERAAP-deficient mice(153), tapasin-deficient mice(130), TAP1-deficient mice(119) and $K^b$-$D^b$ double-deficient mice(17) have been described elsewhere. ERAAP-deficient mice and tapasin-deficient mice were crossed to generate ERAAP and tapasin double-deficient mice. To generate ERAAP-deficient mice on the H-$2^d$ background, B6 ERAAP-deficient mice were crossed with B10.D2 or B6.bBy. Crossing C57Bl/6 mice with B10.D2 mice generated F1 mice and $F_1$ ERAAP KO mice were made by crossing B6 ERAAP-deficient mice with B10.D2 ERAAP-deficient mice. C57BL/6J, B10.D2 and B6.bBy mice were purchased from the Jackson Laboratory (Bar Harbor ME). Use of all mice was done with the approval of the Animal Care and Use Committee of the University of California at Berkeley.

**Antibodies**: The following antibodies used for flow cytometry analysis were purchased from BD Biosciences: anti-H-$2K^b$ (AF6-88.5); anti-H-$2A^b$ (25-9-17); anti-H-$2K^d$ (SF1-1.1.1); FITC IgG2a isotype control; anti-CD8α (53-6.7); anti-CD4 (RM4-5); B220 (RA3-6B2) and anti-IFN-γ (XMG1.2). Antibodies CD16/32 (Fc Block, clone 93); anti-H-$2L^d$/$D^b$ (28-14-8); Gr-1 (RB6-8C5) and F4/80 (BM8) were purchased from ebiosciences. Anti-H-$2E^d$ (14-4-4) and anti-H-$2D^d$ (34-5-8) for surface expression staining were made by southern biotechnology associates.

For *in vivo* depletions, purified anti-NK1.1 antibody (PK136) and anti-CD8α (2.43) from BioXcell or anti-CD4 (GK1.5) and isotype control Rat IgG2b (LTF-2) from the UCSF hybridoma core were used.

To block presentation by MHC I to anti-$tpn^0$ T cell lines, the following culture supernatants were used: anti-H-$2K^b$ (5F1.5), anti-H-$2D^b$ (B22.249) or anti-H-$2A^b$ (M5/114). To block presentation by H-$2^d$ MHC I molecules, anti-H-$2K^d$ (SF1-1.1.1) and anti-H2$D^d$ (34-5-8) made by the Delgado lab, anti-H-$2L^d$ (30-5-7) supernatant generated in house, or anti-H-$2D^d$ (34-2-12) or anti-H-$2A^d$ (39-10-8) from BioLegend were used.

In the immuno-affinity purification of pMHC I complexes for mass spectrometry, anti-H-$2K^b$ (Y3) and anti-H-$2D^b$ (B22.249) were used in the tapasin experiment and anti-H-$2D^d$ (34-5-8), anti-H-$2L^d$ (28-14-8) and anti-H-2Kd (SF1-1.1.1) were used in the ERAAP experiment. Antibody supernatants for mass spectrometry were made by the Delgado Lab at the University of Utah.

Conformation-dependent antibody supernatants were made using the 30-5-7 or 64-3-7 hybridoma cell lines (ATCC). Antibodies were dialyzed in PBS (6 total liters) prior to use in flow cytometry assay.

**Peptides:**

Peptides used in tapasin-stability assays (Chapter 3) were generated by Anaspec Inc. and resuspended to make 1mM stocks. ERAAP $K^d$ and $D^d$ long and short peptides from mass spectrometry were also generated by Anaspec Inc. but were resuspended in DMSO. David King generated all the N-terminally extended SSI9-variant synthetic peptides and their purity was found to be greater than 95%. They were resuspended in purified water.

**DNA Constructs:** MSCV-IRES-GFP was a gift of Dr. William Sha. To clone in $D^d$ and $K^d$, a PCR method was used to generate DNA with adaptors containing XhoI and SalI sites. These

were then digested and ligated into cut MSCV-IRES-GFP vector. $L^d$ was subcloned from the pRSV.5neo backbone using BamHI as well as blunt cutters PvuII (insert)/PmeI (MSCV vector). MHC I expression was verified by transfection into COS7 cells and flow cytometry analysis. pLZRS.UL49.5-IRES-GFP vector was a gift from the Wiertz Lab.

To generate the RPL17 EcoRV fragment pSport:RPL17 was digested with EcoRV and cloned into SAP treated pcDNA1 that had also been digested by EcoRV. To make PCR product deletion mutants of RPL17, PCR primers flanking the desired regions were generated:
5a: CCGAAAAGGATCCAAAATGGTTCGCTACTCTCTTGAC
3f: GATGGCCTCTAGATTAGATCATCTCAATGTGGCA
3g: GATGGCCTCTAGATTAAAATTCAGCACTCTTTTT
3hGATGGCCTCTAGATTAGATATGCATTCCCTTGAT

RPL17 in pSport-6 was used as a template for PCR. PCR products were gel purified, digested with BamHI and XhoI and ligated into pcDNA1.

Ubiquitin-release vector was a gift from Frederic Levy. The SSI9 peptide was cloned into the SacII and Not I sites for release of the complete epitope.

For cloning, all gel purification was done using the PureLink Gel Extraction Kit (Invitrogen). Ligations were done with T4 high-concentration DNA ligase (NEB). Chemically competent bacteria MC1061 (for pcDNA1 backbone plasmids) or Top 10' (all other plasmids) were used (Invitrogen).

**Cell Lines:** ERAAP and TAP double-deficient fibroblasts were previously reported and immortalized ERAAP and tapasin double-deficient fibroblast cell lines were generated in the same manner as previously described(153). The use and generation of b-galactosidase (lacZ)–inducible T cell hybridomas B3Z, 30NXZ, 1AZ, 11P9Z, LPAZ, 27.5Z, BEKo8Z, AI9Z and CTgEZ.4 have been described elsewhere (153, 155, 159, 197). Hybridoma activation was determined by measurement of CPRG (Chlorophenyl red-b-D-galactopyranoside; Roche). Splenocytes from indicated mice treated with 200ng/ml LPS (sigma) for 14-16 hours were used as APCs for T cell hybridomas. $D^d$-L cells expressing B7-2 were made by N. Blanchard. BWZ.36 fusion partner was previously described (198).

Bone Marrow-derived Dendritic Cells were generated using a syringe to harvest marrow from murine leg bones, making a single-cell suspension, washing, and then plating $2x10^6$ cells in a 6-well dish with GM-CSF (10 ng/ml; Peprotech) in cRPMI. Cells were used between days 6-8.

To make RMA and RMA/s cell lines expressing single MHC I molecules, retroviral supernatant from $K^d$, $D^d$ or $L^d$ MSCV-GFP transfected (fugene, Roche) phoenix cells was harvested 2 days after transfection. Viral supernatant was filtered and a spin-infection of either RMA or RMA/s was performed in the presence of 8ug/ml polybrene for 2hr at 850xg. When GFP expression was detectible, GFP-positive cells were single-cell sorted, expanded and subsequently checked for surface expression of Dd, Kd or Ld.

To make J774 cells stably expressing UL49.5, phoenix cells were transfected with the pLZRX.UL49.5-IRES-GFP (fugene, Roche) and supernatant was used to spin-infect J774 cells plated one day prior as done for the RMA cells above. After 2 days, cells were bulk sorted based on GFP expression.

**Generation of FEko7Z Hybridoma:** was generated by fusing BWZ.36 fusion partner with an equal number of FEko T cells using the established protocol (Malarkannan et al). Cells were plated at 3 per well for the first subclone, followed by 1 cell/well for subsequent subclones. Each subclone was screened with $1x10^6$ ERAAP-deficient or WT spleen cells blasted overnight with 200 ng/ml LPS as APCs. CPRG cleavage was used as a readout for hybridoma response.

**Expression Cloning to Identify FEko7Z's epitope:** Library was made as in Mendoza et al. by Fred Gonzalez(189). mRNA harvested from B10.D2 ERAAP-deficient spleens that had been blasted overnight with LPS was the source of the cDNA. Plasmid DNA prepared from bacterial pools was transfected into LMtk- cells stably expressing Dd and B7-2 (Dd-L) using the DEAE/dextran transfection method(189). After 48 hours, the plates were treated with Leucinethiol (LeuSH) and DTT at a final concentration of 30uM and 50uM, respectively. Treatment lasted for 6 hours prior to addition of $10^5$ FEko7Z hybridoma cells. T cell response was assessed by CPRG cleavage after 15-24 hours though measurement at A595.

**Fractionation**: DNA from positive wells was transformed into Top10 or electrocompetent DH5alpha cells (Amp selection). Colonies were selected and plasmid DNA was purified (Qiagen miniprep kit). Indiviudal cDNAs were tested for their ability to stimulate FEko7Z responses through expression in $D^d$-L cells as above. To determine insert sizes and approximate diversity of the pool composition, DNA was digested with NotI/SalI.

**Determining FEKo7Z Restriction via antibody blocking:** Harvested WT and ERAAP KO spleen cells and blasted overnight in 200ng/mL LPS. Washed splenocyte APCs and then performed a 2-fold titration, with $1x10^6$ cells in the first well. The blocking antibody and/or peptide was added to appropriate wells in 50uL volume. Blocking antibodies are listed above. Final [peptide]=10ng/ml of either AI9 or HF10. Allowed APCs with or without peptide and blocking antibodies to incubate on ice for 1 hour before adding $5\text{-}10x10^4$ AI9Z, CTgEZ.4 or FEko7Z hybridoma cells. CPRG was added after overnight incubation to assess T cell response.

**Staining macrophages/DCs with surface MHC I mAb:** To increase the frequency of macrophages and dendritic cells recovered from ERAAP KO and WT spleens, they were treated with DNAse and collagenase prior to generation of a single cell suspension. Spleens were cut into small fragments, incubated for 1 hour in a cRPMI containing collagenase (10mg/ml, Sigma) and DNAse (10mg/ml, Roche). A single-cell suspension was made by grinding the spleens though a nylon filter, red blood cells were lysed using an isotonic buffer and cells were stained with MHC I and cell-type specific antibodies prior to flow cytometry analysis.

**Staining cells intracellularly with conformation dependent Ab:** J774 cells stably expressing UL49.5 or B10.D2 ERAAP KO and WT BMDCs were first stained with Fc block to minimize background staining. Cells were fixed using BD cytofix/cytoperm for 20 minutes on ice. After being washed in BD perm/wash buffer, cells were stained for 20 minutes on ice with dialyzed 30-5-7 or 64-3-7 antibody that had been diluted using perm/wash buffer. Cells were washed in Perm/wash buffer and then stained with APC anti-mouse IgG2a secondary antibody diluted 1:100 in perm/wash buffer. Finally, cells were washed well before being resuspended in FACS buffer (PBS+2.5% FBS) and analyzed by flow cytometry.

**Immunizations and Cytotoxic Lymphocyte Lines (CTLs).** To generate WT anti-tapasin or Tapasin anti-WT T cell lines, female tapasin-deficient or wild-type mice were immunized intraperitoneally with $2x10^7$ spleen cells from male wild-type or tapasin-deficient mice, respectively. Ten days after immunization, spleen cells were restimulated *in vitro*. Cultures contained 20 U/ml (first two restimulations) or 50 U/ml (subsequent restimulations) of hIL-2 (BD Biosciences) and irradiated spleen cells from female mice of the same genotype used for immunization. Additional restimulations were done every 7-10 days.

To generate FEko T cell lines, female $F_1$ mice were immunized with $2x10^7$ spleen cells from male $F_1$ ERAAP-deficient mice. Ten days later, F1 mice were boosted with $2x10^7$ spleen cells from B10.D2 ERAAP-deficient mice. After another ten days, spleen cells were harvested and restimuated *in vitro* as above. EkoF T cell lines were made using the same protocol. Host mice were female $F_1$ ERAAP KO which were immunized first with male F1 spleen cells followed by a boost with B10.D2 WT spleen cells prior to *in vitro* restimulation.

**Measurement of Intracellular IFN-γ production by CTLs.** The $CD8^+$ T cell responses of the immunized mice were measured by assessment of intracellular IFN-γ production. Spleen cell APCs were treated with 200 ng/ml of lipopolysaccharide (LPS, Sigma) overnight and $CD4^+$ and $CD8^+$ cells were depleted using magnetic beads (Dynal Biotech, invitrogen) prior to incubation with restimulated $CD8^+$ T cells. 1μl/ml brefeldin A (GolgiPlug (BD Biosciences)) was added after one hour and total incubation of $CD8^+$ T cells and APCs was 5 hours. Cells were stained for surface markers followed by intracellular staining for IFN-γ. Cells were analyzed by flow cytometry and with FlowJo Software (Treestar). For blocking of particular MHC I molecules, APCs were first incubated for 30-45 minutes on ice with antibody supernatant or commercial antibody at a 1:100 dilution prior to addition of $CD8^+$ T cells as described above. To use RMA cells as APCs, $5x10^4$ RMA or RMA-$K^d$, $D^d$ or $L^d$ were plated in a 96-well round bottom plate and treated overnight with 50uM DTT and 30uM LeuSH as indicated. Ficolled T cells were added directly the following day.

**RMA/s stability assay:** Prior to both surface binding and surface decay assays, flasks containing RMA/s or RMAs-$D^d$ cells in complete RPMI with 10% fetal bovine serum were sealed and left overnight at room temperature followed by three washes in PBS. All subsequent steps were done in PBS with no serum. Ten-fold dilutions of synthetic peptides were made followed by addition of $5x10^5$ washed RMA/s or RMAs-$D^d$ cells to result in the indicated final peptide concentrations. Samples were kept at room temperature for one hour followed by incubation at 37°C for three hours. At the end of the three hours, peptides were washed out, samples were stained with anti-H-$2K^b$, anti-H-$2D^b$ or anti-H-$2D^d$ antibodies, fixed in 1% paraformaldehyde, and analyzed by flow cytometry.

**In vivo cytotoxicity assay.** WT female mice, depleted of NK cells at least 36 hours prior to every immunization, were primed intraperitoneally with $2x10^7$ male WT, $ERAAP^0$ or $Tpn^0$ splenocytes. Mice were challenged on day seven with a 1:1:1 mix of labeled $ERAAP^0$, $Tpn^0$ and WT female APCs. Target cell labels: $ERAAP^0$ labeled with 20μM CellTracker Blue CMAC (7-Amino-4-Chloromethylcoumarin, Invitrogen); $Tpn^0$ targets labeled with 0.125 μM CFSE (low-dose); WT targets labeled with 1.25μM CFSE (high-dose) (Carboxyfluorescein

succinimidyl ester, Invitrogen). 20 hours after challenge with labeled cells, host mice were sacrificed and splenocytes analyzed by flow cytometry to determine percentage of cells remaining. Percent Specific Lysis was calculated as follows: 100 x (1- (ratio of target output)/ (ratio of target input)) where input is determined prior to injection of targets and output represents targets recovered after challenge. To calculate ratios: (% population of interest)/ (%ERAAP$^0$+%Tpn$^0$+%WT).

**In vitro cytotoxicity assay:**
B10.D2 splenocytes (WT) or ERAAP-KO spleen cells (targets) were blasted overnight with 200ng/ml LPS. The following day, target cells were washed well in PBS and labeled for 3 minutes at room temperature with PKH26 cell linker kit for membrane labeling (Sigma). Excess dye was washed away, and target cells were plated at $5x10^4$ cells/well of 96-well plate. T cells were harvested, put over a ficoll gradient (GE healthcare) to remove dead cells and mixed with labeled targets to generate indicated ratios. After 2 hours, Yo-pro-1 dye (Invitrogen) was added to each well at a final concentration of 1uM and the plate was placed on ice for 30 minutes. Cells were then immediately analyzed for the percentage of total target cells that are Yo-Pro-1 positive by flow cytometry (PKH26+YoPro-1+). To calculate relative killing (155): $100*(\%PKH26+YoPRO\text{-}1+_{E:T=X} - \%PKH26+YoPRO\text{-}1+_{E:T=0})/(100 - \%PKH26+YoPRO\text{-}1+_{E:T=0})$

**Large-scale peptide sequencing by MS/MS.** Peptide sequencing using immunoaffinity purification of pMHC complexes from detergent-solubilized spleen lysates was performed as reported previously(199). To detect peptide differences unique to tapasin-deficiency, freshly isolated spleen cells from 25 C57BL/6 and 50 tapasin-deficient mice were lysed and pMHC I was immuno-purified using mAbs Y3 (anti–H-2K$^b$) and B22.249 (anti–H-2D$^b$). In contrast, to detect peptide differences due to loss of ERAAP, freshly isolated spleen cells from 30 B10.D2 and 30 B10.D2xERAAP KO were lysed and immuno-purified using the following mAb: 34-5-8S (anti-H-2D$^d$), SF1-1.1.1( anti-H-2K$^d$) and 28-14-8S (anti-H-2L$^d$). For both experiments, samples were subject to FPLC- HPLC fractionation, and sequence identification by nanochip ESI-QTOF mass spectrometer. Peptides were identified with high confidence using an initial search with Spectrum Mill algorithm followed by expert manual spectral validation(200). To analyze the amino acid conservation of groups more than seven peptides, we used WebLogo program (http://weblogo.berkeley.edu/).

## Chapter 9: References


1. Iwasaki, A., and R. Medzhitov. 2010. Regulation of adaptive immunity by the innate immune system. *Science* 327: 291-295.
2. Starr, T. K., S. C. Jameson, and K. A. Hogquist. 2003. Positive and negative selection of T cells. *Annu Rev Immunol* 21: 139-176.
3. Harty, J. T., A. R. Tvinnereim, and D. W. White. 2000. CD8+ T cell effector mechanisms in resistance to infection. *Annu Rev Immunol* 18: 275-308.
4. Bjorkman, P. J., M. A. Saper, B. Samraoui, W. S. Bennett, J. L. Strominger, and D. C. Wiley. 1987. The foreign antigen binding site and T cell recognition regions of class I histocompatibility antigens. *Nature* 329: 512-518.
5. Falk, K., O. Rotzschke, and H. G. Rammensee. 1990. Cellular peptide composition governed by major histocompatibility complex class I molecules. *Nature* 348: 248-251.
6. Rodgers, J. R., and R. G. Cook. 2005. MHC class Ib molecules bridge innate and acquired immunity. *Nat Rev Immunol* 5: 459-471.
7. Beckman, E. M., S. A. Porcelli, C. T. Morita, S. M. Behar, S. T. Furlong, and M. B. Brenner. 1994. Recognition of a lipid antigen by CD1-restricted alpha beta+ T cells. *Nature* 372: 691-694.
8. Kjer-Nielsen, L., O. Patel, A. J. Corbett, J. Le Nours, B. Meehan, L. Liu, M. Bhati, Z. Chen, L. Kostenko, R. Reantragoon, N. A. Williamson, A. W. Purcell, N. L. Dudek, M. J. McConville, R. A. O'Hair, G. N. Khairallah, D. I. Godfrey, D. P. Fairlie, J. Rossjohn, and J. McCluskey. 2012. MR1 presents microbial vitamin B metabolites to MAIT cells. *Nature* 491: 717-723.
9. Peaper, D. R., and P. Cresswell. 2008. Regulation of MHC class I assembly and peptide binding. *Annu Rev Cell Dev Biol* 24: 343-368.
10. Allen, H., J. Fraser, D. Flyer, S. Calvin, and R. Flavell. 1986. Beta 2-microglobulin is not required for cell surface expression of the murine class I histocompatibility antigen H-2Db or of a truncated H-2Db. *Proc Natl Acad Sci U S A* 83: 7447-7451.
11. Hansen, T. H., N. B. Myers, and D. R. Lee. 1988. Studies of two antigenic forms of Ld with disparate beta 2-microglobulin (beta 2m) associations suggest that beta 2m facilitate the folding of the alpha 1 and alpha 2 domains during de novo synthesis. *J Immunol* 140: 3522-3527.
12. Williams, D. B., B. H. Barber, R. A. Flavell, and H. Allen. 1989. Role of beta 2-microglobulin in the intracellular transport and surface expression of murine class I histocompatibility molecules. *J Immunol* 142: 2796-2806.
13. Zijlstra, M., M. Bix, N. E. Simister, J. M. Loring, D. H. Raulet, and R. Jaenisch. 1990. Beta 2-microglobulin deficient mice lack CD4-8+ cytolytic T cells. *Nature* 344: 742-746.
14. Koller, B. H., P. Marrack, J. W. Kappler, and O. Smithies. 1990. Normal development of mice deficient in beta 2M, MHC class I proteins, and CD8+ T cells. *Science* 248: 1227-1230.

15. Ljunggren, H. G., L. Van Kaer, P. G. Ashton-Rickardt, S. Tonegawa, and H. L. Ploegh. 1995. Differential reactivity of residual CD8+ T lymphocytes in TAP1 and beta 2-microglobulin mutant mice. *Eur J Immunol* 25: 174-178.
16. Ljunggren, H. G., R. Glas, J. K. Sandberg, and K. Karre. 1996. Reactivity and specificity of CD8+ T cells in mice with defects in the MHC class I antigen-presenting pathway. *Immunol Rev* 151: 123-148.
17. Perarnau, B., M. F. Saron, B. Reina San Martin, N. Bervas, H. Ong, M. J. Soloski, A. G. Smith, J. M. Ure, J. E. Gairin, and F. A. Lemonnier. 1999. Single H2Kb, H2Db and double H2KbDb knockout mice: peripheral CD8+ T cell repertoire and anti-lymphocytic choriomeningitis virus cytolytic responses. *Eur J Immunol* 29: 1243-1252.
18. Vugmeyster, Y., R. Glas, B. Perarnau, F. A. Lemonnier, H. Eisen, and H. Ploegh. 1998. Major histocompatibility complex (MHC) class I KbDb -/- deficient mice possess functional CD8+ T cells and natural killer cells. *Proc Natl Acad Sci U S A* 95: 12492-12497.
19. Braaten, D. C., J. S. McClellan, I. Messaoudi, S. A. Tibbetts, K. B. McClellan, J. Nikolich-Zugich, and H. W. Virgin. 2006. Effective control of chronic gamma-herpesvirus infection by unconventional MHC Class Ia-independent CD8 T cells. *PLoS Pathog* 2: e37.
20. Swanson, P. A., 2nd, C. D. Pack, A. Hadley, C. R. Wang, I. Stroynowski, P. E. Jensen, and A. E. Lukacher. 2008. An MHC class Ib-restricted CD8 T cell response confers antiviral immunity. *J Exp Med* 205: 1647-1657.
21. Moore, M. W., F. R. Carbone, and M. J. Bevan. 1988. Introduction of soluble protein into the class I pathway of antigen processing and presentation. *Cell* 54: 777-785.
22. Yewdell, J. W., L. C. Anton, and J. R. Bennink. 1996. Defective ribosomal products (DRiPs): a major source of antigenic peptides for MHC class I molecules? *J Immunol* 157: 1823-1826.
23. Schubert, U., L. C. Anton, J. Gibbs, C. C. Norbury, J. W. Yewdell, and J. R. Bennink. 2000. Rapid degradation of a large fraction of newly synthesized proteins by proteasomes. *Nature* 404: 770-774.
24. Reits, E. A., A. C. Griekspoor, and J. Neefjes. 2000. How does TAP pump peptides? insights from DNA repair and traffic ATPases. *Immunol Today* 21: 598-600.
25. Ostankovitch, M., V. Robila, and V. H. Engelhard. 2005. Regulated folding of tyrosinase in the endoplasmic reticulum demonstrates that misfolded full-length proteins are efficient substrates for class I processing and presentation. *J Immunol* 174: 2544-2551.
26. Apcher, S., C. Daskalogianni, F. Lejeune, B. Manoury, G. Imhoos, L. Heslop, and R. Fahraeus. 2011. Major source of antigenic peptides for the MHC class I pathway is produced during the pioneer round of mRNA translation. *Proc Natl Acad Sci U S A* 108: 11572-11577.
27. Cardinaud, S., S. R. Starck, P. Chandra, and N. Shastri. 2010. The synthesis of truncated polypeptides for immune surveillance and viral evasion. *PLoS One* 5: e8692.
28. Yewdell, J. W., E. Reits, and J. Neefjes. 2003. Making sense of mass destruction: quantitating MHC class I antigen presentation. *Nat Rev Immunol* 3: 952-961.

29. Bullock, T. N., and L. C. Eisenlohr. 1996. Ribosomal scanning past the primary initiation codon as a mechanism for expression of CTL epitopes encoded in alternative reading frames. *J Exp Med* 184: 1319-1329.
30. Schwab, S. R., K. C. Li, C. Kang, and N. Shastri. 2003. Constitutive display of cryptic translation products by MHC class I molecules. *Science* 301: 1367-1371.
31. Groll, M., L. Ditzel, J. Lowe, D. Stock, M. Bochtler, H. D. Bartunik, and R. Huber. 1997. Structure of 20S proteasome from yeast at 2.4 A resolution. *Nature* 386: 463-471.
32. Sijts, E. J., and P. M. Kloetzel. 2011. The role of the proteasome in the generation of MHC class I ligands and immune responses. *Cell Mol Life Sci* 68: 1491-1502.
33. Young, P., Q. Deveraux, R. E. Beal, C. M. Pickart, and M. Rechsteiner. 1998. Characterization of two polyubiquitin binding sites in the 26 S protease subunit 5a. *J Biol Chem* 273: 5461-5467.
34. Nussbaum, A. K., T. P. Dick, W. Keilholz, M. Schirle, S. Stevanovic, K. Dietz, W. Heinemeyer, M. Groll, D. H. Wolf, R. Huber, H. G. Rammensee, and H. Schild. 1998. Cleavage motifs of the yeast 20S proteasome beta subunits deduced from digests of enolase 1. *Proc Natl Acad Sci U S A* 95: 12504-12509.
35. Rock, K. L., I. A. York, and A. L. Goldberg. 2004. Post-proteasomal antigen processing for major histocompatibility complex class I presentation. *Nat Immunol* 5: 670-677.
36. Rock, K. L., C. Gramm, L. Rothstein, K. Clark, R. Stein, L. Dick, D. Hwang, and A. L. Goldberg. 1994. Inhibitors of the proteasome block the degradation of most cell proteins and the generation of peptides presented on MHC class I molecules. *Cell* 78: 761-771.
37. Gaczynska, M., K. L. Rock, and A. L. Goldberg. 1993. Gamma-interferon and expression of MHC genes regulate peptide hydrolysis by proteasomes. *Nature* 365: 264-267.
38. Ustrell, V., G. Pratt, and M. Rechsteiner. 1995. Effects of interferon gamma and major histocompatibility complex-encoded subunits on peptidase activities of human multicatalytic proteases. *Proc Natl Acad Sci U S A* 92: 584-588.
39. Driscoll, K. E., D. G. Hassenbein, J. Carter, J. Poynter, T. N. Asquith, R. A. Grant, J. Whitten, M. P. Purdon, and R. Takigiku. 1993. Macrophage inflammatory proteins 1 and 2: expression by rat alveolar macrophages, fibroblasts, and epithelial cells and in rat lung after mineral dust exposure. *Am J Respir Cell Mol Biol* 8: 311-318.
40. Kuckelkorn, U., S. Frentzel, R. Kraft, S. Kostka, M. Groettrup, and P. M. Kloetzel. 1995. Incorporation of major histocompatibility complex--encoded subunits LMP2 and LMP7 changes the quality of the 20S proteasome polypeptide processing products independent of interferon-gamma. *Eur J Immunol* 25: 2605-2611.
41. Gaczynska, M., K. L. Rock, T. Spies, and A. L. Goldberg. 1994. Peptidase activities of proteasomes are differentially regulated by the major histocompatibility complex-encoded genes for LMP2 and LMP7. *Proc Natl Acad Sci U S A* 91: 9213-9217.
42. Glynne, R., S. H. Powis, S. Beck, A. Kelly, L. A. Kerr, and J. Trowsdale. 1991. A proteasome-related gene between the two ABC transporter loci in the class II region of the human MHC. *Nature* 353: 357-360.
43. Ortiz-Navarrete, V., A. Seelig, M. Gernold, S. Frentzel, P. M. Kloetzel, and G. J. Hammerling. 1991. Subunit of the '20S' proteasome (multicatalytic proteinase) encoded by the major histocompatibility complex. *Nature* 353: 662-664.

44. Basler, M., J. Moebius, L. Elenich, M. Groettrup, and J. J. Monaco. 2006. An altered T cell repertoire in MECL-1-deficient mice. *J Immunol* 176: 6665-6672.
45. Van Kaer, L., P. G. Ashton-Rickardt, M. Eichelberger, M. Gaczynska, K. Nagashima, K. L. Rock, A. L. Goldberg, P. C. Doherty, and S. Tonegawa. 1994. Altered peptidase and viral-specific T cell response in LMP2 mutant mice. *Immunity* 1: 533-541.
46. Nussbaum, A. K., M. P. Rodriguez-Carreno, N. Benning, J. Botten, and J. L. Whitton. 2005. Immunoproteasome-deficient mice mount largely normal CD8+ T cell responses to lymphocytic choriomeningitis virus infection and DNA vaccination. *J Immunol* 175: 1153-1160.
47. Stohwasser, R., U. Kuckelkorn, R. Kraft, S. Kostka, and P. M. Kloetzel. 1996. 20S proteasome from LMP7 knock out mice reveals altered proteolytic activities and cleavage site preferences. *FEBS Lett* 383: 109-113.
48. Fehling, H. J., W. Swat, C. Laplace, R. Kuhn, K. Rajewsky, U. Muller, and H. von Boehmer. 1994. MHC class I expression in mice lacking the proteasome subunit LMP-7. *Science* 265: 1234-1237.
49. Toes, R. E., A. K. Nussbaum, S. Degermann, M. Schirle, N. P. Emmerich, M. Kraft, C. Laplace, A. Zwinderman, T. P. Dick, J. Muller, B. Schonfisch, C. Schmid, H. J. Fehling, S. Stevanovic, H. G. Rammensee, and H. Schild. 2001. Discrete cleavage motifs of constitutive and immunoproteasomes revealed by quantitative analysis of cleavage products. *J Exp Med* 194: 1-12.
50. Osterloh, P., K. Linkemann, S. Tenzer, H. G. Rammensee, M. P. Radsak, D. H. Busch, and H. Schild. 2006. Proteasomes shape the repertoire of T cells participating in antigen-specific immune responses. *Proc Natl Acad Sci U S A* 103: 5042-5047.
51. Kincaid, E. Z., J. W. Che, I. York, H. Escobar, E. Reyes-Vargas, J. C. Delgado, R. M. Welsh, M. L. Karow, A. J. Murphy, D. M. Valenzuela, G. D. Yancopoulos, and K. L. Rock. 2012. Mice completely lacking immunoproteasomes show major changes in antigen presentation. *Nat Immunol* 13: 129-135.
52. Kloetzel, P. M. 2004. Generation of major histocompatibility complex class I antigens: functional interplay between proteasomes and TPPII. *Nat Immunol* 5: 661-669.
53. Geier, E., G. Pfeifer, M. Wilm, M. Lucchiari-Hartz, W. Baumeister, K. Eichmann, and G. Niedermann. 1999. A giant protease with potential to substitute for some functions of the proteasome. *Science* 283: 978-981.
54. Guil, S., M. Rodriguez-Castro, F. Aguilar, E. M. Villasevil, L. C. Anton, and M. Del Val. 2006. Need for tripeptidyl-peptidase II in major histocompatibility complex class I viral antigen processing when proteasomes are detrimental. *J Biol Chem* 281: 39925-39934.
55. Seifert, U., C. Maranon, A. Shmueli, J. F. Desoutter, L. Wesoloski, K. Janek, P. Henklein, S. Diescher, M. Andrieu, H. de la Salle, T. Weinschenk, H. Schild, D. Laderach, A. Galy, G. Haas, P. M. Kloetzel, Y. Reiss, and A. Hosmalin. 2003. An essential role for tripeptidyl peptidase in the generation of an MHC class I epitope. *Nat Immunol* 4: 375-379.
56. Levy, F., L. Burri, S. Morel, A. L. Peitrequin, N. Levy, A. Bachi, U. Hellman, B. J. Van den Eynde, and C. Servis. 2002. The final N-terminal trimming of a subaminoterminal proline-containing HLA class I-restricted antigenic peptide in the cytosol is mediated by two peptidases. *J Immunol* 169: 4161-4171.

57. York, I. A., N. Bhutani, S. Zendzian, A. L. Goldberg, and K. L. Rock. 2006. Tripeptidyl peptidase II is the major peptidase needed to trim long antigenic precursors, but is not required for most MHC class I antigen presentation. *J Immunol* 177: 1434-1443.
58. Kawahara, M., I. A. York, A. Hearn, D. Farfan, and K. L. Rock. 2009. Analysis of the role of tripeptidyl peptidase II in MHC class I antigen presentation in vivo. *J Immunol* 183: 6069-6077.
59. Huai, J., E. Firat, A. Nil, D. Million, S. Gaedicke, B. Kanzler, M. Freudenberg, P. van Endert, G. Kohler, H. L. Pahl, P. Aichele, K. Eichmann, and G. Niedermann. 2008. Activation of cellular death programs associated with immunosenescence-like phenotype in TPPII knockout mice. *Proc Natl Acad Sci U S A* 105: 5177-5182.
60. Firat, E., J. Huai, L. Saveanu, S. Gaedicke, P. Aichele, K. Eichmann, P. van Endert, and G. Niedermann. 2007. Analysis of direct and cross-presentation of antigens in TPPII knockout mice. *J Immunol* 179: 8137-8145.
61. Knight, C. G., P. M. Dando, and A. J. Barrett. 1995. Thimet oligopeptidase specificity: evidence of preferential cleavage near the C-terminus and product inhibition from kinetic analysis of peptide hydrolysis. *Biochem J* 308 ( Pt 1): 145-150.
62. Kessler, J. H., S. Khan, U. Seifert, S. Le Gall, K. M. Chow, A. Paschen, S. A. Bres-Vloemans, A. de Ru, N. van Montfoort, K. L. Franken, W. E. Benckhuijsen, J. M. Brooks, T. van Hall, K. Ray, A. Mulder, Doxiadis, II, P. F. van Swieten, H. S. Overkleeft, A. Prat, B. Tomkinson, J. Neefjes, P. M. Kloetzel, D. W. Rodgers, L. B. Hersh, J. W. Drijfhout, P. A. van Veelen, F. Ossendorp, and C. J. Melief. 2011. Antigen processing by nardilysin and thimet oligopeptidase generates cytotoxic T cell epitopes. *Nat Immunol* 12: 45-53.
63. Saric, T., C. I. Graef, and A. L. Goldberg. 2004. Pathway for degradation of peptides generated by proteasomes: a key role for thimet oligopeptidase and other metallopeptidases. *J Biol Chem* 279: 46723-46732.
64. York, I. A., A. X. Mo, K. Lemerise, W. Zeng, Y. Shen, C. R. Abraham, T. Saric, A. L. Goldberg, and K. L. Rock. 2003. The cytosolic endopeptidase, thimet oligopeptidase, destroys antigenic peptides and limits the extent of MHC class I antigen presentation. *Immunity* 18: 429-440.
65. Stoltze, L., M. Schirle, G. Schwarz, C. Schroter, M. W. Thompson, L. B. Hersh, H. Kalbacher, S. Stevanovic, H. G. Rammensee, and H. Schild. 2000. Two new proteases in the MHC class I processing pathway. *Nat Immunol* 1: 413-418.
66. Kim, E., H. Kwak, and K. Ahn. 2009. Cytosolic aminopeptidases influence MHC class I-mediated antigen presentation in an allele-dependent manner. *J Immunol* 183: 7379-7387.
67. Towne, C. F., I. A. York, L. B. Watkin, J. S. Lazo, and K. L. Rock. 2007. Analysis of the role of bleomycin hydrolase in antigen presentation and the generation of CD8 T cell responses. *J Immunol* 178: 6923-6930.
68. Beninga, J., K. L. Rock, and A. L. Goldberg. 1998. Interferon-gamma can stimulate post-proteasomal trimming of the N terminus of an antigenic peptide by inducing leucine aminopeptidase. *J Biol Chem* 273: 18734-18742.
69. Reits, E., A. Griekspoor, J. Neijssen, T. Groothuis, K. Jalink, P. van Veelen, H. Janssen, J. Calafat, J. W. Drijfhout, and J. Neefjes. 2003. Peptide diffusion, protection, and degradation in nuclear and cytoplasmic compartments before antigen presentation by MHC class I. *Immunity* 18: 97-108.

70. Towne, C. F., I. A. York, J. Neijssen, M. L. Karow, A. J. Murphy, D. M. Valenzuela, G. D. Yancopoulos, J. J. Neefjes, and K. L. Rock. 2005. Leucine aminopeptidase is not essential for trimming peptides in the cytosol or generating epitopes for MHC class I antigen presentation. *J Immunol* 175: 6605-6614.
71. Towne, C. F., I. A. York, J. Neijssen, M. L. Karow, A. J. Murphy, D. M. Valenzuela, G. D. Yancopoulos, J. J. Neefjes, and K. L. Rock. 2008. Puromycin-sensitive aminopeptidase limits MHC class I presentation in dendritic cells but does not affect CD8 T cell responses during viral infections. *J Immunol* 180: 1704-1712.
72. Kisselev, A. F., T. N. Akopian, K. M. Woo, and A. L. Goldberg. 1999. The sizes of peptides generated from protein by mammalian 26 and 20 S proteasomes. Implications for understanding the degradative mechanism and antigen presentation. *J Biol Chem* 274: 3363-3371.
73. Yewdell, J. W. 2001. Not such a dismal science: the economics of protein synthesis, folding, degradation and antigen processing. *Trends Cell Biol* 11: 294-297.
74. Ishii, T., H. Udono, T. Yamano, H. Ohta, A. Uenaka, T. Ono, A. Hizuta, N. Tanaka, P. K. Srivastava, and E. Nakayama. 1999. Isolation of MHC class I-restricted tumor antigen peptide and its precursors associated with heat shock proteins hsp70, hsp90, and gp96. *J Immunol* 162: 1303-1309.
75. Binder, R. J., and P. K. Srivastava. 2005. Peptides chaperoned by heat-shock proteins are a necessary and sufficient source of antigen in the cross-priming of CD8+ T cells. *Nat Immunol* 6: 593-599.
76. Imai, T., Y. Kato, C. Kajiwara, S. Mizukami, I. Ishige, T. Ichiyanagi, M. Hikida, J. Y. Wang, and H. Udono. 2011. Heat shock protein 90 (HSP90) contributes to cytosolic translocation of extracellular antigen for cross-presentation by dendritic cells. *Proc Natl Acad Sci U S A* 108: 16363-16368.
77. Arnold, D., S. Faath, H. Rammensee, and H. Schild. 1995. Cross-priming of minor histocompatibility antigen-specific cytotoxic T cells upon immunization with the heat shock protein gp96. *J Exp Med* 182: 885-889.
78. Binder, R. J., N. E. Blachere, and P. K. Srivastava. 2001. Heat shock protein-chaperoned peptides but not free peptides introduced into the cytosol are presented efficiently by major histocompatibility complex I molecules. *J Biol Chem* 276: 17163-17171.
79. Kunisawa, J., and N. Shastri. 2006. Hsp90alpha chaperones large C-terminally extended proteolytic intermediates in the MHC class I antigen processing pathway. *Immunity* 24: 523-534.
80. Callahan, M. K., M. Garg, and P. K. Srivastava. 2008. Heat-shock protein 90 associates with N-terminal extended peptides and is required for direct and indirect antigen presentation. *Proc Natl Acad Sci U S A* 105: 1662-1667.
81. MacAry, P. A., B. Javid, R. A. Floto, K. G. Smith, W. Oehlmann, M. Singh, and P. J. Lehner. 2004. HSP70 peptide binding mutants separate antigen delivery from dendritic cell stimulation. *Immunity* 20: 95-106.
82. Millar, D. G., K. M. Garza, B. Odermatt, A. R. Elford, N. Ono, Z. Li, and P. S. Ohashi. 2003. Hsp70 promotes antigen-presenting cell function and converts T-cell tolerance to autoimmunity in vivo. *Nat Med* 9: 1469-1476.
83. Lammert, E., D. Arnold, M. Nijenhuis, F. Momburg, G. J. Hammerling, J. Brunner, S. Stevanovic, H. G. Rammensee, and H. Schild. 1997. The endoplasmic reticulum-

resident stress protein gp96 binds peptides translocated by TAP. *Eur J Immunol* 27: 923-927.
84. Arnold, D., C. Wahl, S. Faath, H. G. Rammensee, and H. Schild. 1997. Influences of transporter associated with antigen processing (TAP) on the repertoire of peptides associated with the endoplasmic reticulum-resident stress protein gp96. *J Exp Med* 186: 461-466.
85. Randow, F., and B. Seed. 2001. Endoplasmic reticulum chaperone gp96 is required for innate immunity but not cell viability. *Nat Cell Biol* 3: 891-896.
86. Kubota, H., G. Hynes, and K. Willison. 1995. The chaperonin containing t-complex polypeptide 1 (TCP-1). Multisubunit machinery assisting in protein folding and assembly in the eukaryotic cytosol. *Eur J Biochem* 230: 3-16.
87. Kunisawa, J., and N. Shastri. 2003. The group II chaperonin TRiC protects proteolytic intermediates from degradation in the MHC class I antigen processing pathway. *Mol Cell* 12: 565-576.
88. Vatner, R. E., and P. K. Srivastava. 2010. The tailless complex polypeptide-1 ring complex of the heat shock protein 60 family facilitates cross-priming of CD8 responses specific for chaperoned peptides. *J Immunol* 185: 6765-6773.
89. Pamer, E., and P. Cresswell. 1998. Mechanisms of MHC class I--restricted antigen processing. *Annu Rev Immunol* 16: 323-358.
90. Elliott, T., and A. Williams. 2005. The optimization of peptide cargo bound to MHC class I molecules by the peptide-loading complex. *Immunol Rev* 207: 89-99.
91. Ortmann, B., J. Copeman, P. J. Lehner, B. Sadasivan, J. A. Herberg, A. G. Grandea, S. R. Riddell, R. Tampe, T. Spies, J. Trowsdale, and P. Cresswell. 1997. A critical role for tapasin in the assembly and function of multimeric MHC class I-TAP complexes. *Science* 277: 1306-1309.
92. Schrag, J. D., J. J. Bergeron, Y. Li, S. Borisova, M. Hahn, D. Y. Thomas, and M. Cygler. 2001. The Structure of calnexin, an ER chaperone involved in quality control of protein folding. *Mol Cell* 8: 633-644.
93. Gao, B., R. Adhikari, M. Howarth, K. Nakamura, M. C. Gold, A. B. Hill, R. Knee, M. Michalak, and T. Elliott. 2002. Assembly and antigen-presenting function of MHC class I molecules in cells lacking the ER chaperone calreticulin. *Immunity* 16: 99-109.
94. van Leeuwen, J. E., and K. P. Kearse. 1996. Deglucosylation of N-linked glycans is an important step in the dissociation of calreticulin-class I-TAP complexes. *Proc Natl Acad Sci U S A* 93: 13997-14001.
95. Sadasivan, B., P. J. Lehner, B. Ortmann, T. Spies, and P. Cresswell. 1996. Roles for calreticulin and a novel glycoprotein, tapasin, in the interaction of MHC class I molecules with TAP. *Immunity* 5: 103-114.
96. Farmery, M. R., S. Allen, A. J. Allen, and N. J. Bulleid. 2000. The role of ERp57 in disulfide bond formation during the assembly of major histocompatibility complex class I in a synchronized semipermeabilized cell translation system. *J Biol Chem* 275: 14933-14938.
97. Harris, M. R., Y. Y. Yu, C. S. Kindle, T. H. Hansen, and J. C. Solheim. 1998. Calreticulin and calnexin interact with different protein and glycan determinants during the assembly of MHC class I. *J Immunol* 160: 5404-5409.

98. Jackson, M. R., M. F. Cohen-Doyle, P. A. Peterson, and D. B. Williams. 1994. Regulation of MHC class I transport by the molecular chaperone, calnexin (p88, IP90). *Science* 263: 384-387.
99. Nossner, E., and P. Parham. 1995. Species-specific differences in chaperone interaction of human and mouse major histocompatibility complex class I molecules. *J Exp Med* 181: 327-337.
100. Scott, J. E., and J. R. Dawson. 1995. MHC class I expression and transport in a calnexin-deficient cell line. *J Immunol* 155: 143-148.
101. Kraus, A., J. Groenendyk, K. Bedard, T. A. Baldwin, K. H. Krause, M. Dubois-Dauphin, J. Dyck, E. E. Rosenbaum, L. Korngut, N. J. Colley, S. Gosgnach, D. Zochodne, K. Todd, L. B. Agellon, and M. Michalak. 2010. Calnexin deficiency leads to dysmyelination. *J Biol Chem* 285: 18928-18938.
102. Johnson, S., M. Michalak, M. Opas, and P. Eggleton. 2001. The ins and outs of calreticulin: from the ER lumen to the extracellular space. *Trends Cell Biol* 11: 122-129.
103. Guo, L., K. Nakamura, J. Lynch, M. Opas, E. N. Olson, L. B. Agellon, and M. Michalak. 2002. Cardiac-specific expression of calcineurin reverses embryonic lethality in calreticulin-deficient mouse. *J Biol Chem* 277: 50776-50779.
104. Del Cid, N., E. Jeffery, S. M. Rizvi, E. Stamper, L. R. Peters, W. C. Brown, C. Provoda, and M. Raghavan. 2010. Modes of calreticulin recruitment to the major histocompatibility complex class I assembly pathway. *J Biol Chem* 285: 4520-4535.
105. Fu, H., C. Liu, B. Flutter, H. Tao, and B. Gao. 2009. Calreticulin maintains the low threshold of peptide required for efficient antigen presentation. *Mol Immunol* 46: 3198-3206.
106. Spies, T., M. Bresnahan, S. Bahram, D. Arnold, G. Blanck, E. Mellins, D. Pious, and R. DeMars. 1990. A gene in the human major histocompatibility complex class II region controlling the class I antigen presentation pathway. *Nature* 348: 744-747.
107. Trowsdale, J., I. Hanson, I. Mockridge, S. Beck, A. Townsend, and A. Kelly. 1990. Sequences encoded in the class II region of the MHC related to the 'ABC' superfamily of transporters. *Nature* 348: 741-744.
108. Deverson, E. V., I. R. Gow, W. J. Coadwell, J. J. Monaco, G. W. Butcher, and J. C. Howard. 1990. MHC class II region encoding proteins related to the multidrug resistance family of transmembrane transporters. *Nature* 348: 738-741.
109. Monaco, J. J., S. Cho, and M. Attaya. 1990. Transport protein genes in the murine MHC: possible implications for antigen processing. *Science* 250: 1723-1726.
110. Ma, W., P. J. Lehner, P. Cresswell, J. S. Pober, and D. R. Johnson. 1997. Interferon-gamma rapidly increases peptide transporter (TAP) subunit expression and peptide transport capacity in endothelial cells. *J Biol Chem* 272: 16585-16590.
111. Karttunen, J. T., P. J. Lehner, S. S. Gupta, E. W. Hewitt, and P. Cresswell. 2001. Distinct functions and cooperative interaction of the subunits of the transporter associated with antigen processing (TAP). *Proc Natl Acad Sci U S A* 98: 7431-7436.
112. Nijenhuis, M., S. Schmitt, E. A. Armandola, R. Obst, J. Brunner, and G. J. Hammerling. 1996. Identification of a contact region for peptide on the TAP1 chain of the transporter associated with antigen processing. *J Immunol* 156: 2186-2195.

113. van Endert, P. M., D. Riganelli, G. Greco, K. Fleischhauer, J. Sidney, A. Sette, and J. F. Bach. 1995. The peptide-binding motif for the human transporter associated with antigen processing. *J Exp Med* 182: 1883-1895.
114. Momburg, F., J. Roelse, J. C. Howard, G. W. Butcher, G. J. Hammerling, and J. J. Neefjes. 1994. Selectivity of MHC-encoded peptide transporters from human, mouse and rat. *Nature* 367: 648-651.
115. Burgevin, A., L. Saveanu, Y. Kim, E. Barilleau, M. Kotturi, A. Sette, P. van Endert, and B. Peters. 2008. A detailed analysis of the murine TAP transporter substrate specificity. *PLoS One* 3: e2402.
116. Neisig, A., J. Roelse, A. J. Sijts, F. Ossendorp, M. C. Feltkamp, W. M. Kast, C. J. Melief, and J. J. Neefjes. 1995. Major differences in transporter associated with antigen presentation (TAP)-dependent translocation of MHC class I-presentable peptides and the effect of flanking sequences. *J Immunol* 154: 1273-1279.
117. Rammensee, H. G., T. Friede, and S. Stevanoviic. 1995. MHC ligands and peptide motifs: first listing. *Immunogenetics* 41: 178-228.
118. Spies, T., and R. DeMars. 1991. Restored expression of major histocompatibility class I molecules by gene transfer of a putative peptide transporter. *Nature* 351: 323-324.
119. Van Kaer, L., P. G. Ashton-Rickardt, H. L. Ploegh, and S. Tonegawa. 1992. TAP1 mutant mice are deficient in antigen presentation, surface class I molecules, and CD4-8+ T cells. *Cell* 71: 1205-1214.
120. Wei, M. L., and P. Cresswell. 1992. HLA-A2 molecules in an antigen-processing mutant cell contain signal sequence-derived peptides. *Nature* 356: 443-446.
121. van Hall, T., E. Z. Wolpert, P. van Veelen, S. Laban, M. van der Veer, M. Roseboom, S. Bres, P. Grufman, A. de Ru, H. Meiring, A. de Jong, K. Franken, A. Teixeira, R. Valentijn, J. W. Drijfhout, F. Koning, M. Camps, F. Ossendorp, K. Karre, H. G. Ljunggren, C. J. Melief, and R. Offringa. 2006. Selective cytotoxic T-lymphocyte targeting of tumor immune escape variants. *Nat Med* 12: 417-424.
122. Weinzierl, A. O., D. Rudolf, N. Hillen, S. Tenzer, P. van Endert, H. Schild, H. G. Rammensee, and S. Stevanovic. 2008. Features of TAP-independent MHC class I ligands revealed by quantitative mass spectrometry. *Eur J Immunol* 38: 1503-1510.
123. Helenius, A., and M. Aebi. 2004. Roles of N-linked glycans in the endoplasmic reticulum. *Annu Rev Biochem* 73: 1019-1049.
124. Ellgaard, L., and L. W. Ruddock. 2005. The human protein disulphide isomerase family: substrate interactions and functional properties. *EMBO Rep* 6: 28-32.
125. Smith, J. D., J. C. Solheim, B. M. Carreno, and T. H. Hansen. 1995. Characterization of class I MHC folding intermediates and their disparate interactions with peptide and beta 2-microglobulin. *Mol Immunol* 32: 531-540.
126. Dong, G., P. A. Wearsch, D. R. Peaper, P. Cresswell, and K. M. Reinisch. 2009. Insights into MHC class I peptide loading from the structure of the tapasin-ERp57 thiol oxidoreductase heterodimer. *Immunity* 30: 21-32.
127. Peaper, D. R., P. A. Wearsch, and P. Cresswell. 2005. Tapasin and ERp57 form a stable disulfide-linked dimer within the MHC class I peptide-loading complex. *Embo J* 24: 3613-3623.
128. Wearsch, P. A., and P. Cresswell. 2007. Selective loading of high-affinity peptides onto major histocompatibility complex class I molecules by the tapasin-ERp57 heterodimer. *Nat Immunol* 8: 873-881.

129. Garbi, N., S. Tanaka, F. Momburg, and G. J. Hammerling. 2006. Impaired assembly of the major histocompatibility complex class I peptide-loading complex in mice deficient in the oxidoreductase ERp57. *Nat Immunol* 7: 93-102.
130. Grandea, A. G., 3rd, T. N. Golovina, S. E. Hamilton, V. Sriram, T. Spies, R. R. Brutkiewicz, J. T. Harty, L. C. Eisenlohr, and L. Van Kaer. 2000. Impaired assembly yet normal trafficking of MHC class I molecules in Tapasin mutant mice. *Immunity* 13: 213-222.
131. Suh, W. K., M. A. Derby, M. F. Cohen-Doyle, G. J. Schoenhals, K. Fruh, J. A. Berzofsky, and D. B. Williams. 1999. Interaction of murine MHC class I molecules with tapasin and TAP enhances peptide loading and involves the heavy chain alpha3 domain. *J Immunol* 162: 1530-1540.
132. Tan, P., H. Kropshofer, O. Mandelboim, N. Bulbuc, G. J. Hammerling, and F. Momburg. 2002. Recruitment of MHC class I molecules by tapasin into the transporter associated with antigen processing-associated complex is essential for optimal peptide loading. *J Immunol* 168: 1950-1960.
133. Simone, L. C., C. J. Georgesen, P. D. Simone, X. Wang, and J. C. Solheim. 2012. Productive association between MHC class I and tapasin requires the tapasin transmembrane/cytosolic region and the tapasin C-terminal Ig-like domain. *Mol Immunol* 49: 628-639.
134. Dick, T. P., N. Bangia, D. R. Peaper, and P. Cresswell. 2002. Disulfide bond isomerization and the assembly of MHC class I-peptide complexes. *Immunity* 16: 87-98.
135. Bangia, N., P. J. Lehner, E. A. Hughes, M. Surman, and P. Cresswell. 1999. The N-terminal region of tapasin is required to stabilize the MHC class I loading complex. *Eur J Immunol* 29: 1858-1870.
136. Garbi, N., N. Tiwari, F. Momburg, and G. J. Hammerling. 2003. A major role for tapasin as a stabilizer of the TAP peptide transporter and consequences for MHC class I expression. *Eur J Immunol* 33: 264-273.
137. Park, B., S. Lee, E. Kim, and K. Ahn. 2003. A single polymorphic residue within the peptide-binding cleft of MHC class I molecules determines spectrum of tapasin dependence. *J Immunol* 170: 961-968.
138. Sieker, F., T. P. Straatsma, S. Springer, and M. Zacharias. 2008. Differential tapasin dependence of MHC class I molecules correlates with conformational changes upon peptide dissociation: a molecular dynamics simulation study. *Mol Immunol* 45: 3714-3722.
139. Simone, L. C., A. Tuli, P. D. Simone, X. Wang, and J. C. Solheim. 2012. Analysis of major histocompatibility complex class I folding: novel insights into intermediate forms. *Tissue Antigens* 79: 249-262.
140. Zarling, A. L., C. J. Luckey, J. A. Marto, F. M. White, C. J. Brame, A. M. Evans, P. J. Lehner, P. Cresswell, J. Shabanowitz, D. F. Hunt, and V. H. Engelhard. 2003. Tapasin is a facilitator, not an editor, of class I MHC peptide binding. *J Immunol* 171: 5287-5295.
141. Lewis, J. W., and T. Elliott. 1998. Evidence for successive peptide binding and quality control stages during MHC class I assembly. *Curr Biol* 8: 717-720.
142. Chen, M., and M. Bouvier. 2007. Analysis of interactions in a tapasin/class I complex provides a mechanism for peptide selection. *Embo J* 26: 1681-1690.

143. Howarth, M., A. Williams, A. B. Tolstrup, and T. Elliott. 2004. Tapasin enhances MHC class I peptide presentation according to peptide half-life. *Proc Natl Acad Sci U S A* 101: 11737-11742.
144. Serwold, T., F. Gonzalez, J. Kim, R. Jacob, and N. Shastri. 2002. ERAAP customizes peptides for MHC class I molecules in the endoplasmic reticulum. *Nature* 419: 480-483.
145. Cui, X., F. Hawari, S. Alsaaty, M. Lawrence, C. A. Combs, W. Geng, F. N. Rouhani, D. Miskinis, and S. J. Levine. 2002. Identification of ARTS-1 as a novel TNFR1-binding protein that promotes TNFR1 ectodomain shedding. *J Clin Invest* 110: 515-526.
146. Hattori, A., K. Kitatani, H. Matsumoto, S. Miyazawa, T. Rogi, N. Tsuruoka, S. Mizutani, Y. Natori, and M. Tsujimoto. 2000. Characterization of recombinant human adipocyte-derived leucine aminopeptidase expressed in Chinese hamster ovary cells. *J Biochem* 128: 755-762.
147. Tsujimoto, M., and A. Hattori. 2005. The oxytocinase subfamily of M1 aminopeptidases. *Biochim Biophys Acta* 1751: 9-18.
148. Nguyen, T. T., S. C. Chang, I. Evnouchidou, I. A. York, C. Zikos, K. L. Rock, A. L. Goldberg, E. Stratikos, and L. J. Stern. 2011. Structural basis for antigenic peptide precursor processing by the endoplasmic reticulum aminopeptidase ERAP1. *Nat Struct Mol Biol* 18: 604-613.
149. Chang, S. C., F. Momburg, N. Bhutani, and A. L. Goldberg. 2005. The ER aminopeptidase, ERAP1, trims precursors to lengths of MHC class I peptides by a "molecular ruler" mechanism. *Proc Natl Acad Sci U S A* 102: 17107-17112.
150. Evnouchidou, I., F. Momburg, A. Papakyriakou, A. Chroni, L. Leondiadis, S. C. Chang, A. L. Goldberg, and E. Stratikos. 2008. The internal sequence of the peptide-substrate determines its N-terminus trimming by ERAP1. *PLoS One* 3: e3658.
151. Brouwenstijn, N., T. Serwold, and N. Shastri. 2001. MHC class I molecules can direct proteolytic cleavage of antigenic precursors in the endoplasmic reticulum. *Immunity* 15: 95-104.
152. Kanaseki, T., N. Blanchard, G. E. Hammer, F. Gonzalez, and N. Shastri. 2006. ERAAP synergizes with MHC class I molecules to make the final cut in the antigenic peptide precursors in the endoplasmic reticulum. *Immunity* 25: 795-806.
153. Hammer, G. E., F. Gonzalez, M. Champsaur, D. Cado, and N. Shastri. 2006. The aminopeptidase ERAAP shapes the peptide repertoire displayed by major histocompatibility complex class I molecules. *Nat Immunol* 7: 103-112.
154. Hammer, G. E., F. Gonzalez, E. James, H. Nolla, and N. Shastri. 2007. In the absence of aminopeptidase ERAAP, MHC class I molecules present many unstable and highly immunogenic peptides. *Nat Immunol* 8: 101-108.
155. Nagarajan, N. A., F. Gonzalez, and N. Shastri. 2012. Nonclassical MHC class Ib-restricted cytotoxic T cells monitor antigen processing in the endoplasmic reticulum. *Nat Immunol* 13: 579-586.
156. York, I. A., M. A. Brehm, S. Zendzian, C. F. Towne, and K. L. Rock. 2006. Endoplasmic reticulum aminopeptidase 1 (ERAP1) trims MHC class I-presented peptides in vivo and plays an important role in immunodominance. *Proc Natl Acad Sci U S A* 103: 9202-9207.
157. Yan, J., V. V. Parekh, Y. Mendez-Fernandez, D. Olivares-Villagomez, S. Dragovic, T. Hill, D. C. Roopenian, S. Joyce, and L. Van Kaer. 2006. In vivo role of ER-associated

peptidase activity in tailoring peptides for presentation by MHC class Ia and class Ib molecules. *J Exp Med* 203: 647-659.
158. Firat, E., L. Saveanu, P. Aichele, P. Staeheli, J. Huai, S. Gaedicke, A. Nil, G. Besin, B. Kanzler, P. van Endert, and G. Niedermann. 2007. The role of endoplasmic reticulum-associated aminopeptidase 1 in immunity to infection and in cross-presentation. *J Immunol* 178: 2241-2248.
159. Blanchard, N., T. Kanaseki, H. Escobar, F. Delebecque, N. A. Nagarajan, E. Reyes-Vargas, D. K. Crockett, D. H. Raulet, J. C. Delgado, and N. Shastri. 2010. Endoplasmic reticulum aminopeptidase associated with antigen processing defines the composition and structure of MHC class I peptide repertoire in normal and virus-infected cells. *J Immunol* 184: 3033-3042.
160. Tanioka, T., A. Hattori, S. Mizutani, and M. Tsujimoto. 2005. Regulation of the human leukocyte-derived arginine aminopeptidase/endoplasmic reticulum-aminopeptidase 2 gene by interferon-gamma. *Febs J* 272: 916-928.
161. Saveanu, L., O. Carroll, V. Lindo, M. Del Val, D. Lopez, Y. Lepelletier, F. Greer, L. Schomburg, D. Fruci, G. Niedermann, and P. M. van Endert. 2005. Concerted peptide trimming by human ERAP1 and ERAP2 aminopeptidase complexes in the endoplasmic reticulum. *Nat Immunol* 6: 689-697.
162. Zervoudi, E., A. Papakyriakou, D. Georgiadou, I. Evnouchidou, A. Gajda, M. Poreba, G. S. Salvesen, M. Drag, A. Hattori, L. Swevers, D. Vourloumis, and E. Stratikos. 2011. Probing the S1 specificity pocket of the aminopeptidases that generate antigenic peptides. *Biochem J* 435: 411-420.
163. Birtley, J. R., E. Saridakis, E. Stratikos, and I. M. Mavridis. 2012. The crystal structure of human endoplasmic reticulum aminopeptidase 2 reveals the atomic basis for distinct roles in antigen processing. *Biochemistry* 51: 286-295.
164. Harmer, D., M. Gilbert, R. Borman, and K. L. Clark. 2002. Quantitative mRNA expression profiling of ACE 2, a novel homologue of angiotensin converting enzyme. *FEBS Lett* 532: 107-110.
165. Danilov, S. M., E. Sadovnikova, N. Scharenborg, I. V. Balyasnikova, D. A. Svinareva, E. L. Semikina, E. N. Parovichnikova, V. G. Savchenko, and G. J. Adema. 2003. Angiotensin-converting enzyme (CD143) is abundantly expressed by dendritic cells and discriminates human monocyte-derived dendritic cells from acute myeloid leukemia-derived dendritic cells. *Exp Hematol* 31: 1301-1309.
166. Saijonmaa, O., T. Nyman, and F. Fyhrquist. 2007. Atorvastatin inhibits angiotensin-converting enzyme induction in differentiating human macrophages. *Am J Physiol Heart Circ Physiol* 292: H1917-1921.
167. Shen, X. Z., S. Billet, C. Lin, D. Okwan-Duodu, X. Chen, A. E. Lukacher, and K. E. Bernstein. 2011. The carboxypeptidase ACE shapes the MHC class I peptide repertoire. *Nat Immunol* 12: 1078-1085.
168. Eisenlohr, L. C., I. Bacik, J. R. Bennink, K. Bernstein, and J. W. Yewdell. 1992. Expression of a membrane protease enhances presentation of endogenous antigens to MHC class I-restricted T lymphocytes. *Cell* 71: 963-972.
169. Kim, S., S. Lee, J. Shin, Y. Kim, I. Evnouchidou, D. Kim, Y. K. Kim, Y. E. Kim, J. H. Ahn, S. R. Riddell, E. Stratikos, V. N. Kim, and K. Ahn. 2011. Human cytomegalovirus microRNA miR-US4-1 inhibits CD8(+) T cell responses by targeting the aminopeptidase ERAP1. *Nat Immunol*.

170. Fruci, D., P. Giacomini, M. R. Nicotra, M. Forloni, R. Fraioli, L. Saveanu, P. van Endert, and P. G. Natali. 2008. Altered expression of endoplasmic reticulum aminopeptidases ERAP1 and ERAP2 in transformed non-lymphoid human tissues. *J Cell Physiol* 216: 742-749.
171. Burton, P. R., D. G. Clayton, L. R. Cardon, N. Craddock, P. Deloukas, A. Duncanson, D. P. Kwiatkowski, M. I. McCarthy, W. H. Ouwehand, N. J. Samani, J. A. Todd, P. Donnelly, J. C. Barrett, D. Davison, D. Easton, D. M. Evans, H. T. Leung, J. L. Marchini, A. P. Morris, C. C. Spencer, M. D. Tobin, A. P. Attwood, J. P. Boorman, B. Cant, U. Everson, J. M. Hussey, J. D. Jolley, A. S. Knight, K. Koch, E. Meech, S. Nutland, C. V. Prowse, H. E. Stevens, N. C. Taylor, G. R. Walters, N. M. Walker, N. A. Watkins, T. Winzer, R. W. Jones, W. L. McArdle, S. M. Ring, D. P. Strachan, M. Pembrey, G. Breen, D. St Clair, S. Caesar, K. Gordon-Smith, L. Jones, C. Fraser, E. K. Green, D. Grozeva, M. L. Hamshere, P. A. Holmans, I. R. Jones, G. Kirov, V. Moskivina, I. Nikolov, M. C. O'Donovan, M. J. Owen, D. A. Collier, A. Elkin, A. Farmer, R. Williamson, P. McGuffin, A. H. Young, I. N. Ferrier, S. G. Ball, A. J. Balmforth, J. H. Barrett, T. D. Bishop, M. M. Iles, A. Maqbool, N. Yuldasheva, A. S. Hall, P. S. Braund, R. J. Dixon, M. Mangino, S. Stevens, J. R. Thompson, F. Bredin, M. Tremelling, M. Parkes, H. Drummond, C. W. Lees, E. R. Nimmo, J. Satsangi, S. A. Fisher, A. Forbes, C. M. Lewis, C. M. Onnie, N. J. Prescott, J. Sanderson, C. G. Matthew, J. Barbour, M. K. Mohiuddin, C. E. Todhunter, J. C. Mansfield, T. Ahmad, F. R. Cummings, D. P. Jewell, J. Webster, M. J. Brown, M. G. Lathrop, J. Connell, A. Dominiczak, C. A. Marcano, B. Burke, R. Dobson, J. Gungadoo, K. L. Lee, P. B. Munroe, S. J. Newhouse, A. Onipinla, C. Wallace, M. Xue, M. Caulfield, M. Farrall, A. Barton, I. N. Bruce, H. Donovan, S. Eyre, P. D. Gilbert, S. L. Hilder, A. M. Hinks, S. L. John, C. Potter, A. J. Silman, D. P. Symmons, W. Thomson, J. Worthington, D. B. Dunger, B. Widmer, T. M. Frayling, R. M. Freathy, H. Lango, J. R. Perry, B. M. Shields, M. N. Weedon, A. T. Hattersley, G. A. Hitman, M. Walker, K. S. Elliott, C. J. Groves, C. M. Lindgren, N. W. Rayner, N. J. Timpson, E. Zeggini, M. Newport, G. Sirugo, E. Lyons, F. Vannberg, A. V. Hill, L. A. Bradbury, C. Farrar, J. J. Pointon, P. Wordsworth, M. A. Brown, J. A. Franklyn, J. M. Heward, M. J. Simmonds, S. C. Gough, S. Seal, M. R. Stratton, N. Rahman, M. Ban, A. Goris, S. J. Sawcer, A. Compston, D. Conway, M. Jallow, K. A. Rockett, S. J. Bumpstead, A. Chaney, K. Downes, M. J. Ghori, R. Gwilliam, S. E. Hunt, M. Inouye, A. Keniry, E. King, R. McGinnis, S. Potter, R. Ravindrarajah, P. Whittaker, C. Widden, D. Withers, N. J. Cardin, T. Ferreira, J. Pereira-Gale, I. B. Hallgrimsdo'ttir, B. N. Howie, Z. Su, Y. Y. Teo, D. Vukcevic, D. Bentley, S. L. Mitchell, P. R. Newby, O. J. Brand, J. Carr-Smith, S. H. Pearce, J. D. Reveille, X. Zhou, A. M. Sims, A. Dowling, J. Taylor, T. Doan, J. C. Davis, L. Savage, M. M. Ward, T. L. Learch, M. H. Weisman, and M. Brown. 2007. Association scan of 14,500 nonsynonymous SNPs in four diseases identifies autoimmunity variants. *Nat Genet* 39: 1329-1337.
172. Harvey, D., J. J. Pointon, D. M. Evans, T. Karaderi, C. Farrar, L. H. Appleton, R. D. Sturrock, M. A. Stone, U. Oppermann, M. A. Brown, and B. P. Wordsworth. 2009. Investigating the genetic association between ERAP1 and ankylosing spondylitis. *Hum Mol Genet* 18: 4204-4212.
173. Halenius, A., S. Hauka, L. Dolken, J. Stindt, H. Reinhard, C. Wiek, H. Hanenberg, U. H. Koszinowski, F. Momburg, and H. Hengel. 2011. Human cytomegalovirus disrupts

the major histocompatibility complex class I peptide-loading complex and inhibits tapasin gene transcription. *J Virol* 85: 3473-3485.
174. Park, B., Y. Kim, J. Shin, S. Lee, K. Cho, K. Fruh, and K. Ahn. 2004. Human cytomegalovirus inhibits tapasin-dependent peptide loading and optimization of the MHC class I peptide cargo for immune evasion. *Immunity* 20: 71-85.
175. Lybarger, L., X. Wang, M. R. Harris, H. W. t. Virgin, and T. H. Hansen. 2003. Virus subversion of the MHC class I peptide-loading complex. *Immunity* 18: 121-130.
176. Jiang, Q., H. Y. Pan, D. X. Ye, P. Zhang, L. P. Zhong, and Z. Y. Zhang. 2010. Downregulation of tapasin expression in primary human oral squamous cell carcinoma: association with clinical outcome. *Tumour Biol* 31: 451-459.
177. Garbi, N., P. Tan, A. D. Diehl, B. J. Chambers, H. G. Ljunggren, F. Momburg, and G. J. Hammerling. 2000. Impaired immune responses and altered peptide repertoire in tapasin-deficient mice. *Nat Immunol* 1: 234-238.
178. Li, L., B. A. Sullivan, C. J. Aldrich, M. J. Soloski, J. Forman, A. G. Grandea, 3rd, P. E. Jensen, and L. Van Kaer. 2004. Differential requirement for tapasin in the presentation of leader- and insulin-derived peptide antigens to Qa-1b-restricted CTLs. *J Immunol* 173: 3707-3715.
179. Barber, L. D., M. Howarth, P. Bowness, and T. Elliott. 2001. The quantity of naturally processed peptides stably bound by HLA-A*0201 is significantly reduced in the absence of tapasin. *Tissue Antigens* 58: 363-368.
180. Boulanger, D. S., R. Oliveira, L. Ayers, S. H. Prior, E. James, A. P. Williams, and T. Elliott. 2010. Absence of tapasin alters immunodominance against a lymphocytic choriomeningitis virus polytope. *J Immunol* 184: 73-83.
181. Aladin, F., G. Lautscham, E. Humphries, J. Coulson, and N. Blake. 2007. Targeting tumour cells with defects in the MHC Class I antigen processing pathway with CD8+ T cells specific for hydrophobic TAP- and Tapasin-independent peptides: the requirement for directed access into the ER. *Cancer immunology, immunotherapy : CII* 56: 1143-1152.
182. Cifaldi, L., E. Lo Monaco, M. Forloni, E. Giorda, S. Lorenzi, S. Petrini, E. Tremante, D. Pende, F. Locatelli, P. Giacomini, and D. Fruci. 2011. Natural killer cells efficiently reject lymphoma silenced for the endoplasmic reticulum aminopeptidase associated with antigen processing. *Cancer Res* 71: 1597-1606.
183. Rammensee, H. G., K. Falk, and O. Rotzschke. 1993. Peptides naturally presented by MHC class I molecules. *Annu Rev Immunol* 11: 213-244.
184. Praveen, P. V., R. Yaneva, H. Kalbacher, and S. Springer. 2010. Tapasin edits peptides on MHC class I molecules by accelerating peptide exchange. *Eur J Immunol* 40: 214-224.
185. Matsunaga, T., and E. Simpson. 1978. H-2 complementation in anti-H-Y cytotoxic T-cell responses can occur in chimeric mice. *Proc Natl Acad Sci U S A* 75: 6207-6210.
186. Shastri, N., S. Schwab, and T. Serwold. 2002. Producing nature's gene-chips: the generation of peptides for display by MHC class I molecules. *Annu Rev Immunol* 20: 463-493.
187. Neefjes, J., E. Gottfried, J. Roelse, M. Gromme, R. Obst, G. J. Hammerling, and F. Momburg. 1995. Analysis of the fine specificity of rat, mouse and human TAP peptide transporters. *Eur J Immunol* 25: 1133-1136.

188. Burrows, S. R., J. Rossjohn, and J. McCluskey. 2006. Have we cut ourselves too short in mapping CTL epitopes? *Trends Immunol* 27: 11-16.
189. Mendoza, L. M., S. Malarkannan, and N. Shastri. 2001. Identification of CD8+ T-cell-stimulating antigen genes in cDNA libraries. *Methods Mol Biol* 156: 255-263.
190. Simone, L. C., X. Wang, A. Tuli, and J. C. Solheim. 2010. Effect of a tapasin mutant on the assembly of the mouse MHC class I molecule H2-K(d). *Immunol Cell Biol* 88: 57-62.
191. Sieker, F., S. Springer, and M. Zacharias. 2007. Comparative molecular dynamics analysis of tapasin-dependent and -independent MHC class I alleles. *Protein Sci* 16: 299-308.
192. Williams, D. B., and T. H. Watts. 1995. Molecular chaperones in antigen presentation. *Curr Opin Immunol* 7: 77-84.
193. Elliott, T. 2009. More images that yet fresh images Beget. *Immunity* 30: 1-2.
194. Lewis, J. W., A. Sewell, D. Price, and T. Elliott. 1998. HLA-A*0201 presents TAP-dependent peptide epitopes to cytotoxic T lymphocytes in the absence of tapasin. *Eur J Immunol* 28: 3214-3220.
195. Peh, C. A., S. R. Burrows, M. Barnden, R. Khanna, P. Cresswell, D. J. Moss, and J. McCluskey. 1998. HLA-B27-restricted antigen presentation in the absence of tapasin reveals polymorphism in mechanisms of HLA class I peptide loading. *Immunity* 8: 531-542.
196. Hansen, T. H., and M. Bouvier. 2009. MHC class I antigen presentation: learning from viral evasion strategies. *Nat Rev Immunol* 9: 503-513.
197. Blanchard, N., F. Gonzalez, M. Schaeffer, N. T. Joncker, T. Cheng, A. J. Shastri, E. A. Robey, and N. Shastri. 2008. Immunodominant, protective response to the parasite Toxoplasma gondii requires antigen processing in the endoplasmic reticulum. *Nat Immunol* 9: 937-944.
198. Malarkannan, S., L. M. Mendoza, and N. Shastri. 2001. Generation of antigen-specific, lacZ-inducible T-cell hybrids. *Methods Mol Biol* 156: 265-272.
199. Delgado, J. C., H. Escobar, D. K. Crockett, E. Reyes-Vargas, and P. E. Jensen. 2009. Identification of naturally processed ligands in the C57BL/6 mouse using large-scale mass spectrometric peptide sequencing and bioinformatics prediction. *Immunogenetics* 61: 241-246.
200. Escobar, H., E. Reyes-Vargas, P. E. Jensen, J. C. Delgado, and D. K. Crockett. 2011. Utility of characteristic QTOF MS/MS fragmentation for MHC class I peptides. *J Proteome Res* 10: 2494-2507.

# Appendix: Tables 2-7

## Table 2: $D^b$ peptides from WT and tapasin-deficient spleen cells

| Data Set | Peptide Sequence | Length | Accession Number | Source Protein Name |
|---|---|---|---|---|
| tpn0 | AALQNLEQL | 9 | Q9WTK5 | Nuclear factor NF-kappa-B p100 subunit |
| tpn0 | AGILNGKLV | 9 | Q922D8 | C-1-tetrahydrofolate synthase, cytoplasmic |
| tpn0 | FSHPNVLPV | 9 | O55222 | Integrin-linked protein kinase |
| tpn0 | FSPLNPVRV | 9 | O35737 | Heterogeneous nuclear ribonucleoprotein H |
| tpn0 | GGPENTLVF | 9 | Q8BX02 | KN motif and ankyrin repeat domain-containing protein 2 |
| tpn0 | GINVNAAPF | 9 | Q60865 | Caprin-1 |
| tpn0 | NSGINVMQV | 9 | O89090 | Transcription factor Sp1 |
| tpn0 | SSLLSPMSV | 9 | P80315 | T-complex protein 1 subunit delta |
| tpn0 | YSSENISNF | 9 | O70400 | PDZ and LIM domain protein 1 |
| tpn0 | YVFPGASHN | 9 | Q60710 | SAM domain and HD domain-containing protein 1 |
| tpn0 | SLLGGHPRL | 9 | Q69ZK6 | Probable JmjC domain-containing histone demethylation protein 2C |
| tpn0 | LHLGVTPSVL | 10 | O89023 | Tripeptidyl-peptidase 1 |
| tpn0 | SNLYNHPQLI | 10 | Q6NSQ7 | Protein LTV1 homolog |
| tpn0 | VGPLGSTIPM | 10 | Q9DCP9 | DAZ-associated protein 2 |
| tpn0 | VMSGMMMSHM | 10 | Q9R1C7 | Pre-mRNA-processing factor 40 homolog A |
| tpn0 | VSGVNGPLVI | 10 | P62814 | V-type proton ATPase subunit B, brain isoform |
| tpn0 | WAPENAPLKS | 10 | P18760 | Cofilin-1 |
| tpn0 | AQYNLDQFTPV | 11 | P47754 | F-actin-capping protein subunit alpha-2 |
| tpn0 | FAPVAPKFTPV | 11 | Q62523 | Zyxin |
| tpn0 | FAPVNVTTEVK | 11 | P10126 | Elongation factor 1-alpha 1 |
| tpn0 | LLTSGVEFESL | 11 | Q3U0M1 | Trafficking protein particle complex subunit 9 |
| tpn0 | SAPSADAPMFV | 11 | P16858 | Glyceraldehyde-3-phosphate dehydrogenase |
| tpn0 | SLGVGYRTQPM | 11 | Q8C2Q3 | RNA-binding protein 14 |
| tpn0 | FALQNATGDGKF | 12 | Q6P2L6 | Histone-lysine N-methyltransferase NSD3 |
| tpn0 | FVHPGAATVPTM | 12 | Q9DCP9 | DAZ-associated protein 2 |
| tpn0 | SQYGWSGNMERI | 12 | P08113 | Endoplasmin |
| B6 | IRMMLEII | 8 | Q8CHY3 | Dymeclin |

| | | | | |
|---|---|---|---|---|
| B6 | AALLNFDEF | 9 | Q6P9Q4 | FH1/FH2 domain-containing protein 1 |
| B6 | AALLNTDLV | 9 | Q91WM3 | U3 small nucleolar RNA-interacting protein 2 |
| B6 | AALQNAVAF | 9 | Q80VI1 | Tripartite motif-containing protein 56 |
| B6 | AALQNLVKI | 9 | P70168 | Importin subunit beta-1 |
| B6 | AALVNLDSL | 9 | Q8CHU3 | Epsin-2 |
| B6 | AAMLNYTHI | 9 | Q8VDB2 | Dolichyl-P-Man:Man(7)GlcNAc(2)-PP-dolichyl-alpha-1,6-mannosyltransferase |
| B6 | AAPFDTVHI | 9 | Q8BNV1 | tRNA (uracil-5-)-methyltransferase homolog A |
| B6 | AAPINTQGL | 9 | Q8BIH0 | Histone deacetylase complex subunit SAP130 |
| B6 | AAPISPWTM | 9 | Q3U133 | Zinc finger protein 746 |
| B6 | AAPRSFIFL | 9 | Q3UIK4 | Methyltransferase-like protein KIAA1627 |
| B6 | AAPSNLPYL | 9 | Q8BFV3 | Dual specificity protein phosphatase 4 |
| B6 | AAVLNPRFL | 9 | Q7TPS5 | Uncharacterized protein KIAA0528 |
| B6 | AGTRNIYYL | 9 | Q9CQN1 | Heat shock protein 75 kDa, mitochondrial |
| B6 | AKIQMLDAL | 9 | Q9D757 | Death-associated protein-like 1 |
| B6 | AMLTNLESL | 9 | Q8BZQ7 | Anaphase-promoting complex subunit 2 |
| B6 | AMNVNDLFL | 9 | P61021 | Ras-related protein Rab-5B |
| B6 | AMNVNEIFM | 9 | P35278 | Ras-related protein Rab-5C |
| B6 | AMYVHAYTL | 9 | O70435 | Proteasome subunit alpha type-3 |
| B6 | ASMINVEYL | 9 | O88491 | Histone-lysine N-methyltransferase, H3 lysine-36 and H4 lysine-20 specific |
| B6 | ASVLNVNHI | 9 | Q99NH0 | Ankyrin repeat domain-containing protein 17 |
| B6 | ASVSNPLFL | 9 | P70428 | Exostosin-2 |
| B6 | ATIINEEVL | 9 | P14576 | Signal recognition particle 54 kDa protein |
| B6 | ATVSNGPFL | 9 | Q69ZF8 | Male-specific lethal 2 homolog |
| B6 | EAVKNLEWI | 9 | Q02788 | Collagen alpha-2(VI) chain |
| B6 | ERAQLAAQL | 9 | P70436 | Homeobox protein DLX-4 |
| B6 | FAHTNIESL | 9 | P27773 | Protein disulfide-isomerase A3 |
| B6 | FAIDDHDYL | 9 | Q91XU3 | Phosphatidylinositol-5-phosphate 4-kinase type-2 gamma |
| B6 | FAIQNPTLI | 9 | Q9D2H6 | Transcription factor Sp2 |
| B6 | FAPKNIYSI | 9 | P09581 | Macrophage colony-stimulating factor 1 receptor |
| B6 | FAPYNKPSL | 9 | Q8R3P2 | Protein deltex-2 |
| B6 | FGPINSVAF | 9 | Q9QZD9 | Eukaryotic translation initiation factor 3 subunit I |
| B6 | FIMTNVDQI | 9 | Q9D3J9 | Uncharacterized protein CXorf21 homolog |

| | | | | |
|---|---|---|---|---|
| B6 | FSFVNSEFL | 9 | P68404 | Protein kinase C beta type |
| B6 | FSLQNQLRL | 9 | Q9JJ28 | Protein flightless-1 homolog |
| B6 | FSPFNPTSL | 9 | Q9Z2U4 | ETS-related transcription factor Elf-4 |
| B6 | FSVTNPHTM | 9 | Q8CDD9 | Uncharacterized protein C1orf103 homolog |
| B6 | FSYLNPQEL | 9 | Q8C2S5 | F-box/LRR-repeat protein 5 |
| B6 | GALKNIVAV | 9 | Q3ULJ0 | Glycerol-3-phosphate dehydrogenase 1-like protein |
| B6 | GAPLNLVDL | 9 | Q9QWT9 | Kinesin-like protein KIFC1 |
| B6 | GAVKNLTYF | 9 | Q91Y74 | CMP-N-acetylneuraminate-beta-galactosamide-alpha-2,3-sialyltransferase |
| B6 | GMIENGPFL | 9 | Q80SU7 | Interferon-induced very large GTPase 1 |
| B6 | GQVINLDQL | 9 | Q3UVG3 | Protein FAM91A1 |
| B6 | GSVVNSVAL | 9 | P59326 | YTH domain family protein 1 |
| B6 | IAPTNAEVL | 9 | Q80U28 | MAP kinase-activating death domain protein |
| B6 | IAVANAQEL | 9 | P62075 | Mitochondrial import inner membrane translocase subunit Tim13 |
| B6 | IGPKNYEFL | 9 | Q8BHY8 | Sorting nexin-14 |
| B6 | ILHTNLVYL | 9 | Q62280 | Protein SSXT |
| B6 | IQIANVTTL | 9 | Q9CU65 | Zinc finger MYM-type protein 2 |
| B6 | IQLMNTAHL | 9 | Q9DC50 | Peroxisomal carnitine O-octanoyltransferase |
| B6 | IRPGATAVI | 9 | Q9WTR6 | Cystine/glutamate transporter |
| B6 | ISPENHISL | 9 | Q9WTX2 | Interferon-inducible double stranded RNA-dependent protein kinase activator A |
| B6 | ISPFNFTAI | 9 | Q8CHT0 | Delta-1-pyrroline-5-carboxylate dehydrogenase, mitochondrial |
| B6 | ISPVNPVAI | 9 | Q91WT8 | RNA-binding protein 47 |
| B6 | KAIVNVIGM | 9 | Q99NB9 | Splicing factor 3B subunit 1 |
| B6 | KGVFNVEVV | 9 | Q8R1A4 | Dedicator of cytokinesis protein 7 |
| B6 | KSVENFVSL | 9 | Q8C3J5 | Dedicator of cytokinesis protein 2 |
| B6 | KSVINTTLV | 9 | O35114 | Lysosome membrane protein 2 |
| B6 | LAIRNDEEL | 9 | Q8CGP5 | Histone H2A type 1-F |
| B6 | LGLSNLTHL | 9 | Q9EQU3 | Toll-like receptor 9 |
| B6 | LLASHRTWI | 9 | Q921L5 | Conserved oligomeric Golgi complex subunit 2 |
| B6 | LQLLNTDYL | 9 | Q9R0L6 | Pericentriolar material 1 protein |
| B6 | LSHTNILVL | 9 | Q9EQU3 | Toll-like receptor 9 |
| B6 | LSLPNTDYI | 9 | Q9WTX2 | Interferon-inducible double stranded RNA-dependent protein kinase activator A |

| | | | | |
|---|---|---|---|---|
| B6 | LSNINSVFL | 9 | Q9Z0M6 | CD97 antigen |
| B6 | MGILNTDTL | 9 | Q8C4V1 | Rho GTPase-activating protein 24 |
| B6 | NGVINAAFM | 9 | Q61548 | Clathrin coat assembly protein AP180 |
| B6 | NMPWNVDTL | 9 | Q61081 | Hsp90 co-chaperone Cdc37 |
| B6 | QPPYNPTYM | 9 | Q9D7I0 | Protein shisa-5 |
| B6 | QSLTNILHL | 9 | Q7TMR0 | Lysosomal Pro-X carboxypeptidase |
| B6 | RALQLLDEV | 9 | P97471 | Mothers against decapentaplegic homolog 4 |
| B6 | RALSNLESI | 9 | Q8R317 | Ubiquilin-1 |
| B6 | RSLLLLAPL | 9 | Q9R0E2 | Procollagen-lysine,2-oxoglutarate 5-dioxygenase 1 |
| B6 | SAIINEDNL | 9 | Q8BG67 | Protein EFR3 homolog A |
| B6 | SAISNLDYI | 9 | Q9R0C8 | Guanine nucleotide exchange factor VAV3 |
| B6 | SALANYIHL | 9 | Q8BPS4 | Integral membrane protein GPR180 |
| B6 | SALINLVEF | 9 | P97313 | DNA-dependent protein kinase catalytic subunit |
| B6 | SALLLKDVL | 9 | Q8BZ36 | RAD50-interacting protein 1 |
| B6 | SAPINSVLL | 9 | Q8C4N4 | PQ-loop repeat-containing protein 2 |
| B6 | SATINAEFV | 9 | Q66K08 | Cartilage intermediate layer protein 1 |
| B6 | SGIRNISFM | 9 | O35598 | ADAM 10 |
| B6 | SGLLNQQSL | 9 | Q9DB40 | Mediator of RNA polymerase II transcription subunit 27 |
| B6 | SGLQNFEAL | 9 | Q99KD5 | Protein unc-45 homolog A |
| B6 | SGVWNVTEL | 9 | P70257 | Nuclear factor 1 X-type |
| B6 | SHVTNVDFL | 9 | Q05BC3 | Echinoderm microtubule-associated protein-like 1 |
| B6 | SILVNQEVL | 9 | P42228 | Signal transducer and activator of transcription 4 |
| B6 | SKLANIDYL | 9 | Q811L6 | Microtubule-associated serine/threonine-protein kinase 4 |
| B6 | SLIILKQVM | 9 | Q9Z2U1 | Proteasome subunit alpha type-5 |
| B6 | SLITNKVVM | 9 | P23492 | Purine nucleoside phosphorylase |
| B6 | SMAENSIPL | 9 | P58462 | Forkhead box protein P1 |
| B6 | SMGVNDIDI | 9 | Q3TIV5 | Zinc finger CCCH domain-containing protein 15 |
| B6 | SMVQNRVFL | 9 | Q8C3J5 | Dedicator of cytokinesis protein 2 |
| B6 | SQISNTEFL | 9 | Q3TCJ1 | Protein FAM175B |
| B6 | SQVINPTAI | 9 | Q61191 | Host cell factor |
| B6 | SSLINGSFL | 9 | Q4JIM5 | Tyrosine-protein kinase ABL2 |
| B6 | SSLMLESFF | 9 | Q91XQ0 | Dynein heavy chain 8, axonemal |
| B6 | SSLQNYAKI | 9 | P41251 | Natural resistance-associated macrophage protein 1 |

| | | | | |
|---|---|---|---|---|
| B6 | SSPVNPVVF | 9 | Q9D868 | Peptidyl-prolyl cis-trans isomerase H |
| B6 | SSVLNLTEL | 9 | Q8BW56 | Glycosyltransferase-like domain-containing protein 1 |
| B6 | STIRLLTSL | 9 | P80318 | T-complex protein 1 subunit gamma |
| B6 | STLINSLFL | 9 | P42209 | Septin-1 |
| B6 | STLVNSLFL | 9 | P28661 | Septin-4 |
| B6 | SVLFNLTTM | 9 | Q8K2L8 | Tetratricopeptide repeat protein 15 |
| B6 | TALENLSTL | 9 | P19096 | Fatty acid synthase |
| B6 | TAPVNIAVI | 9 | Q99JF5 | Diphosphomevalonate decarboxylase |
| B6 | TQPLNHYFI | 9 | A3KGF7 | 1-phosphatidylinositol-4,5-bisphosphate phosphodiesterase beta-2 |
| B6 | TSLLNLTVI | 9 | Q8BM54 | E3 ubiquitin-protein ligase MYLIP |
| B6 | VAPYNTTQF | 9 | Q8R409 | Protein HEXIM1 |
| B6 | VAVVNKVDI | 9 | O35604 | Niemann-Pick C1 protein |
| B6 | VAYMNPIAM | 9 | Q9CVI2 | Protein FAM133B |
| B6 | VGIENFELL | 9 | Q8C050 | Ribosomal protein S6 kinase alpha-5 |
| B6 | VGLTNINVV | 9 | Q61419 | Cytidine monophosphate-N-acetylneuraminic acid hydroxylase |
| B6 | VGVENVAEL | 9 | Q9ET01 | Glycogen phosphorylase, liver form |
| B6 | VGVNNPVFL | 9 | Q9DBN5 | Peroxisomal Lon protease homolog 2 |
| B6 | VMLENYSHL | 9 | Q60585 | Zinc finger protein 30 |
| B6 | VQNINIENL | 9 | P27005 | Protein S100-A8 |
| B6 | VQPFNYVTL | 9 | Q9Z2G1 | Protein fem-1 homolog A-A |
| B6 | VSLLDIDHL | 9 | Q8BQM4 | HEAT repeat-containing protein 3 |
| B6 | VSLNLRQVL | 9 | Q99N32 | Beta-klotho |
| B6 | VSPLNVTAV | 9 | Q9CR27 | Coiled-coil domain-containing protein 53 |
| B6 | VSVANVDLL | 9 | Q80Y17 | Lethal(2) giant larvae protein homolog 1 |
| B6 | VVVENGELI | 9 | P08775 | DNA-directed RNA polymerase II subunit RPB1 |
| B6 | WAVSNREML | 9 | Q80YQ8 | Protein RMD5 homolog A |
| B6 | WKVVNPYYL | 9 | Q5EG47 | 5'-AMP-activated protein kinase catalytic subunit alpha-1 |
| B6 | YALANAQQV | 9 | Q8VBU8 | Protein BANP |
| B6 | YAPDNVWFI | 9 | Q80V94 | AP-4 complex subunit epsilon-1 |
| B6 | YAPINANAI | 9 | Q9R190 | Metastasis-associated protein MTA2 |
| B6 | YQLLLKDFL | 9 | Q9CWR0 | Guanine nucleotide exchange factor GEFT |
| B6 | YQQMNPEAL | 9 | P54841 | Transcription factor MafB |

| | | | | |
|---|---|---|---|---|
| B6 | YSIVNASVL | 9 | Q9ERE3 | Serine/threonine-protein kinase Sgk3 |
| B6 | SLPTNLIHL | 9 | Q6WKZ8 | E3 ubiquitin-protein ligase UBR2 |
| B6 | YVVDNIDHL | 9 | Q9R1A8 | E3 ubiquitin-protein ligase RFWD2 |
| B6 | ASLVNSPSYL | 10 | Q3U3D7 | Transmembrane protein 131-like |
| B6 | FALANHLIKV | 10 | Q9WVK4 | EH domain-containing protein 1 |
| B6 | FAVVNHQGTL | 10 | Q5DU02 | Ubiquitin carboxyl-terminal hydrolase 22 |
| B6 | GALENAKAEI | 10 | Q9DBS8 | Uncharacterized protein C5orf37 homolog |
| B6 | LSLENGTHTL | 10 | P13864 | DNA (cytosine-5)-methyltransferase 1 |
| B6 | RSLDNGGYYI | 10 | P16277 | Tyrosine-protein kinase BLK |
| B6 | SAHQNYAEWL | 10 | Q99PL5 | Ribosome-binding protein 1 |
| B6 | SAIHNFYDNI | 10 | Q99K90 | Mitogen-activated protein kinase kinase kinase 7-interacting protein 2 |
| B6 | SALENGRYEL | 10 | O88379 | Bromodomain adjacent to zinc finger domain protein 1A |
| B6 | SAPVNGSVFI | 10 | Q91XF4 | E3 ubiquitin-protein ligase RNF167 |
| B6 | SAVENILEHL | 10 | P58064 | 28S ribosomal protein S6, mitochondrial |
| B6 | SAVRNGLLLL | 10 | Q80TT8 | p53-associated parkin-like cytoplasmic protein |
| B6 | SAYLNMFEHI | 10 | Q99N16 | Cytochrome P450 4F3 |
| B6 | SGPTNEDLYI | 10 | Q01237 | 3-hydroxy-3-methylglutaryl-coenzyme A reductase |
| B6 | SMAGNIIPAI | 10 | Q9Z1F9 | SUMO-activating enzyme subunit 2 |
| B6 | SSAEVIITTL | 10 | P0C5E4 | Phosphotidylinositol phosphatase PTPRQ |
| B6 | SSIRNFLIYV | 10 | B1AXP6 | Mitochondrial import receptor subunit TOM5 homolog |
| B6 | TAIENSWIHL | 10 | Q9CQG2 | Putative methyltransferase METT10D |
| B6 | VGLPNESQAL | 10 | Q00175 | Progesterone receptor |
| B6 | VMVSNPATRM | 10 | Q61191 | Host cell factor |
| B6 | VSLLNPPETL | 10 | P51943 | Cyclin-A2 |
| B6 | YAGSNFPEHI | 10 | P61161 | Actin-related protein 2 |
| B6 | YALENFVENL | 10 | Q8VI75 | Importin-4 |
| B6 | YGPENTLPTL | 10 | Q5RJY2 | G2/M phase-specific E3 ubiquitin-protein ligase-like protein |
| B6 | YSVANHNSFL | 10 | Q9D3G9 | Rho-related GTP-binding protein RhoH |
| B6 | AAAKNLSDMTL | 11 | Q8K1H7 | T-complex protein 11-like protein 2 |
| B6 | AAPQNFTPSMI | 11 | Q9Z1T1 | AP-3 complex subunit beta-1 |
| B6 | AAVQNPALTAL | 11 | Q3U1N2 | Sterol regulatory element-binding protein 2 |
| B6 | AQYGNILKHVM | 11 | Q8R4R6 | Nucleoporin NUP53 |

| | | | | |
|---|---|---|---|---|
| **B6** | ASPMSIPTNTM | 11 | Q9WVG6 | Histone-arginine methyltransferase CARM1 |
| **B6** | ATAINMKNEAL | 11 | Q91YK0 | Leucine-rich repeat-containing protein 49 |
| **B6** | FSLENLRTMNT | 11 | Q80TG1 | Uncharacterized protein KIAA1267 |
| **B6** | PGSANETSSIL | 11 | Q80X90 | Filamin-B |
| **B6** | SAIMNPASKVI | 11 | Q68FD5 | Clathrin heavy chain 1 |
| **B6** | SKFDVSGYPTI | 11 | P08003 | Protein disulfide-isomerase A4 |
| **B6** | SSIQNFQKGTL | 11 | Q8BX57 | PX domain-containing protein kinase-like protein |
| **B6** | SSPASTPLSPM | 11 | Q91YK2 | Ribosomal RNA processing protein 1 homolog B |
| **B6** | YQFDKVGILTL | 11 | Q8BKT7 | THO complex subunit 5 homolog |
| **B6** | VSYPLVTSFPPL | 12 | O54957 | Linker for activation of T-cells family member 1 |
| **B6** | SVMENSKVLGEAM | 13 | P26039 | Talin-1 |
| **B6** | SVMENSKVLGESM | 13 | Q71LX4 | Talin-2 |
| shared | AAGVGDMVM | 9 | P62830 | 60S ribosomal protein L23 |
| shared | AIVEHLVTL | 9 | Q9Z1E3 | NF-kappa-B inhibitor alpha |
| shared | AMGVNLTSM | 9 | P17918 | Proliferating cell nuclear antigen |
| shared | FAYEGRDYI | 9 | P01899 | H-2 class I histocompatibility antigen, D-B alpha chain |
| shared | FGPVNHEEL | 9 | P46414 | Cyclin-dependent kinase inhibitor 1B |
| shared | FININSLRL | 9 | P16460 | Argininosuccinate synthase |
| shared | FQIVNPHLL | 9 | P07742 | Ribonucleoside-diphosphate reductase large subunit |
| shared | FSPLNPMRV | 9 | P70333 | Heterogeneous nuclear ribonucleoprotein H2 |
| shared | FSPMGVDHM | 9 | P70372 | ELAV-like protein 1 |
| shared | GGVVNMYHM | 9 | P28063 | Proteasome subunit beta type-8 |
| shared | GMGFGLERM | 9 | Q9D0E1 | Heterogeneous nuclear ribonucleoprotein M |
| shared | IGIENIHYL | 9 | Q9DB27 | Malignant T cell amplified sequence 1 |
| shared | IQAENAEFM | 9 | P14901 | Heme oxygenase 1 |
| shared | KALINADEL | 9 | P16546 | Spectrin alpha chain, brain |
| shared | MAPQNLSTF | 9 | Q99KV1 | DnaJ homolog subfamily B member 11 |
| shared | NGPQNIYNL | 9 | Q8K3C0 | Ribonuclease kappa |
| shared | NSMVLFDHM | 9 | Q64511 | DNA topoisomerase 2-beta |
| shared | RAIENIDTL | 9 | Q3UM45 | Protein phosphatase 1 regulatory subunit 7 |
| shared | SAPVAAEPF | 9 | Q60597 | 2-oxoglutarate dehydrogenase E1 component, mitochondrial |
| shared | SAVVDKDFL | 9 | P55264 | Adenosine kinase |
| shared | SSPSNMLPV | 9 | Q99KN9 | Clathrin interactor 1 |

| | | | | |
|---|---|---|---|---|
| shared | VGIENIHVM | 9 | Q8VE11 | Myotubularin-related protein 6 |
| shared | VMVTNVTSL | 9 | P26039 | Talin-1 |
| shared | YGLKNLTAL | 9 | Q9EQ32 | Phosphoinositide 3-kinase adapter protein 1 |
| shared | FAPVNVTTEV | 10 | P10126 | Elongation factor 1-alpha 1 |
| shared | FGIHNGVETL | 10 | Q8C0L9 | Putative glycerophosphodiester phosphodiesterase 5 |
| shared | NSPFNSKFPA | 10 | Q80VH0 | B-cell scaffold protein with ankyrin repeats |
| shared | RQPSIELPSM | 10 | P19973 | Lymphocyte-specific protein 1 |
| shared | SAPRNFVENF | 10 | Q91WG4 | Elongator complex protein 2 |
| shared | SAPSAIALPV | 10 | Q9JHC9 | ETS-related transcription factor Elf-2 |
| shared | SAPVAAEPFL | 10 | Q60597 | 2-oxoglutarate dehydrogenase E1 component, mitochondrial |
| shared | SGPRNPFPPP | 10 | Q60843 | Krueppel-like factor 2 |
| shared | AQYNMDQFTPV | 11 | P47753 | F-actin-capping protein subunit alpha-1 |
| shared | SLGKNPTDAYL | 11 | Q3THE2 | Myosin regulatory light chain MRLC2 |
| shared | AQPGASGMLTPM | 12 | Q7TN29 | Stromal membrane-associated protein 2 |
| shared | SAPSADAPMFVM | 12 | P16858 | Glyceraldehyde-3-phosphate dehydrogenase |
| shared | FAPVNVTTEVKSV | 13 | P10126 | Elongation factor 1-alpha 1 |

**Table 3: $K^b$ peptides from WT and tapasin-deficient spleen cells**

| Data Set | Peptide Sequence | Length | Accession Number | Source Protein Name |
|---|---|---|---|---|
| **tpn0** | ISPYFINT | 8 | P63038 | 60 kDa heat shock protein, mitochondrial |
| **tpn0** | KAPAMFNI | 8 | P97351 | 40S ribosomal protein S3a |
| **tpn0** | SIFQFGKP | 8 | Q8K3Z9 | Nuclear envelope pore membrane protein POM 121 |
| **tpn0** | SLNRFIPL | 8 | Q8VBV7 | COP9 signalosome complex subunit 8 |
| **tpn0** | VIPQFQTV | 8 | O89090 | Transcription factor Sp1 |
| **tpn0** | VNDIFERI | 8 | Q64475 | Histone H2B type 1-B |
| **tpn0** | VADGFISRM | 9 | P24452 | Macrophage-capping protein |
| **tpn0** | VGQQFGAVGV | 10 | Q8K2F8 | Protein LSM14 homolog A |
| **tpn0** | VNRQFMAETQF | 11 | Q60865 | Caprin-1 |
| **B6** | AALIYTSV | 8 | Q8R1Q8 | Cytoplasmic dynein 1 light intermediate chain 1 |
| **B6** | AAYEFTTL | 8 | P32233 | Developmentally-regulated GTP-binding protein 1 |
| **B6** | AIFNFQSL | 8 | Q9CR64 | Transmembrane protein 167A |
| **B6** | AIVEFATV | 8 | Q91WT4 | DnaJ homolog subfamily C member 17 |
| **B6** | ANYEFSQV | 8 | P56528 | ADP-ribosyl cyclase 1 |
| **B6** | AQYKFIYV | 8 | P29351 | Tyrosine-protein phosphatase non-receptor type 6 |
| **B6** | ASYLLAAL | 8 | P99027 | 60S acidic ribosomal protein P2 |
| **B6** | ATYIFNGL | 8 | Q9QXK3 | Coatomer subunit gamma-2 |
| **B6** | AVFTFEQL | 8 | Q3UW53 | Protein Niban |
| **B6** | AVIKFLEL | 8 | P43247 | DNA mismatch repair protein Msh2 |
| **B6** | AVYAFLGL | 8 | Q9JJU8 | SH3 domain-binding glutamic acid-rich-like protein |
| **B6** | AVYSFEAL | 8 | Q99KC8 | Loss of heterozygosity 11 chromosomal region 2 gene A protein homolog |
| **B6** | AVYTFETL | 8 | Q8R1F1 | Niban-like protein 1 |
| **B6** | AWIKVEQL | 8 | Q922P9 | Nuclear protein NP60 |
| **B6** | EAYRFTGL | 8 | Q8K015 | Centromere protein O |
| **B6** | EIVTFERL | 8 | Q61584 | Fragile X mental retardation syndrome-related protein 1 |
| **B6** | FAYRFSNL | 8 | Q8BU03 | Periodic tryptophan protein 2 homolog |
| **B6** | FNLVYENL | 8 | Q8R4V1 | NFAT activation molecule 1 |
| **B6** | FQQEFPSL | 8 | Q3TLH4 | BAT2 domain-containing protein 1 |
| **B6** | FVYIFQEV | 8 | Q99K51 | Plastin-3 |

| | | | | |
|---|---|---|---|---|
| **B6** | GVLRFVNL | 8 | Q3UGP8 | Putative alpha-1,2-glucosyltransferase ALG10-B |
| **B6** | HGYTFANL | 8 | Q9R1T2 | SUMO-activating enzyme subunit 1 |
| **B6** | HVYYFAHL | 8 | Q80SU7 | Interferon-induced very large GTPase 1 |
| **B6** | IAFIFNNL | 8 | Q6ZQ08 | CCR4-NOT transcription complex subunit 1 |
| **B6** | IALRYVAL | 8 | Q9JIF7 | Coatomer subunit beta |
| **B6** | IAVSFREL | 8 | Q8BJW5 | Nucleolar protein 11 |
| **B6** | IAYAFFHL | 8 | Q8K4P7 | Suppressor of tumorigenicity protein 7-like protein |
| **B6** | IIAAMPNL | 8 | O89090 | Transcription factor Sp1 |
| **B6** | IIITFNDL | 8 | Q9JI78 | Peptide-N(4)-(N-acetyl-beta-glucosaminyl)asparagine amidase |
| **B6** | IIPMFSNL | 8 | Q76MZ3 | Serine/threonine-protein phosphatase 2A 65 kDa regulatory subunit A alpha isoform |
| **B6** | IIQEFPAL | 8 | Q9QZ05 | Eukaryotic translation initiation factor 2-alpha kinase 4 |
| **B6** | IIVSFVNA | 8 | Q921M3 | Splicing factor 3B subunit 3 |
| **B6** | INFDFNTI | 8 | Q8CDD8 | BTB/POZ domain-containing protein KCTD20 |
| **B6** | IRYIFAYL | 8 | Q9JHF7 | Glutathione-requiring prostaglandin D synthase |
| **B6** | ISFKFDHL | 8 | P47753 | F-actin-capping protein subunit alpha-1 |
| **B6** | ISPLFAEL | 8 | Q99KH8 | Serine/threonine-protein kinase 24 |
| **B6** | ISYLYNKL | 8 | Q61471 | Protein Tob1 |
| **B6** | ISYQFSNL | 8 | Q99PQ1 | Tripartite motif-containing protein 12 |
| **B6** | IVPLFTNL | 8 | Q7TNP2 | Serine/threonine-protein phosphatase 2A 65 kDa regulatory subunit A beta isoform |
| **B6** | IWIRVASL | 8 | Q8BRG6 | Kelch-like protein 24 |
| **B6** | KSYLFQLL | 8 | P97377 | Cell division protein kinase 2 |
| **B6** | LIYKFLNV | 8 | Q6P5F9 | Exportin-1 |
| **B6** | LQYEFTHL | 8 | Q9JL26 | Formin-like protein 1 |
| **B6** | LQYEFTKL | 8 | A2APV2 | Formin-like protein 2 |
| **B6** | LSYQYSGL | 8 | Q2TBA3 | Mucosa-associated lymphoid tissue lymphoma translocation protein 1 homolog |
| **B6** | LVYQFKEM | 8 | Q60775 | ETS-related transcription factor Elf-1 |
| **B6** | MSFQFAHL | 8 | Q80TY5 | Vacuolar protein sorting-associated protein 13B |
| **B6** | NNYVYAGL | 8 | Q8CIK8 | RING finger and WD repeat domain-containing protein 3 |
| **B6** | PNQLFINL | 8 | Q9JJ28 | Protein flightless-1 homolog |
| **B6** | QSIEFSRL | 8 | P23116 | Eukaryotic translation initiation factor 3 subunit A |
| **B6** | RNFIFSRL | 8 | Q60848 | Lymphocyte-specific helicase |

| | | | | |
|---|---|---|---|---|
| **B6** | RNYQFDFL | 8 | Q8K4Z5 | Splicing factor 3 subunit 1 |
| **B6** | RSLKFYSL | 8 | Q99KP6 | Pre-mRNA-processing factor 19 |
| **B6** | RSYDFEFM | 8 | P40336 | Vacuolar protein sorting-associated protein 26A |
| **B6** | RTYIFTFL | 8 | Q8JZL7 | Ras-GEF domain-containing family member 1B |
| **B6** | RVLIFSQM | 8 | P40201 | Chromodomain-helicase-DNA-binding protein 1 |
| **B6** | SAFEFNEL | 8 | Q9Z2C4 | Myotubularin-related protein 1 |
| **B6** | SAFSFRTL | 8 | Q8BMI0 | F-box only protein 38 |
| **B6** | SALIYSNL | 8 | O55013 | Trafficking protein particle complex subunit 3 |
| **B6** | SALRFLNL | 8 | Q3TAA7 | Serine/threonine kinase 11-interacting protein |
| **B6** | SALVFTRL | 8 | Q9JHJ3 | Uncharacterized protein C1orf85 homolog |
| **B6** | SAMVFSAM | 8 | P63082 | V-type proton ATPase 16 kDa proteolipid subunit |
| **B6** | SAPEYVFL | 8 | Q7TNB8 | Protein strawberry notch homolog 2 |
| **B6** | SAPLYTNL | 8 | Q8K4S1 | 1-phosphatidylinositol-4,5-bisphosphate phosphodiesterase epsilon-1 |
| **B6** | SGFVFTRL | 8 | Q6PCN7 | Helicase-like transcription factor |
| **B6** | SIANFTNV | 8 | Q91V92 | ATP-citrate synthase |
| **B6** | SIIIFTNT | 8 | Q4FZF3 | Probable ATP-dependent RNA helicase DDX49 |
| **B6** | SILQYSNV | 8 | Q9WUE4 | Tumor suppressor candidate 4 |
| **B6** | SIVQFYYM | 8 | Q9R190 | Metastasis-associated protein MTA2 |
| **B6** | SNLKYILV | 8 | A2AWL7 | MAX gene-associated protein |
| **B6** | SNYIFTAI | 8 | O88427 | Voltage-dependent T-type calcium channel subunit alpha-1H |
| **B6** | SNYVFVFL | 8 | Q9Z0S9 | Prenylated Rab acceptor protein 1 |
| **B6** | SQYVFTEM | 8 | Q5SYH2 | Transmembrane protein 199 |
| **B6** | SSFVFLNL | 8 | Q64310 | Surfeit locus protein 4 |
| **B6** | SSFVFSTV | 8 | Q01237 | 3-hydroxy-3-methylglutaryl-coenzyme A reductase |
| **B6** | SSIVFAEL | 8 | Q9Z2R9 | Eukaryotic translation initiation factor 2-alpha kinase 1 |
| **B6** | SSYDFTSI | 8 | Q8VCW8 | Acyl-CoA synthetase family member 2, mitochondrial |
| **B6** | SSYFFGKL | 8 | Q99P81 | ATP-binding cassette sub-family G member 3 |
| **B6** | SSYTFPKM | 8 | Q9WUR2 | Peroxisomal 3,2-trans-enoyl-CoA isomerase |
| **B6** | STFIYNSI | 8 | Q01514 | Interferon-induced guanylate-binding protein 1 |
| **B6** | STFTFADL | 8 | Q9ERU9 | E3 SUMO-protein ligase RanBP2 |
| **B6** | STVEFTNL | 8 | O54692 | Centromere/kinetochore protein zw10 homolog |
| **B6** | STYKFFEV | 8 | Q9CZM2 | 60S ribosomal protein L15 |

| | | | | |
|---|---|---|---|---|
| **B6** | SVIKFENL | 8 | Q9CPV7 | Probable palmitoyltransferase ZDHHC6 |
| **B6** | SVITYVGL | 8 | Q91ZE5 | EGF-like module-containing mucin-like hormone receptor-like 4 |
| **B6** | SVVRYVQL | 8 | O35900 | U6 snRNA-associated Sm-like protein LSm2 |
| **B6** | TAFQFLQL | 8 | P51945 | Cyclin-G1 |
| **B6** | TAFRFSEL | 8 | A3KGB4 | TBC1 domain family member 8B |
| **B6** | TAFVFPRL | 8 | Q8BK62 | Olfactomedin-like protein 3 |
| **B6** | TAPEYVFL | 8 | Q689Z5 | Protein strawberry notch homolog 1 |
| **B6** | TAYAFHFL | 8 | Q9R0H0 | Peroxisomal acyl-coenzyme A oxidase 1 |
| **B6** | TAYEFAKL | 8 | Q9EQ06 | Estradiol 17-beta-dehydrogenase 11 |
| **B6** | TIYEYGAL | 8 | P46412 | Glutathione peroxidase 3 |
| **B6** | TIYRFLKL | 8 | Q8CEF1 | Protein fem-1 homolog C |
| **B6** | TNLVYPAL | 8 | Q8BLR9 | Hypoxia-inducible factor 1-alpha inhibitor |
| **B6** | TNYIFDSL | 8 | Q9CXF4 | TBC1 domain family member 15 |
| **B6** | TNYKFFML | 8 | Q5Y5T1 | Probable palmitoyltransferase ZDHHC20 |
| **B6** | TQYTFSSI | 8 | Q08943 | FACT complex subunit SSRP1 |
| **B6** | TSLRFVFL | 8 | Q9CQV4 | Protein FAM134C |
| **B6** | TSYRFLAL | 8 | Q8QZX2 | Uncharacterized protein C4orf15 homolog |
| **B6** | TTLIFQKL | 8 | P15307 | C-Rel proto-oncogene protein |
| **B6** | VALKFSQI | 8 | Q62187 | Transcription termination factor 1 |
| **B6** | VALLFRQL | 8 | Q6ZPE2 | Myotubularin-related protein 5 |
| **B6** | VAPGYPLL | 8 | P21995 | Embigin |
| **B6** | VAYKFPEL | 8 | Q6WKZ8 | E3 ubiquitin-protein ligase UBR2 |
| **B6** | VAYTYDNL | 8 | Q6ZQ93 | Ubiquitin carboxyl-terminal hydrolase 34 |
| **B6** | VFRLLPQL | 8 | Q9EST5 | Acidic leucine-rich nuclear phosphoprotein 32 family member B |
| **B6** | VFTEVANL | 8 | Q62141 | Paired amphipathic helix protein Sin3b |
| **B6** | VGFRFPIL | 8 | Q9QUG9 | RAS guanyl-releasing protein 2 |
| **B6** | VIAELVNV | 8 | Q8K2X8 | General transcription factor IIH subunit 5 |
| **B6** | VIISFNSL | 8 | Q5I012 | Putative sodium-coupled neutral amino acid transporter 10 |
| **B6** | VIQVFQQL | 8 | Q8BHC4 | Dephospho-CoA kinase domain-containing protein |
| **B6** | VIVRFLTV | 8 | P62245 | 40S ribosomal protein S15a |
| **B6** | VMYRVIQV | 8 | Q61069 | Upstream stimulatory factor 1 |
| **B6** | VNVDYSKL | 8 | Q62425 | NADH dehydrogenase [ubiquinone] 1 alpha subcomplex subunit 4 |
| **B6** | VSFTYRYL | 8 | Q920Q4 | Vacuolar protein sorting-associated protein 16 homolog |

| | | | | |
|---|---|---|---|---|
| **B6** | VSIQFYHL | 8 | Q5H8C4 | Vacuolar protein sorting-associated protein 13A |
| **B6** | VSYLFSHV | 8 | Q9D7G0 | Ribose-phosphate pyrophosphokinase 1 |
| **B6** | VSYVFTEV | 8 | Q8K2V6 | Importin-11 |
| **B6** | VTVDFSKL | 8 | Q6NVF4 | DNA helicase B |
| **B6** | VVFFFTRL | 8 | P50615 | Protein BTG3 |
| **B6** | VVFQFQHI | 8 | P70658 | C-X-C chemokine receptor type 4 |
| **B6** | VVYIYHSL | 8 | Q8CD15 | Myc-induced nuclear antigen |
| **B6** | AMYIFLHTV | 9 | Q9CQZ0 | ORM1-like protein 2 |
| **B6** | AVLSFSTRL | 9 | P46978 | Dolichyl-diphosphooligosaccharide--protein glycosyltransferase subunit STT3A |
| **B6** | ELFPVFTQL | 9 | Q99KU6 | Uncharacterized protein C6orf89 homolog |
| **B6** | IGPTYYQRL | 9 | Q8CFI7 | DNA-directed RNA polymerase II subunit RPB2 |
| **B6** | KIFEFKETL | 9 | Q8BW96 | Calcium/calmodulin-dependent protein kinase type 1D |
| **B6** | KNYDFAQVL | 9 | Q8BGF7 | PAB-dependent poly(A)-specific ribonuclease subunit 2 |
| **B6** | QILSDFPKL | 9 | Q99ME9 | Nucleolar GTP-binding protein 1 |
| **B6** | QSLAFLKDI | 9 | Q6NVF4 | DNA helicase B |
| **B6** | QVYTFTERM | 9 | Q9R2B6 | Alpha-N-acetyl-neuraminyl-2,3-beta-galactosyl-1,3-N-acetyl-galactosaminide alpha-2,6-sialyltransferase |
| **B6** | RNYEYLIRL | 9 | Q8R3L2 | Transcription factor 25 |
| **B6** | RVAEFTTNL | 9 | Q8VDD5 | Myosin-9 |
| **B6** | RVYEFLDKL | 9 | P14685 | 26S proteasome non-ATPase regulatory subunit 3 |
| **B6** | SGYDFENRL | 9 | Q8VE09 | Tetratricopeptide repeat protein 39C |
| **B6** | SIAAFIQRL | 9 | Q9Z1R2 | Large proline-rich protein BAT3 |
| **B6** | SIINFIERL | 9 | Q9QZ09 | Putative homeodomain transcription factor 1 |
| **B6** | TGYAYTQGL | 9 | Q9JHI9 | Solute carrier family 40 member 1 |
| **B6** | TILEFSQNM | 9 | Q6P5F9 | Exportin-1 |
| **B6** | TIQEFLERI | 9 | P57725 | SAM domain-containing protein SAMSN-1 |
| **B6** | VGFTFPNRL | 9 | Q9Z0E0 | Neurochondrin |
| **B6** | VGYRFVTAI | 9 | Q80TM9 | Nischarin |
| **B6** | VIYPFMQGL | 9 | Q91VV4 | DENN domain-containing protein 2D |
| **B6** | VNFEKFWEL | 9 | Q8JZL7 | Ras-GEF domain-containing family member 1B |
| **B6** | VNFPFLVKL | 9 | P05132 | cAMP-dependent protein kinase catalytic subunit alpha |
| **B6** | VNLREYPSL | 9 | Q8BVK9 | Sp110 nuclear body protein |

| | | | | |
|---|---|---|---|---|
| **B6** | VNYRHLALL | 9 | P08775 | DNA-directed RNA polymerase II subunit RPB1 |
| **B6** | VTYSFRQSF | 9 | Q8R0S2 | IQ motif and SEC7 domain-containing protein 1 |
| **B6** | RELFPVFTQL | 10 | Q99KU6 | Uncharacterized protein C6orf89 homolog |
| shared | ASYEFTTL | 8 | Q9QXB9 | Developmentally-regulated GTP-binding protein 2 |
| shared | ATLVFHNL | 8 | P42227 | Signal transducer and activator of transcription 3 |
| shared | HIYEFPQL | 8 | Q8C4B4 | Protein unc-119 homolog B |
| shared | INFDFPKL | 8 | P54823 | Probable ATP-dependent RNA helicase DDX6 |
| shared | KILTFDQL | 8 | P35980 | 60S ribosomal protein L18 |
| shared | SGPQFVQL | 8 | Q64693 | POU domain class 2-associating factor 1 |
| shared | SNYLFTKL | 8 | P97481 | Endothelial PAS domain-containing protein 1 |
| shared | SVYVYKVL | 8 | Q64475 | Histone H2B type 1-B |
| shared | TIIIFHSL | 8 | O08575 | Eyes absent homolog 2 |
| shared | VAFDFTKV | 8 | Q7M6Y3 | Phosphatidylinositol-binding clathrin assembly protein |
| shared | VNFEFPEF | 8 | P62082 | 40S ribosomal protein S7 |
| shared | VNIEFKDL | 8 | Q64343 | ATP-binding cassette sub-family G member 1 |
| shared | ASYEFVQRL | 9 | Q9JHU4 | Cytoplasmic dynein 1 heavy chain 1 |

**Table 4: Selected peptides used for Tapasin stability and decay assays**

| Sequence | Length | MHC I |
|---|---|---|
| FSPLNPVRV | 9 | $D^b$ |
| FVHPGAATVPTM | 12 | $D^b$ |
| SNLYNHPQLI | 10 | $D^b$ |
| WAPENAPLKS | 10 | $D^b$ |
| FAPVAPKFTPV | 11 | $D^b$ |
| SLNRFIPL | 8 | $K^b$ |
| ISPYFINT | 8 | $K^b$ |
| VGQQFGAVGV | 10 | $K^b$ |

**Table 5: $L^d$ peptides from WT and ERAAP-deficient spleen cells**

| Data Set | Peptide Sequence | Length | Accession Number | Source Protein Name |
|---|---|---|---|---|
| **WT** | VPFKALDL | 8 | Q11204 | CMP-N-acetylneuraminate-beta-galactosamide-alpha-2,3-sialyltransferase |
| **WT** | FPELKAEL | 8 | Q3U1Y4 | DENN domain-containing protein 4B |
| **WT** | HSVLPLLL | 8 | Q6PNC0 | DmX-like protein 1 |
| **WT** | LPYFLRYI | 8 | A2AN08 | E3 ubiquitin-protein ligase UBR4 |
| **WT** | HPSRDFFL | 8 | Q8BQM8 | Echinoderm microtubule-associated protein-like 5 |
| **WT** | RALGPKPF | 8 | Q8BRH4 | Histone-lysine N-methyltransferase MLL3 |
| **WT** | LPRPSDFI | 8 | P21812 | Mast cell protease 4 |
| **WT** | FPRDAVEI | 8 | Q91ZV0 | Melanoma inhibitory activity protein 2 |
| **WT** | PASGLHLF | 8 | Q9EQ32 | Phosphoinositide 3-kinase adapter protein 1 |
| **WT** | HPNFEKLL | 8 | Q6A070 | Protein FAM179B |
| **WT** | YPVDWWSL | 8 | Q9JJX8 | Serine/threonine-protein kinase 32B |
| **WT** | IPFRAADL | 8 | O88307 | Sortilin-related receptor |
| **WT** | LPQRGNIF | 8 | Q9D8Y1 | Transmembrane protein 126A |
| **WT** | HVIPRSDF | 8 | Q99MV1 | Tudor domain-containing protein 1 |
| **WT** | FPELNYQL | 8 | P42227 | Signal transducer and activator of transcription 3 |

| | | | | |
|---|---|---|---|---|
| **WT** | FPHPSQLDL | 9 | P54923 | [Protein ADP-ribosylarginine] hydrolase |
| **WT** | IPAESYTFF | 9 | Q9CX56 | 26S proteasome non-ATPase regulatory subunit 8 |
| **WT** | TPKPNFFDF | 9 | Q9D061 | Acyl-CoA-binding domain-containing protein 6 |
| **WT** | IPEALVTNL | 9 | Q9R158 | ADAM 26A |
| **WT** | TPLTLRYSI | 9 | Q02357 | Ankyrin-1 |
| **WT** | WPHQPIENL | 9 | Q9DCX2 | ATP synthase subunit d, mitochondrial |
| **WT** | RPSAAGINL | 9 | O70133 | ATP-dependent RNA helicase A |
| **WT** | KPANVQPYY | 9 | Q5SQX6 | Cytoplasmic FMR1-interacting protein 2 |
| **WT** | EAMRALEYL | 9 | Q8CIQ7 | Dedicator of cytokinesis protein 3 |
| **WT** | VPHTVYRNL | 9 | Q8C147 | Dedicator of cytokinesis protein 8 |
| **WT** | LPHVGVSDF | 9 | Q8CFI7 | DNA-directed RNA polymerase II subunit RPB2 |
| **WT** | TPSPTKYSL | 9 | Q9ERU9 | E3 SUMO-protein ligase RanBP2 |
| **WT** | FPQFSALRF | 9 | Q7TMY8 | E3 ubiquitin-protein ligase HUWE1 |
| **WT** | VPIKPGQQG | 9 | P70429 | Ena/VASP-like protein |
| **WT** | FPQMGRFTL | 9 | Q8R050 | Eukaryotic peptide chain release factor GTP-binding subunit ERF3A |
| **WT** | VPFHLHINL | 9 | Q8R1B4 | Eukaryotic translation initiation factor 3 subunit C |
| **WT** | IPQEAYNAV | 9 | Q3UA37 | Glutamine-rich protein 1 |
| **WT** | MPSPIQHDF | 9 | P14220 | Glycophorin |
| **WT** | LPHVGYLYM | 9 | Q91VB4 | Hermansky-Pudlak syndrome 3 protein homolog |

| | | | | |
|---|---|---|---|---|
| **WT** | IPQSGLFVV | 9 | Q2TB54 | High affinity immunoglobulin alpha and immunoglobulin mu Fc receptor |
| **WT** | VPLASKYNL | 9 | Q9WU62 | Inner centromere protein |
| **WT** | YPEQETVSL | 9 | Q5SF07 | Insulin-like growth factor 2 mRNA-binding protein 2 |
| **WT** | IPKSAVGEL | 9 | P11835 | Integrin beta-2 |
| **WT** | LPHASSYSL | 9 | Q9Z0R6 | Intersectin-2 |
| **WT** | VPHSQFINM | 9 | Q61168 | Lysosomal-associated transmembrane protein 5 |
| **WT** | VPQESRFNL | 9 | Q80YQ2 | Mediator of RNA polymerase II transcription subunit 23 |
| **WT** | LPHPAYFGL | 9 | P41251 | Natural resistance-associated macrophage protein 1 |
| **WT** | IPSQHYVYM | 9 | Q09014 | Neutrophil cytosol factor 1 |
| **WT** | IPSQLNVNF | 9 | Q9DC50 | Peroxisomal carnitine O-octanoyltransferase |
| **WT** | LPAKYPELF | 9 | Q5BL07 | Peroxisome biogenesis factor 1 |
| **WT** | SPIAARDLL | 9 | Q9QY23 | Plakophilin-3 |
| **WT** | HAHQWITAL | 9 | P31360 | POU domain, class 3, transcription factor 2 |
| **WT** | FPQELKDLL | 9 | Q80UZ2 | Protein SDA1 homolog |
| **WT** | FSGSFASIF | 9 | P11157 | Ribonucleoside-diphosphate reductase subunit M2 |
| **WT** | SPHGIPIDL | 9 | Q9WTM5 | RuvB-like 2 |
| **WT** | HPFFNTIDF | 9 | Q7TSJ6 | Serine/threonine-protein kinase LATS2 |
| **WT** | FPQRLRHLL | 9 | P52633 | Signal transducer and transcription activator 6 |

| | | | | |
|---|---|---|---|---|
| **WT** | IPQQQVFAL | 9 | Q5DU57 | Spermatogenesis-associated protein 13 |
| **WT** | YPLEKPFDF | 9 | Q8R0X7 | Sphingosine-1-phosphate lyase 1 |
| **WT** | VPFNIPLEL | 9 | Q6P5D8 | Structural maintenance of chromosomes flexible hinge domain-containing protein 1 |
| **WT** | MPYLNKFIL | 9 | Q6A028 | Switch-associated protein 70 |
| **WT** | LPAQGLIEF | 9 | P42669 | Transcriptional activator protein Pur-alpha |
| **WT** | LPGPLVDSF | 9 | Q9EPW0 | Type I inositol-3,4-bisphosphate 4-phosphatase |
| **WT** | MPMMPGPPM | 9 | Q62241 | U1 small nuclear ribonucleoprotein C |
| **WT** | YPHAAVNGL | 9 | Q9DB76 | UPF0172 protein FAM158A |
| **WT** | EPFRLQHNL | 9 | Q8CIE2 | Zinc finger MIZ domain-containing protein 2 |
| **WT** | IPQDVGVNL | 9 | Q9DC48 | Pre-mRNA-processing factor 17 |
| **WT** | PVGFSLPSHL | 10 | P05622 | Beta-type platelet-derived growth factor receptor |
| **WT** | VPGTHPLLVF | 10 | Q6NS52 | Diacylglycerol kinase beta |
| **WT** | SPQELQLHYF | 10 | Q8K5B2 | Multiple coagulation factor deficiency protein 2 homolog |
| **WT** | FPIEAQDHVL | 10 | Q08481 | Platelet endothelial cell adhesion molecule |
| **WT** | LPHRIKGYLL | 10 | P59729 | Ras and Rab interactor 3 |
| **WT** | IPSVVTGTDI | 10 | Q9Z2H2 | Regulator of G-protein signaling 6 |
| **WT** | LPQGPLGTSF | 10 | Q8BG60 | Thioredoxin-interacting protein |

| | | | | |
|---|---|---|---|---|
| **WT** | VPSGHSLLAM | 10 | O35239 | Tyrosine-protein phosphatase non-receptor type 9 |
| **WT** | LPYDASKWEF | 10 | P35969 | Vascular endothelial growth factor receptor 1 |
| **WT** | LSVVSGKEFL | 10 | Q80YY7 | Zinc finger protein 618 |
| **WT** | VPIFSFGENNL | 11 | Q80W94 | 2-acylglycerol O-acyltransferase 2 |
| **WT** | ESKDGEENVGL | 11 | Q8CH18 | Cell division cycle and apoptosis regulator protein 1 |
| **WT** | APGTHPPFITF | 11 | Q9QYB1 | Chloride intracellular channel protein 4 |
| **WT** | IPQQVFQEVGI | 11 | Q8K2D3 | Enhancer of mRNA-decapping protein 3 |
| **WT** | VPCFRTPLGPL | 11 | Q3UCQ1 | Forkhead box protein K2 |
| **WT** | IPHLLGDVVFL | 11 | Q791T5 | Mitochondrial carrier homolog 1 |
| **WT** | IPYGNSSELVF | 11 | Q2TBA3 | Mucosa-associated lymphoid tissue lymphoma translocation protein 1 homolog |
| **WT** | YPVPSGYPEPV | 11 | Q9JIZ9 | Phospholipid scramblase 3 |
| **WT** | LSTQPVQTLDL | 11 | B2RUI1 | Zinc finger protein 551 |
| **WT** | IPDEINDRVRFL | 12 | Q8VE70 | Programmed cell death protein 10 |
| **WT** | IPSSTKNIDLSF | 12 | Q9QUK6 | Toll-like receptor 4 |
| **Shared** | IPASGLHLF | 9 | Q9EQ32 | Phosphoinositide 3-kinase adapter protein 1 |
| **Shared** | LSRPDLPF | 8 | P36371 | Antigen peptide transporter 2 |
| **Shared** | LPHEILEM | 8 | Q91VC3 | Eukaryotic initiation factor 4A-III |
| **Shared** | KPTLALNL | 8 | P09450 | Transcription factor jun-B |
| **Shared** | LPDQLFHNL | 9 | Q9QWK5 | Baculoviral IAP repeat-containing protein 1a |

| | | | | |
|---|---|---|---|---|
| **Shared** | VPFEAGQYF | 9 | Q6P8I6 | Cytochrome c oxidase assembly protein COX11, mitochondrial |
| **Shared** | KPQLLQENL | 9 | Q8C3J5 | Dedicator of cytokinesis protein 2 |
| **Shared** | RPGSSYFNL | 9 | Q6NZB0 | DnaJ homolog subfamily C member 8 |
| **Shared** | APSTVIFHL | 9 | Q9DBG6 | Dolichyl-diphosphooligosaccharide--protein glycosyltransferase subunit 2 |
| **Shared** | KPNEGYLEF | 9 | Q9D0M0 | Exosome complex exonuclease RRP42 |
| **Shared** | VPALAKVLL | 9 | P97480 | Eyes absent homolog 3 |
| **Shared** | APQPGKYVI | 9 | Q8BTM8 | Filamin-A |
| **Shared** | MPSESKFLF | 9 | Q60760 | Growth factor receptor-bound protein 10 |
| **Shared** | IPNEIIHAL | 9 | Q9D0E1 | Heterogeneous nuclear ribonucleoprotein M |
| **Shared** | VPFENKLYL | 9 | Q6GQU2 | Kelch-like protein 23 |
| **Shared** | MPEKLGYNL | 9 | O09046 | L-amino-acid oxidase |
| **Shared** | APFKGGTLF | 9 | Q61033 | Lamina-associated polypeptide 2, isoforms alpha/zeta |
| **Shared** | LPQDGVYYL | 9 | P41155 | Lymphotoxin-beta |
| **Shared** | HPRINVFDF | 9 | Q8R151 | NFX1-type zinc finger-containing protein 1 |
| **Shared** | RPSANVYDL | 9 | Q8R151 | NFX1-type zinc finger-containing protein 1 |
| **Shared** | MPGRIINGL | 9 | Q9DBN5 | Peroxisomal Lon protease homolog 2 |
| **Shared** | APGAHGPFL | 9 | Q8R089 | Probable fibrosin-1 long transcript protein |
| **Shared** | EPILNIHDL | 9 | P61290 | Proteasome activator complex subunit 3 |
| **Shared** | VSEPHHSTL | 9 | Q6ZQ06 | Protein QN1 homolog |

| | | | | |
|---|---|---|---|---|
| **Shared** | LPHAAQETF | 9 | P13405 | Retinoblastoma-associated protein |
| **Shared** | VPLPTYHNL | 9 | Q8VH51 | RNA-binding protein 39 |
| **Shared** | RPAGAKYFF | 9 | Q60838 | Segment polarity protein dishevelled homolog DVL-2 |
| **Shared** | VPLAGHVGF | 9 | Q9R1T4 | Septin-6 |
| **Shared** | KNLLLIHNL | 9 | P42228 | Signal transducer and activator of transcription 4 |
| **Shared** | LPAKAVYDF | 9 | Q3UTJ2 | Sorbin and SH3 domain-containing protein 2 |
| **Shared** | YPNVNIHNF | 9 | Q62261 | Spectrin beta chain, brain 1 |
| **Shared** | YPHVNVTNF | 9 | P15508 | Spectrin beta chain, erythrocyte |
| **Shared** | FPGQLNADL | 9 | Q7TMM9 | Tubulin beta-2A chain |
| **Shared** | IVQFPGLYF | 9 | P32972 | Tumor necrosis factor ligand superfamily member 8 |
| **Shared** | IPQQLVERL | 9 | Q6A4J8 | Ubiquitin carboxyl-terminal hydrolase 7 |
| **Shared** | SPSLVQYDL | 9 | Q80X50 | Ubiquitin-associated protein 2-like |
| **Shared** | SPYQGGVFF | 9 | P62838 | Ubiquitin-conjugating enzyme E2 D2 |
| **Shared** | SPGRILHDL | 9 | Q8C263 | Uncharacterized protein C13orf3 homolog |
| **Shared** | EPFRLEHNL | 9 | Q6P1E1 | Zinc finger MIZ domain-containing protein 1 |
| **Shared** | KPANVQPYYL | 10 | Q5SQX6 | Cytoplasmic FMR1-interacting protein 2 |
| **Shared** | KPHSGFHVAF | 10 | Q8CD10 | EF-hand domain-containing family member A1 |
| **Shared** | VPIKPGQQGF | 10 | P70429 | Ena/VASP-like protein |
| **Shared** | APAPVNPFQV | 10 | Q8CHU3 | Epsin-2 |
| **Shared** | LPQKAGGFLM | 10 | P09411 | Phosphoglycerate kinase 1 |

| | | | | |
|---|---|---|---|---|
| **Shared** | HPMGPPPPFM | 10 | Q8BHS3 | Pre-mRNA-splicing factor RBM22 |
| **Shared** | KPQEILTFDF | 10 | Q922X9 | Protein arginine N-methyltransferase 7 |
| **Shared** | APYPLYPAEL | 10 | Q9WVB0 | RNA-binding protein with multiple splicing |
| **Shared** | YPHEVQFFDL | 10 | Q3TIR3 | Synembryn-A |
| **Shared** | IPIAGRDITYF | 11 | Q641P0 | Actin-related protein 3B |
| **Shared** | VPHKIPDSLLL | 11 | P59598 | Putative Polycomb group protein ASXL1 |
| **Shared** | IPQELNNITKL | 11 | Q5SFM8 | RNA-binding protein 27 |
| **Shared** | IPALCVVFSSF | 11 | Q5GH67 | XK-related protein 4 |
| **ERAAP KO** | LPQRVLEQHKL | 11 | P26041 | Moesin |
| **ERAAP KO** | IPMKPSWKTAF | 11 | O35892 | Nuclear autoantigen Sp-100 |
| **ERAAP KO** | QPQPGFGYSM | 10 | Q68FD5 | Clathrin heavy chain 1 |
| **ERAAP KO** | KPHSGFHVAF | 10 | Q8CD10 | EF-hand domain-containing family member A1 |
| **ERAAP KO** | CVQWIVKFI | 9 | Q80YQ2 | Mediator of RNA polymerase II transcription subunit 23 |
| **ERAAP KO** | HPAPMPPML | 9 | Q62203 | Splicing factor 3A subunit 2 |
| **ERAAP KO** | LVPFTLFEL | 9 | Q8BYY4 | Tetratricopeptide repeat protein 39B |
| **ERAAP KO** | IPQDLEDFI | 9 | Q3UP75 | UDP-glucuronosyltransferase 3A1 |
| **ERAAP KO** | VPNESFFNF | 9 | Q78ZA7 | Nucleosome assembly protein 1-like 4 |
| **ERAAP KO** | HPYLAIYDL | 9 | P97813 | Phospholipase D2 |
| **ERAAP KO** | RNAVIGLNL | 9 | P97287 | Induced myeloid leukemia cell differentiation protein Mcl-1 homolog |
| **ERAAP KO** | RPAQLHIGF | 9 | Q02053 | Ubiquitin-like modifier-activating enzyme 1 |

| | | | | |
|---|---|---|---|---|
| **ERAAP KO** | LNKLGGVEF | 9 | O08997 | Copper transport protein ATOX1 |
| **ERAAP KO** | TPQILVNNL | 9 | Q6Q899 | Probable ATP-dependent RNA helicase DDX58 |
| **ERAAP KO** | SPGRILHDL | 9 | Q8C263 | Uncharacterized protein C13orf3 homolog |
| **ERAAP KO** | HPMRAIFMI | 9 | Q9JI10 | Serine/threonine-protein kinase 3 |
| **ERAAP KO** | IPQEKPIFL | 9 | P19096 | Fatty acid synthase |
| **ERAAP KO** | QPFSAKDL | 8 | P52633 | Signal transducer and transcription activator 6 |
| **ERAAP KO** | IPGHPLQL | 8 | Q99KC8 | Loss of heterozygosity 11 chromosomal region 2 gene A protein homolog |
| **ERAAP KO** | LPSHPLEL | 8 | Q9CQT5 | Proteasome maturation protein |

**Table 6: $D^d$ peptides from WT and ERAAP-deficient spleen cells**

| Sample | Sequence | Length | Uniprot Id | Source Protein |
|---|---|---|---|---|
| WT | EGKHLYTL | 8 | P68040 | Guanine nucleotide-binding protein subunit beta-2-like 1 |
| WT | GPVIKVKI | 8 | Q9CQT2 | RNA-binding protein 7 |
| WT | GPLHLFRL | 8 | Q6S5C2 | N-acetylglucosamine-1-phosphotransferase subunit gamma |
| WT | GPERILSI | 8 | P61979 | Heterogeneous nuclear ribonucleoprotein K |
| WT | GPLRTVWI | 8 | Q8BL97 | Splicing factor, arginine/serine-rich 7 |
| WT | SPLRSLLF | 8 | P21460 | Cystatin-C |
| WT | NPLRILNI | 8 | Q810L4 | Transmembrane protein 39B |
| WT | GPEHIIKM | 8 | Q8CHI8 | E1A-binding protein p400 |
| WT | GPPHFKTI | 8 | Q5SQX6 | Cytoplasmic FMR1-interacting protein 2 |
| WT | GPVRGIDF | 8 | Q8CIE6 | Coatomer subunit alpha |
| WT | VGVYRSPI | 8 | P55200 | Histone-lysine N-methyltransferase HRX |
| WT | SPYHVDLL | 8 | Q9Z1S0 | Mitotic checkpoint serine/threonine-protein kinase BUB1 beta |
| WT | AGPQSQLL | 8 | Q9QYB8 | Beta-adducin |
| WT | LGFMGNLLI | 9 | O70342 | Neuropeptide Y receptor type 5 |
| WT | TAPVRSLFL | 9 | Q8BSF4 | Phosphatidylserine decarboxylase proenzyme |
| WT | YGPLRTVWI | 9 | Q8BL97 | Splicing factor, arginine/serine-rich 7 |
| WT | MGPSHIINI | 9 | Q91WD1 | DNA-directed RNA polymerase III subunit RPC4 |
| WT | AGPEIRDAI | 9 | Q8BHZ0 | Protein FAM49A |
| WT | ASPLRSLLF | 9 | P21460 | Cystatin-C |
| WT | VGPALLQSL | 9 | Q571H0 | Nucleolar pre-ribosomal-associated protein 1 |

| | | | | |
|---|---|---|---|---|
| WT | GGPLRDYQI | 9 | Q6PGB8 | Probable global transcription activator SNF2L1 |
| WT | DGPARLLNL | 9 | Q8BRH4 | Histone-lysine N-methyltransferase MLL3 |
| WT | LGPEKTSFF | 9 | P14869 | 60S acidic ribosomal protein P0 |
| WT | TGPWRSLWI | 9 | Q8R2T8 | General transcription factor 3C polypeptide 5 |
| WT | DGPTKNLFI | 9 | P70188 | Kinesin-associated protein 3 |
| WT | VLASRLFQL | 9 | Q3UYK3 | TBC1 domain family member 9 |
| WT | SGASRGVGF | 9 | Q91W59 | RNA-binding motif, single-stranded-interacting protein 1 |
| WT | IGMTKADLI | 9 | P07901 | Heat shock protein HSP 90-alpha |
| WT | YGPIADVSI | 9 | P62996 | Splicing factor, arginine/serine-rich 10 |
| WT | IGPLRLSTL | 9 | Q8BKX6 | Serine/threonine-protein kinase SMG1 |
| WT | IGAERSLVL | 9 | Q03267 | DNA-binding protein Ikaros |
| WT | AGPVIKVKI | 9 | Q9CQT2 | RNA-binding protein 7 |
| WT | AGPDRFVLL | 9 | Q3UPF5 | Zinc finger CCCH-type antiviral protein 1 |
| WT | SGPERILSI | 9 | P61979 | Heterogeneous nuclear ribonucleoprotein K |
| WT | SGPLHLFRL | 9 | Q6S5C2 | N-acetylglucosamine-1-phosphotransferase subunit gamma |
| WT | STPLRSGLL | 9 | Q8C0R0 | Ubiquitin carboxyl-terminal hydrolase 37 |
| WT | SGPNRFILI | 9 | O08696 | Forkhead box protein M1 |
| WT | SGPVHAPVF | 9 | Q91WM1 | Spermatid perinuclear RNA-binding protein |
| WT | LGIHGLGGI | 9 | Q8CIZ9 | NADPH oxidase 1 |
| WT | IGPRAVDVL | 9 | Q7TSQ8 | Pyruvate dehydrogenase phosphatase regulatory subunit, mitochondrial |
| WT | VGPDGKELI | 9 | O70279 | Protein DGCR14 |
| WT | IGPNLSIKI | 9 | P27641 | ATP-dependent DNA helicase 2 subunit 2 |

| | | | | |
|---|---|---|---|---|
| WT | **GGLQHLYNI** | 9 | Q3UFS0 | Protein zyg-11 homolog B |
| WT | **GGPVRVYSL** | 9 | Q62507 | Cochlin |
| WT | **TGPNRYLLF** | 9 | Q9DC69 | NADH dehydrogenase [ubiquinone] 1 alpha subcomplex subunit 9, mitochondrial |
| WT | **LGPRNVLLF** | 9 | Q9R1Q9 | V-type proton ATPase subunit S1 |
| WT | **VGASKAVFL** | 9 | O54927 | WD repeat and SOCS box-containing protein 1 |
| WT | **FGPGREYNF** | 9 | Q8CDD8 | BTB/POZ domain-containing protein KCTD20 |
| WT | **YGPEHLLTF** | 9 | P59016 | Vacuolar protein sorting-associated protein 33B |
| WT | **SGPFRTITV** | 9 | P13864 | DNA (cytosine-5)-methyltransferase 1 |
| WT | **GGPDRFYFL** | 9 | P13864 | DNA (cytosine-5)-methyltransferase 1 |
| WT | **VGPNHAAFL** | 9 | Q80TP3 | E3 ubiquitin-protein ligase UBR5 |
| WT | **QGFQLTHSL** | 9 | Q7TMM9 | Tubulin beta-2A chain |
| WT | **KGPVIALEF** | 9 | Q9EPK2 | Protein XRP2 |
| WT | **YGPYKPFQL** | 9 | Q3UM29 | Conserved oligomeric Golgi complex subunit 7 |
| WT | **LGPEHIIKM** | 9 | Q8CHI8 | E1A-binding protein p400 |
| WT | **WGAFRHFQL** | 9 | P19096 | Fatty acid synthase |
| WT | **VGPPHFKTI** | 9 | Q5SQX6 | Cytoplasmic FMR1-interacting protein 2 |
| WT | **FGPYHFNVL** | 9 | Q9D7B7 | Probable glutathione peroxidase 8 |
| WT | **EGPKVIFRF** | 9 | Q3U0J8 | TBC1 domain family member 2B |
| WT | **SGPLKGIEL** | 9 | Q80Y81 | Zinc phosphodiesterase ELAC protein 2 |
| WT | **IGLPATRAF** | 9 | Q6GQT1 | Alpha-2-macroglobulin-P |
| WT | **IGPLYPHAF** | 9 | Q8C547 | HEAT repeat-containing protein 5B |
| WT | **VSPVKINQI** | 9 | Q5KU39 | Vacuolar protein sorting-associated protein 41 homolog |

| | | | | |
|---|---|---|---|---|
| WT | **AGPRYEYHW** | 9 | Q921Y0 | Mps one binder kinase activator-like 1B |
| WT | **VGPIEATTF** | 9 | O35228 | Interleukin-27 subunit beta |
| WT | **VGPFQEAAF** | 9 | Q9CWW6 | Peptidyl-prolyl cis-trans isomerase NIMA-interacting 4 |
| WT | **LGPEIFQAY** | 9 | Q8VHY0 | Chondroitin sulfate proteoglycan 4 |
| WT | **RGPFELEAF** | 9 | Q61699 | Heat shock protein 105 kDa |
| WT | **VGARVLDAL** | 9 | Q9CQA1 | Trafficking protein particle complex subunit 5 |
| WT | **FGPMKGGNF** | 9 | P49312 | Heterogeneous nuclear ribonucleoprotein A1 |
| WT | **VGPGSTVTL** | 9 | Q6NZQ4 | ETS-related transcription factor |
| WT | **VGPAAAQQI** | 9 | Q8BHL6 | Fanconi anemia-associated protein of 24 kDa |
| WT | **QGPVAAVLL** | 9 | Q8C9V1 | Carabin |
| WT | **GGPVKIGQL** | 9 | Q9QY24 | Z-DNA-binding protein 1 |
| WT | **NGSTELVAL** | 9 | Q9EPE9 | Probable cation-transporting ATPase 13A1 |
| WT | **LGPQRVSGL** | 9 | Q9JL16 | Interferon-stimulated gene 20 kDa protein |
| WT | **IGPGMVQQI** | 9 | P63037 | DnaJ homolog subfamily A member 1 |
| WT | **YGPMKGGSF** | 9 | Q8BG05 | Heterogeneous nuclear ribonucleoprotein A3 |
| WT | **AGPVYSHTL** | 9 | Q91V83 | Uncharacterized protein KIAA0406 homolog |
| WT | **IGPSKPNEI** | 9 | Q8K4Z5 | Splicing factor 3 subunit 1 |
| WT | **SGPFRHVGL** | 9 | Q3TBD2 | Minor histocompatibility protein HA-1 |
| WT | **VGAERNVLI** | 9 | P63017 | Heat shock cognate 71 kDa protein |
| WT | **AGPKLQEEL** | 9 | Q2EMV9 | Poly [ADP-ribose] polymerase 14 |
| WT | **QGPKTIDQI** | 9 | Q6NZJ6 | Eukaryotic translation initiation factor 4 gamma 1 |
| WT | **KGPEALQEF** | 9 | Q3UA37 | Glutamine-rich protein 1 |

| | | | | |
|---|---|---|---|---|
| WT | VGPELHEKL | 9 | Q9QXS1 | Plectin-1 |
| WT | VGPDRLEKL | 9 | Q8JZQ9 | Eukaryotic translation initiation factor 3 subunit B |
| WT | KGPYDFDQI | 9 | Q6NVE8 | WD repeat-containing protein 44 |
| WT | AGPSRTVGLF | 10 | Q64521 | Glycerol-3-phosphate dehydrogenase, mitochondrial |
| WT | TGPSKDALHL | 10 | Q571H0 | Nucleolar pre-ribosomal-associated protein 1 |
| WT | YGQISEVVVV | 10 | P60824 | Cold-inducible RNA-binding protein |
| WT | VGPNHAAFLL | 10 | Q80TP3 | E3 ubiquitin-protein ligase UBR5 |
| WT | VGPERDLAEL | 10 | Q00417 | Transcription factor 7 |
| WT | SSGPERILSI | 10 | P61979 | Heterogeneous nuclear ribonucleoprotein K |
| WT | VAPVSDIIEI | 10 | Q99LC5 | Electron transfer flavoprotein subunit alpha, mitochondrial |
| WT | NGPPEEAEKF | 10 | Q9JL04 | Formin-2 |
| WT | FPGPLKEENL | 10 | Q91X84 | CREB-regulated transcription coactivator 3 |
| WT | VGPVEEVKEL | 10 | P18242 | Cathepsin D |
| WT | APGPNRTLLL | 10 | Q80TT8 | p53-associated parkin-like cytoplasmic protein |
| WT | LPSQLLVPNL | 10 | Q6PGF3 | Mediator of RNA polymerase II transcription subunit 16 |
| WT | LGVSPNRILL | 10 | O09130 | NFATC2-interacting protein |
| WT | PSGPFRHVGL | 10 | Q3TBD2 | Minor histocompatibility protein HA-1 |
| WT | EGLPVGLSAI | 10 | Q8VDV3 | Guanine nucleotide exchange factor for Rab3A |
| WT | GGRNHLVLSL | 10 | Q9JKV7 | Exostosin-like 1 |
| WT | IGASCTLSLL | 10 | Q91W10 | Zinc transporter ZIP8 |
| WT | DGGPVKIGQL | 10 | Q9QY24 | Z-DNA-binding protein 1 |
| WT | APGPVHTQEI | 10 | Q61210 | Rho guanine nucleotide exchange factor 1 |

| | | | | |
|---|---|---|---|---|
| WT | IGPIKNEQQL | 10 | Q61216 | Double-strand break repair protein MRE11A |
| WT | AGPSRTVGLFL | 11 | Q64521 | Glycerol-3-phosphate dehydrogenase, mitochondrial |
| WT | DSSGPERILSI | 11 | P61979 | Heterogeneous nuclear ribonucleoprotein K |
| WT | YGIPFAAPTAL | 11 | Q91VX2 | Ubiquitin-associated protein 2 |
| WT | PDSSGPERILSI | 12 | P61979 | Heterogeneous nuclear ribonucleoprotein K |
| WT | GPNPFPQKEDTL | 12 | Q6WKZ8 | E3 ubiquitin-protein ligase UBR2 |
| WT | VPDSSGPERILSI | 13 | P61979 | Heterogeneous nuclear ribonucleoprotein K |
| Shared | GPLKAFNL | 8 | P26369 | Splicing factor U2AF 65 kDa subunit |
| Shared | MGPWTHSL | 8 | P97821 | Dipeptidyl-peptidase 1 |
| Shared | RLPLRIFLI | 9 | P13516 | Acyl-CoA desaturase 1 |
| Shared | VGAAAWWFI | 9 | O55143 | Sarcoplasmic/endoplasmic reticulum calcium ATPase 2 |
| Shared | FGPYKQLFL | 9 | Q8CIE6 | Coatomer subunit alpha |
| Shared | RGPIKFNVW | 9 | Q61820 | GTP-binding nuclear protein Ran, testis-specific isoform |
| Shared | TGPLLKFQI | 9 | P62342 | Selenoprotein T |
| Shared | VGPEHGTEI | 9 | Q80SU7 | Interferon-induced very large GTPase 1 |
| Shared | NGPQNIYNL | 9 | Q8K3C0 | Ribonuclease kappa |
| Shared | VGPVTVVRL | 9 | Q9DAK3 | Rho-related BTB domain-containing protein 1 |
| Shared | GGPQALVNI | 9 | Q02248 | Catenin beta-1 |
| Shared | NGPIHWNEL | 9 | Q9D6N1 | Carbonic anhydrase 13 |
| Shared | HGPLITFHL | 9 | Q3UHC0 | Trinucleotide repeat-containing gene 6C protein |
| Shared | TGPSVYELI | 9 | Q8BFQ8 | Parkinson disease 7 domain-containing protein 1 |
| Shared | VGPTQRLLL | 9 | Q3UDR8 | Protein YIPF3 |

| | | | | |
|---|---|---|---|---|
| Shared | AGPMRQISL | 9 | Q80T69 | Round spermatid basic protein 1 |
| Shared | IGPTYYQRL | 9 | Q8CFI7 | DNA-directed RNA polymerase II subunit RPB2 |
| Shared | GGPQQLYHL | 9 | Q9CQJ2 | PIH1 domain-containing protein 1 |
| Shared | KGPEVLDFI | 9 | P43404 | Tyrosine-protein kinase ZAP-70 |
| Shared | SGPERILSI | 9 | P61979 | Heterogeneous nuclear ribonucleoprotein K |
| Shared | GGPFRFVDL | 9 | Q8BMS1 | Trifunctional enzyme subunit alpha, mitochondrial |
| Shared | VGPTLKATF | 9 | Q8CDM1 | ATPase family AAA domain-containing protein 2 |
| Shared | SVPTRALLL | 9 | P17427 | AP-2 complex subunit alpha-2 |
| Shared | IGPSSIDLI | 9 | Q80WQ6 | Rhomboid family member 2 |
| Shared | SGPIHVLLI | 9 | Q61502 | Transcription factor E2F5 |
| Shared | KGATIVDAL | 9 | P45700 | Mannosyl-oligosaccharide 1,2-alpha-mannosidase IA |
| Shared | AGPVHALAI | 9 | Q9D8S9 | BolA-like protein 1 |
| Shared | RGPFADENF | 9 | Q9D868 | Peptidyl-prolyl cis-trans isomerase H |
| Shared | VGPTILNKI | 9 | Q8QZS3 | Folliculin |
| Shared | IGPKNYEFL | 9 | Q8BHY8 | Sorting nexin-14 |
| Shared | LGPKVSVLI | 9 | P46061 | Ran GTPase-activating protein 1 |
| Shared | YGPLRSVWV | 9 | P84104 | Splicing factor, arginine/serine-rich 3 |
| Shared | SGPPVSELI | 9 | P15864 | Histone H1.2 |
| Shared | VGAIKLTYI | 9 | Q8BUL6 | Pleckstrin homology domain-containing family A member 1 |
| Shared | SGPTIQDYL | 9 | Q9CVI2 | Protein FAM133B |
| Shared | YGPGRLFTL | 9 | Q8R1U1 | Conserved oligomeric Golgi complex subunit 4 |
| Shared | VGGTLKDFL | 9 | Q9ERL9 | Guanylate cyclase soluble subunit alpha-3 |

| | | | | |
|---|---|---|---|---|
| Shared | VGPGHGIQL | 9 | Q9JMH7 | Sialidase-3 |
| Shared | TGPPVSELI | 9 | P43276 | Histone H1.5 |
| Shared | AGPLRIVAL | 9 | Q9D8T0 | Protein FAM3A |
| Shared | SGPQLFQTF | 9 | Q8BFX3 | BTB/POZ domain-containing protein KCTD3 |
| Shared | MGPYRQDLL | 9 | Q64727 | Vinculin |
| Shared | TGPLVINRV | 9 | P47911 | 60S ribosomal protein L6 |
| Shared | TGFSHIDLI | 9 | Q9Z1F9 | SUMO-activating enzyme subunit 2 |
| Shared | LGPDAAINL | 9 | Q99KJ8 | Dynactin subunit 2 |
| Shared | DGPVRGIDF | 9 | Q8CIE6 | Coatomer subunit alpha |
| Shared | AGPRLIVYI | 9 | Q64324 | Syntaxin-binding protein 2 |
| Shared | NGPQKLIEI | 9 | Q99PP2 | Zinc finger protein 318 (Fragment) |
| Shared | VGPPHFQVI | 9 | Q7TMB8 | Cytoplasmic FMR1-interacting protein 1 |
| Shared | IGAEVYHNL | 9 | P17182 | Alpha-enolase |
| Shared | TGPLVEDFL | 9 | Q02053 | Ubiquitin-like modifier-activating enzyme 1 |
| Shared | ELGAQLVII | 9 | Q91ZW8 | CD209 antigen-like protein D |
| Shared | GGPAHITSL | 9 | Q62137 | Tyrosine-protein kinase JAK3 |
| Shared | RGPVRGISI | 9 | P63276 | 40S ribosomal protein S17 |
| Shared | YGPMKSGNF | 9 | O88569 | Heterogeneous nuclear ribonucleoproteins A2/B1 |
| Shared | STPQRNFEI | 9 | Q8VCX5 | Calcium-binding atopy-related autoantigen |
| Shared | LGAGRQSLL | 9 | Q921C3 | Bromodomain and WD repeat-containing protein 1 |
| Shared | MGPGRTVVI | 9 | Q9JL15 | Galectin-8 |
| Shared | SGGQRVITI | 9 | P81069 | GA-binding protein subunit beta-2 |

| | | | | |
|---|---|---|---|---|
| **Shared** | **GVGPIRKVLL** | 10 | Q8BH60 | Golgi-associated PDZ and coiled-coil motif-containing protein |
| **Shared** | **GPGPGRLLLL** | 10 | P11276 | Fibronectin |
| **Shared** | **YGPVGLRDFI** | 10 | Q8VEB6 | Zinc phosphodiesterase ELAC protein 1 |
| **Shared** | **SSGPERILSI** | 10 | P61979 | Heterogeneous nuclear ribonucleoprotein K |
| **Shared** | **NPGPDKYFTL** | 10 | O88958 | Glucosamine-6-phosphate isomerase 1 |
| **Shared** | **DSSGPERILSI** | 11 | P61979 | Heterogeneous nuclear ribonucleoprotein K |
| **Shared** | **PDSSGPERILSI** | 12 | P61979 | Heterogeneous nuclear ribonucleoprotein K |
| **ERAAP KO** | **SPLRSLLF** | 8 | P21460 | Cystatin-C |
| **ERAAP KO** | **GPPHFKTI** | 8 | Q5SQX6 | Cytoplasmic FMR1-interacting protein 2 |
| **ERAAP KO** | **GPLHLFRL** | 8 | Q6S5C2 | N-acetylglucosamine-1-phosphotransferase subunit gamma |
| **ERAAP KO** | **GPEFKDKL** | 8 | Q9QXS1 | Plectin-1 |
| **ERAAP KO** | **GPLRTVWI** | 8 | Q8BL97 | Splicing factor, arginine/serine-rich 7 |
| **ERAAP KO** | **GAPELEVAR** | 9 | Q8BHJ6 | Serine incorporator 5 |
| **ERAAP KO** | **AGPIRVVTI** | 9 | Q3THG9 | Alanyl-tRNA synthetase domain-containing protein 1 |
| **ERAAP KO** | **AGASRIIGI** | 9 | Q64437 | Alcohol dehydrogenase class 4 mu/sigma chain |
| **ERAAP KO** | **SGPSKWNWL** | 9 | Q810A7 | ATP-dependent RNA helicase DDX42 |
| **ERAAP KO** | **RAPVIWDNI** | 9 | Q9EQQ9 | Bifunctional protein NCOAT |
| **ERAAP KO** | **VGALMYHTI** | 9 | O88712 | C-terminal-binding protein 1 |
| **ERAAP KO** | **ASPLRSLLF** | 9 | P21460 | Cystatin-C |
| **ERAAP KO** | **VGPPHFKTI** | 9 | Q5SQX6 | Cytoplasmic FMR1-interacting protein 2 |
| **ERAAP KO** | **FGGQRRPLL** | 9 | Q8C9B9 | Death-inducer obliterator 1 |
| **ERAAP KO** | **GGPDRFYFL** | 9 | P13864 | DNA (cytosine-5)-methyltransferase 1 |

| | | | | |
|---|---|---|---|---|
| **ERAAP KO** | **IGAERSLVL** | 9 | Q03267 | DNA-binding protein Ikaros |
| **ERAAP KO** | **VGPNHAAFL** | 9 | Q80TP3 | E3 ubiquitin-protein ligase UBR5 |
| **ERAAP KO** | **FSPNRVIGL** | 9 | Q9DCH4 | Eukaryotic translation initiation factor 3 subunit F |
| **ERAAP KO** | **FGPINSVAF** | 9 | Q9QZD9 | Eukaryotic translation initiation factor 3 subunit I |
| **ERAAP KO** | **LGSAEQFLL** | 9 | Q76LL6 | FH1/FH2 domain-containing protein 3 |
| **ERAAP KO** | **AAPYKSDFL** | 9 | Q9JL62 | Glycolipid transfer protein |
| **ERAAP KO** | **EGPEYWERI** | 9 | P01897 | H-2 class I histocompatibility antigen, L-D alpha chain |
| **ERAAP KO** | **SQVMNLHNL** | 9 | P29812 | L-dopachrome tautomerase |
| **ERAAP KO** | **GGPAIVHGL** | 9 | Q9CZW4 | Long-chain-fatty-acid--CoA ligase 3 |
| **ERAAP KO** | **SAPKYIDYL** | 9 | Q8BPB0 | Mps one binder kinase activator-like 1A |
| **ERAAP KO** | **AGPKYEYHW** | 9 | Q8BPB0 | Mps one binder kinase activator-like 1A |
| **ERAAP KO** | **AGPRYEYHW** | 9 | Q921Y0 | Mps one binder kinase activator-like 1B |
| **ERAAP KO** | **SGPLHLFRL** | 9 | Q6S5C2 | N-acetylglucosamine-1-phosphotransferase subunit gamma |
| **ERAAP KO** | **VAPSKLEAL** | 9 | Q8C4Y3 | Negative elongation factor B |
| **ERAAP KO** | **TGPAHWELL** | 9 | Q9JHW2 | Nitrilase homolog 2 |
| **ERAAP KO** | **STAARTFYL** | 9 | Q9EQ61 | Pescadillo homolog 1 |
| **ERAAP KO** | **VGPEFKDKL** | 9 | Q9QXS1 | Plectin-1 |
| **ERAAP KO** | **RGPGTSFEF** | 9 | Q99LX0 | Protein DJ-1 |
| **ERAAP KO** | **AGPEIRDAI** | 9 | Q8BHZ0 | Protein FAM49A |
| **ERAAP KO** | **LGGARVTLL** | 9 | Q811G0 | Protein PTHB1 |
| **ERAAP KO** | **RGPFIIRQL** | 9 | Q80WQ2 | Protein VAC14 homolog |
| **ERAAP KO** | **VGALLVYDI** | 9 | P62492 | Ras-related protein Rab-11A |

| | | | | |
|---|---|---|---|---|
| **ERAAP KO** | **LGPVLSWQF** | 9 | Q9WVL2 | Signal transducer and activator of transcription 2 |
| **ERAAP KO** | **NGPEIISKF** | 9 | Q3UMC0 | Spermatogenesis-associated protein 5 |
| **ERAAP KO** | **YGPLRTVWI** | 9 | Q8BL97 | Splicing factor, arginine/serine-rich 7 |
| **ERAAP KO** | **AGPPNDFGL** | 9 | P26039 | Talin-1 |
| **ERAAP KO** | **EGPKVIFRF** | 9 | Q3U0J8 | TBC1 domain family member 2B |
| **ERAAP KO** | **NGPEIMSKL** | 9 | Q01853 | Transitional endoplasmic reticulum ATPase |
| **ERAAP KO** | **KGPSRRPSL** | 9 | Q9DCF1 | Transmembrane protein 25 |
| **ERAAP KO** | **SNPLRILNI** | 9 | Q810L4 | Transmembrane protein 39B |
| **ERAAP KO** | **YGPDFTQHL** | 9 | Q9D8Y7 | Tumor necrosis factor, alpha-induced protein 8-like protein 2 |
| **ERAAP KO** | **LGPIKLELL** | 9 | Q8R5L3 | Vam6/Vps39-like protein |
| **ERAAP KO** | **TAPVRSVDF** | 9 | Q8BHD1 | WD repeat-containing protein 51B |
| **ERAAP KO** | **GGPVKIGQL** | 9 | Q9QY24 | Z-DNA-binding protein 1 |
| **ERAAP KO** | **AGPDRFVLL** | 9 | Q3UPF5 | Zinc finger CCCH-type antiviral protein 1 |
| **ERAAP KO** | **SGPLKGIEL** | 9 | Q80Y81 | Zinc phosphodiesterase ELAC protein 2 |
| **ERAAP KO** | **GGPNYQEGL** | 9 | Q91V92 | ATP-citrate synthase |
| **ERAAP KO** | **TGPISAHSL** | 9 | P61460 | DEP domain-containing protein 5 |
| **ERAAP KO** | **KGPPYSDTF** | 9 | Q922Y0 | Dual specificity tyrosine-phosphorylation-regulated kinase 3 |
| **ERAAP KO** | **SGAERDLLL** | 9 | Q8BNW9 | Kelch repeat and BTB domain-containing protein 11 |
| **ERAAP KO** | **SGPLYTDRM** | 9 | Q8CIF6 | SID1 transmembrane family member 2 |
| **ERAAP KO** | **SGPAAHDLF** | 9 | Q8C754 | Vacuolar protein sorting-associated protein 52 homolog |
| **ERAAP KO** | **SGGPVRVYSL** | 10 | Q62507 | Cochlin |
| **ERAAP KO** | **SSGPFRTITV** | 10 | P13864 | DNA (cytosine-5)-methyltransferase 1 |

| | | | | |
|---|---|---|---|---|
| ERAAP KO | IGPIKNEQQL | 10 | Q61216 | Double-strand break repair protein MRE11A |
| ERAAP KO | RGPPKGILLF | 10 | Q8BPY9 | Fidgetin-like protein 1 |
| ERAAP KO | RGPSLATLLF | 10 | P11032 | Granzyme A |
| ERAAP KO | PSGPFRHVGL | 10 | Q3TBD2 | Minor histocompatibility protein HA-1 |
| ERAAP KO | LSADTASRFL | 10 | P60882 | Multiple epidermal growth factor-like domains 8 |
| ERAAP KO | AGPITDRIFL | 10 | Q5SUA5 | Myosin-Ig |
| ERAAP KO | VGPELHDRLL | 10 | Q9QXS1 | Plectin-1 |
| ERAAP KO | LGSFPGNVIL | 10 | Q921K8 | Protein FAM115C |
| ERAAP KO | GAGPEIRDAI | 10 | Q8BHZ0 | Protein FAM49A |
| ERAAP KO | QGPYKGYIGV | 10 | O55201 | Transcription elongation factor SPT5 |
| ERAAP KO | AAGPDRFVLL | 10 | Q3UPF5 | Zinc finger CCCH-type antiviral protein 1 |
| ERAAP KO | FSGPLKGIEL | 10 | Q80Y81 | Zinc phosphodiesterase ELAC protein 2 |
| ERAAP KO | LGLPRDEVLQ | 10 | Q61216 | Double-strand break repair protein MRE11A |
| ERAAP KO | IGPIKNEQQL | 10 | Q9R0N0 | Galactokinase |
| ERAAP KO | LGPQPPLRSA | 10 | Q9WTM3 | Semaphorin-6C |
| ERAAP KO | AFPGPLKEENL | 11 | Q91X84 | CREB-regulated transcription coactivator 3 |
| ERAAP KO | SQGGPDRFYFL | 11 | P13864 | DNA (cytosine-5)-methyltransferase 1 |
| ERAAP KO | STPVTAASELL | 11 | P43352 | DNA repair protein RAD52 homolog |
| ERAAP KO | IGPIKNEQQLF | 11 | Q61216 | Double-strand break repair protein MRE11A |
| ERAAP KO | VGPVVGGNQQI | 11 | Q8CHI8 | E1A-binding protein p400 |
| ERAAP KO | AGPSRTVGLFL | 11 | Q64521 | Glycerol-3-phosphate dehydrogenase, mitochondrial |
| ERAAP KO | RGPSLATLLFL | 11 | P11032 | Granzyme A |

| | | | | |
|---|---|---|---|---|
| **ERAAP KO** | **KLVEVEWEQHL** | 11 | Q3U1G5 | Interferon-stimulated 20 kDa exonuclease-like 2 |
| **ERAAP KO** | **HGPERDFPLYL** | 11 | Q5PSV9 | Mediator of DNA damage checkpoint protein 1 |
| **ERAAP KO** | **QGPARDVIAQL** | 11 | Q3U0J8 | TBC1 domain family member 2B |
| **ERAAP KO** | **KAAGPDRFVLL** | 11 | Q3UPF5 | Zinc finger CCCH-type antiviral protein 1 |
| **ERAAP KO** | **AAFPGPLKEENL** | 12 | Q91X84 | CREB-regulated transcription coactivator 3 |
| **ERAAP KO** | **IGAERSLVLDRL** | 12 | Q03267 | DNA-binding protein Ikaros |
| **ERAAP KO** | **RGPFRGNFEELI** | 12 | Q99ML9 | E3 ubiquitin-protein ligase Arkadia |
| **ERAAP KO** | **NAGPSRTVGLFL** | 12 | Q64521 | Glycerol-3-phosphate dehydrogenase, mitochondrial |
| **ERAAP KO** | **VGAERGEATDLL** | 12 | O54724 | Polymerase I and transcript release factor |
| **ERAAP KO** | **SSPGPSRIADYL** | 12 | Q8K4K4 | Tribbles homolog 1 |
| **ERAAP KO** | **KGPVREGDVLTLL** | 13 | P62858 | 40S ribosomal protein S28 |
| **ERAAP KO** | **TGPQKTEDAYTIS** | 13 | Q5SNZ0 | Girdin |
| **ERAAP KO** | **SVPDSSGPERILSI** | 14 | P61979 | Heterogeneous nuclear ribonucleoprotein K |
| **ERAAP KO** | **VSVPDSSGPERILSI** | 15 | P61979 | Heterogeneous nuclear ribonucleoprotein K |

**Table 7: $K^d$ peptides from WT and ERAAP-deficient spleen cells**

| Sample | Sequence | Length | Uniprot Id | Source Protein |
|---|---|---|---|---|
| ERAAP KO | SYVTTSTRTY | 10 | P20152 | Vimentin |
| ERAAP KO | KYFEVPSVLL | 10 | Q9QZB7 | Actin-related protein 10 |
| ERAAP KO | SLVSCFAGGVFL | 12 | Q9QZ03 | Zinc transporter ZIP1 |
| ERAAP KO | AYAPAAATV | 9 | O88532 | Zinc finger RNA-binding protein |
| ERAAP KO | PYKSILSEL | 9 | Q6P1B1 | Xaa-Pro aminopeptidase 1 |
| ERAAP KO | KYAPSGFYI | 9 | O88342 | WD repeat-containing protein 1 |
| ERAAP KO | TYQAMVHEL | 9 | P97390 | Vacuolar protein sorting-associated protein 45 |
| ERAAP KO | NYQEALRYI | 9 | Q91W86 | Vacuolar protein sorting-associated protein 11 homolog |
| ERAAP KO | TFINLMTHI | 9 | Q8BVE3 | V-type proton ATPase subunit H |
| ERAAP KO | VYQQTASLL | 9 | Q3U269 | Uncharacterized protein C9orf97 homolog |
| ERAAP KO | GYIESIQHI | 9 | Q9CXC3 | Uncharacterized protein C20orf72 homolog |
| ERAAP KO | YSQVLLRCL | 9 | Q8BFT2 | Uncharacterized protein C14orf94 homolog |
| ERAAP KO | SFGVTLHEL | 9 | P52332 | Tyrosine-protein kinase JAK1 |
| ERAAP KO | SYLEDKDLV | 9 | P52332 | Tyrosine-protein kinase JAK1 |
| ERAAP KO | DYLGSRQYV | 9 | P52332 | Tyrosine-protein kinase JAK1 |
| ERAAP KO | KYTPSLTVI | 9 | Q8CHB8 | Tubulin polyglutamylase TTLL5 |
| ERAAP KO | TYYAAQMLI | 9 | Q9D8N3 | Transmembrane protein 86A |
| ERAAP KO | KYITTLEDL | 9 | Q7TN22 | Thioredoxin domain-containing protein 16 |
| ERAAP KO | RYLQLTQSEL | 10 | Q810A3 | Tetratricopeptide repeat protein 9C |
| ERAAP KO | TYSCREGFIL | 10 | A2AVA0 | Sushi, von Willebrand factor type A, EGF and pentraxin domain-containing protein 1 |
| ERAAP KO | KYQIAVTKV | 9 | Q9CU62 | Structural maintenance of chromosomes protein 1A |
| ERAAP KO | TYRELIEQL | 9 | Q60864 | Stress-induced-phosphoprotein 1 |
| ERAAP KO | SYKPVFVTEI | 10 | Q78PY7 | Staphylococcal nuclease domain-containing protein 1 |
| ERAAP KO | LYQAVATIL | 9 | Q9CZV5 | STAGA complex 65 subunit gamma |
| ERAAP KO | SYYGPLNLL | 9 | O09005 | Sphingolipid delta(4)-desaturase DES1 |
| ERAAP KO | HYEITKQDI | 9 | Q62245 | Son of sevenless homolog 1 |
| ERAAP KO | SYRDVIQEL | 9 | Q921I6 | SH3 domain-binding protein 4 |
| ERAAP KO | EYISKMGYL | 9 | Q7TSJ6 | Serine/threonine-protein kinase LATS2 |
| ERAAP KO | AYNPLPLTRL | 10 | Q62388 | Serine-protein kinase ATM |
| ERAAP KO | ISYEELSQI | 9 | Q9WUH7 | Semaphorin-4G |
| ERAAP KO | HYLPSYYHL | 9 | Q9DAR7 | Scavenger mRNA-decapping enzyme DcpS |

| | | | | |
|---|---|---|---|---|
| **ERAAP KO** | KYEPIFQDI | 9 | Q64700 | Retinoblastoma-like protein 2 |
| **ERAAP KO** | SFRIYKGVI | 9 | Q99P72 | Reticulon-4 |
| **ERAAP KO** | YYKQGFSLI | 9 | Q8CHX7 | Raftlin-2 |
| **ERAAP KO** | SYVDIHTGL | 9 | Q9DCC4 | Pyrroline-5-carboxylate reductase 3 |
| **ERAAP KO** | AYVLMIKTL | 9 | P55086 | Proteinase-activated receptor 2 |
| **ERAAP KO** | GYVYGISAI | 9 | Q9EQQ2 | Protein YIPF5 |
| **ERAAP KO** | IYQYFEIFV | 9 | P61620 | Protein transport protein Sec61 subunit alpha isoform 1 |
| **ERAAP KO** | GYHPMPPQPGM | 11 | Q9D7I0 | Protein shisa-5 |
| **ERAAP KO** | KYNKLRQPFF | 10 | Q9EQU5 | Protein SET |
| **ERAAP KO** | LYTHIVTDI | 9 | Q80UZ2 | Protein SDA1 homolog |
| **ERAAP KO** | KFVAALSVL | 9 | Q9CTG6 | Probable cation-transporting ATPase 13A2 |
| **ERAAP KO** | SFNETMSQL | 9 | Q9JLG4 | Polycystic kidney disease 2-like 2 protein |
| **ERAAP KO** | GYLQPAGDL | 9 | Q9JHK5 | Pleckstrin |
| **ERAAP KO** | RYHAALAVI | 9 | Q9JJW0 | Peroxisomal membrane protein 4 |
| **ERAAP KO** | KYRQQFEEL | 9 | Q6ZQH8 | Nucleoporin NUP188 homolog |
| **ERAAP KO** | SYSATKETL | 9 | P09405 | Nucleolin |
| **ERAAP KO** | FFVENVSEL | 9 | Q6KCD5 | Nipped-B-like protein |
| **ERAAP KO** | SYNQGIVVI | 9 | Q5NCX5 | NHR domain-containing protein KIAA1787 |
| **ERAAP KO** | RFIPSQHYV | 9 | Q09014 | Neutrophil cytosol factor 1 |
| **ERAAP KO** | NYIWALSEI | 9 | Q60867 | Neurogenic differentiation factor 1 |
| **ERAAP KO** | EITLSFKTL | 9 | Q9CS84 | Neurexin-1-alpha |
| **ERAAP KO** | HYQPSVNNI | 9 | Q91XQ5 | N-acetylgalactosamine 4-sulfate 6-=- sulfotransferase |
| **ERAAP KO** | VYSNPVSTL | 9 | Q8CFN5 | Myocyte-specific enhancer factor 2C |
| **ERAAP KO** | KYLQNDLYI | 9 | O89050 | Muskelin |
| **ERAAP KO** | HYWPVHNEL | 9 | P97471 | Mothers against decapentaplegic homolog 4 |
| **ERAAP KO** | RYKKLLSLL | 9 | P53349 | Mitogen-activated protein kinase kinase kinase 1 |
| **ERAAP KO** | KYLSVQGQLF | 10 | Q791T5 | Mitochondrial carrier homolog 1 |
| **ERAAP KO** | IYKDSSTFL | 9 | Q3UIK4 | Methyltransferase-like protein KIAA1627 |
| **ERAAP KO** | KYFDTNSEI | 9 | Q5UAK0 | Mesoderm induction early response protein 1 |
| **ERAAP KO** | IYAFRSQEL | 9 | Q01727 | Melanocyte-stimulating hormone receptor |
| **ERAAP KO** | ALPVNAEGGEI | 11 | P43430 | Mast cell protease 8 |
| **ERAAP KO** | LYGTSLEAI | 9 | O88910 | MAGUK p55 subfamily member 3 |
| **ERAAP KO** | SYTFLREAL | 9 | Q8VC16 | Leucine-rich repeat-containing protein 14 |
| **ERAAP KO** | KYLENPNAL | 9 | Q8BX02 | KN motif and ankyrin repeat domain-containing protein 2 |
| **ERAAP** | VYAPLKELL | 9 | Q9D0F1 | Kinetochore protein NDC80 homolog |

| | | | | |
|---|---|---|---|---|
| **KO** | | | | |
| **ERAAP KO** | KYGSVIQLL | 9 | P70227 | Inositol 1,4,5-trisphosphate receptor type 3 |
| **ERAAP KO** | SGSRSGSDYSLTISSL | 16 | P01639 | Ig kappa chain V-V region MOPC 41 |
| **ERAAP KO** | AYLEQLESL | 9 | Q3UXZ9 | Histone demethylase JARID1A |
| **ERAAP KO** | NYGPMKGGSF | 10 | Q8BG05 | Heterogeneous nuclear ribonucleoprotein A3 |
| **ERAAP KO** | YTSSSAPSAI | 10 | Q64314 | Hematopoietic progenitor cell antigen CD34 |
| **ERAAP KO** | SYQAGPSAGAGGAGI | 15 | P49710 | Hematopoietic lineage cell-specific protein |
| **ERAAP KO** | VYIPSKTDL | 9 | Q9CRB2 | H/ACA ribonucleoprotein complex subunit 2 |
| **ERAAP KO** | GYVDNKEFV | 9 | P01899 | H-2 class I histocompatibility antigen, D-B alpha chain |
| **ERAAP KO** | AYAPSGNFV | 9 | P62880 | Guanine nucleotide-binding protein G(I)/G(S)/G(T) subunit beta-2 |
| **ERAAP KO** | VYSNTIQSI | 9 | P08752 | Guanine nucleotide-binding protein G(i), alpha-2 subunit |
| **ERAAP KO** | SYSQLITLV | 9 | Q6PAR5 | GTPase-activating protein and VPS9 domain-containing protein |
| **ERAAP KO** | QFNSSLHNI | 9 | O35166 | Golgi SNAP receptor complex member 2 |
| **ERAAP KO** | FYTPIPNGL | 9 | O08573 | Galectin-9 |
| **ERAAP KO** | AYNRILDAL | 9 | Q68FD7 | Folliculin-interacting protein 1 |
| **ERAAP KO** | KYKDMGTVVL | 10 | Q8R050 | Eukaryotic peptide chain release factor GTP-binding subunit ERF3A |
| **ERAAP KO** | FFSPTGSPL | 9 | P17679 | Erythroid transcription factor |
| **ERAAP KO** | YYLEVGKTLI | 10 | Q2HXL6 | ER degradation-enhancing alpha-mannosidase-like 3 |
| **ERAAP KO** | SYLDIERIL | 9 | Q6P1E8 | EF-hand calcium-binding domain-containing protein 6 |
| **ERAAP KO** | AYSIVIRQI | 9 | Q80TP3 | E3 ubiquitin-protein ligase UBR5 |
| **ERAAP KO** | TYMALEERL | 9 | O55176 | E3 ubiquitin-protein ligase Praja1 |
| **ERAAP KO** | TFASTLSHL | 9 | Q8CFI7 | DNA-directed RNA polymerase II subunit RPB2 |
| **ERAAP KO** | TYQDIQNTI | 9 | P08775 | DNA-directed RNA polymerase II subunit RPB1 |
| **ERAAP KO** | TYIGSVELV | 9 | Q01320 | DNA topoisomerase 2-alpha |
| **ERAAP KO** | YYLQIHPQEL | 10 | Q3U1J4 | DNA damage-binding protein 1 |
| **ERAAP KO** | IFYQSVLNI | 9 | Q8CIG0 | DEP domain-containing protein 1A |
| **ERAAP KO** | SYRKILNDL | 9 | Q01147 | Cyclic AMP-responsive element-binding protein 1 |
| **ERAAP KO** | HYLDTTTLI | 9 | P47941 | Crk-like protein |
| **ERAAP KO** | AYLPSSDTPLL | 11 | Q9Z160 | Conserved oligomeric Golgi complex subunit 1 |
| **ERAAP KO** | EYTRMSTSELI | 11 | Q9WVD4 | Chloride channel protein 5 |
| **ERAAP KO** | TYSPPLNKL | 9 | P02340 | Cellular tumor antigen p53 |
| **ERAAP KO** | EYIHSKNFI | 9 | Q9DC28 | Casein kinase I isoform delta |
| **ERAAP KO** | YYHEAALGEAL | 11 | O89001 | Carboxypeptidase D |
| **ERAAP KO** | YYVENTDTKM | 10 | Q8CGN4 | BCL-6 corepressor |
| **ERAAP KO** | SYKRSNFYI | 9 | Q9Z2H5 | Band 4.1-like protein 1 |

| | | | | |
|---|---|---|---|---|
| **ERAAP KO** | SYSSETDLTL | 10 | Q3UUF8 | Ankyrin repeat domain-containing protein 34B |
| **ERAAP KO** | SYFPTVNDI | 9 | Q8VHI4 | Amyotrophic lateral sclerosis 2 chromosomal region candidate gene 8 protein homolog |
| **ERAAP KO** | KFLAAGTHL | 9 | P14206 | 40S ribosomal protein SA |
| **ERAAP KO** | SYVVSSFTEL | 10 | A3KGF7 | 1-phosphatidylinositol-4,5-bisphosphate phosphodiesterase beta-2 |
| **ERAAP KO** | TYHASGTEL | 9 | Q3U1N2 | Sterol regulatory element-binding protein 2 |
| **ERAAP KO** | SYNQLTRL | | Q52KR2 | Leucine-rich repeats and immunoglobulin-like domains protein 2 |
| **Shared** | RYQEVIQEL | 9 | Q5DU37 | Zinc finger FYVE domain-containing protein 26 |
| **Shared** | LLEQANNAI | | Q8BND3 | WD repeat-containing protein 35 |
| **Shared** | NYQDTIGRL | 9 | P20152 | Vimentin |
| **Shared** | SYENMVTEI | 9 | P54728 | UV excision repair protein RAD23 homolog B |
| **Shared** | SYTSVLSRL | 9 | Q80TA9 | UPF0493 protein KIAA1632 |
| **Shared** | SYFGSSSSL | 9 | Q80U62 | Uncharacterized protein KIAA0226 |
| **Shared** | RYQEALSEL | 9 | Q8R092 | Uncharacterized protein C1orf43 homolog |
| **Shared** | SYAVSVNHV | 9 | Q8K387 | Ubiquitin carboxyl-terminal hydrolase 45 |
| **Shared** | AYQNNKELL | 9 | P57080 | Ubiquitin carboxyl-terminal hydrolase 25 |
| **Shared** | KYLINLETL | 9 | Q62120 | Tyrosine-protein kinase JAK2 |
| **Shared** | SYFPEITHI | 9 | P52332 | Tyrosine-protein kinase JAK1 |
| **Shared** | SFLETVNQL | 9 | Q9EP52 | Twisted gastrulation protein homolog 1 |
| **Shared** | AYLLNLNHL | 9 | Q91V04 | Translocation-associated membrane protein 1 |
| **Shared** | SYLENPTSYHL | 11 | Q9R210 | Transcription factor EB |
| **Shared** | TYGALVTQL | 9 | O55013 | Trafficking protein particle complex subunit 3 |
| **Shared** | SYLHSLQEV | 9 | Q5SSZ5 | Tensin-3 |
| **Shared** | GYLELLDHV | 9 | P26039 | Talin-1 |
| **Shared** | TFITDKTVL | 9 | P01849 | T-cell receptor alpha chain C region |
| **Shared** | SYSSLIRNL | 9 | Q64324 | Syntaxin-binding protein 2 |
| **Shared** | GYLGQVTTI | 9 | Q9Z1F9 | SUMO-activating enzyme subunit 2 |
| **Shared** | YYIHGPKGNEI | 11 | Q6P5D8 | Structural maintenance of chromosomes flexible hinge domain-containing protein 1 |
| **Shared** | NFIGTKTVI | 9 | Q9R1J0 | Sterol-4-alpha-carboxylate 3-dehydrogenase, decarboxylating |
| **Shared** | SYGDLKNAI | 9 | O35326 | Splicing factor, arginine/serine-rich 5 |
| **Shared** | YYFPVKNVI | 9 | Q921M3 | Splicing factor 3B subunit 3 |
| **Shared** | NYISGIQTI | 9 | Q921M3 | Splicing factor 3B subunit 3 |
| **Shared** | SYLKSELGL | 9 | Q922B9 | Sperm-specific antigen 2 homolog |
| **Shared** | VYLPLTSHI | 9 | Q8CFD4 | Sorting nexin-8 |
| **Shared** | RYLEQLHQL | 9 | P42227 | Signal transducer and activator of transcription 3 |
| **Shared** | KYVENFGLI | 9 | Q9CYN2 | Signal peptidase complex subunit 2 |
| **Shared** | KYYVQLEQL | 9 | Q9Z131 | SH3 domain-binding protein 5 |
| **Shared** | NYLDIKGLL | 9 | Q9WTX5 | S-phase kinase-associated protein 1 |

| | | | | |
|---|---|---|---|---|
| **Shared** | GYLKGYTLV | 9 | Q9CWZ3 | RNA-binding protein 8A |
| **Shared** | TYGLTPHYI | 9 | Q62176 | RNA-binding protein 38 |
| **Shared** | SYLFSHVPL | 9 | Q9D7G0 | Ribose-phosphate pyrophosphokinase 1 |
| **Shared** | TYELHRDF | 8 | Q6Y5D8 | Rho GTPase-activating protein 10 |
| **Shared** | IFDRVLTEL | 9 | P28700 | Retinoic acid receptor RXR-alpha |
| **Shared** | IYKGVIQAI | 9 | Q99P72 | Reticulon-4 |
| **Shared** | KYLNSVQYI | 9 | Q9ERD6 | Ras-specific guanine nucleotide-releasing factor RalGPS2 |
| **Shared** | KYQDILNEI | 9 | Q3UQ44 | Ras GTPase-activating-like protein IQGAP2 |
| **Shared** | RYQELINDI | 9 | Q9JKF1 | Ras GTPase-activating-like protein IQGAP1 |
| **Shared** | YYGPLKTLL | 9 | P58069 | Ras GTPase-activating protein 2 |
| **Shared** | NFLITQTEL | 9 | Q6ZPV2 | Putative DNA helicase INO80 complex homolog 1 |
| **Shared** | TYAPPKPRSEL | 11 | Q8BKS9 | Pumilio domain-containing protein KIAA0020 |
| **Shared** | SYIGSPRAV | 9 | Q8BJS4 | Protein unc-84 homolog B |
| **Shared** | SYKQNLENL | 9 | Q8BGX1 | Protein FAM113B |
| **Shared** | GYIKLINFI | 9 | Q922H1 | Protein arginine N-methyltransferase 3 |
| **Shared** | NYVNGKTFL | 9 | P49722 | Proteasome subunit alpha type-2 |
| **Shared** | GYLPGNEKL | 9 | P97372 | Proteasome activator complex subunit 2 |
| **Shared** | KFIATLQYI | 9 | Q9QUR6 | Prolyl endopeptidase |
| **Shared** | RYLPLNTAL | 9 | Q9D8M7 | PHD finger protein 10 |
| **Shared** | IYSEVATLI | 9 | Q9R0L6 | Pericentriolar material 1 protein |
| **Shared** | GYLAIVEHL | 9 | Q9Z1E3 | NF-kappa-B inhibitor alpha |
| **Shared** | VYSRTFTWL | 9 | Q9WTI7 | Myosin-Ic |
| **Shared** | KYKDIYTEL | 9 | P97434 | Myosin phosphatase Rho-interacting protein |
| **Shared** | KYFPSRVSI | 9 | Q6PEB6 | Mps one binder kinase activator-like 3 |
| **Shared** | YSSLNRAQL | | Q69ZX6 | MORC family CW-type zinc finger protein 2A |
| **Shared** | KYIHSADII | 9 | P47811 | Mitogen-activated protein kinase 14 |
| **Shared** | KYIHSANVL | 9 | P63085 | Mitogen-activated protein kinase 1 |
| **Shared** | SYLPPGTSL | 9 | Q8VCF0 | Mitochondrial antiviral-signaling protein |
| **Shared** | KYLGQLTSI | 9 | Q8K2Y9 | Malcavernin |
| **Shared** | GYLPLAHVL | 9 | Q9CZW4 | Long-chain-fatty-acid--CoA ligase 3 |
| **Shared** | SYLVSKQEL | 9 | Q3UM18 | Large subunit GTPase 1 homolog |
| **Shared** | IFTSVRSEL | 9 | Q3UWM4 | JmjC domain-containing histone demethylation protein 1D |
| **Shared** | KFTETLTNI | 9 | Q80SU7 | Interferon-induced very large GTPase 1 |
| **Shared** | VYGSLASVL | 9 | Q8JZK9 | Hydroxymethylglutaryl-CoA synthase, cytoplasmic |
| **Shared** | AYLPNGTVL | 9 | Q80Y84 | Histone demethylase JARID1B |
| **Shared** | RYFDSFGDL | 9 | P02088 | Hemoglobin subunit beta-1 |
| **Shared** | KFLASVSTV | 9 | P01942 | Hemoglobin subunit alpha |
| **Shared** | QYLPAIRAL | 9 | P27601 | Guanine nucleotide-binding protein subunit alpha-13 |
| **Shared** | NYFPSKQDI | 9 | P27600 | Guanine nucleotide-binding protein subunit alpha-12 |
| **Shared** | AYAPSGNYV | 9 | P62874 | Guanine nucleotide-binding protein G(I)/G(S)/G(T) subunit beta-1 |

| | | | | |
|---|---|---|---|---|
| **Shared** | YYLNDLERI | 9 | P08752 | Guanine nucleotide-binding protein G(i), alpha-2 subunit |
| **Shared** | NYIESKESL | 9 | Q75N62 | GTPase IMAP family member 8 |
| **Shared** | NYLPAINGI | 9 | P36536 | GTP-binding protein SAR1a |
| **Shared** | GYLPNKQVL | 9 | Q05915 | GTP cyclohydrolase 1 |
| **Shared** | SYNPSSQAL | 9 | Q2NL51 | Glycogen synthase kinase-3 alpha |
| **Shared** | TYLVFVQGI | 9 | Q8BZM1 | Glomulin |
| **Shared** | VYVDGKEEI | 9 | Q9WUD8 | Fas apoptotic inhibitory molecule 1 |
| **Shared** | RYLPAPTAL | 9 | Q9JL70 | Fanconi anemia group A protein homolog |
| **Shared** | KYVPLVTGL | 9 | Q8BMI0 | F-box only protein 38 |
| **Shared** | RYLQTLTTI | 9 | P54116 | Erythrocyte band 7 integral membrane protein |
| **Shared** | AYQSIQSYL | 9 | Q925U4 | ER degradation-enhancing alpha-mannosidase-like 1 |
| **Shared** | YYSPTKNEI | 9 | Q4PZA2 | Endothelin-converting enzyme 1 |
| **Shared** | GYLPVQTVL | 9 | P11531 | Dystrophin |
| **Shared** | TYTSARTLL | 9 | Q61881 | DNA replication licensing factor MCM7 |
| **Shared** | KYQQLFEDI | 9 | P49717 | DNA replication licensing factor MCM4 |
| **Shared** | VYTRHPLF | | Q9CWR8 | DNA (cytosine-5)-methyltransferase 3-like |
| **Shared** | TYLVSKESI | 9 | Q6PNC0 | DmX-like protein 1 |
| **Shared** | YLPMAQSV | 8 | Q9DCP9 | DAZ-associated protein 2 |
| **Shared** | AYLNMFEHI | 9 | Q99N16 | Cytochrome P450 4F3 |
| **Shared** | AYVPGFAHI | 9 | Q9CXX9 | CUE domain-containing protein 2 |
| **Shared** | SFVDTRTLL | 9 | Q01149 | Collagen alpha-2(I) chain |
| **Shared** | KYGVVLDEI | 9 | O89079 | Coatomer subunit epsilon |
| **Shared** | DYQALRTSI | 9 | Q68FD5 | Clathrin heavy chain 1 |
| **Shared** | SYIGGHEGL | 9 | P40201 | Chromodomain-helicase-DNA-binding protein 1 |
| **Shared** | SFLPAQHTV | 9 | Q8K4Q7 | Ceramide kinase |
| **Shared** | SYSLQRQSL | | Q9CWM2 | Cell division cycle-associated protein 4 |
| **Shared** | KYQEVTNNL | 9 | Q60865 | Caprin-1 |
| **Shared** | KFNQILTAL | 9 | Q9QZK2 | Breast cancer anti-estrogen resistance protein 3 |
| **Shared** | KYLTVKDYL | 9 | Q8CDM1 | ATPase family AAA domain-containing protein 2 |
| **Shared** | SFLPSGSEI | 9 | Q9JKC7 | AP-4 complex subunit mu-1 |
| **Shared** | SYGTAVTHI | 9 | P27808 | Alpha-1,3-mannosyl-glycoprotein 2-beta-N-acetylglucosaminyltransferase |
| **Shared** | KLVTTVTEI | 9 | P40124 | Adenylyl cyclase-associated protein 1 |
| **Shared** | SYALHQVTL | 9 | Q99J27 | Acetyl-coenzyme A transporter 1 |
| **Shared** | VYNASNNEL | 9 | P62242 | 40S ribosomal protein S8 |
| **Shared** | KYFEVPSVL | 9 | Q9QZB7 | Actin-related protein 10 |
| **Shared** | KYSGVLSSI | 9 | Q791T5 | Mitochondrial carrier homolog 1 |
| **Shared** | VYLPTHTSL | 9 | Q8BM54 | E3 ubiquitin-protein ligase MYLIP |
| **Shared** | VYLPTHTSLL | 10 | Q8BM54 | E3 ubiquitin-protein ligase MYLIP |
| **WT** | NYSLSRELL | 9 | Q03385 | Ral guanine nucleotide dissociation stimulator |
| **WT** | GYVQSKEMI | 9 | P14685 | 26S proteasome non-ATPase regulatory subunit 3 |
| **WT** | GYKAGMTHI | 9 | P27659 | 60S ribosomal protein L3 |

| | | | | |
|---|---|---|---|---|
| WT | KYFEVPSVL | 9 | Q9QZB7 | Actin-related protein 10 |
| WT | DFYKDLEKI | 9 | O88444 | Adenylate cyclase type 1 |
| WT | DYLQTITNI | 9 | Q8K4T1 | Alpha-2,8-sialyltransferase 8F |
| WT | YLQTITNI | 8 | Q8K4T1 | Alpha-2,8-sialyltransferase 8F |
| WT | LYLKTENYL | 9 | O08739 | AMP deaminase 3 |
| WT | SFTGTKTSL | 9 | A2A4P0 | ATP-dependent RNA helicase DHX8 |
| WT | TYSPSRVLI | 9 | Q91XU0 | ATPase WRNIP1 |
| WT | VYTLTIQNI | 9 | P15530 | B-cell antigen receptor complex-associated protein beta-chain |
| WT | KYFGGVTAL | 9 | Q9JJ04 | Beta-1,4-galactosyltransferase 4 |
| WT | QYNPVKQQL | 9 | Q9DBL7 | Bifunctional coenzyme A synthase |
| WT | SFLPTLREL | 9 | P28653 | Biglycan |
| WT | GYISIANGL | 9 | Q99LC2 | Cleavage stimulation factor 50 kDa subunit |
| WT | TYIESSTKV | 9 | Q8VBZ3 | Cleft lip and palate transmembrane protein 1 homolog |
| WT | TYAPVKSFL | 9 | Q11204 | CMP-N-acetylneuraminate-beta-galactosamide-alpha-2,3-sialyltransferase |
| WT | IYASSKDAI | 9 | P18760 | Cofilin-1 |
| WT | SFIPAVNDL | 9 | Q8BHX1 | Coiled-coil domain-containing protein 5 |
| WT | RYAALRELI | 9 | Q9DBT3 | Coiled-coil domain-containing protein 97 |
| WT | RYKQLLTYI | 9 | P61202 | COP9 signalosome complex subunit 2 |
| WT | FFSTIRTEL | 9 | P50172 | Corticosteroid 11-beta-dehydrogenase isozyme 1 |
| WT | RYMELYTHV | 9 | Q9WTX6 | Cullin-1 |
| WT | TWNKLLTTI | 9 | Q9D4H8 | Cullin-2 |
| WT | KYVNSIWDL | 9 | Q9JLV5 | Cullin-3 |
| WT | LYLPMAQSV | 9 | Q9DCP9 | DAZ-associated protein 2 |
| WT | HYKDMLSEL | 9 | Q8BZN6 | Dedicator of cytokinesis protein 10 |
| WT | SYLPVGSHNL | 10 | Q9WVF7 | DNA polymerase epsilon catalytic subunit A |
| WT | SYNKAISYL | 9 | A2ALW5 | DnaJ homolog subfamily C member 25 |
| WT | YLPTHTSL | 8 | Q8BM54 | E3 ubiquitin-protein ligase MYLIP |
| WT | SYLTSASSL | 9 | Q80TP3 | E3 ubiquitin-protein ligase UBR5 |
| WT | DYQPGITFI | 9 | Q8CJG0 | Eukaryotic translation initiation factor 2C 2 |
| WT | SYNRLKSLI | 9 | Q920E5 | Farnesyl pyrophosphate synthetase |
| WT | DYIGVRQHL | 9 | Q5H8B9 | FRAS1-related extracellular matrix protein 3 |
| WT | KYSISQGTI | 9 | Q9WVF6 | Group IID secretory phospholipase A2 |
| WT | HGEYPAKAL | 9 | P35492 | Histidine ammonia-lyase |
| WT | AYLAALTQL | 9 | P54310 | Hormone-sensitive lipase |
| WT | KYLSDNVHL | 9 | Q61081 | Hsp90 co-chaperone Cdc37 |
| WT | SYWLVRTEL | 9 | P42859 | Huntingtin |
| WT | SYKLGQVSI | 9 | P42859 | Huntingtin |
| WT | IYAPIREAL | 9 | Q8BTX9 | Hydroxysteroid dehydrogenase-like protein 1 |
| WT | KYLATSQVL | 9 | P01872 | Ig mu chain C region secreted form |
| WT | SLQSLKTRI | 9 | O88351 | Inhibitor of nuclear factor kappa-B kinase subunit beta |
| WT | LYQSLLTQV | 9 | Q7TQK1 | Integrator complex subunit 7 |

| | | | | |
|---|---|---|---|---|
| WT | NYFESKGIL | 9 | P15092 | Interferon-activable protein 204 |
| WT | KYMETIEKL | 9 | Q3TDD9 | KLRAQ motif-containing protein 1 |
| WT | SYNQLTRL | 8 | Q52KR2 | Leucine-rich repeats and immunoglobulin-like domains protein 2 |
| WT | TYKNITVRL | 9 | Q149R9 | Lysophosphatidic acid receptor 5 |
| WT | NYYPVNTRI | 9 | O09159 | Lysosomal alpha-mannosidase |
| WT | SYMEVPTYL | 9 | Q61168 | Lysosomal-associated transmembrane protein 5 |
| WT | AYIAQKTLL | 9 | Q62234 | Myomesin-1 |
| WT | SFVNTMTSL | 9 | P28660 | Nck-associated protein 1 |
| WT | TYNMAPSAL | 9 | Q61985 | Nuclear factor erythroid 2-related factor 1 |
| WT | LYGLLDPSI | 9 | Q8BHY2 | Nucleolar complex protein 4 homolog |
| WT | GYQVLRSVL | 9 | Q8R5K4 | Nucleolar protein 6 |
| WT | QFWGTRSEL | 9 | Q8R5K4 | Nucleolar protein 6 |
| WT | TYMEALSHL | 9 | O35904 | Phosphatidylinositol-4,5-bisphosphate 3-kinase catalytic subunit delta isoform |
| WT | AYFHLLNQI | 9 | Q3V0K9 | Plastin-1 |
| WT | TYLPAGQSV | 9 | P67778 | Prohibitin |
| WT | SYLIGRQKI | 9 | Q91ZX7 | Prolow-density lipoprotein receptor-related protein 1 |
| WT | SFSVIGFSVL | 10 | P70263 | Prostaglandin D2 receptor |
| WT | IFEEEISEL | 9 | Q8VCU0 | Protein angel homolog 1 |
| WT | GYIDTHKL | 8 | A6X919 | Protein dpy-19 homolog 1 |
| WT | AYAGVISAL | 9 | Q8BMB0 | Protein EMSY |
| WT | SYHPSGLSL | 9 | Q8BXQ8 | Protein FAM53C |
| WT | TYAVRVFAL | 9 | Q4QQM5 | Protein FAM73A |
| WT | AFLSSLTDV | 9 | Q3UVL4 | Protein fat-free homolog |
| WT | HYFNTPFQL | 9 | Q6NVE9 | Protein phosphatase PTC7 homolog |
| WT | KYQDILSEL | 9 | Q8C9X1 | Protein S100-A1-like |
| WT | YYKASVTRL | 9 | Q9QVP9 | Protein tyrosine kinase 2 beta |
| WT | GYQRLLELI | 9 | A2AIV2 | Protein virilizer homolog |
| WT | SYLLQSTEL | 9 | P59729 | Ras and Rab interactor 3 |
| WT | YYSPLRDLL | 9 | Q60790 | Ras GTPase-activating protein 3 |
| WT | MYFQTHDQI | 9 | Q9EPU0 | Regulator of nonsense transcripts 1 |
| WT | SYSMPLTSI | 9 | Q6PDX6 | RING finger protein 220 |
| WT | SYMPTVSHL | 9 | Q9Z2E9 | Seipin |
| WT | KYGPVVSLL | 9 | P97343 | Serine/threonine-protein kinase Kist |
| WT | SFGRTSTVTL | 10 | Q9EQY0 | Serine/threonine-protein kinase/endoribonuclease IRE1 |
| WT | IFFPSVTGI | 9 | Q9JIS8 | Solute carrier family 12 member 4 |
| WT | IYFPSVTGI | 9 | Q91V14 | Solute carrier family 12 member 5 |
| WT | YYGILQEKI | 9 | P97858 | Solute carrier family 35 member B1 |
| WT | TYAWPLSNL | 9 | Q8R4U0 | Stabilin-2 |
| WT | LFSEIQTTL | 9 | Q8C2E7 | Strumpellin |
| WT | SYLDGKGNL | 9 | Q8R2K4 | TAF6-like RNA polymerase II p300/CBP-associated factor-associated factor 65 kDa subunit 6L |
| WT | GYFVEACKL | 9 | A2ASS6 | Titin |

| | | | | |
|---|---|---|---|---|
| **WT** | KYQEALDVI | 9 | Q8BWZ3 | TPR repeat-containing protein C12orf30 homolog |
| **WT** | TYPGQAHPAL | 10 | P35428 | Transcription factor HES-1 |
| **WT** | KFLPSSQEL | 9 | O70472 | Transmembrane protein 131 |
| **WT** | AYKFGKTVV | 9 | Q8R3Q0 | Transmembrane protein 66 |
| **WT** | HYLQVNSTI | 9 | P32972 | Tumor necrosis factor ligand superfamily member 8 |
| **WT** | MYQDILTEL | 9 | Q6P1Y8 | Type II inositol-3,4-bisphosphate 4-phosphatase |
| **WT** | KYQEALSYL | 9 | Q5I043 | Ubiquitin carboxyl-terminal hydrolase 28 |
| **WT** | YYINGKTGL | 9 | Q6ZQ93 | Ubiquitin carboxyl-terminal hydrolase 34 |
| **WT** | SLVSDTETSI | 10 | Q6ZQ93 | Ubiquitin carboxyl-terminal hydrolase 34 |
| **WT** | KYVAVYNLI | 9 | Q80U87 | Ubiquitin carboxyl-terminal hydrolase 8 |
| **WT** | WYNPILNRV | 9 | Q9Z222 | UDP-GlcNAc:betaGal beta-1,3-N-acetylglucosaminyltransferase 2 |
| **WT** | SFVSVLHAL | 9 | Q91V83 | Uncharacterized protein KIAA0406 homolog |
| **WT** | LWEAHTNIL | 9 | Q505K2 | UPF0518 protein FAM160A1 |
| **WT** | TYIRSSLDI | 9 | Q8CII0 | Zinc finger and BTB domain-containing protein 8 |